



THE UNIVERSITY OF QUEENSLAND
AUSTRALIA

Gestational hypoxia and programming of disease

Sarah Louise Walton

Bachelor of Biomedical Science (Honours)

A thesis submitted for the degree of Doctor of Philosophy at

The University of Queensland in 2016

School of Biomedical Sciences

Abstract

Fetal hypoxia remains the most common complication throughout pregnancy and has a wide aetiology including, but not limited to, placental insufficiency, high altitude living and maternal factors such as smoking and pulmonary disease. Intrauterine growth restriction and subsequent low birth weight are common features of pregnancies complicated by reduced oxygenation. Suboptimal organ development may arise, thereby substantially increasing vulnerability to cardiovascular and renal diseases in adulthood. Recently it has been established that prenatally programmed vulnerability to disease may be exacerbated by a postnatal 'second-hit', such as a high salt diet or ageing. The primary aim of this thesis was to investigate the effects of maternal hypoxia on the programming of cardiovascular and renal disease in mice, and secondly whether excess dietary salt intake throughout life may exacerbate disease outcomes.

Pregnant CD1 mice were housed in a hypoxia chamber set to 12% oxygen throughout the last five days of pregnancy, from embryonic day (E) 14.5 until birth (P0). Control animals remained in normoxic room conditions (21% oxygen) throughout pregnancy. Upon littering, animals were removed from the hypoxia chamber and raised in normoxic room conditions. A subset of mice was fed a high salt diet from 10 weeks of age until post-mortem. Mice were housed in metabolic cages for 24 hours to assess renal function under basal conditions, and in response to a 24 hour water deprivation challenge, at 4 and 12 months of age. Blood pressure and microvascular function and structure were assessed in offspring at 12 months of age. Kidneys, hearts and aortas were collected for stereological and histological analyses.

Prenatal hypoxia reduced nephron number in the kidneys of male offspring, leading to glomerular hypertrophy, renal fibrosis and mild albuminuria by 12 months of age. However, female offspring exposed to the same hypoxic insult *in utero* presented with normal number of glomeruli and renal pathology equivalent to control animals by 12 months of age. Both male and female hypoxia-exposed offspring had elevated mean arterial pressure at 12 months of age. A high salt diet throughout adult life increased cardiac tissue fibrosis, particularly in male hypoxia-exposed offspring, and exacerbated renal pathology in male hypoxia-exposed offspring only. Pressurized myography was performed at the time of post-mortem to assess functional, structural and mechanical properties of mesenteric resistance arteries at 12 months of age. Both male and female offspring exposed to maternal hypoxia had significantly

impaired endothelial function, which was not exacerbated by the high salt diet. The combination of prenatal hypoxia and a postnatal high salt diet caused marked stiffening of the microvasculature as well as loss of elastin integrity and increased collagen content in the aorta, consistent with vascular stiffness. This suggests that kidneys from female offspring are somehow protected from the *in utero* insult; however, this protection does not extend to the cardiovascular system.

We also investigated the impact of prenatal hypoxia on the renal tubule system and collecting ducts. First, we developed a methodology to estimate lengths of renal tubules and collecting ducts using a combination of immunohistochemistry and design-based stereology. We have demonstrated that the renal tubules and collecting ducts undergo significant elongation postnatally. Furthermore, salt-induced renal hypertrophy was associated with elongation of the thin descending limb of Henle and the proximal tubule. We applied this technique to the kidneys of male hypoxia-exposed offspring with a congenital nephron deficit, and observed significant elongation of the proximal and distal tubule compared to controls. Male hypoxia-exposed offspring had an altered response to a 24 h water deprivation challenge at 12 months of age, which was associated with altered cellular composition of the collecting duct and reduced Aquaporin 2 expression and distribution in the kidney. This highlights that renal tubule segments and collecting ducts are susceptible to prenatal insult and may, in combination with reduced nephron number, contribute to the predisposition to cardiovascular and renal disease.

In conclusion, this thesis has demonstrated that prenatal hypoxia increases vulnerability of offspring, particularly males, to cardiovascular and renal disease in adulthood. Furthermore, a postnatal diet high in salt exacerbated microvascular stiffness, cardiac fibrosis and renal histopathology, suggesting that consumption of a healthier diet may attenuate predisposition to disease. This indicates that the postnatal environment is an important consideration in disease progression, particularly for those born of low birth weight.

Declaration by author

This thesis is composed of my original work, and contains no material previously published or written by another person except where due reference has been made in the text. I have clearly stated the contribution by others to jointly authored works that I have included in my thesis.

I have clearly stated the contribution of others to my thesis as a whole, including statistical assistance, survey design, data analysis, significant technical procedures, professional editorial advice, and any other original research work used or reported in my thesis. The content of my thesis is the result of work I have carried out since the commencement of my research higher degree candidature and does not include a substantial part of work that has been submitted to qualify for the award of any other degree or diploma in any university or other tertiary institution. I have clearly stated which parts of my thesis, if any, have been submitted to qualify for another award.

I acknowledge that an electronic copy of my thesis must be lodged with the University Library and, subject to the policy and procedures of The University of Queensland, the thesis be made available for research and study in accordance with the *Copyright Act 1968* unless a period of embargo has been approved by the Dean of the Graduate School.

I acknowledge that copyright of all material contained in my thesis resides with the copyright holder(s) of that material. Where appropriate I have obtained copyright permission from the copyright holder to reproduce material in this thesis.

Publications during candidature

Peer reviewed papers

1. Cuffe, J.S.M., **Walton, S.L.**, Singh, R.R., Spiers, J.G., Bielefeldt-Ohmann, H., Wilkinson, L., Little, M.H., & Moritz, K.M. (2014). *Mid- to late term hypoxia in the mouse alters placental morphology, glucocorticoid regulatory pathways and nutrient transporters in a sex-specific manner*. The Journal of Physiology, 592(14): 3127-41
2. Cuffe, J.S.M., **Walton, S.L.**, Steane, S.E., Singh, R.R., Simmons, D.G., & Moritz, K.M. (2014). *The effects of gestational age and maternal hypoxia on the placental renin angiotensin system in the mouse*. Placenta, 35(11): 953-61
3. **Walton, S.L.**, Singh, R.R., Tan, T., Paravicini, T.M., & Moritz, K.M. (2016). *Late gestational hypoxia and a postnatal high salt diet programs endothelial dysfunction and arterial stiffness in adult mouse offspring*. The Journal of Physiology, 594(5): 1451-63

Book chapters

1. Cuffe, J.S.M., **Walton, S.L.**, & Moritz, K.M. (2015). *The developmental origins of renal dysfunction*. Book chapter in “The Epigenome and Developmental Origins of Health and Disease”, Editor: Rosenfeld, C, Publisher: Elsevier

Conference abstracts

International

1. Ding, A., **Walton, S.L.**, Moritz, K.M., & Phillips, J.K., *Nephron endowment in a rodent model of polycystic kidney disease*. FASEB Science Research Conference: Polycystic Kidney Disease, Lucca, Italy, 2014
2. **Walton, S.L.**, Singh, R.R., Li, J., Bielefeldt-Ohmann, H., Paravicini, T.M., Little, M.H., & Moritz, K.M., *The effect of prenatal hypoxia and a postnatal high salt diet on renal structure in the aged mouse*. Kidney Week, hosted by the American Society of Nephrology, San Diego, USA, 2015 (presenting author).

3. **Walton, S.L.**, Singh, R.R, Li, J., Bielefeldt-Ohmann, H., Paravicini, T.M., Little, M.H., & Karen M Moritz., *The effect of prenatal hypoxia and a postnatal high-salt diet on microvascular structure and function*. Developmental Origins of Health and Disease, Cape Town, South Africa, 2015 (presented on my behalf by Prof Karen Moritz).
4. Combes, A.N., Wilson, S., Phipson, B., Binnie, B., Ju, A., Cebrian, C., **Walton, S.L.**, Moritz, K., Oshlack, A., & Little, M.H., *Heterozygosity for Six2 increases ureteric branching and final nephron number*. Kidney Week, hosted by the American Society of Nephrology, Chicago, USA, 2016

National

1. **Walton, S.L.**, Singh, R.R., Paravicini T.M., Wilkinson, L., Little, M.H., & Moritz, K.M., *Chronic mid-late gestational hypoxia alters renal structure and function, and leads to hypertension in adult offspring*. SBMS Symposium, Brisbane, 2013 (presenting author).
2. **Walton, S.L.**, Singh, R.R., Paravicini T.M., Wilkinson, L., Little, M.H., Moritz, K.M., *Chronic mid-late gestational hypoxia alters renal structure and function in adult male mouse offspring*. Australian and New Zealand Society of Nephrology, Brisbane, 2013 (presenting author).
3. **Walton, S.L.**, Singh, R.R., Paravicini T.M., Wilkinson, L., Little, M.H., Moritz, K.M., *Chronic mid-late gestational hypoxia leads to hypertension in male and female mouse offspring*. High Blood Pressure Research Council of Australia, Melbourne, 2013 (presenting author).
4. **Walton, S.L.**, Singh, R.R., Little, M.H., & Moritz, K.M., *Urine-concentrating defect associated with reduced nephron number and proximal and distal tubule elongation in male but not female offspring exposed to late-gestational hypoxia*. Australian and New Zealand Society of Nephrology, Melbourne, 2013 (presenting author).
5. **Walton, S.L.**, Singh, R.R., Little, M.H., & Moritz, K.M., *Urine-concentrating defect associated with altered renal structure and function in male but not female offspring exposed to late-gestational hypoxia*. SBMS Symposium, Brisbane, 2014 (presenting author).

6. **Walton, S.L.**, Singh, R.R, Paravicini, T.M., Little, M.H., & Karen M Moritz., *Hypoxia-induced growth restriction leads to sexually dimorphic changes to the renal and cardiovascular systems in adult mouse offspring*. The Australian Physiology Society, Brisbane, 2014 (presenting author).
7. **Walton, S.L.**, Singh, R.R, Paravicini, T.M., Bielefeldt-Ohmann, H., Little, M.H., & Karen M Moritz., *Late gestational hypoxia alters renal structure and function in male but not female mouse offspring*. The Fetal and Neonatal Workshop of Australia and New Zealand, Melbourne, 2015 (presenting author).
8. **Walton, S.L.**, Singh, R.R, Li, J., Bielefeldt-Ohmann, H., Paravicini, T.M., Little, M.H., & Karen M Moritz., *Prenatal hypoxia combined with a postnatal high salt diet alters renal structure in the aged mouse*. SBMS Symposium, Brisbane, 2015 (presenting author).
9. **Walton, S.L.**, Singh, R.R, Paravicini, T.M., & Karen M Moritz., *Chronic hypoxia during late gestation alters renal structure and leads to hypertension in mouse offspring*. Developmental Origins of Health and Disease, Melbourne, 2015 (presenting author).
10. Li, J., Kartopawiro, J., **Walton, S.L.**, Flores, T., Black, J., Bertram, J., Trnka, P., Hoy, W., & Moritz, K.M., *Factors affecting postnatal kidney development and implications for adult disease*. Children's Health Queensland Research Day, Brisbane, 2015
11. **Walton, S.L.**, Singh, R.R., Bielefeldt-Ohmann, H., Paravicini, T.M., Little, M.H., & Moritz, K.M., *Prenatal hypoxia combined with a high-salt diet increases risk of renal and cardiovascular impairments in adult mice*. The Fetal and Neonatal Workshop of Australia and New Zealand, Magnetic Island, 2016 (presenting author).
12. **Walton, S.L.**, Singh, R.R., Li, J., Bielefeldt-Ohmann, H., Paravicini, T.M., Little, M.H., & Moritz, K.M., *Prenatal hypoxia increases susceptibility to renal and cardiovascular impairments in mouse offspring*. The Australian Society for Medical Research Queensland Postgraduate Student Conference, Brisbane, 2016 (presenting author).
13. **Walton, S.L.**, Singh, R.R., Li, J., Bielefeldt-Ohmann, H., Paravicini, T.M., Little, M.H., & Moritz, K.M., *Prenatal hypoxia increases susceptibility to renal and cardiovascular impairments in mouse offspring*. Queensland Perinatal Consortium, Brisbane, 2016 (presenting author).

Publications included in this thesis

Walton, S.L., Singh, R.R., Tan, T., Paravicini, T.M., & Moritz, K.M. (2016). *Late gestational hypoxia and a postnatal high salt diet programs endothelial dysfunction and arterial stiffness in adult mouse offspring*. The Journal of Physiology, 594(5): 1451-63

Incorporated as Chapter 3.

Contributor	Statement of contribution
Walton, S.L.	Animal treatment and tissue collection (80%) Pressurised myography (50%) Histological analysis (100%) Interpreting results (70%) Writing and editing manuscript (60%) Study design (10%)
Singh, R.R.	Animal treatment and tissue collection (20%) Study design (20%) Writing and editing manuscript (10%)
Tan, T.	Pressurised myography (50%)
Paravicini, T.M.	Interpreting results (15%) Writing and editing manuscript (15%) Study design (35%)
Moritz, K.M.	Interpreting results (15%) Writing and editing manuscript (15%) Study design (35%)

Contributions by others to the thesis

The majority of work completed throughout this thesis was undertaken by SL Walton. Help was provided for the conception and design of the project as well as interpretation of results and critical revision of work by Professor Karen M. Moritz, Professor Melissa H. Little, Dr Reetu R. Singh, Dr Helle Bielefeldt-Ohmann and Dr Joan Li. Radiotelemetry surgeries were performed by Dr Tamara M. Paravicini. T Tan assisted with pressurised myography experiments. Dr Helle Bielefeldt-Ohmann carried out histopathological analyses.

Statement of parts of the thesis submitted to qualify for the award of another degree

None.

Acknowledgements

First I would like to convey my gratitude to Professor Karen Moritz for guiding me throughout my candidature. Your support and mentorship at all times has been invaluable with all aspects of my project as well as my career development. I would also like to thank Dr Joan Li, who has been a tremendous help to me and has always generously devoted time to providing insightful ideas for my project. Special thanks must go to Professor Melissa Little for assisting with this project and providing great expertise in the field. In addition, I would like to extend my thanks to Dr Reetu Singh. You have continued to support me and provide guidance since my Honours year which I am so grateful for (especially given the countless hours we have spent talking about tubules across Australia and now internationally!) To Dr Helle Bielefeldt-Ohmann, I am indebted to your work on my project, which really has gone above and beyond, and I have learned so much from your efforts and guidance.

I would also like to thank all members of the Moritz laboratory, most especially Dr James Cuffe and Sarah Steane for the great collaborative efforts on this project. To Richard Schlegel and Jacinta Kalisch-Smith, you have made my time here the best of fun and you were always there to help whenever times were tough. I will always look fondly on our trips to the Ville for pizzas and ice creams, and I will never forget the time you foraged for my breakfast in Melbourne when I was sick. Thank you also to Emily Dorey and Lisa Akison for constant support and encouragement, and Tiffany Tan for her assistance with myography. Special thanks must go to Dr Tamara Paravicini for the long hours spent in the animal house, and to Kym French for her kindness and dedication to assisting with my project over several years.

I would also like to acknowledge the Australian Postgraduate Award which has supported me throughout my candidature, and the School of Biomedical Sciences at the University of Queensland and the Australian & New Zealand Society of Nephrology for supporting my conference travels.

Most of all I would to thank my parents, Kathryn and David, for always looking out for me and supporting me throughout my university years! I am very grateful for everything you have done for me. Also a big thank you to the rest of my family – Emma and Liam, and my grandparents, Granny & Grandad Walton, and Moya and Grandstan Taschke. I cannot thank you all enough!

Keywords

hypoxia, maternal, programming, development, kidney, cardiovascular, renal, vascular, salt, stereology

Australian and New Zealand Standard Research Classifications (ANZSRC)

ANZSRC code: 060603, Animal Physiology – Systems (60%)

ANZSRC code: 111401, Foetal Development and Medicine (25%)

ANZSRC code: 111103, Nutritional Physiology (15%)

Fields of Research (FoR) Classification

FoR code: 1114, Paediatrics and Reproductive Medicine, 70%

FoR code: 1116, Medical Physiology, 30%

Table of Contents

List of figures	17
List of tables	18
List of abbreviations	19
Chapter 1: Introduction	23
1.1 Overview of the increasing rates of non-communicable diseases worldwide	23
1.2 Cardiovascular disease	23
1.3 Chronic kidney disease	26
1.4 Associations between CKD and CVD	29
1.5 Developmental Origins of Health and Disease	30
1.6 Human evidence for developmental programming	30
1.7 Animal models of developmental programming	30
1.7.1 Maternal undernutrition	31
1.7.2 Fetal glucocorticoid exposure	34
1.7.3 Uteroplacental insufficiency	35
1.8 Hypoxia during gestation	36
1.8.1 Acute hypoxia	37
1.8.2 Chronic hypoxia	37
1.8.3 High altitude	38
1.8.4 Maternal diseases and sleep disorders	40
1.9 Common outcomes of hypoxia-exposed offspring	41
1.9.1 Effects of prenatal hypoxia on the placenta	41
1.9.2 Prenatal hypoxia and brain sparing	42
1.9.3 Effects of prenatal hypoxia on the heart	42
1.9.3 Effects of prenatal hypoxia on the vasculature	43

1.9.4	Effects of prenatal hypoxia on the kidney	43
1.10	Mechanisms of hypoxia-induced damage and avenues for intervention	48
1.11	Developmental programming of the kidney and renal dysfunction in offspring	49
1.12	Postnatal development of the kidney	52
1.13	Low nephron number in developmental programming	52
1.13.1	Molecular mechanisms contributing to altered renal development	57
1.13.2	Renal tubules.....	58
1.13.3	Sodium channels and transporters	58
1.13.4	Renin-angiotensin system	60
1.14	The importance of the kidney in blood pressure regulation	64
1.15	Sex differences in developmental programming	66
1.16	The ‘second hit’ hypothesis	66
1.16.1	Overview	66
1.16.2	High salt diet	67
1.17	Rationale	70
1.18	Hypotheses and aims.....	70
Chapter 2:	General methods.....	72
2.1	Ethics approval.....	72
2.2	Animal treatment: maternal hypoxia	72
2.3	Tissue collection from juvenile animals	75
2.3.1	Fetal post-mortem	75
2.3.2	Post-mortem on day-of-birth.....	75
2.3.3	Early juvenile post-mortem.....	75
2.3.4	Post-mortem at weaning	75
2.3.5	Post-mortem at 2 months of age	75
2.4	Dietary intervention: chronic high salt diet	76
2.4.1	Post-mortem at 4 months of age	76

2.5	Animal physiological studies	76
2.5.1	Metabolic cages	76
2.5.2	Water deprivation challenge	76
2.6	Blood pressure by radiotelemetry	77
2.6.1	Surgical preparation	77
2.6.2	Restraint stress	78
2.7	Pressure myography	78
2.7.1	Mesenteric artery dissection and cannulation	78
2.7.2	Vessel imaging and image capture	78
2.7.3	Equilibration	79
2.7.4	Maximum vessel contractility using $KPSS_{max}$	79
2.7.5	Vasoconstrictive response to phenylephrine	79
2.7.6	Endothelium-dependent vasodilation	79
2.7.7	Endothelium-independent vasodilation	79
2.7.8	Vascular structure and mechanics	79
2.7.9	Data analysis	80
2.8	Quantitative real-time PCR	81
2.9	Histological studies	81
2.9.1	Tissue collection	81
2.9.2	Paraffin processing and staining	81
2.9.3	Staining	82
2.9.4	Stereology	84
2.9.5	Histomorphometric analyses	86
2.10	Statistical analyses	88
Chapter 3	89
	Late gestational hypoxia and a postnatal high salt diet programs endothelial dysfunction and arterial stiffness in adult mouse offspring	90

Chapter 4	126
Prenatal hypoxia combined with a high-salt diet predisposes mouse offspring to renal and cardiovascular impairments.	127
Chapter 5	169
Lengths of nephron tubule segments and collecting ducts in the CD-1 mouse kidney: an ontogeny study.	170
Chapter 6	198
The impact of prenatal hypoxia on renal medulla and papilla structure and functional maturation in the mouse.	198
Chapter 7: General Discussion	234
7.1 Thesis summary	234
7.2 Modelling prenatal hypoxia in the mouse.....	236
7.3 Quantifying fetal, placental and maternal hypoxia	237
7.4 Fetal and early offspring growth following prenatal hypoxia	237
7.5 Responses to maternal hypoxia.....	238
7.6 Catch-up growth.....	240
7.7 Effect of maternal hypoxia on early postnatal kidney structure and function	241
7.7.1 Reduced nephron number and proximal/distal tubule hypertrophy in male offspring	241
7.7.2 Mechanisms of the sex-specific reduction in nephron number	244
7.7.3 Examining renal function under a water deprivation challenge	247
7.7.4 Measuring renal function in mice	247
7.8 Effect of maternal hypoxia on cardiovascular function and structure	248
7.8.1 Elevated mean arterial pressure	248
7.8.2 Vascular function	251
7.8.3 Vascular stiffening	251
7.8.4 Role of sex hormones in mediating offspring outcomes	252
7.8.5 Renal nerves	252

7.9	The impact of high dietary salt intake.....	253
7.10	Methodology to determine tubule and collecting duct lengths in the mouse kidney 255	
7.11	Limitations and future directions	257
7.11.1	Cardiovascular and renal measurements.....	257
7.11.2	Developmental programming of the renal medulla and papilla.....	258
7.12	Conclusion	260
	References.....	261

List of figures

- Figure 1.1.** Comparative timeline of nephrogenesis in different species.
- Figure 1.2.** The Brenner Hypothesis depicting the mechanisms through which a congenital nephron deficit may contribute to hypertension and renal disease in adulthood.
- Figure 1.3.** Potential pre- and postnatal pathways through which a suboptimal in utero environment may contribute to the programming of chronic kidney disease.
- Figure 2.1.** Diagram of major time points within this model of maternal hypoxia exposure throughout late gestation, and its influence on renal and cardiovascular outcomes.
- Figure 1.4.** The pressure-natriuresis mechanism.
- Figure 7.1.** A summary of the major time points within this model and long-term health outcomes of offspring exposed to maternal hypoxia during late gestation.
- Figure 7.2.** Potential mechanisms that may drive increased blood pressure following reduced renal mass.

List of tables

- Table 1.1.** Criteria for CKD
- Table 1.2.** Prognosis of CKD by GFR and albuminuria categories
- Table 1.3.** A summary of fetal and postnatal growth and metabolic, cardiovascular and renal outcomes in animal studies of hypoxia.
- Table 1.4.** Birth weight and arterial pressure in animal models of reduced nephron endowment
- Table 1.5.** NHMRC recommendations for average intake and upper level of intake of sodium by life stage.
- Table 7.1.** Summary of the effects of maternal hypoxia on body and organ weights compared to control offspring at late gestation (E18.5) and weaning (P21)
- Table 7.2.** Summary of renal outcomes in young mice
- Table 7.3.** Summary of cardiovascular outcomes in 12-month-old hypoxia-exposed offspring fed the normal-salt and high salt diet.
- Table 7.4.** Summary of renal outcomes in offspring fed normal salt and high salt diets at 12 months of age

List of abbreviations

ΣP , number of test points per kidney
11BHSD2, 11 beta hydroxysteroid dehydrogenase type 2
A, area
Ace, angiotensin-converting enzyme
Ace2, angiotensin-converting enzyme 2
ACh, acetylcholine
Agtr1a, angiotensin II type 1 receptor a
Agtr1b, angiotensin II type 1 receptor b
Agtr2, angiotensin II type 2 receptor
ANOVA, analysis of variance
 $a(p)$, area associated with each test point
AQP2, aquaporin 2
AUC, area under curve
bpm, beats per minute
BSA, bovine serum albumin
Bw, body weight
C, control
CaO₂, arterial oxygen content
CAKUT, congenital abnormalities of the kidney and urinary tract
CCD, cortical collecting duct
CD, collecting duct
cDNA, complementary DNA
CHS, control offspring fed a high salt diet
CKD, chronic kidney disease
Cl⁻, chloride
CNS, control offspring fed a normal salt diet
CSA, cross sectional area
CVD, cardiovascular disease
DBP, diastolic blood pressure
DNA, deoxyribonucleic acid
DOHaD, Developmental Origins of Health and Disease

DT, distal tubule
E, embryonic day
EC₅₀, half maximal effective concentration
ECF, extracellular fluid
eGFR, estimated glomerular filtration rate
ENaC, amiloride-sensitive epithelial sodium channel
GFR, glomerular filtration rate
GLUT1, glucose transporter protein type 1
H, hypoxia
HCO₃⁻, bicarbonate
HHS, hypoxia offspring fed a high salt diet
HIF1 α , hypoxia inducible factor 1-alpha
HNS, hypoxia offspring fed a normal salt diet
HR, heart rate
HS, high salt
ID, inner diameter of vessel
Igf2, insulin-like growth factor 2
I_i, number of intersections between cycloid and tubules
IUGR, intrauterine growth restriction
K⁺, potassium
KPSS, high potassium physiological salt solution
KPSS_{max}, maximum vessel contraction to KPSS
l, unit length of cycloid
 \hat{L} , length (m)
LBW, low birth weight
L_v, length density ($\times 10^{-4} \mu\text{m}^{-2}$)
MANOVA, multivariate analysis of variance
MAP, mean arterial pressure
MCD, medullary collecting duct
mRNA, messenger RNA
Na⁺, sodium
NCC, electroneutral sodium-chloride symporter
NCD, non-communicable disease

NHE3, sodium-hydrogen exchanger 3
NKCC2, type 2 Na-K-Cl cotransporter
NO, nitric oxide
NS, normal salt
O₂, oxygen
OD, outer diameter of vessel
P, postnatal day
PAS, period acid-Schiff
PB, phosphate buffer
PCR, polymerase chain reaction
PE, phenylephrine
PFA, paraformaldehyde
 P_i , number of test points per section
PNA, peanut agglutinin
PP, pulse pressure
PT, proximal tubule
qPCR, quantitative PCR
RAS, renin angiotensin system
 R_{max} , maximum relaxation
RNA, ribonucleic acid
ROS, reactive oxygen species
RSNA, renal sympathetic nerve activity
SaO₂, arterial oxygen saturation
SEM, standard error of the mean
Slc2a1, glucose transporter protein type 1
SNGFR, single nephron glomerular filtration rate
SNP, sodium nitroprusside
SpO₂, peripheral capillary oxygen saturation
SSF, section sampling fraction
TDLH, thin descending limb of Henle
TGF, tubuloglomerular feedback
UACR, urinary albumin to creatinine ratio
U_{Cl}V, urinary chloride excretion ($\mu\text{mol}/24\text{h}$)

$U_K V$, urinary potassium excretion ($\mu\text{mol}/24\text{h}$)

$U_{\text{Na}} V$, urinary sodium excretion ($\mu\text{mol}/24\text{h}$)

V-ATPase, vacuolar-type H^+ -ATPase

VEGF, vascular endothelial growth factor

V_{kid} , volume of kidney

VUR, vertical uniform random

WT, wall thickness of vessel

Chapter 1: Introduction

Parts of this chapter have been published in:

Cuffe, J.S.M., **Walton, S.L.**, & Moritz, K.M. (2015). *The developmental origins of renal dysfunction*. Book chapter in “The Epigenome and Developmental Origins of Health and Disease”, Editor: Rosenfeld, C, Publisher: Elsevier

1.1 Overview of the increasing rates of non-communicable diseases worldwide

The World Health Organisation (2015) reports that non-communicable diseases (NCDs) are responsible for 38 million deaths worldwide every year. There are four main types of NCDs: cardiovascular disease, cancers, chronic respiratory diseases and diabetes. NCDs are present in individuals from all age groups and socio-economic backgrounds. However, NCD-related deaths affect low- and middle-income countries disproportionately, with 28 million deaths each year (almost three-quarters of NCD-related deaths worldwide) (Black *et al.*, 2008; World Health Organisation, 2015). Risk factors contributing to NCDs include unhealthy diets, physical inactivity, smoking, alcohol consumption and ageing (Ezzati *et al.*, 2002; Danaei *et al.*, 2009; Ezzati & Riboli 2013). Many of these risk factors can be modified by behaviour, such as diet, tobacco use and physical activity. Therefore, interventions to encourage healthy lifestyles may prove greatly effective in reducing NCD rates. More recently, an association between NCDs and poor fetal growth and subsequent low birth weight has been identified (Barker, 2007). Suboptimal fetal development may be the result of factors including maternal undernutrition, placental insufficiency and prenatal stress, and it appears that this non-modifiable risk factor may profoundly influence health in later life.

1.2 Cardiovascular disease

Cardiovascular diseases (CVD), a group of disorders that affect the heart and vasculature, are the most predominant form of NCDs, and the greatest cause of death globally (World Health Organisation, 2009; Yusuf *et al.*, 2015). These include conditions such as coronary heart disease, cerebrovascular disease, stroke, and ischaemic heart disease. The majority of these

deaths are in low- and middle-income countries, where access to affordable and effective health care services can be lacking.

Elevated blood pressure, or hypertension, (defined as systolic and/or diastolic blood pressure $\geq 140/90$ mmHg) is one of the greatest risk factors for CVD (Lim *et al.*, 2012), responsible for 13.5% of all deaths worldwide. The World Health Organisation also reported that approximately 40% of adults over the age of 25 had been diagnosed with hypertension in 2008 (World Health Organisation, 2009). Hypertension is also more prevalent in low- and middle-income countries, compared to high-income countries (World Health Organisation, 2009). However, hypertension is greatly under-diagnosed as the majority of hypertensive people do not exhibit any symptoms. Therefore regular blood pressure measurement is vital for timely diagnosis before life-threatening complications develop. Improved control of hypertension on a global scale may significantly reduce the economic and public health burden of cardiovascular disease (Chow *et al.*, 2013; Yusuf *et al.*, 2015).

Increased arterial pressure places greater force on the arterial walls, leading to altered functional and structural characteristics of the vasculature. In particular, hypertension is associated with thickening of the walls of both small and large arteries, known as arteriosclerosis (Otsuka *et al.*, 2015). This loss of arterial compliance can lead to altered vessel wall properties and an exaggerated response to vasoconstrictors, both of which increase peripheral vascular resistance. Increased arterial stiffness has been shown to contribute to elevated blood pressure in the human population (te Velde *et al.*, 2004), and is strongly associated with CVD in adulthood (Benetos *et al.*, 2002). CVD, in particular heart failure, is also associated with abnormal vascular reactivity. Dysfunction of the vascular endothelium, the epithelial lining of blood vessels that regulates vascular tone, is a hallmark of CVD (Benetos *et al.*, 2002; Matsuzawa *et al.*, 2015). Endothelial dysfunction is characterised by reduced bioavailability of vasodilators, notably nitric oxide and increased endothelial vasoconstrictors, overall leading to a reduced ability for endothelium-dependent vasodilation (Benetos *et al.*, 2002). Hypertension and endothelial dysfunction frequently co-exist, however it is not clear whether hypertension is the cause of the result of endothelial damage. Regardless, endothelial dysfunction has been shown to be an accurate predictor of CVD in the human population (Hadi *et al.*, 2005).

Impaired arterial structure and function has flow-on effects to other organ systems by reducing blood flow to the heart, kidneys, brain and extremities. Uncontrolled hypertension also lead to coronary artery disease, left ventricular hypertrophy and ultimately heart failure (Hadi *et al.*, 2015). Hypertension also increases the risk of aneurysms developing in the vasculature. In addition, reduced blood flow to the brain as a result of hypertension is strongly associated with stroke and dementia (Ilulita & Girouard, 2016). Interestingly, a recent study revealed that increased vascular stiffness is a superior predictor of declining cognitive function to blood pressure (Hajjar *et al.*, 2016). This suggests that blood pressure measurements should be considered in conjunction with other cardiovascular parameters such as vascular stiffness.

Hypertension is also a strong risk factor for the development of atherosclerosis, a type of arteriosclerosis which involves the formation of plaques within the vasculature (Al Rifai *et al.*, 2015). Although the cause of atherosclerosis is not fully understood, damage to the endothelium, the inner lining of the arterial wall, due to hypertension has been recognised as a contributor. Atherosclerotic plaques are comprised of cholesterol, triglycerides, calcium and cellular content, particularly accumulating white blood cells, and increase in size over the lifespan (Wang & Bennett, 2012). Presence of atherosclerotic plaques reduce elasticity of the arterial walls, leading to increased vascular stiffness and widened pulse pressure, both of which are significant risk factors for CVD. Over time, increased plaque size can disrupt blood flow through the vasculature, the consequences of which are specific to the site of the lesion (Otsuka *et al.*, 2015; Wang & Bennett, 2012). Atherosclerosis of the coronary arteries, for example, leads to coronary artery disease whereby the individual experiences reduced cardiac blood flow and susceptibility to heart attack (Otsuka *et al.*, 2015). Plaques in arteries that direct blood away from the heart and brain can cause peripheral vascular disease, which increases risk of infection, tissue ischaemia and ultimately limb loss if left untreated. Renal artery atherosclerosis can also reduce renal blood flow and ultimately lead to the development of chronic kidney disease (CKD) (Sarnak *et al.*, 2003). The associations between CVD and kidney damage will be discussed in greater detail in Section 1.5.

As noted above, many risk factors associated with hypertension are modifiable, including smoking, physical inactivity, and dietary excess of calories, saturated fat and salt. Salt reduction initiatives will be discussed in Section 1.16.2. However, a growing body of

evidence has shown an association between the early life environment, such as maternal and child undernutrition, and risk of CVD (Black *et al.*, 2008). Hypertension and vascular dysfunction, in particular, are common findings in individuals born of low birth weight (Martin *et al.*, 2000; Barker *et al.*, 2007). The early origins of CVD will be discussed in further detail in Section 1.5.

1.3 Chronic kidney disease

Chronic kidney disease (CKD) is part of the increasing burden of non-communicable diseases, with prevalence rates of 8% to 16% worldwide (Jha *et al.*, 2013). It is amongst the fastest-growing chronic diseases, with deaths attributable to CKD increasing by more than 80% over the past 20 years (Radhakrishnan *et al.*, 2014). Diabetes mellitus is the most common cause of CKD globally. Other risk factors for developing CKD have been identified, including hypertension, obesity, herbal medicines, nephropathies, ease of access to water, and water quality (Jha *et al.*, 2013). Of particular concern, many young people without comorbidities such as hypertension or diabetes are developing CKD. Complications from CKD include anaemia, CKD-associated mineral and bone disorders, dyslipidemia, nutritional deficits and cardiovascular disease (Thomas *et al.*, 2008).

CKD is currently defined as abnormalities of kidney structure or function, persisting for greater than 3 months (National Kidney Foundation, 2002). This includes a decline in glomerular filtration rate (GFR) and one or markers of kidney damage (Table 1.1) (National Kidney Foundation, 2002; Levey *et al.*, 2003).

Table 1.1. Criteria for CKD (either of the following present for >3 months)

Markers of kidney damage (one or more)	Albuminuria Urine sediment abnormalities Electrolyte and other abnormalities due to tubular disorders Abnormalities detected by histology Structural abnormalities detected by imaging History of kidney transplantation
Decreased GFR	GFR <60 ml/min/1.73 m ²

Abbreviations: CKD, chronic kidney disease; GFR, glomerular filtration rate

CKD is classified using a five-stage system based on estimated GFR (eGFR) (Table 1.2) (KDIGO, 2013). Diagnosis of CKD usually occurs at later stages (stages 3-5) when eGFR has declined by more than 50%. Renal replacement therapy is required for patients with Stage 5 renal failure (Sarnak *et al.*, 2003). Late diagnosis may be attributed to the fact that kidney disease progression is frequently asymptomatic.

Table 1.2. Prognosis of CKD by GFR and albuminuria categories

				Persistent albuminuria categories		
				Description and range		
				A1	A2	A3
				Normal to mildly increased	Moderately increased	Severely increased
				<30 mg/g	30-300 mg/g	>300 mg/g
eGFR categories (ml/min/1.73 m²)	G1	Normal or high	≥90			
	G2	Mildly decreased	60-89			
	G3a	Mildly to moderately decreased	45-59			
	G3b	Moderately to severely decreased	30-44			
	G4	Severely decreased	15-29			
	G5	Kidney failure	<15			

Green: low risk; Yellow: moderately increased risk; Orange: high risk; Red, very high risk

Adapted from: (KDIGO, 2013).

Lack of awareness of CKD, by both patients and physicians, appears to be a global phenomenon (Stevens *et al.*, 2005; Minutolo *et al.*, 2008). This can result in delayed diagnosis and therefore significant adverse outcomes for the patients. The AusDiab Kidney Study examining 11,247 Australians revealed approximately 16% of those studied had at least one indicator of kidney damage (proteinuria, hematuria and/or reduced GFR) (Chadban *et al.*, 2003). Although knowledge of renal impairment was not examined in this study, approximately 50% of patients had hypertension or diabetes mellitus but were unaware of their diagnosis. Systematic screening for CKD is not widely practiced in Australia, as it is thought to be ineffective and costly unless directed towards high-risk groups (Boulware *et al.*, 2003). Similarly, a study of almost half a million people in Taiwan revealed 12% of the population show evidence of CKD but only 3% of these patients were aware (Wen *et al.*, 2008). A study in Guangzhou in southern China revealed 12.1% present with evidence of kidney damage, but only 9.6% of patients aware (Chen *et al.*, 2009). However, urinalysis is more common in Japan and has successfully been used for early detection of CKD (Yamagata *et al.*, 2002). Initiatives have arisen worldwide to increase kidney awareness, most notably the World Kidney Day campaign, and although these have had a positive impact (Chin *et al.*, 2010), the rates of CKD are still increasing every year (Atkins, 2005). Early recognition of declining renal function is vital as lifestyle interventions and treatment of comorbid conditions (hypertension and/or diabetes) can dramatically slow the progression to renal failure, or at least facilitate a smoother transition to dialysis or transplant. Furthermore, CKD is rarely considered in young people but earlier diagnosis of mild renal dysfunction in early life may significantly reduce rates of CKD and end-stage renal disease.

1.4 Associations between CKD and CVD

Individuals with CKD are in the highest risk group in the population for cardiovascular events. Patients with low GFR and albuminuria are more likely to develop CVD, and cardiovascular mortality is 10 to 30 times higher in patients with end-stage kidney disease (controlled for age, ethnicity and sex) (Foley *et al.*, 1998). Furthermore, patients on dialysis with declining renal function (Foley *et al.*, 1995; Herzog *et al.*, 1998) or kidney transplant recipients (Ojo *et al.*, 2000) are more likely to experience a cardiovascular event than the general population. Care for advanced stages of chronic kidney disease requires large expenditure, which is prohibitive in some parts of the poorer parts of the world. Consequently, prevention and/or early detection of chronic kidney disease are strongly desirable for the individual, but also to reduce cost of care and limit the burden on health services. As will be discussed in Section 1.11, congenital alterations to kidney structure may underlie the pathophysiology of CKD and CVD.

1.5 Developmental Origins of Health and Disease

In 1986, a team of scientists led by David Barker described an association between high infant mortality and CVD-related deaths in specific locations in the United Kingdom. The geographical locations with the highest rates of infant mortality and CVD were also lower-income (Barker & Osmond, 1986). Further research showed that low body weight from birth until 1 year of age correlated with risk of hypertension and CVD, suggesting poor nutrition *in utero* or as a neonate increases susceptibility to CVD (Barker *et al.*, 1989). This provided the first epidemiological evidence that prenatal and neonatal environments can profoundly influence adult health outcomes, and became known as the ‘Barker Hypothesis’. Over subsequent decades of research, the Barker Hypothesis evolved to become the theory of the “Developmental Origins of Health and Disease” (DOHaD), or simply “developmental programming”.

1.6 Human evidence for developmental programming

Low birth weight, a surrogate marker of a poor in utero environment, has been directly associated with increased risk of NCDs including CVD, CKD, metabolic diseases, and mental disorders. Two powerful examples in human history are the Great Chinese Famine of 1959-1961 and the Dutch Winter Famine of 1944. Retrospective studies of women who were pregnant during the Dutch Winter Famine have shown their children were more likely to be born small (Lumey, 1992) and develop diseases in adulthood. These include elevated blood pressure (Painter *et al.*, 2006; Stein *et al.*, 2006), schizophrenia (Susser & Lin, 1992) and impaired glucose tolerance (Ravelli *et al.*, 1998; De Rooij *et al.*, 2006). Similarly, the Great Chinese Famine revealed babies were more likely to be born small, and develop chronic diseases including hypertension (Li *et al.*, 2011), hyperglycaemia and type 2 diabetes (Li *et al.*, 2010), and schizophrenia (St Clair *et al.*, 2005). Low birth weight followed by accelerated weight gain in early childhood has also been shown to aggravate risk of adult disease (Eriksson *et al.*, 2000; Eriksson *et al.*, 2001). These studies demonstrated that adverse maternal environment, particularly malnutrition and stress, could lead to reduced fetal growth and increased vulnerability to adult disease. Although low birth weight is the clinical surrogate marker of poor fetal development, programming of adult disease can occur across the birth weight range (for review, see Moritz *et al.*, 2009b) which suggests it is likely that failure to reach growth potential is more important.

1.7 Animal models of developmental programming of CKD

Epidemiological studies cannot elucidate the mechanisms involved in developmental programming of disease, therefore necessitating the use of animals to provide further insight. Early descriptive

studies relied on large animals such as the sheep, which readily allow *in utero* cannulation of the fetus for physiological measures. Recently the rat and mouse have become widely used in developmental programming studies. This is because physiological measurements are still possible (albeit restricted compared to the sheep), gestation time is short (19-22 days), average litter size is large, and tools for molecular work are more readily available than for larger animals. Animal models of developmental programming have predominantly used perturbations resulting in growth restriction, including maternal protein/calorie restriction, placental insufficiency and glucocorticoid exposure. These perturbations are designed to mimic common conditions affecting the mother and/or the fetus, and allow researchers to examine physiological consequences in offspring (including blood pressure, glucose regulation, heart function, vascular function and renal function) but also investigate the molecular mechanisms responsible for regulating disease outcomes. Increasingly other factors capable of programming disease outcomes have been identified, including reduced fetal oxygen supply (hypoxia) and maternal substance abuse (such as alcohol, tobacco, nicotine and cocaine).

The following sections will discuss studies examining offspring outcomes following maternal undernutrition, excess glucocorticoid exposure and gestational hypoxia. Studies have identified that multiple body systems are affected by *in utero* perturbations (Gluckman & Hanson, 2006; Warner & Ozanne, 2010), but this thesis shall focus on the renal and cardiovascular systems. As discussed in detail later (section 1.11), the kidney seems to be particularly susceptible to prenatal insult. This may be due in part to the fact that all nephrons, the functional units of the kidney, are formed before birth in humans, and by the first week after birth in rodents. Notably many questions remain regarding the effect of gestational hypoxia on long-term adult health outcomes, particularly with regards to the kidney.

1.7.1 Suboptimal maternal nutrition

Many animal models of programmed disease have utilized global calorie restriction, protein deficient diets, or diets lacking particular nutrients to demonstrate that poor maternal nutrition can result in impaired nephrogenesis and hypertension in offspring. Such studies have been extensively discussed in earlier reviews (Bagby, 2007; Moritz *et al.*, 2008a). In summary, studies in the rat have demonstrated that protein restriction (9% casein diet compared to 18%) can regulate nephron number depending on the timing and severity of the exposure as well as the sex of the animal. When rats were protein restricted in just the first week of pregnancy, no effect on nephron development was observed at any age. In contrast, when rats were exposed to a low protein diet

through gestation or through the second or third week of pregnancy, nephron number was reduced at 4 weeks of age at which time blood pressure was increased and glomerular filtration rate unaffected (Langley-Evans *et al.*, 1999). A similar study demonstrated that protein restriction throughout gestation reduced birth weight, reduced adult nephron number and glomerular filtration rate, and increased blood pressure (Woods *et al.*, 2001; Woods *et al.*, 2004). These outcomes were at least in part dependent upon the sex of offspring. In female offspring, a more severe protein restriction (5% casein diet) was required to program hypertension (Woods *et al.*, 2004; Woods *et al.*, 2005). In addition, the postnatal diet influenced long-term outcomes as male rats exposed to a low protein diet throughout pregnancy and then maintained on a low protein diet throughout life did not develop hypertension despite a nephron deficit and reduced GFR (Hoppe *et al.*, 2007a; Hoppe *et al.*, 2007b). A number of studies have shown a maternal low protein diet throughout pregnancy results in offspring with altered electrolyte handling. This includes increased sodium excretion, which was associated with a decrease in expression and activity of the Na⁺,K⁺-ATPase pump, in the collecting ducts (Alwaseel & Ashton, 2009). The authors found that the renal sodium loss resulted in increased sodium appetite, suggesting that the increased salt (and thus food intake) drove accelerated growth and increased blood pressure (Alwaseel *et al.*, 2012).

Overnutrition and/or maternal obesity have been shown to program for disease outcomes in multiple animal models. Worldwide, 1.4 billion people are overweight or obese (World Health Organisation, 2012), and the prevalence rates during pregnancy are thought to be approximately 40% in Western nations (Athukorala *et al.*, 2010). While maternal obesity has been long associated with increased birth weight, low birth weight is an equally common outcome (Blackmore & Ozanne, 2013). This U-shaped association suggests that the programming of disease outcomes by maternal obesity is complex. With respect to the programming of CKD, there are clear links between obesity, renal function, and cardiovascular disease in adults, with obesity being the greatest risk factor for CKD (Wickman & Kramer, 2013). Models of maternal overnutrition and/or obesity usually include feeding rodents a high fat or a high fat/high carbohydrate diet prior to pregnancy to induce an obesogenic state, although many of these may not mimic aspects of human obesity. Relatively short-term exposure of rats to a high fat diet (for 10 days prior to pregnancy until the end of lactation) has been shown to result in female specific hypertension at 12 months in association with normal nephron endowment but reduced renal renin and Na⁺,K⁺-ATPase activity (Armitage *et al.*, 2005). Several rodent studies have taken a longer-term approach to determine the effects of overnutrition prior to, during gestation and during lactation on long-term kidney health. Feeding rats a high fat/high fructose diet from 6 weeks prior to mating, throughout pregnancy and subsequent lactation, resulted in offspring that developed albuminuria, which was exacerbated by

postnatal overnutrition causing tubulointerstitial fibrosis and increased TGF- β expression (Jackson *et al.*, 2012). In a separate study, inducing obesity in rats 5 weeks prior to mating results in the programming of increased adiposity in offspring, hyperleptinemia and hypertension in offspring in association with increased renal norepinephrine and increased renal renin expression (Samuelsson *et al.*, 2010).

In many such studies, it is unclear as to whether nutrient excess or maternal obesity itself is regulating kidney development. An interesting observation is that excess glucose levels, either caused by simple glucose infusion during nephrogenesis or beta cell destruction using streptozotocin, reduces nephron number in rats (Amri *et al.*, 1999). Similarly, streptozotocin-induced maternal diabetes in mice results in offspring hypertension in association with glomerular hypertrophy, increased extracellular matrix accumulation, as well as increased expression of components of the renin-angiotensin system and fibrosis genes (Chen *et al.*, 2010). Additional studies have suggested that changes in the hormonal profile associated with increased food intake can lead to programming of disease outcomes. Rabbits exposed to a high fat diet during pregnancy deliver offspring who later develop stress-induced hypertension, increased heart rate, and increased renal sympathetic nerve activity in association with ghrelin and leptin resistance (Prior *et al.*, 2014). While it is clear that calorie excess results in disturbed fetal development and long-term disease outcomes, it is interesting to note that foods rich in calories are often poor in micronutrient levels.

In addition to global undernutrition, an estimated 2 billion people in the world suffer from at least one type of micronutrient deficiency (World Health Organisation, 2001). These deficiencies can occur in well-fed women and may include, but are not limited to, iron, zinc, vitamin A, and vitamin D deficiencies. Outcomes range from poor pregnancy outcomes, increased risk of postnatal morbidity and mortality, and impaired physical and cognitive abilities. The World Health Organisation (2001) reports that iron deficiency is the most common, and estimates suggest that nearly one in two women in developing countries is iron deficient both before and during pregnancy, highlighting the importance of considering both the pre-/periconceptual period and the prenatal period in the context of developmental programming. Rodent models of maternal iron and vitamin A deficiencies in utero have shown a reduction in nephron endowment (Lelièvre-Pégorier *et al.*, 1998; Lewis *et al.*, 2002; Tomat *et al.*, 2008), and maternal anaemia has been shown to result in increased blood pressure in adult offspring (Crowe *et al.*, 1995). A comprehensive study of renal function in male rat offspring born to zinc-restricted mothers demonstrated reduced GFR and proteinuria, which was associated with increased systolic blood pressure (Tomat *et al.*, 2008). An emerging area of great interest is the long-term effects of maternal vitamin D deficiency. A model

of vitamin D deficiency during pregnancy in rats has reported a 20% increase in nephron number in offspring kidneys, with an overall decrease in size of the renal corpuscle (Maka *et al.*, 2008). Whether increased nephron endowment confers an advantage or disadvantage is unknown, as the necessary functional studies have not yet been performed.

1.7.2 Fetal glucocorticoid exposure

A common maternal perturbation known to occur during pregnancy is that of increased glucocorticoid exposure. Maternal glucocorticoid administration during pregnancy is standard clinical practice for women at risk of preterm delivery. Additionally, naturally synthesized glucocorticoids (predominantly cortisol in the human and sheep and corticosterone in the rodent) are elevated in times of stress. Many of the animal models used to explore the mechanisms of developmental programming are likely to include a maternal stress component. Whilst the placenta is thought to inactivate a significant proportion of maternal glucocorticoids via the actions of the enzyme 11 beta hydroxysteroid dehydrogenase type II (11BHSD2), it is now recognized that this system has distinct limitations and in times of maternal stress, the fetus is also likely to be exposed to elevated glucocorticoid concentrations. There is considerable literature to support a role for elevated glucocorticoids in altering renal development prenatally as well as inducing long-term renal pathologies in offspring. The majority of this research has been performed using synthetic glucocorticoids such as betamethasone or dexamethasone in sheep and rodent models. Studies in sheep (term = 150 days) demonstrated that maternal administration of dexamethasone at a dose of 0.48 mg/h for 48 h during early nephron endowment, increased glomerular volume, enlarged and dilated proximal tubules, and tubulointerstitial and vascular periadventitial fibrosis at 7 years of age (Wintour *et al.*, 2003). These renal pathologies are likely to have contributed toward the observed hypertension in these animals. More recent studies have shown that betamethasone administration in mid-pregnancy (0.17 mg/kg/day on days 80/81) induces a 26% nephron deficit in males and females and reduced GFR in males. These sheep also developed hypertension, but there was no correlation between nephron number and blood pressure on an individual animal level suggesting that while nephron number may have contributed to the observed hypertension, additional factors may have been involved (Zhang *et al.*, 2010). When betamethasone was administered in late pregnancy in the sheep (0.5 mg/kg on days 104, 111, and 118), kidney weight was temporarily reduced at day 116 and 122 but was of normal size thereafter (Li *et al.*, 2013). Dexamethasone administration during mid-gestation in the spiny mouse also reduced nephron number, and this was associated with changes in mRNA expression of genes that regulate kidney development. Although offspring did not have alterations in blood pressure at 20 weeks of age, they had elevations in heart rate after surgical stress suggesting programming of cardiovascular responses to stress (Dickinson

et al., 2007). Other studies have demonstrated that dexamethasone can also reduce nephron endowment and lead to hypertension in rats (Ortiz *et al.*, 2003) and mice (O'Sullivan *et al.*, 2013), although outcomes were dependent upon the sex of the offspring, the timing of exposure, and the dose used.

While less well characterized, sheep and rodent studies have also demonstrated the effects of endogenous glucocorticoids on the developing kidney. Administration of cortisol (5 mg/h) for 48 h from day 26 of gestation in the sheep induced a greater nephron deficit (40%) than did maternal dexamethasone exposure (0.48 mg/h, 25%) when assessed at day 140 of gestation (Moritz *et al.*, 2011). Offspring exposed to either glucocorticoid were programmed to have altered mRNA levels of genes that regulate sodium transport. Furthermore, mean glomerular volume was increased by maternal cortisol exposure but was not affected by maternal dexamethasone exposure, and blood pressure was elevated in four- to five-year-old female sheep in cortisol-exposed offspring (Moritz *et al.*, 2011). More recently, corticosterone administered to rats has been shown to increase mean arterial pressure, reduce nephron number, and alter kidney gene expression including components of the renin-angiotensin system (discussed in detail below) (Singh *et al.*, 2007). These studies demonstrate that both natural and synthetic glucocorticoids can severely impair renal development and contribute to programming of hypertension and renal dysfunction.

1.7.3 Uteroplacental insufficiency

Inadequate blood supply to the fetus, as occurs with uteroplacental insufficiency, is the most common cause of fetal growth restriction in the Western world and results in insufficient nutrient and oxygen supply to the developing fetus. This has been modelled in a number of experimental studies. In the rat, uteroplacental insufficiency can be induced by ligation of the uterine arteries and/or veins. If the ligation occurs around day 14 in the rat, the dam develops characteristics of preeclampsia including late-gestation hypertension and proteinuria (Li *et al.*, 2012). If performed at day 18 of pregnancy, the model results in late-gestation growth restriction and programming of a number of sex-specific deficits including a reduction in nephron endowment (both males and females), increases in blood pressure (in male offspring) (Wlodek *et al.*, 2008), and increases in serum creatinine (in aged females) (Moritz *et al.*, 2009a). Interestingly, the nephron deficit and hypertension in male offspring could be ameliorated by cross-fostering growth-restricted pups onto a control dam on day 1 of life (Wlodek *et al.*, 2007), suggesting improved nutrition can stimulate the late stages of nephrogenesis. Whilst this would not be an effective strategy to improve nephron endowment in a growth-restricted term infant where nephrogenesis is likely to be complete, it is

relevant to the treatment and care of premature babies where nephrogenesis is ongoing. Other models of uteroplacental insufficiency have been developed in the sheep where removal of placentation sites or injection of microspheres limits blood supply to the fetus. This has been shown to result in fetal growth restriction and a decrease in nephron number in late gestation (Zohdi *et al.*, 2007).

1.8 Hypoxia during gestation

An adequate oxygen supply throughout pregnancy is vital for optimal fetal development. Notably, the fetus develops under conditions of relative hypoxia compared with the adult, leading Sir Joseph Barcroft, a pioneering physiologist of Cambridge University, to describe fetal life as ‘living on Mount Everest’. However, further reductions in fetal oxygenation initiate a range of protective mechanisms in the fetus in order to maximise survival and growth of critical organs. This may be beneficial for short-term survival, however suboptimal growth of organs may predispose offspring to adverse health outcomes in later life.

Normal fetal blood oxygenation is achieved through the uteroplacental and umbilical circulations. Poor fetal underoxygenation can arise through a number of mechanisms, which Kingdom and Kaufmann (1997) have broadly classified into 3 major categories:

1. Preplacental hypoxia, where oxygen content in the maternal blood is reduced and in turn leads to hypoxia of the placenta and fetus. This may be due to high-altitude living, maternal smoking, maternal anaemia and pre-existing maternal cardiovascular conditions such as pulmonary hypertension and congenital heart disease.
2. Uteroplacental hypoxia, where poor placentation leads to a hypoxic placenta and in turn, fetal hypoxia. This occurs without any maternal under-oxygenation, and can be due to occlusion of uteroplacental arterioles or failed trophoblast invasion.
3. Postplacental hypoxia, where impairment of fetoplacental perfusion leads to fetal hypoxia, without hypoxia of the mother or placenta.

Additionally, birth asphyxia is a common event that arises from complications during labour and delivery. This may cause hypoxic ischaemic organ damage, which has a high rate neonatal mortality, and for those infants who survive, a high rate of severe morbidity (Low, 2004a). Major causes of fetal hypoxia will be discussed in detail further on. Fetal hypoxia can be further categorised by duration of the hypoxic episode, with acute hypoxia defined as episodes of reduced

fetal hypoxia lasting minutes, and chronic hypoxia considered to last hours, days or weeks (Giussani *et al.*, 2016; Morrison, 2008).

1.8.1 Acute hypoxia

The supply of oxygen is plentiful outside the womb, however fetal oxygen supply is primarily constrained by the placenta. Consequently, the cardiovascular system, rather than the ventilator system, responds to hypoxic episodes in the fetus. Acute episodes of hypoxia are associated with parturition, caused by uterine contractions or umbilical cord compression during prolonged labour (Huch *et al.*, 1977). Antepartum fetal asphyxia contributes to intrauterine growth restriction and prevalence of stillbirths (Low, 2004b). These hypoxic events are common, and consequently the fetus has unique cardiovascular responses to acute hypoxia to increase the chance of survival. The primary defence mechanism to hypoxia involves the redistribution of cardiac output away from peripheral vascular beds to preferentially perfuse the brain, heart and adrenals. This response involves detection of low oxygen partial pressures by the carotid body of chemoreceptors, triggering the release of vasoconstrictor agents into the fetal circulation including vasopressin (Rurak, 1978), catecholamines (Cohen *et al.*, 1982) and renin (Robillard *et al.*, 1981). Local vasodilators such as nitric oxide and adenosine increase blood flow to the cerebral, myocardial and adrenal circulations whilst sympathetic activation of peripheral vasoconstriction reduces blood flow to the peripheral, gastrointestinal and renal circulations (Robillard *et al.*, 1981; Iwamoto *et al.*, 1983; Kamitomo *et al.*, 1993). Fetal haemoglobin has greater oxygen affinity relative to adult haemoglobin, and fetal shunts such as the *ductus venosus* and *ductus arteriosus* ensure blood is preferentially distributed to the heart and brain during fetal distress (Rudolph & Heymann, 1968; Edelstone *et al.*, 1980; Barcroft *et al.*, 1940). These fetal defence mechanisms to hypoxia can allow the fetus to tolerate lower oxygen tensions in the short term and maximise chance of survival.

1.8.2 Chronic hypoxia

Chronic hypoxia, lasting weeks to months, is encountered clinically due to placental complications including placental insufficiency and preeclampsia. In addition, other medical conditions including maternal haematological and cardiovascular disorders or environmental factors which induce hypobaric hypoxia (living at high altitudes) can affect oxygen transfer from the mother to the fetus (Hutter *et al.*, 2010). Maternal hypoxia introduces an additional layer of complexity to the fetal hypoxic response, as the placenta is required to adapt to maximise oxygen transfer to the fetus (Sulyok *et al.*, 1979). Studies have demonstrated that redistribution of fetal cardiac output, initiated in response to acute hypoxia, is maintained in chronic hypoxia. Given oxygen availability is crucial

for organogenesis, a constant state of relative hypoxia in developing peripheral tissues such as the kidneys can have tremendous consequences for the fetus.

A common finding in pregnancies complicated by hypoxia is fetal growth restriction and subsequent low birth weight. Table 1.3 displays a range of human and animal studies that focus on the effect of maternal hypoxia on growth as well as metabolic, cardiovascular and renal outcomes in offspring, both in fetal and adult life. Notably, the cardiovascular and metabolic outcomes following fetal hypoxia have been well-characterised in animal models, particularly the rodent; however, studies examining the impact of prenatal hypoxia on nephron endowment and predisposition to kidney disease are relatively scarce. These outcomes will be discussed in detail in Section 1.9. The rat model of late-gestational hypoxia is common and allows for extensive research into pathophysiological changes in the cardiovascular system. The mouse model is less common, possibly due to increased difficulty of measuring blood pressure and renal function. However, the ability to combine the extensive array of murine molecular tools with physiological measurements suggests the mouse model is relatively underutilised. Regardless of the animal model used, it is clear that intrauterine growth restriction and subsequent birth weight is a common thread connecting these hypoxia models.

The following section will discuss several common causes of gestational hypoxia in the human population.

1.8.3 High altitude

An estimated 140 million persons worldwide live permanently at high altitude, defined as elevations above 2500 m, as this is the elevation at which haemoglobin oxygen saturation declines in most individuals (Hornbein & Schoene, 2001). Many more travellers visit high-altitude locations each year. Barometric pressure and absolute concentration of oxygen decline with increasing altitude. For example, at altitudes of 4000 m, typical of the Tibetan Plateau, oxygen concentration is only 60% of the oxygen available at sea level, and at 5380 m (Everest Base Camp), oxygen concentration is only 50% of the oxygen available at sea level. For every 1000-meter elevation in altitude, average birth weight declines by 100 grams (Jensen *et al.*, 1999; Giussani *et al.*, 2001). Furthermore, a study on fetal biometry at high altitude (4300 m) compared to sea level in Peru has shown that chronically hypoxemic fetuses slow growth between gestational week 25 to 31, a time in normal pregnancies at which fetal growth increases exponentially (Krampl *et al.*, 2000). Most high altitude populations are impoverished; however these findings may be complicated by economic

status. A study comparing wealthy and impoverished communities in high altitude (La Paz, 3649 m above sea level) and low altitude (437 m above sea level) localities in Bolivia revealed birth weight was reduced in babies born at high altitude, regardless of economic status (Giussani *et al.*, 2001). Interestingly multigenerational high-altitude inhabitants have a reduced decline in birth weight compared to individuals recently relocating from low-altitude to high-altitude (Zamudio *et al.*, 1993; Moore *et al.*, 2001; Julian *et al.*, 2007); however, birth weight in these multigenerational high-altitude families still remains lower than those inhabiting low altitude environments. Indeed, indigenous high-altitude populations have well-described adaptations, particularly pulmonary and haematological factors, to chronic hypoxia exposure. Notably, greater uterine artery diameter and increased blood flow has been reported in Andean residents of La Paz, Bolivia (3600m) compared to European residents, resulting in increased uteroplacental oxygen delivery to the fetus near term (Wilson *et al.*, 2006). Increased uterine artery blood flow (Moore *et al.*, 2001) has also been observed in pregnant Tibetan women at high altitude, compared to Han women, native to China, living in Tibet. This increase in uteroplacental oxygen delivery may attenuate the decrease in birth weight typically observed in high altitude living. It has been suggested that the protective effect of high-altitude ancestry is related to genetics, rather than a consequence of being born and raised at high-altitude specifically (Moore, 2001). Differential regulation of the vasoconstrictor endothelin-1, a hypoxia-inducible factor (HIF) regulated gene, has been reported in pregnancies of Andean compared to European women at high altitude (Moore *et al.*, 2004). A further 40 genes within the HIF pathway have been identified through genomic analysis to be involved in natural selection to high altitude (Bigham *et al.*, 2009). It is unclear how many generations of high-altitude living confer these functional advantages, as there is controversy in the literature regarding how to assess duration of high altitude habitation (Moore *et al.*, 2001). Archaeological data suggests that Tibetan populations first habituated the Himalayas 25,000 years ago, whereas the Andes appears to be habituated only 11,000 years ago, and interestingly these two populations have well-characterised differences in physiological adaptations to high altitude (Bigham *et al.*, 2009). Tibetans, for example, have lower haemoglobin concentrations compared to Andeans, which may be a functional advantage to reduce blood viscosity (Bigham *et al.*, 2009). Differences in HIF-related genes have also been identified between Tibetan and Andean populations (Bigham *et al.*, 2013; Moore *et al.*, 2011). Whether these differences are due to duration of high-altitude living remain unclear.

Maternal ventilation increases by 25% during pregnancy due to progesterone and estrogen increasing hypoxic chemosensitivity, as well as a higher basal metabolic rate (Moore *et al.*, 2001; Moore *et al.*, 2011). At high altitude but not low altitude, this increase in ventilation is associated with increased maternal arterial oxygen saturation (SaO₂). Additionally, there is rise in plasma

volume but red blood cell volume does not increase to the same extent, meaning haemoglobin concentration declines in pregnancy (Moore *et al.*, 2011). In high-altitude pregnancies, haematocrit tends to be higher compared low-altitude pregnancies. Consequently, increased ventilation combined with elevated haematocrit means pregnancies at high-altitude can maintain arterial oxygen content (CaO_2) close to low-altitude values (Moore *et al.*, 2011). Given CaO_2 appears similar in low- and high-altitude pregnancies (Zamudio *et al.*, 1993; Moore *et al.*, 2001; Julian *et al.*, 2007), fetal growth restriction at high altitude is likely caused by other mechanisms. These may include reduced uterine artery blood flow, which has been observed in pregnant residents of high altitude (Zamudio *et al.*, 1995b), or placental adaptations to hypoxia and abnormal placental development (Kingdom & Kaufmann, 1997; Moore, 2003).

1.8.4 Maternal diseases and sleep disorders

Hypoxia is a central feature of many diseases such as anaemia and sleep disorders such as snoring and sleep apnoea. Maternal anaemia, as mentioned previously, is the result of low haemoglobin levels and is a prevalent nutritional deficiency problem in pregnancy women. Maternal anaemia is associated with intrauterine growth restriction, and is known to stimulate placental angiogenesis resulting in larger placentae, which is thought to be a compensatory adaptation to reduced fetal oxygenation (Godfrey *et al.*, 1991; Burton *et al.*, 1996; Kadyrov *et al.*, 1998; Kadyrov *et al.*, 2003). Newborns of anaemic mothers have increased risk of preterm delivery, preterm birth and poor perinatal outcomes (Lone *et al.*, 2004). Maternal asthma is the most common chronic respiratory disease, affecting 12% of pregnant Australian women (Wilson *et al.*, 2006). Asthma is thought to impair fetal oxygenation, and is associated with increased risk of stillbirth in the male fetus and poor fetal growth (Cousins, 1999; Clifton *et al.*, 2009). Obstructive sleep apnoea is characterised by periodic apnoea during sleep, leading to episodic hypoxia and hypercapnia and associated with loud frequent snoring. Five percent of the population is affected by obstructive sleep apnoea and the prevalence is thought to increase during pregnancy, although the exact rates are unclear (Domingo *et al.*). The frequency of snoring increases during the third trimester of pregnancy (Izci *et al.*, 2005), and maternal obesity is associated with significantly more sleep-related disorders (Maasilta *et al.*, 2001). This suggests that maternal sleep disorders leading to hypoxia may profoundly affect fetal development, particularly during late gestation. Indeed, obstructive sleep apnoea and other sleep-related disorders have been associated with intrauterine growth restriction, reduced birth weight and poor fetal outcomes (Sahin *et al.*, 2008; Fung *et al.*, 2013; Ding *et al.*, 2014). Together, these studies suggest that maternal hypoxia is strongly associated with adverse fetal outcomes. However,

these diseases are multi-factorial and therefore the use of animal models to examine the effects of hypoxia alone is desirable to elucidate the underlying mechanisms.

1.9 Common outcomes of hypoxia-exposed offspring

1.9.1 Effects of prenatal hypoxia on the placenta

The placenta plays a vital role in mediating fetal growth through oxygen and nutrient delivery. As such, small changes to placental function may have tremendous impact on fetal development. Oxygen tension has been shown to regulate several stages of placental development and the cell fate of placental cell types (Adelman *et al.*, 2000), with initial placental development beginning in a relatively hypoxic environment. Oxygen sensing molecules such as hypoxia inducible factor 1 alpha (HIF1a) transcriptionally regulate the expression of many genes including those involved in placental vascularization and nutrient transport (Feldser *et al.*, 1999). Metabolic demands of the fetus increase with advancing gestational age, therefore sufficient oxygen tension becomes increasingly important for optimal fetal growth. Thus, hypoxia is potentially most detrimental to the growing fetus when occurring in mid and late gestation (Hutter *et al.*, 2010).

Sheep studies have shown that a hypoxia-induced rise in maternal catecholamines, which can cross the placenta, as well as the production of prostaglandins in the placenta may in turn enter the fetal circulation and induce cardiovascular responses (Anderson *et al.*, 1989; Cowley, 1992). Although cardiac output is reduced, fetal haemoglobin synthesis is increased to maintain near-normal oxygen delivery (Iwamoto & Rudolph, 1985). As discussed earlier, fetal haemoglobin is able to bind with greater affinity to oxygen than the adult form, meaning the fetus has greater access to oxygen from the maternal blood stream. As such there is likely to be differential levels of hypoxia between the mother, placenta and fetus, with the fetus less affected.

During the course of my PhD, our group demonstrated that late-gestational hypoxia in the mouse altered placental vascular development, growth factor and nutrient transport expression, and placental glucocorticoid signalling in late-term mice (Cuffe *et al.*, 2014a). Maternal hypoxia led to fetal growth restriction and increased HIF1a staining of the placenta and fetal livers, suggesting maternal hypoxia did translate to fetal hypoxia in this model. Fetal sex determined the placental adaptations to hypoxia, with placental adaptations to low maternal oxygen tension most evident in female hypoxia-exposed fetuses. Furthermore the placental renin-angiotensin system, an important mediator of placental development, was perturbed by maternal hypoxia in a sexually dimorphic manner (Cuffe *et al.*, 2014b). This likely contributes to impaired placental vascularisation and fetal

growth restriction as previously reported (Cuffe *et al.*, 2014a). In these studies, maternal corticosterone, the endogenous rodent stress hormone, and plasma glucose were elevated, suggesting maternal hypoxia induces a stress response. Given excess glucocorticoid exposure and maternal hyperglycaemia are well described in the literature, it is likely that placental alterations and fetal growth restriction are not due solely to reduced oxygen tension.

1.9.2 Prenatal hypoxia and brain sparing

Growth restriction is frequently asymmetric, with preservation of brain size at the expense of the trunk size. This phenomenon is known as brain sparing and has been reported in pregnancies complicated by hypoxia (for review, see Giussani, 2016). A human epidemiological study of pregnancies at high altitude has shown that babies are born asymmetrically growth-restricted, being thin for their length but with an increased head circumference (Giussani *et al.*, 2001). Brain sparing has been observed in models of chronic hypoxia in the chick (Giussani *et al.*, 2007), rat (Williams *et al.*, 2005a), pig (Burke *et al.*, 2006) and sheep (Morrison, 2008; Allison *et al.*, 2016). Persistent redistribution of blood towards the brain at the expense of peripheral organs during chronic hypoxia may explain reduced nephron number in the kidney or reduced beta-cell mass in the pancreas following an in utero insult.

1.9.3 Effects of prenatal hypoxia on the heart

The cardiovascular health outcomes in hypoxia-exposed offspring have been well described in a variety of animal models, particularly in the rat (Table 1.3). Terminal differentiation of the heart is complete in early postnatal life and thus cardiac growth is primarily reliant on hypertrophic growth of individual cardiomyocytes. A reduction in cardiomyocyte number has been observed in fetal hypoxia (Bae *et al.*, 2003) as well as a range of other *in utero* perturbation models including maternal nutrient restriction (Corstius *et al.*, 2005), glucocorticoid exposure (Vries *et al.*, 2006) and placental restriction (Morrison *et al.*, 2007). It has been reported that chronic gestational hypoxia increases fetal cardiac afterload, which places strain on the heart and associated vessels. As a result, ventricular aortic thickening has been reported in chicks (Rouwet *et al.*, 2002; Salinas *et al.*, 2010) and rats exposed to chronic prenatal hypoxia (Camm *et al.*, 2010; Giussani *et al.*, 2012b).

In contrast, more severe hypoxia in mid-gestation (8% O₂; E11.5-12.5) in the mouse caused myocardial thinning due to decreased myocardial proliferation (Ream *et al.*, 2008). The hypoxic chick embryo has also shown myocardial thinning, as well as a reduction in cardiomyocyte number and compromised cardiac function (Tintu *et al.*, 2009). This cardiomyopathy persisted into

adulthood. Experiments have shown that prenatal hypoxia can impair cardiac performance. Notably, cardiac vulnerability to ischemia-reperfusion injury has been identified in numerous studies following prenatal hypoxia (Li *et al.*, 2003; Xue & Zhang, 2009; Rueda-Clausen *et al.*, 2010; Rueda-Clausen *et al.*, 2012a). Diastolic dysfunction and associated pathological myocardial fibrosis is another common feature in adult rats exposed to hypoxia *in utero* (Xu *et al.*, 2006; Rueda-Clausen *et al.*, 2008). Interestingly, assessment of blood pressure in rodents using radiotelemetry, the gold standard of blood pressure measurement, has not yet been performed in a model of prenatal hypoxia.

1.9.3 Effects of prenatal hypoxia on the vasculature

Alterations to vascular structure have also been highlighted as partial contributors to perturbed haemodynamic regulation in hypoxia-exposed animals (Rouwet *et al.*, 2002; Rueda-Clausen *et al.*, 2008; Camm *et al.*, 2010). Particularly, the vascular endothelium is susceptible to programming with a strong association observed between low birth weight babies and endothelial dysfunction in young adult life (Leeson *et al.*, 2001). Animal studies have also linked vascular endothelial dysfunction with hypoxia-associated growth restriction. In the chicken, exposure to chronic hypoxia *in ovo* reduced endothelium-dependent relaxation of arteries in fetal offspring (Villamor *et al.*, 2004). Furthermore, adult rat offspring exposed to prenatal hypoxia have presented with increased myogenic tone and impaired endothelial function in the peripheral arteries (Hemmings *et al.*, 2005; Williams *et al.*, 2005b). Endothelial dysfunction is a precursor to atherosclerosis, suggesting these offspring may be susceptible to atherosclerotic diseases late in life.

1.9.4 Effects of prenatal hypoxia on the kidney

As can be seen in Table 1.3 below, relatively little is known regarding long-term renal outcomes following prenatal hypoxia. Given the kidney is the major long-term regulator of blood pressure, impaired development can translate to poor renal and cardiovascular outcomes. A study in fetal lambs during acute bouts of maternal hypoxemia showed an increase in renal vascular resistance and a reduction in renal blood flow by 20% (Cohn *et al.*, 1974; Robillard *et al.*, 1981; Weismann & Robillard, 1988). Glomerular filtration rate was maintained suggesting renal vasoconstriction at the efferent arteriolar level (Robillard *et al.*, 1981). The reduction in renal blood flow increased the levels of plasma renal and vasopressin, leading to increased water reabsorption. Furthermore, the reduced renal blood flow reduced renal oxygen delivery and ultimately renal oxygen consumption. In addition, the renal metabolism of carbohydrate can be altered by changes in fetal oxygenation (Iwamoto & Rudolph, 1985). Lack of blood flow to the kidney during periods of fetal hypoxia may therefore compromise kidney development.

Renal damage following prenatal hypoxia has been reported in several animal models, although studies are relatively scarce compared to studies examining cardiovascular outcomes (see Table 1.3 below). Maternal hypoxia induced by a tracheostomy catheter in sheep at 116 days gestation showed increased expression of immune and inflammatory genes, indicative of ischaemic renal damage (Chang et al 2016). Decreased number of nephrons, the functional filtration units of the kidney, has been reported in several animal models of prenatal hypoxia. Rats exposed to prenatal hypoxia during the last third of pregnancy showed decreased nephron number in male and female offspring (Gonzalez-Rodriguez *et al.*, 2013). Contrary to current literature that states nephrogenesis is complete in early postnatal life, nephron number was shown to increase almost 2-fold from P7 to 3 months of age with a nephron deficit remaining in the hypoxia-exposed offspring (Gonzalez-Rodriguez *et al.*, 2013). However, the acid maceration technique was used to quantify nephron number, which is not as reliable as the physical-disector fractionator method, the current gold standard of glomerular number estimation (Cullen-McEwen *et al.*, 2012). In a recent study, midgestation, moderate hypoxia (E12.5, 12% maternal O₂) for 48 hours in the mouse caused fetal growth restriction, suppression of branching morphogenesis in the kidney and reduced nephron number (Wilkinson *et al.*, 2015). The same study also demonstrated that severe, short-term hypoxia (5.5-7.5% maternal O₂ for 10 h from E9.5-10.5) resulted in congenital abnormalities of the kidney and urinary tract. Delayed renal development in a mouse model of maternal cigarette smoke exposure has been reported, with fewer nephrons and evidence albuminuria in male offspring compared to non-exposed control offspring (Al-Odat *et al.*, 2014). A model of birth asphyxia in the spiny mouse revealed signs of acute kidney injury in offspring (Ellery *et al.*, 2013), however the long-term health outcomes of these offspring have not yet been described.

Together these studies demonstrate that the kidney is susceptible to a hypoxic insult during development. Furthermore, the timing, severity and nature of the hypoxic insult can influence renal outcomes. Investigation of the impact of prenatal hypoxia on renal impairments and long-term health is warranted, given the close relationship between CKD and CVD.

Table 1.3. A summary of fetal and postnatal growth and metabolic, cardiovascular and renal outcomes in animal studies of hypoxia.

Study	Species	Gestational duration	Outcome	Citing
GROWTH AND METABOLIC DISEASE				
High altitude (4300 m)	Humans	Chronic	Slowed growth from gestational week 25 to 31	(Weber, 1989)
High altitude (>3500 m)	Humans	Chronic	LBW Increased head circumference:birth weight ratio	(Giussani <i>et al.</i> , 2001)
Hypoxic chamber (13-14% O ₂)	Rat	Day 14-21	Asymmetric IUGR Increased IGFBP-1 and -2	(Tapanainen <i>et al.</i> , 1994)
Hypoxic chamber (12% O ₂)	Rat	Day 15-20	IUGR Fetal hypoxia and acidosis Fetal lactate accumulation Increased glucose utilisation of specific fetal tissues	(Werns <i>et al.</i> , 1989)
Hypoxic chamber (14% O ₂)	Rat	Day 18-21	IUGR IUGR prevented by maternal endothelin receptor A antagonism	(Deane & Masson, 1951)
Hypoxic chamber (10% O ₂)	Rat	Day 5 –birth	LBW Impaired circadian rhythms	(Gezmish <i>et al.</i> , 2010)
Hypoxic chamber (11.5% O ₂)	Rat	Day 15-21	IUGR Increased susceptibility to high-fat diet-induced metabolic syndrome	(Ojeda <i>et al.</i> , 2007b; Rueda-Clausen <i>et al.</i> , 2008)
Incubator (14% O ₂)	Chicken	Day 0-hatch Day 0-10 Day 10-hatch	IUGR reversed by restoration of normoxia mid-incubation	(Zambrano <i>et al.</i> , 2005)

Study	Species	Gestational duration	Outcome	Citing
CARDIOVASCULAR				
Hypoxic chamber	Mouse	Variable	Embryonic lethality IUGR Ventricular dilation Myocardial hypoplasia	(Ream <i>et al.</i> , 2008)
Hypoxic chamber (12% O ₂)	Rat	Day 15-21	Asymmetric growth restriction Regional changes to fetal vascular function	(Ojeda <i>et al.</i> , 2007a)
Hypoxic chamber	Rat	Day 15-20	IUGR Altered cardiac structure Altered vascular reactivity Insulin resistance markers	(Camm <i>et al.</i> , 2010)
Hypoxic chamber	Rat	Day 15- 21	IUGR Altered cardiac structure Chronic cardiopulmonary dysfunction during ageing	(Rueda-Clausen <i>et al.</i> , 2008)
Hypoxic chamber (10.5% O ₂)	Rat	Day 15-21	Asymmetric IUGR Increased apoptosis in fetal heart	(Bae <i>et al.</i> , 2003)
Hypoxic chamber (12% O ₂)	Rat	Day 15-21	Impaired endothelium-dependent relaxation at 4mth Reduced NO mediation of endothelial function at 7mth	(Williams <i>et al.</i> , 2005b)
Hypoxic chamber (12% O ₂)	Rat	Day 15-21	Increased myogenic tone in aged male but not female offspring	(Hemmings <i>et al.</i> , 2005)
Hypoxic chamber (12% O ₂)	Rat	Day 15-21	Progressive cardiac remodelling Diastolic dysfunction Impaired post-ischemic recovery	(Xu <i>et al.</i> , 2006)
Hypoxic chamber (10.5% O ₂)	Rat	Day 15-21	Epigenetic programming of PKC ϵ gene expression in hearts	(Skarsgard <i>et al.</i> , 1997)
Hypoxic chamber (10% O ₂)	Rat	Day 15-20	Asymmetric IUGR Aortic thickening Altered aortic vascular reactivity	(Camm <i>et al.</i> , 2010)
High altitude (3820m)	Sheep	Day 30-135	Redistribution of fetal cardiac output to favour brain, heart and adrenal glands.	(Kamitomo <i>et al.</i> , 1993)
High altitude (3820m)	Sheep	Day 30-140	Decreased right ventricle contractility Altered cardiac contractile protein expression	(Low, 2004a)

Study	Species	Gestational duration	Outcome	Citing
RENAL				
Birth asphyxia	Spiny mouse	Day 38 (Term ~39days)	Acute kidney injury 24h after birth Maternal creatine treatment prevents acute kidney injury	(Lueder <i>et al.</i> , 1995)
Hypoxic chamber (10.5% O ₂)	Rat	Day 15-21	LBW Reduced kidney weight Altered angiotensin-II receptor expression patterns Reduced nephron number	(Camm <i>et al.</i> , 2011)
High altitude	Sheep	Day 30 – birth	Renal tubular alterations Altered RAS expression	(Tazuke <i>et al.</i> , 1998)
Cigarette smoke exposure	Mouse	Throughout gestation and lactation	LBW Reduced kidney weight Reduced nephron number Increased urinary albumin:creatinine Increased renal oxidative stress	(Al-Odat <i>et al.</i> , 2014; Stangenberg <i>et al.</i> , 2015)

LBW: low birth weight. IUGR: Intrauterine growth restriction. IGFBP: insulin-like growth-factor binding protein. RAS: renin-angiotensin system. NO: nitric oxide

1.10 Mechanisms of hypoxia-induced damage and avenues for intervention

Two inter-related hypotheses concerning prenatal hypoxia-induced origins of cardiovascular disease have been put forward: (1) oxidative stress underlies the development of cardiovascular disease in offspring prenatally exposed to hypoxia and (2) these changes can be ameliorated using maternal antioxidant therapy (Giussani *et al.*, 2012). Hypoxia is a potent stimulus for the generation of reactive oxygen species (ROS), with excess ROS generation and/or a decline in the body's antioxidant capabilities leading to cellular oxidative stress (Halliwell & Gutteridge, 1999). Pregnancies at high altitude have associated reduced partial pressure of oxygen with reduced activity of placental antioxidant enzymes as well as increased nitrate stress (Zamudio *et al.*, 2007; Parraguez *et al.*, 2011). Additionally, Giussani and colleagues (2012) have reported increased levels of maternal circulating and placental molecular indices of oxidative stress in a rat model of chronic gestational hypoxia (13% O₂; E6-E20). Increased cardiac oxidative stress has also been reported in the rat (11.5% O₂; E15-E21) (Rueda-Clausen *et al.*, 2012b) and guinea pigs (10.5% O₂; 14 d before term [term = 65 d]) (Evans *et al.*, 2012) exposed to prenatal hypoxia. Increased renal oxidative stress has also been reported in chronic cigarette exposure *in utero* (Stangenberg *et al.*, 2015).

Recent work in animal models suggests that deficits associated with developmental programming may be ameliorated, or in some cases reversed, by nutritional or pharmacological interventions during critical windows of development. In line with the oxidative stress hypothesis detailed above, antioxidant therapies are becoming increasingly common and range from maternal Vitamin C, melatonin and creatine supplementation. Maternal supplementation with the antioxidant Vitamin C has been shown to prevent developmental programming of cardiovascular dysfunction in rats (Giussani *et al.*, 2012a). Melatonin, a hormone produced from the pineal gland, has been used as a supplement in compromised pregnancy due to its actions as an antioxidant and free radical scavenger. It has been shown to successfully to attenuate neonatal ischaemic brain injury in rats as well as provide partial neural protection after asphyxia in preterm fetal sheep (Zamudio *et al.*, 1995a; Palmer *et al.*, 1999). More recently, melatonin has been used as a preventative measure in a model of prenatal dexamethasone (Krampl *et al.*, 2000), where melatonin therapy prevented the reduction in nephron number and as well as the associated increase in blood pressure in adult offspring.

Supplementation of the maternal diet with creatine has been highlighted as another potential prophylactic therapy for pregnancies at risk of fetal hypoxia. Low oxygen levels reduce the capacity to produce ATP, leading to a reliance on anaerobic respiration and ultimately the production of

reactive oxygen species. Creatine kinase, however, can phosphorylate ADP to ATP in hypoxic conditions, without the production of toxic by-products (Wallimann *et al.*, 1992). Creatine can also act as a direct antioxidant against free radicals and reactive oxygen species (Lawler *et al.*, 2002). This process can be enhanced by increasing the intracellular pools of creatine and phosphocreatine. Hence, maternal creatine supplementation when inspired oxygen levels are low may increase cellular energy reserves and allow normal ATP turnover. Creatine pretreatment in the spiny mouse has been shown to improve neonatal survival, ameliorate brain and kidney damage and improve postnatal growth following a bout of birth asphyxia (Ireland *et al.*, 2008; Cannata *et al.*, 2010; Ireland *et al.*, 2011). More recently, a natural polyphenol found in red grape skins known as resveratrol has been used as a therapy to prevent adverse cardiovascular outcomes associated with prenatal hypoxia. Resveratrol has been shown to have anti-inflammatory actions as well as mitigating oxidative stress, and has been successfully used to improve recovery from cardiac ischemia/reperfusion injury which, as discussed above, is impaired in hypoxia-exposed rodents (Shah *et al.*, 2016).

1.11 Developmental programming of the kidney and renal dysfunction in offspring

Susceptibility to CKD is likely due, in part, to altered renal development. Nephrons, the functional filtration units of the kidney, are complex structures comprising of the glomerulus to filter blood and an associated renal tubule system where reabsorption and secretion of electrolytes and water occurs. The development of the mammalian kidney involves the formation of three excretory organs: the pronephros, mesonephros and metanephros (Moritz *et al.*, 2008a). The pronephros and mesonephros are transitory structures in development. The metanephros is the definitive kidney, beginning development during the fifth week of gestation in the humans. Metanephric kidney development is marked by the formulation of nephrons through a process termed *nephrogenesis*.

The mammalian metanephric kidney arises through reciprocal and sequential interactions between the ureteric bud (epithelial outgrowth from the nephric duct) and metanephric mesenchyme, both of which are derived from the intermediate mesoderm. The metanephric mesenchyme signals the ureteric bud to grow and branch to generate the collecting duct system. Simultaneously, nephrons develop from progenitor cells (also known as cap mesenchyme cells), which are a subset of the metanephric mesenchyme. This occurs by the ureteric bud tips signalling for proliferation of cap mesenchyme cells for the mesenchyme to aggregate to form a pretubular aggregate and mesenchymal-to-epithelial transition to form an epithelial renal vesicle. Polarised gene expression within the renal vesicle promotes distinct tubular segments to form (tubulogenesis) through folding,

elongation, segmentation and cellular differentiation. The nephron connects to the collecting ducts, formed from the Wolffian duct. Ureteric branching and nephron formation persists until postnatal day 3 (P3) in the mouse (Hartman *et al.*, 2007; Rumballe *et al.*, 2011). In contrast, nephrogenesis is complete by ~36 weeks gestation in humans; therefore, term babies are born with the final number of nephrons that will support them throughout their lifespan.

Surprisingly, there is a 10-fold range in normal nephron number in the human population, from 200,000 to 2 million (Luyckx *et al.*, 2013). Females have fewer nephrons per kidney than males (Nyengaard & Bendtsen, 1992), and ethnicity is associated with differences in nephron number (Hoy *et al.*, 1999; Hoy *et al.*, 2006; Hughson *et al.*, 2006). However, the reasons for this large variation in nephron number are largely unknown. It is likely that some variation can be explained by suboptimal development of the kidney *in utero*. Indeed, fetal growth is strongly correlated with nephron number, with an estimated increase of 250-,000-350,000 nephrons for every kilogram increase in birth weight (Hughson *et al.*, 2003). The importance of reduced nephron number will be discussed in detail in the following section (section 1.13).

There are major differences in the timing of nephrogenesis in other mammalian species, compared to humans (Figure 1.1). Many rodents (rats and mice) are altricial species and are therefore born with relatively immature kidneys. Nephrogenesis persists postnatally until ~7 days post-birth (Cebrian *et al.*, 2004; Hartman *et al.*, 2007) to yield ~14,000 nephrons in the mouse (Cullen-McEwen *et al.*, 2003; Hartman *et al.*, 2007; Walker *et al.*, 2012), and 8-11 days post-birth to yield ~30,000 nephrons in the rat (Cullen-McEwen *et al.*, 2011). In contrast to most rodents, the spiny mouse is relatively mature at birth, with nephrogenesis complete 2 days before birth (with a 40-day gestation) (Dickinson *et al.*, 2005). The sheep has a long gestational period, similar to humans, and also completes nephrogenesis before birth (Gimonet *et al.*, 1998; Wintour *et al.*, 2003). Consequently the sheep has been used many times to study how *in utero* insults affect nephrogenesis and ultimately final nephron endowment (Wintour *et al.*, 2003; Zohdi *et al.*, 2007; Moritz *et al.*, 2011).

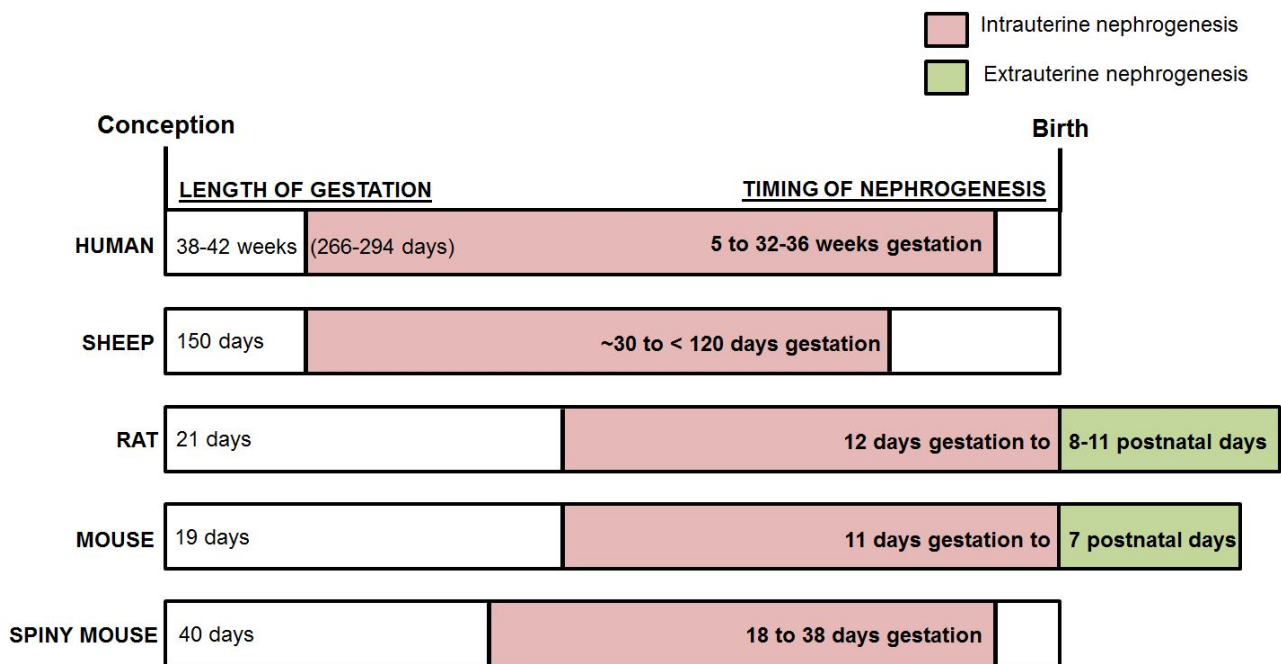


Figure 1.1. Comparative timeline of nephrogenesis in different species.

Coloured bars represent the percentage of gestation in which nephrogenesis (intrauterine: pink; extrauterine: green) occurs in different mammalian species. In the human (Hinchliffe *et al.*, 1991b), sheep (Gimonet *et al.*, 1998; Wintour *et al.*, 1999) and spiny mouse (Dickinson *et al.*, 2005), nephrogenesis is completed before birth. Nephrogenesis continues postnatally in the rat (Cullen-McEwen *et al.*, 2011) and mouse (Cebrian *et al.*, 2004; Hartman *et al.*, 2007). Figure adapted from (Cullen-McEwen *et al.*, 2016).

1.12 Postnatal development of the kidney

Upon birth, placental support is lost requiring the kidney to perform the infant's body fluid homeostasis. Increased renal blood flow and GFR cause the glomeruli, renal tubules and collecting duct system undergo a tremendous process of postnatal maturation (Arant, 1978). This is marked by hypertrophy of glomeruli, increased length and diameter of the proximal tubules and infolding of the apical and basolateral proximal tubule membranes to maximise reabsorptive area (Aperia & Larsson, 1979). There is also a marked increase in sodium channel and transporter expression along the nephron segments. At birth in the rodent and human, the renal papillary lobe(s) are short and underdeveloped; rapid elongation occurs during the first two weeks of life by extension of papillary tubules (Wilkinson *et al.*, 2012). Consequently, the fetal and early neonatal kidney produces hypotonic urine as there is limited ability to reabsorb sodium in the underdeveloped medulla and papillary structures. Full urine concentration capacity is achieved 12 months after birth in humans (Atiyeh *et al.*, 1996) following establishment of an osmotic gradient from the cortico-medullary boundary to the papillary tip by countercurrent multiplication (Layton *et al.*, 2009). All filtration units of the nephron drain through the collecting ducts of the papilla, which are responsible for the final control of water excretion and therefore urine concentration. This is achieved by the presence of principal cells in the collecting duct, which express aquaporin 2 (AQP2) and are the site of sodium reabsorption and aldosterone and vasopressin action. Very little is known about the development of the renal papilla in humans, and this therefore warrants investigation given reduced urine concentrating capacity is observed in CKD (Nieto *et al.*, 2008).

1.13 Low nephron number in developmental programming

The importance of nephron number, the functional filtration units of the kidney, was first proposed by Brenner who postulated that a low number of nephrons in the kidney is correlated with low birth weight and can increase the risk of hypertension and renal disease (Brenner *et al.*, 1988; Brenner & Chertow, 1994). The reduction in filtration surface area increases the filtered load placed upon each glomerulus of the nephron, leading to consequential glomerular hypertension and scarring. This feeds into a positive feedback loop, where hypertension is worsened by the progressive glomerular damage (Figure 1.2). A landmark study by Keller found that the number of glomeruli (nephrons) was lower in patients with hypertension than matched normotensive controls (Keller *et al.*, 2003). This was also shown in studies of children with unilateral renal agenesis (one kidney) of which 50% have reduced GFR and develop hypertension and albuminuria by the age of 18. Ethnicities with a predisposition to hypertension have on average fewer glomeruli but of greater glomerular volume (Schmidt *et al.*, 1992; Hughson *et al.*, 2003; Hughson *et al.*, 2006). The pathogenesis of essential

hypertension is closely related to renal haemodynamics and structure, with cross-transplantation experiments showing that hypertension develops in previously normotensive recipients that receive tissue from a hypertensive donor (Bianchi *et al.*, 1974; Dahl *et al.*, 1974; Curtis *et al.*, 1983; Rettig *et al.*, 1990).

THE BRENNER HYPOTHESIS

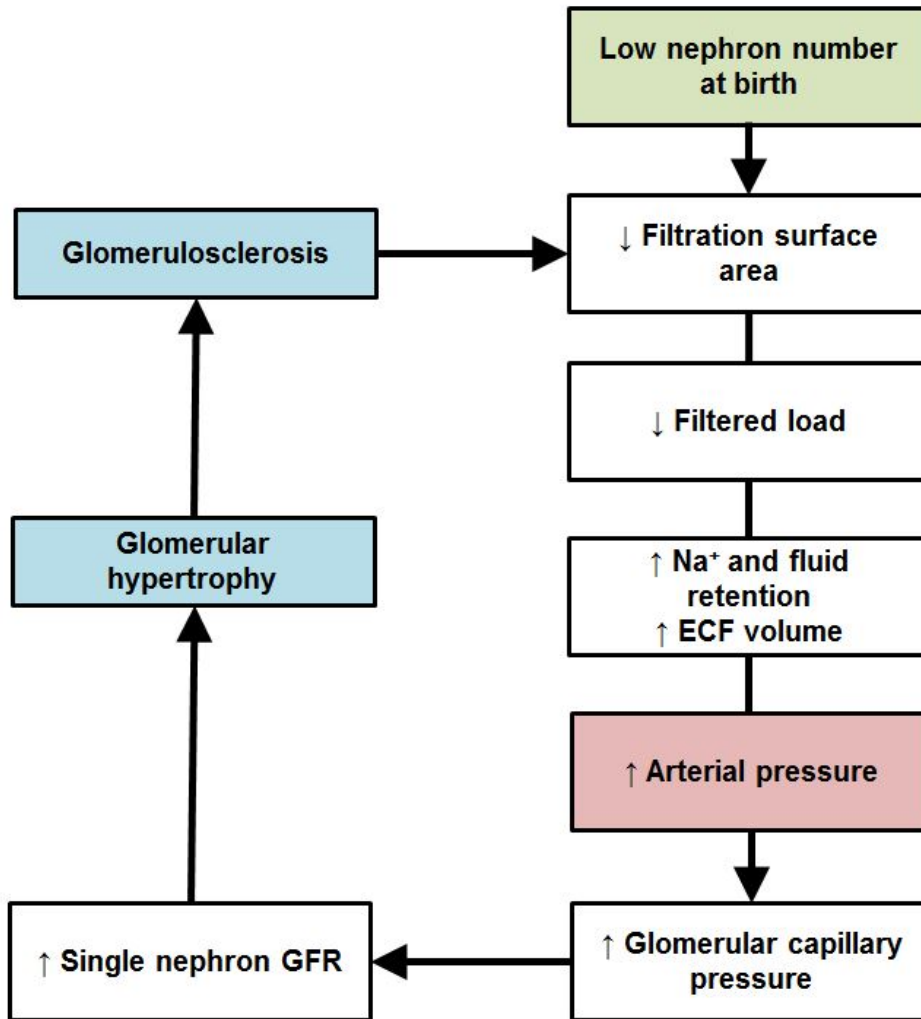


Figure 1.2. The Brenner Hypothesis depicting the mechanisms through which a congenital nephron deficit may contribute to hypertension and renal disease in adulthood.

Decreased filtration surface area, due to a nephron deficit or reduction in individual glomerular filtration surface area, leads to renal sodium (Na^+) retention, increased extracellular fluid (ECF) volume and thus increased arterial pressure. This results in increased single nephron glomerular filtration rate (GFR). Systemic hypertension promotes glomerular hypertrophy and eventual sclerosis, thereby further reducing functional filtration surface area.

Similarly, reduced fetal growth has been associated with low nephron number in a range of animal studies, however, it is important to note that a nephron deficit does not always lead to hypertension. Table 1.4 provides a brief summary of the outcomes recorded in a range of animal models. This is not a comprehensive list, but a selection to highlight the wide range of perturbations that affect kidney development. Species differences in the timing of nephrogenesis must be considered. In a species such as the sheep or spiny mouse, nephrogenesis is complete prior to birth as is the case with humans. However, nephrogenesis in the mouse and rat persists throughout early postnatal life.

Table 1.4. Birth weight and arterial pressure in animal models of reduced nephron endowment

Maternal Perturbation	Species	Sexes Studied	Fetal weight/Birth Weight	Reduction in Nephron Endowment	Functional Renal Outcomes	Change in Arterial Pressure
UNDERNUTRITION						
9% Casein diet (Langley-Evans <i>et al.</i> , 1999)	Rat	Pooled	↔	↓ 13%	↔ GFR	↑ 13 mmHg
8.5% Low protein diet (Woods <i>et al.</i> , 2004; Woods <i>et al.</i> , 2005)	Rat	Males Females	↓	↓ 25% males ↔ females	↓ GFR males ↔ females	↑ 10 mmHg ↔ females
50% Nutrient restriction (Alwasel & Ashton, 2009)	Sheep	Males	↔	↓ 11%	Impaired sodium handling	↑ 17 mmHg
OVERNUTRITION						
High fat/high fructose (Prior <i>et al.</i> , 2014)	Rat	Pooled	↑	–	Albuminuria	↑ 17 mmHg
MICRONUTRIENT DEFICIENCIES						
Iron deficiency (Lewis <i>et al.</i> , 2002)	Rat	Males Females	↓	↓	–	↑ 18 mmHg
Vitamin A deficiency (Lelièvre-Pégorier <i>et al.</i> , 1998)	Rat	Pooled	↔	↓ 20%	–	–
Zinc deficiency (Tomat <i>et al.</i> , 2008)	Rat	Males	↓	↓	↓ GFR Proteinuria	↑ SBP
Vitamin D deficiency (Maka <i>et al.</i> , 2008)	Rat	-	↔	↑ 20%	–	–
HYPOXIA						
Maternal hypoxia (Gonzalez-Rodriguez <i>et al.</i> , 2013)	Rat	Males Females	↓	↓ 25% males ↓ 52% females	–	–
Maternal hypoxia (Wilkinson <i>et al.</i> , 2015)	Mouse	Pooled	↓	↓	–	–
Cigarette smoke exposure (Al-Odat <i>et al.</i> , 2014)	Rat	Males	↔	↓	Albuminuria	–
Uteroplacental insufficiency (Wlodek <i>et al.</i> , 2008; Moritz <i>et al.</i> , 2009a)	Rat	Males Females	↓	↓	↑ plasma creatinine, aged females	↑ SBP in males
GLUCOCORTICOID EXPOSURE						
Dexamethasone (Wintour <i>et al.</i> , 2003)	Sheep	Females	↔	↓ 38%	–	↑ 10 mmHg
Betamethasone (Zhang <i>et al.</i> , 2010)	Sheep	Males Females	↔	↓ 26% males and females	↓ GFR in males	↑ 7-9 mmHg
Corticosterone (Singh <i>et al.</i> , 2007)	Rat	Males Females	↔	↓ 21% males ↓ 19% females	–	↑ 10 mmHg
Dexamethasone (Dickinson <i>et al.</i> , 2007)	Spiny mouse	Males Females	↔	↓ 13% males ↓ 17% females	–	↔
Corticosterone (O'Sullivan <i>et al.</i> , 2015)	Mouse	Males Females	↓	↓ 33% males ↓ 25% females	Albuminuria	↓ 10 mmHg
ETHANOL CONSUMPTION						
Intravenous ethanol infusion (Gray <i>et al.</i> , 2008)	Sheep	Pooled	↔	↓ 11%	–	–
Ethanol (gavage) (Gray <i>et al.</i> , 2010)	Rat	Males Females	↓	↓ 15% males ↓ 10% females	↑ GFR males ↓ GFR females Proteinuria	↑ 10%

Abbreviation: GFR, glomerular filtration rate.

1.13.1 Molecular mechanisms contributing to altered renal development

As the Brenner hypothesis suggests, a nephron deficit caused by a prenatal perturbation, combined with alterations in renal function, particularly sodium excretion, are likely to contribute to the adult disease outcomes. This leads to two important questions: firstly, what are the molecular pathways through which a prenatal perturbation can inhibit nephrogenesis; and secondly, what are the long-term “programmed” renal changes that result in altered function in the adult offspring? Below we shall focus our discussion on these questions with emphasis on the important role of factors controlling sodium homeostasis, that is, the renal sodium channels and the renal renin-angiotensin system. Figure 1.3 outlines the links between the disturbances in kidney development with impairments in offspring renal function that may ultimately contribute to chronic kidney disease. It must be recognised that nephron formation could be restricted at any stage of nephrogenesis: branching morphogenesis, condensation of the mesenchyme around the epithelium, mesenchymal-to-epithelial transition, or the cessation of nephrogenesis. Thus, maternal perturbations during particular “critical windows” of renal development may impact different stages of nephrogenesis, and of relevance to animal studies, this may occur at different stages of gestation (Figure 1.2 above).

There is a relative paucity of information concerning the mechanisms that result in disruptions to the fetal kidney following insult. Impaired branching morphogenesis has been reported in several studies of developmental programming. *In vitro* metanephric organ cultures have shown dexamethasone (Singh *et al.*, 2007), a synthetic glucocorticoid administered to pre-term infants to accelerate lung maturation, and ethanol (Gray *et al.*, 2012) directly inhibit branching morphogenesis. Reduced glomerular number was reported *in vivo models* glucocorticoid and alcohol exposure. Maternal dexamethasone treatment at midgestation in the spiny mouse led to increased mRNA expression of branching morphogenesis antagonists *Bmp4* and *Tgf- β 1* in the fetal kidneys and reduced nephron number (Dickinson *et al.*, 2007). Mid-gestational maternal corticosterone exposure in the rat was associated with changes in the renal renin-angiotensin (RAS) system, namely increased mRNA expression of angiotensin II receptors (*Agtr1a* and *Agtr2*) in kidneys from offspring at embryonic day 16 and postnatal day 30 (Singh *et al.*, 2007). These offspring had reduced nephron number and developed elevated blood pressure in adulthood. The role of the renal RAS will be discussed in detail further on (section 1.13.4). Similarly, maternal ethanol consumption during mid-gestation in the rat was associated with reduced expression of the branching morphogenesis gene *Gdnf* and its receptor, *c-Ret* (Gray *et al.*, 2010). Mid-gestational transient hypoxia (12% O₂, 48 h, 12.5-14.5) was shown to reduce ureteric branching and glomerular number in mouse offspring (Wilkinson *et al.*, 2015). This was driven by suppression of β -catenin

signalling, which contributes to branching morphogenesis, nephron induction, nephron elongation and medullary development (Park *et al.*, 2007; Bridgewater *et al.*, 2008; Marose *et al.*, 2008). Activation of apoptotic pathways in the developing kidney has been proposed as a contributing mechanism to low nephron endowment. This has been observed in a model of maternal low protein consumption in the rat (Welham *et al.*, 2002) and hypoxia (Xia *et al.*, 2015). Collectively, these suggest that a nephron deficit may be due to suppression of key genes in the nephrogenic pathway, and activation of apoptotic pathways. It is important to note that most of these studies have examined mRNA expression rather than protein, and many components of the nephrogenic process have not been detailed in full for each study. Therefore, a thorough examination into the mechanisms of reduced nephron endowment is warranted in the future.

1.13.2 Renal tubules

While much research has focused on glomerular (nephron) number in offspring following a prenatal perturbation, the importance of the renal tubules has received little acknowledgement. This is surprising as the renal tubules perform the bulk of fluid and electrolyte homeostasis in adulthood, and the remarkable compensatory capacity of the renal tubules has long been known. Nephrectomised patients who have lost ~50% of renal mass experience substantial hypertrophy of the remaining kidney. This is also observed in rodent and sheep models of nephrectomy. Compensatory growth has primarily been attributed to the proximal tubule, which is the major site of sodium reabsorption in the nephron, and secondly to the distal tubular segments. An early study reported hypertrophy and hyperplasia of proximal and distal tubular segments following uninephrectomy in the adult rat (Hayslett *et al.*, 1968), and a model of diabetic nephropathy in the rat also showed hypertrophy of the proximal and distal tubular segments (Nyengaard *et al.*, 1993). Reduction in renal mass as a result of uninephrectomy requires remaining nephrons to undergo significant increases in single nephron GFR (Aperia *et al.*, 1977). The outcomes of tubular hypertrophy are likely to maintain sodium homeostasis in response to the increase in GFR and increased tubular fluid delivery (Baum *et al.*, 2003). As such, an examination of tubular structure in a maternal programming model is needed to determine if, or indeed how, the kidney adapts to a significant reduction (albeit to a lesser extent than nephrectomy) in nephron number.

1.13.3 Sodium channels and transporters

The mammalian fetus has limited ability to reabsorb sodium in the kidney, leading to the production of hypotonic urine compared to the adult (Moritz *et al.*, 2008b). Postnatal maturation of the kidney is associated with marked expression of sodium channels and transporters to increase sodium

reabsorption. The predominant sodium transporter responsible for sodium balance is the sodium-hydrogen exchanger 3 (NHE3) expressed in the apical membrane and brush border of the proximal tubule and the thick ascending limb of Henle. NHE3 absorbs large amounts of sodium reabsorption in the kidney at high capacity, and performs the majority of HCO_3^- absorption. The electroneutral sodium-chloride cotransporter (NCC) is another major contributor to sodium reabsorption and is expressed along the distal tubule segment. The amiloride-sensitive epithelial sodium channel (ENaC) expressed in the collecting duct, antiporter enzyme $\text{Na}^+, \text{K}^+, \text{ATPase}$ expressed in the plasma membrane of tubular cells, and the type-2 Na-K-2Cl cotransporter in the thick ascending limb of Henle (NKCC2) also contribute to sodium reabsorption.

The importance of these sodium channels and transporters has been demonstrated in genetically modified mouse studies and congenital defects in humans. The spontaneously hypertensive rat (SHR) has impaired control of the $\text{Na}^+, \text{K}^+, \text{ATPase}$ in proximal tubule segments, increasing sodium reabsorption in the proximal tubules and possibly contributing to the hypertensive phenotype (Gurich & Beach, 1994). In humans, loci of adducin, a cytoskeletal protein capable of modulating $\text{Na}^+, \text{K}^+, \text{ATPase}$ pump activity, are strongly associated with essential hypertension (Casari *et al.*, 1995). Bartter syndrome in the human population is caused by a congenital mutation in the NKCC2 transporters, leading to severe volume depletion and excess polyhydramnios (excess amniotic fluid), frequently leading to premature birth (Simon *et al.*, 1996). Similarly, a mutation in the NCC transporter leads to a renal tubular disorder known as Gitelman syndrome, which involves abnormal fluid and electrolyte homeostatic mechanisms (de Jong *et al.*, 2002). Partial inactivity of the ENaC $\alpha 1$ subunit in the mouse leads to a salt-wasting phenotype (Wang *et al.*, 2001) and NHE3 knockout mice have hypotension and a marked inability to reabsorb bicarbonate and fluid in the proximal tubules (Schultheis *et al.*, 1998).

Alterations to renal handling of sodium and water have increasingly reported in developmental programming studies, particularly in protein-deprived models in rats. Offspring born to mothers fed a low protein (9% w/w protein) diet had normal GFR, although urinary sodium excretion was increased suggesting impaired tubular reabsorption of sodium (Alwasel & Ashton, 2009). *Nkcc2* mRNA levels were elevated in the kidney, with no changes to *Ncc*. This combined with immunohistochemical evidence that the $\text{Na}^+, \text{K}^+, \text{ATPase}$ $\alpha 1$ subunit was lost from the inner medulla suggesting that the programming of hypertension and impaired sodium handling is intricately linked to the expression of sodium channels. These observations were also observed in a similar model of low protein (6% w/w protein) diet in rats during the latter half of pregnancy, with offspring being born with reduced numbers of glomeruli per kidney (Manning *et al.*, 2002). With age, these

offspring exhibit hypertension, slightly lower GFR, and significantly increased expression of NKCC2 (or butemide-sensitive cotransporter BSC1) and thiazide-sensitive Na-Cl cotransporter (TSC) in the kidney. This suggests that renal sodium handling and reabsorption may be programmed by a maternal insult.

Singh and colleagues (Singh *et al.*, 2010) reported that sheep uninephrectomised in fetal life develop hypertension and low GFR. Deficits in renal sodium handling were observed in response to a salt load, and apical *Nhe3*, *Enac* β and γ subunits, and basolateral $Na^+,K^+,ATPase$ β and γ subunits were significantly elevated in uninephrectomised animals, while *Enac* α -subunit expression was reduced. Similar increases in sodium channel and transporter expression were observed in a model of dexamethasone treatment for 2 days mid-gestation in the rat, with increased protein levels of NHE3 exchanger at the proximal tubules as well as a 50% increase in activity (Dagan *et al.*, 2007). Together these data suggest that maternal perturbations can program changes in renal sodium handling as well as a reduction in nephron number, of which both may be implicated in the progression of hypertension in adult life.

1.13.4 Renin-angiotensin system

The renin angiotensin system (RAS) is a complex systemic cascade of interacting peptides and enzymes known to play a key role in the regulation of adult fluid and electrolyte homeostasis. Angiotensinogen is produced primarily in the liver and is secreted into the systemic circulation where it is converted into angiotensin I by the enzyme renin, which is secreted from the juxtaglomerular apparatus of the kidney. While other tissues express the gene responsible for producing the active renin enzyme, it is only the kidney that secretes the active renin, which is fully capable of enzymatic cleavage of angiotensinogen. Angiotensin I is converted into Angiotensin II by the angiotensin-converting enzyme (ACE) localized to endothelial cells throughout the body as well as the brush border of the renal proximal tubules. Angiotensin II is the most biologically active effector peptide of the RAS and binds to either the angiotensin II type 1 (*Agtr1*) receptor located within the renal tubule to increase sodium reabsorption or the *Agtr2* receptor to decrease sodium reabsorption. While in species such as the human and sheep, a single *Agtr1* isoform exists, in the rodent, two genes collectively perform these functions, namely *Agtr1a* and *Agtr1b*. In addition to the direct role of *Agtr1* and *Agtr2* in the kidney itself, signalling through these receptors in other tissues can indirectly influence renal function via adrenal production of aldosterone or through vascular effects. In addition to this predominant arm of the RAS, a number of additional peptides, enzymes, and receptors have all been shown to play a role in renal function and adult disease. This

includes angiotensin (1-7) [Ang 1-7], a small peptide generated from angiotensin II through the action of angiotensin-converting enzyme 2 (ACE2) (Santos, 2014). Recently it has become clear that Ang 1-7 exerts protective effects on the cardiovascular system through its receptor, Mas by promoting vasodilation, decreased blood pressure and anti-fibrotic effects. This process antagonises the angiotensin II/*Agtr1* axis and therefore Ang 1-7 is considered to have potential as a cardiovascular therapeutic agent (Galandrin *et al.*, 2016; Santos, 2014). Interestingly, in many organs, including the kidney, all components of the RAS are thought to coexist suggesting a role for a complete local RAS in such tissues. Programmed alterations to this system can have profound effects on both renal function and cardiovascular outcomes.

In addition to its role in adult physiology, the RAS is known to be involved in the development of many fetal organs and plays a key role in renal organogenesis. This is supported by the fact that when genes for *renin*, *Ace*, or *Agtr1* are knocked out of the genome, mice develop a number of congenital abnormalities of the kidney and have decreased survival rates (reviewed by Kobori *et al.*, 2007). During development, *Agtr1* signalling is generally accepted to have proliferative effects while the activation of *Agtr2* is thought to lead to antiproliferative, apoptotic phenotypes. Thus while decreased activation of *Agtr1* in adult life may reduce sodium reabsorption and reduce blood pressure, in fetal life, this may result in impairment of renal formation. Given the dual roles of the RAS in renal development and adult renal function, it is not surprising that the RAS is one of the best characterized systems shown to be programmed by in utero insults (for review, see Moritz *et al.*, 2010). It is also interesting to note that there are sex differences in the basal expression of many components of the renal RAS, however, the sex of the fetus has not been taken into account when investigating the renal RAS in programming models (Dagan *et al.*, 2007).

Renal expression of renin, ACE and angiotensin II receptors have all been shown to be programmed in offspring prenatally exposed to a number of maternal perturbations (summarized in Table 1.4). Maternal exposure to a low protein diet throughout pregnancy in the rat has been shown to reduce nephron number and increase blood pressure in offspring in association with a decrease in offspring *Agtr2* mRNA levels (McMullen *et al.*, 2004). A similar study in the rat demonstrated that protein restriction reduces renal *renin* mRNA levels, renal renin concentrations, and renal tissue angiotensin II levels (Woods *et al.*, 2001). In addition, in the previously mentioned rat model of high fat intake during pregnancy and lactation, offspring developed increased blood pressure despite a reduction in renal renin activity (Armitage *et al.*, 2005).

In addition to these postnatal programmed changes to the renal RAS, dysregulation of the fetal renal RAS has been shown to be a common finding in both rodent and sheep models of maternal insult (summarized in Table 1.4). A notable study demonstrated that dexamethasone exposure for 48 h from D27 of pregnancy in the sheep induces high blood pressure in offspring in association with increased mRNA levels of renal *angiotensinogen*, *Agtr1*, and *Agtr2* at 130 days of gestation (Moritz *et al.*, 2002). In a number of programming studies, fetal adaptations to the renal RAS and programmed changes to the RAS in the kidneys of offspring occur in response to the same maternal challenge suggesting that adaptive or maladaptive changes to the renal RAS that occur in utero may persist into adult life where they may have opposing effects on adult physiology. An example of this age-dependent dysregulation of the RAS is demonstrated in the rat model of corticosterone exposure discussed previously. Renal *Agtr1a* and *Agtr2* were increased and *Agtr1b* was decreased during nephrogenesis and both *Agtr1b* and *Agtr2* were increased in adolescent offspring, at which time *Agtr1* was unaffected (Singh *et al.*, 2007). Similarly, in a rat model of protein restriction, *Agtr1b* was decreased during kidney development and *Agtr1a* was increased in postnatal life (Vehaskari *et al.*, 2004). This biphasic fetal and postnatal dysregulation of the RAS has also been demonstrated in a model of intrauterine growth restriction induced through uteroplacental insufficiency that is known to induce hypertension in offspring. In this model, renal *renin* and *angiotensinogen* mRNA levels were decreased at birth but were increased in adult offspring. This was additionally associated with an increase in offspring ACE activity (Grigore *et al.*, 2007). Finally, in a model of fetal hypoxia known to impair nephron endowment, while AGTR1 protein levels were unchanged during nephrogenesis, AGTR1 protein levels as well as *Agtr1a* and *Agtr1b* mRNA levels were decreased in adult offspring (Gonzalez-Rodriguez *et al.*, 2013). It is interesting to note that, in some of the models described above, alterations to the fetal renal RAS may be protective in the short term but in the longer term are detrimental to offspring health. Additionally, few studies have examined the role of the Ang 1-7/Mas arm of the RAS with relation to developmentally-programmed cardiovascular and renal dysfunction, and this warrants investigation in the future given its protective role against increased blood pressure.

The pathogenesis of hypertension has also been linked to abnormalities of renal sodium handling. An inherited nephron deficit results in a diminished filtration surface area and hence a reduced capacity of the kidney to excrete normal sodium load. Sodium retention leads to the expansion of extracellular fluid volume and plasma volume, which acts to increase cardiac output, total peripheral resistance and mean arterial pressure. The increase in mean arterial pressure resets the pressure-natriuresis balance (Guyton *et al.*, 1972). Humoral alterations to ANP and PRA ultimately affect single nephron glomerular filtration rate, leading to progressive glomerular sclerosis and

therefore further reduction in filtration surface area. Brenner describes this as a vicious cycle, with progressive deterioration of the kidney and worsening of systemic hypertension (Brenner *et al.*, 1988). Ethnicity, gender and age are all important factors when considering susceptibility to hypertension. Females tend to have greater age-related increases in blood pressure, related to menopause and the alterations of oestrogen levels (Parraguez *et al.*, 2011). It has been suggested that fact that females tend to have smaller kidneys than males with slightly fewer glomeruli may contribute to increased susceptibility to hypertension (Halliwell & Gutteridge, 1999). There is also an age-related decline in nephrons that correlates with an age-related increase in the incidence of hypertension (Zamudio *et al.*, 2007). Although a nephron deficit may not directly lead to hypertension and cardiovascular disease, offspring with decreased nephron and cardiomyocyte number may be less able to adapt to the demands of a poor lifestyle or diet, such as a high-salt diet.

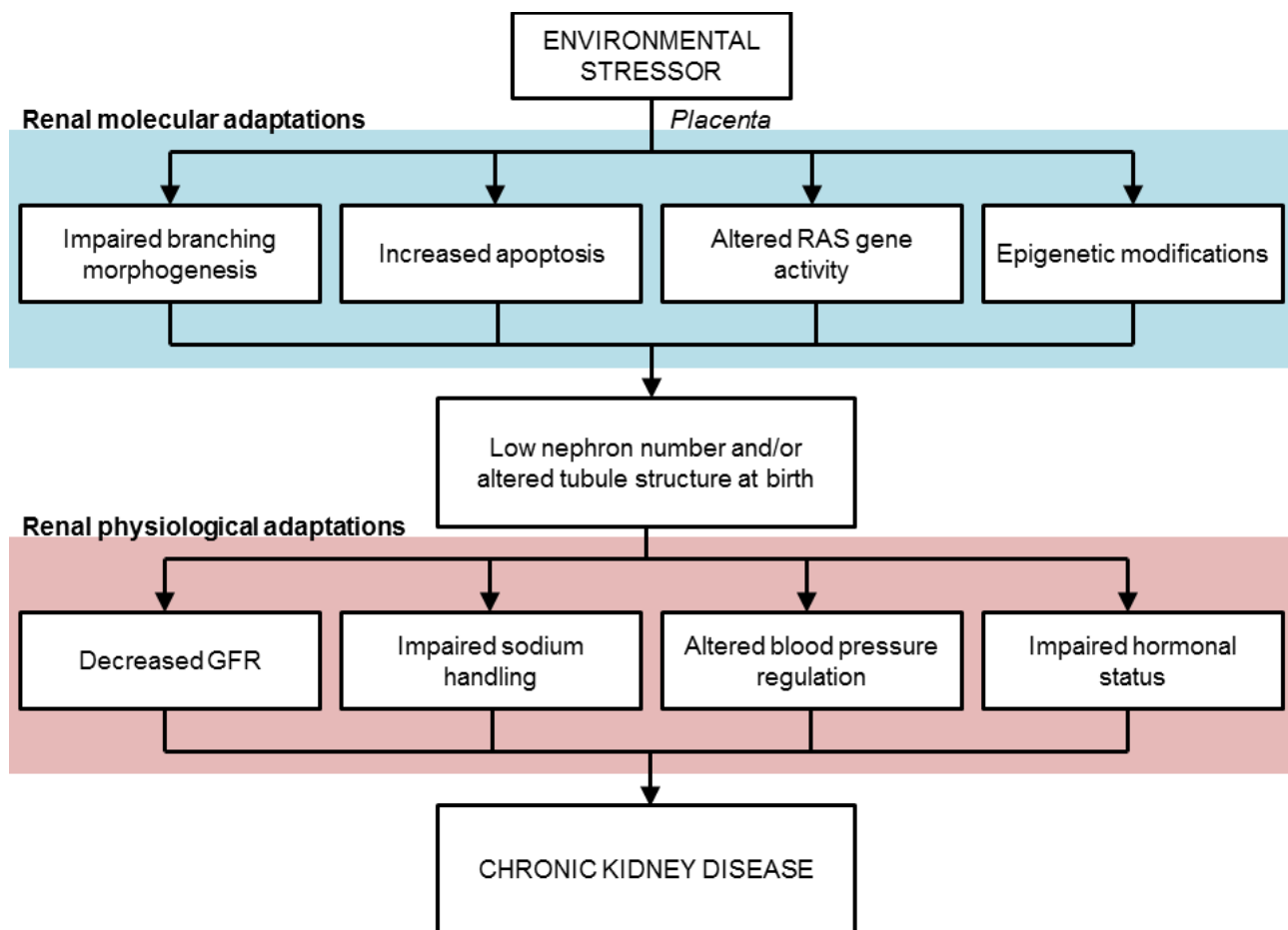


Figure 1.3. Potential pre- and postnatal pathways through which a suboptimal in utero environment may contribute to the programming of chronic kidney disease.

Abbreviations: RAS, renin angiotensin system. GFR, glomerular filtration rate.

1.14 The importance of the kidney in blood pressure regulation

The control of arterial pressure is a tightly regulated process. Arterial pressure is determined by cardiac output and total systemic vascular resistance; when arterial pressure is perturbed, these parameters are adjusted to return mean arterial pressure to normal (Cowley, 1992). In the short term (seconds to minutes), this regulation is due to the carotid baroreceptor reflex, which results in the inhibition of the sympathetic nervous system to lower arterial pressure (Bartelds *et al.*, 1993). Elevated sympathetic activity has been associated with hypertension (Anderson *et al.*, 1989). Long-term control of arterial pressure over minutes to day primarily involves fluid volume regulation by the renal system (Guyton *et al.*, 1972). The kidney is responsible for fluid and electrolyte balance into the body through a process of filtration by the glomerulus and reabsorption by the tubules. The kidney has a great capacity to cope with changing physiological conditions. Particularly, the ability of the kidney to excrete concentrated urine is vital in types of volume depletion and severe dehydration. Guyton's paper (1972) used computer modelling to explain the pressure-natriuresis mechanism. Elevations in arterial pressure increase the excretion of sodium and water to surpass that of sodium and water intake, until arterial pressure lowers to a point of equilibrium (Figure 1.4). This point represents the arterial pressure at which the intake of sodium and water matches renal output. This mechanism operates with an infinite feedback gain, as the renal output of water and sodium always returns to equilibrium with the body's intake of water and sodium. There are two major determinants of the long-term control of arterial pressure: (1) sodium and water intake, and (2) a pressure shift in the renal output curve in response to sodium and water. Consequently, hypertension can occur when there is either (1) a chronic increase in sodium and water intake beyond that which the kidney is capable of excreting, and (2) arterial pressure that enables sodium and water excretion is permanently shifted to a higher value.

It is important to note that the Guyton model of pressure-natriuresis does not consider the role of ex-renal organs in blood pressure regulation. Although the kidney is the decisive factor in blood pressure regulation, the skin and immune system have recently been indentified in water and electrolyte homeostasis (Machnik *et al.*, 2009; Titze, 2015; Wiig *et al.*, 2013). Electrolytes (sodium and chloride) are sequestered in the skin interstitium as an ex-renal regulatory mechanism for electrolyte balance of the interstitial fluid. In periods of osmotic stress, mononuclear phagocyte system (MPS) cells are recruited to the skin and activate the tonicity-responsive enhancer-binding protein (TONEBP) (Machnik *et al.*, 2009). This leads to the expression of vascular endothelial growth factor-C (*Vegf-c*), which is secreted by macrophages to promote electrolyte clearance through lymphatic vessels and increased eNOS vascular expression to encourage vasodilation (Wiig

et al., 2013). Failure of this process has been associated with electrolyte accumulation in the skin and hypertension (Titze, 2015; Wiig *et al.*, 2013).

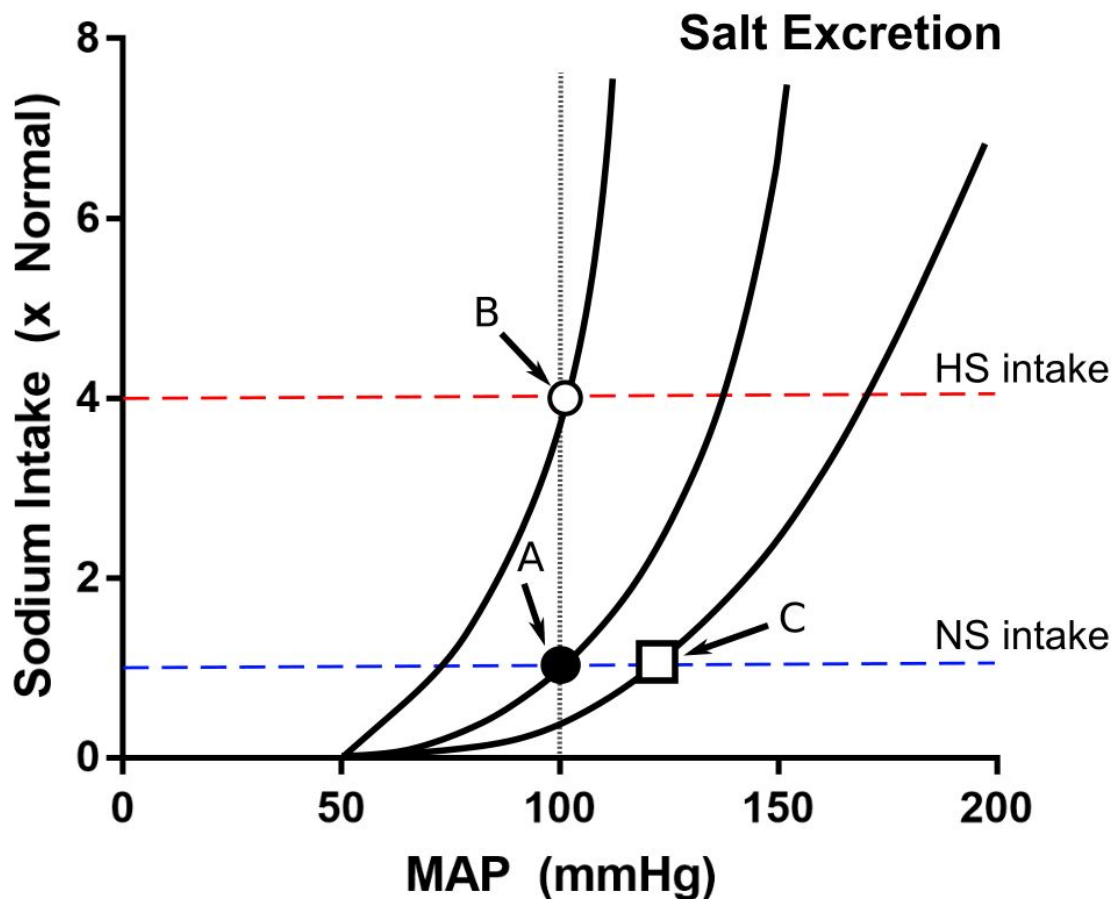


Figure 1.4. *The pressure-natriuresis mechanism.*

Renal function curve showing the effect of mean arterial pressure (MAP) on renal sodium excretion under normal salt (NS) and high salt (HS) dietary intake. *A*: The equilibrium point marks the pressure level at which the kidney-fluid mechanism will control arterial pressure. *B*: Chronic increases in dietary sodium causes a leftward shift of the renal function curve to increase sodium excretion at any given pressure. *C*: Failure of this process leads to a rightward shift in the renal function curve so that a higher equilibrium pressure is required to match sodium output to input. Adapted from Guyton, 1990.

1.15 Sex differences in developmental programming

Intriguingly, the extent to which a developmental insult may affect the offspring also depends upon the sex of the fetus or neonate with male offspring tended to develop more exaggerated disease states in adult life. A study by Hemmings and colleagues (2005) reported that both male and female offspring exposed to hypoxia during pregnancy displayed vascular changes in adulthood, however only males had overt changes that may have contributed to increased peripheral resistance and cardiovascular disease. The group has proposed that female offspring may have greater vascular compensatory mechanisms after birth, possibly due to sex-specific differences in the modulation of vasodilation (Skarsgard *et al.*, 1997). Sexual dimorphism in response to a gestational hypoxic insult has otherwise been given little attention, with the majority of studies either pooling the sexes or study males only. As strong evidence exists for the differential health trajectory of male and female growth-restricted offspring, attention needs to be placed upon both sexes. The mechanisms by which male and female offspring differ in response to a developmental insult remain unknown. Three main hypotheses have been proposed: (1) male and female offspring adapt differently to a developmental insult (Zambrano *et al.*, 2005), (2) sex hormones, particularly testosterone in the male offspring, interact to affect the sexes differentially (Ojeda *et al.*, 2007a; Ojeda *et al.*, 2007b), and (3) innate differences between the sexes, irrespective of sex hormones, may influence the susceptibility to developmental insult (Gilbert & Nijland, 2008).

1.16 The ‘second hit’ hypothesis

1.16.1 Overview

Increasingly, the importance of the postnatal environment is recognised in developmental programming. An *in utero* perturbation may not directly lead to an overt disease phenotype, but only a susceptibility to developing disease in later life. Underlying deficits in organ function may be unmasked when a ‘second hit’ is applied in later life. This can be seen in the Australian context, where a number of Indigenous communities appear to be particularly susceptible to the programming of renal dysfunction. The Australian Aboriginal people have amongst the highest rates of CKD worldwide, and this is associated with increased rates of low birth weight babies (Hoy *et al.*, 1999) and increased proteinuria in children. However, this population also has high prevalence of early life infections resulting in post-streptococcal glomerulonephritis (Hoy *et al.*, 2016) and likely worsens the renal phenotype. This highlights the important interactions between the pre- and postnatal environments; a poor intrauterine environment may contribute to increased disease risk due to the low birth weight with the postnatal environment providing a “second hit” that further increases risk of disease.

A common challenge includes childhood obesity, which has also been shown to exacerbate poor renal outcomes in Aboriginal children of a low birth weight. Similarly, rapid postnatal growth is associated with poorer outcomes in children born of low birth weight. Increasingly studies in animals have examined the effects of a poor postnatal diet, such as low protein (Hoppe *et al.*, 2007b), high fat (Shah *et al.*, 2016) and high salt (Ruta *et al.*, 2010). In this thesis, we have examined additional ‘second hits’ of ageing as well as a diet high in salt.

1.16.2 High salt diet

The customary quantities of salt in the modern Western diet are in far excess of what it required to maintain sodium balance in the body, with the daily intake of humans now 10-fold higher than that of our ancestors. Epidemiological studies have long associated dietary sodium intake in communities with the incidence and severity of hypertension (Weinberger & Fineberg, 1991; Sacks *et al.*, 2001). The Yanomami Indians, a population of northern Brazil and southern Venezuela, survive on less than 0.5 g of salt per day, and show no evidence of hypertension or obesity. Additionally, there are no recorded age-related increases in blood pressure (Arant, 1978; Aperia *et al.*, 1981). In contrast, societies that consume a modern Western diet, which is considered to be sodium-rich but potassium-poor, have high rates of hypertension and cardiovascular disease.

The role of dietary sodium in the pathogenesis of hypertension has remained controversial, as studies show heterogeneity of blood pressure responses to extracellular volume depletion and sodium intake in both normotensive and hypotensive patients (Kawasaki *et al.*, 1978; Weinberger & Fineberg, 1991). Despite this, a severe reduction in dietary sodium is generally agreed upon as an effective treatment of hypertension. Improvements of methodologies has allowed more sensitive measurements of blood pressure, with most now acknowledging the importance of dietary sodium influences on blood pressure. Most notably, the Dietary Approaches to Stop Hypertension (DASH) trial showed that a low sodium diet rich in fruits, vegetables and low-fat dairy products reduced body fat composition and significantly lower blood pressure (Sacks *et al.*, 2001). Therefore, dietary sodium restriction across a population is likely to reduce the risk and thus overall occurrence of cardiovascular diseases. Although resistance is often found to low-salt diets, several studies have shown that modest, incremental reductions in dietary sodium may go undetected (Rodgers & Neal, 1999; Girgis *et al.*, 2003). Recent efforts have seen an Australian food producer reformulate 12 breakfast cereal products, with an average sodium reduction of 40% (from 85-429 mg sodium per 100 g) (Williams *et al.*, 2003). A second Australian study showed that gradual sodium reduction of 25% in bread was undetectable by taste (Girgis *et al.*, 2003). Furthermore, these sustained

reductions of dietary sodium have been shown to shift taste preferences towards a lower salt diet (Bertino *et al.*, 1982). These studies are promising, as they suggest that an overall societal reduction in sodium intake may not be as unattainable as previously thought, and could have significant impact in the treatment of elevated blood pressure and consequential cardiovascular diseases.

Animal studies have demonstrated similar associations between dietary sodium intake and blood pressure elevation. Structural changes have been observed, with elevated dietary sodium linked to both renal and left ventricular hypertrophy (Fields *et al.*, 1991; Yuan & Leenen, 1991; Lal *et al.*, 2003; Mohri *et al.*, 2003), possibly due to widespread fibrosis and increased TGF- β 1 (Yu *et al.*, 1998), as well as elevated blood pressure. Left ventricular hypertrophy has also been observed in normotensive and hypotensive humans in response to high dietary sodium (Du Cailar *et al.*, 1992), both of which are contributors to hypertension. High dietary sodium intake does not always lead to hypertension; sometimes, impairments in either the cardiovascular or renal systems such as a nephron deficit may not cope with the added stress of a high sodium load and this could in turn lead to hypertension. A high degree of renal mass ablation (70%) in the rat leads to both glomerular and systemic hypertension, without the secondary impact of high dietary sodium. More modest renal mass reduction, however, does not always lead to systemic hypertension. However, these animals fed on a diet high in sodium then became susceptible to hypertension. These data are important, as it suggests that those born of low birth weight with poorly developed kidneys may be at a higher risk of developing cardiovascular disease if dietary sodium intake remains high. Studies have shown that both children and adults with low birth weight and reduced renal mass are at higher risk for lower renal function and increased salt sensitivity (Phipps *et al.*, 1993; Barker *et al.*, 2010).

Based on this literature, the National Health and Research Council of Australia (2006) has set guidelines for adequate sodium intake and the upper levels of sodium intake across the lifespan (Table 1.5). Adequate sodium intake increases with age, with infants requiring very little sodium in the diet (120 mg/day) to both males and females requiring 460-920 mg of sodium daily. A suggested daily sodium intake has been set at 1,600 mg for both male and female adults, which equates to approximately 4 grams of salt. The upper level of intake of 2,300 mg of sodium per day was set as it was “the highest average daily intake level likely to pose no adverse health effects to almost all individuals in the general population”. Despite these guidelines, the FSANZ report has estimated that the mean sodium intake across all Australians is approximately 2,500 mg per day (110 mmol/day), a level that exceeds the suggested upper limit of daily dietary sodium intake (Boorman *et al.*, 2008). A recent estimate from a report commissioned by FSANZ has suggested that reduction in sodium levels in processed foods, which accounts for 75% of dietary sodium

consumption, would reduce the population incidence of myocardial infarction and stroke significantly.

Table 1.5. NHMRC recommendations for average intake and upper level of intake of sodium by life stage.

Age	Adequate Intake of Sodium	Upper Level of Intake of Sodium
<i>Infants</i>		
0-6 months	120 mg/day (5.2 mmol)	Unable to establish. Source of intake should be through breast milk, formula and food only.
7-12 months	170 mg/day (7.4 mmol)	
<i>Children & adolescents</i>		
1-3 years	200-400 mg/day (9-17 mmol)	1000 mg/day (43 mmol)
4-8 years	300-600 mg/day (13-26 mmol)	1,400 mg/day (60 mmol)
9-13 years	400-800 mg/day (17-34 mmol)	2,000 mg/day (86 mmol)
14-18 years	460-920 mg/day (20-40 mmol)	2,300 mg/day (100 mmol)
<i>Adults</i>		
19+ years	460-920mg/day (20-40 mmol)	2,300 mg/day (100mmol)

1.17 Rationale

Prenatal hypoxia is a common pregnancy complication that increases risk of cardiovascular and metabolic disease in adulthood. To date, no study has examined whether offspring exposed to prenatal hypoxia develop renal impairments that may contribute to CKD. The impact of prenatal hypoxia on the kidney is vital to understand, given the kidney's role in the long-term regulation of arterial pressure. A broad range of studies have demonstrated that the fetal kidney is highly susceptible to *in utero* insult, and it is well known that *in utero* hypoxia directly reduces blood flow to the fetal kidneys in favour of the heart, brain and adrenal glands. Overall, this suggests that describing alterations to renal structure following a hypoxic *in utero* insult will provide further insight into the cardiovascular impairments previously observed in ageing offspring. The present set of studies have utilised a mouse model of late gestational maternal hypoxia to examine the effects on blood pressure, microvascular function, and renal function in the ageing offspring. Furthermore, the implications of high dietary sodium intake for long-term cardiovascular and renal health were examined, given this is endemic in Western societies.

1.18 Hypotheses and aims

Overall aims:

- To determine if maternal hypoxia during mid-late gestation can lead to structural changes in the kidneys, heart and vasculature.
- To determine if maternal hypoxia during mid-late gestation can lead to changes in blood pressure, microvascular function and renal function in adult offspring.
- To determine whether high dietary sodium intake can exacerbate the observed renal and cardiovascular deficits.

Overall hypotheses:

- Maternal hypoxia during late gestation will impair nephrogenesis *in utero* and also postnatal maturation of the kidney.
- Maternally induced fetal hypoxia during mid-late gestation will predispose offspring to developing cardiovascular and renal disease in adulthood.
- High dietary intake of sodium will exacerbate functional impairments of the renal and cardiovascular systems.

To achieve these overall aims and hypotheses, four separate but related studies were undertaken:

1. Study 1 (Chapter 3) investigated the effects of prenatal hypoxia and a postnatal high salt diet on microvascular function and structure in offspring.
2. Study 2 (Chapter 4) examined the impact of prenatal hypoxia on nephron endowment, blood pressure and renal function, as well as susceptibility to dietary salt-induced organ injury.
3. Study 3 (Chapter 5) developed a design-based stereology method to estimate the lengths of renal tubules and collecting ducts in the rodent kidney.
4. Study 4 (Chapter 6) investigated the impact of prenatal hypoxia on urine-concentrating capacity and renal medullary structure, in part using the technique developed in study 3, in offspring.

Chapter 2: General methods

2.1 Ethics approval

All experiments were approved in advance by the University of Queensland animal ethics committee (AEC numbers 484/09 and 496/12) and were conducted in accordance with the Australian Code of Practice for the Care and Use of Animals for Scientific Purposes.

2.2 Animal treatment: maternal hypoxia

CD1 mice were used for all experiments within this thesis. CD1 mice have multiple benefits compared to other mouse strains. These include: (1) large litter sizes (average 14-16 pups), (2) good mothering abilities to reduce fetal loss, (3) large body size for ease of physiological measurements, and (4) heterogeneity compared to inbred strains, which more accurately mimics the diversity of the human population.

At embryonic day (E) 14.5 of pregnancy, time-mated CD1 mice were randomly allocated to normoxic room conditions (control; N=21) or housed inside a hypoxic chamber continuously flushed with nitrogen gas to maintain an oxygen concentration of 12% (hypoxia; N=22) for the remainder of pregnancy (see Figure 2.1). Food and water was provided *ad libitum*. Body weight, food and water consumption were monitored daily throughout the experimental protocol. The dams were removed from the hypoxic chamber upon littering down (postnatal day 0 [P0]).

Benefits and limitations of the mouse model of maternal hypoxia

This experimental protocol does not result in changes in maternal food intake and weight gain, and is thus not compromised by maternal undernutrition (Cuffe *et al.*, 2014a). This allows us to examine the effect of hypoxia alone on the mouse offspring, which is not possible in models of maternal hypoxia in the rat where reduced food intake is frequently reported (Williams *et al.*, 2005a; Williams *et al.*, 2005b). It is important to note that this is a global model of maternal hypoxia exposure, as opposed to a model of isolated fetal hypoxia. This reflects conditions whereby maternal oxygen exposure is reduced, such as smoking, high

altitude living and maternal conditions such as anaemia, as discussed in Section 1.8.2. However, these forms of maternal hypoxia frequently co-exist with other features such as nicotine/tobacco exposure in smoking, reduced atmospheric pressure and undernourishment in high altitude living, and iron deficiency in maternal anaemia. Our mouse model of maternal hypoxia allows us to isolate the effects of hypoxia specifically, although additional studies are required if direct parallels are to be drawn with these maternal conditions. Use of larger animals such as the sheep allow direct fetal cannulation and induction of fetal hypoxia without affecting maternal oxygen inspiration. Compared to mice, larger animals are more costly, have significantly longer gestational periods and fewer molecular tools are available for analysis of tissue from non-murine species.

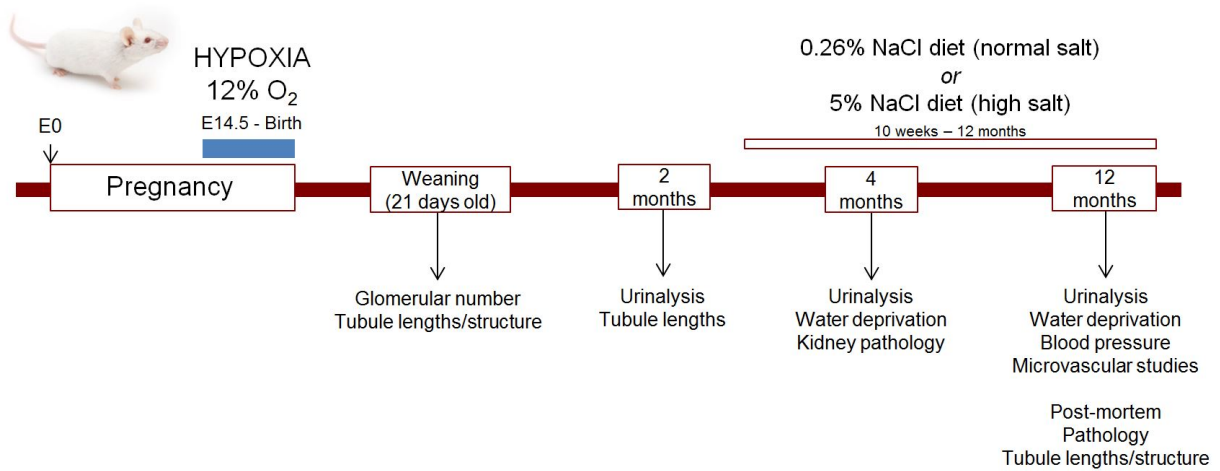


Figure 2.1. Diagram of major time points within this model of maternal hypoxia exposure throughout late gestation, and its influence on renal and cardiovascular outcomes.

2.3 Tissue collection from juvenile animals

2.3.1 Fetal post-mortem

Pregnant dams at E18.5 (N=8 per treatment group) were euthanised by cervical dislocation. Fetuses were immediately removed from the uterine horn, weighed and swiftly decapitated. Kidneys, hearts and brains were dissected and weighed. Tails were taken for identification of fetal sex by genotyping.

2.3.2 Post-mortem on day-of-birth

An additional subset of dams and offspring (C: N=10; H: N=11) were culled at P0 by cervical dislocation and decapitation respectively. Pup body weights were recorded. Maternal and pup blood was collected for measurement of haematocrit in duplicate.

2.3.3 Early juvenile post-mortem

Male offspring at P6 (N=4 from separate litters) were culled. Kidneys were removed and immediately immersion fixed in 4% neutral buffered paraformaldehyde (PFA) for subsequent histological processing.

2.3.4 Post-mortem at weaning

At P21, male and female offspring (N=2 animals per litter, from 11 separate litters per treatment group) were culled by cervical dislocation. Body weight was measured before organs (heart, kidney, brain) were dissected, weighed and snap frozen in liquid nitrogen and stored at -80°C for molecular studies or immersion fixed in 4% paraformaldehyde for subsequent histological processing.

2.3.5 Post-mortem at 2 months of age

Male offspring at 2 months of age (N=6 per treatment group) were culled by cervical dislocation. Body weight was measured before kidneys were dissected, weighed and immersion fixed in 4% paraformaldehyde for subsequent histological processing.

2.4 Dietary intervention: chronic high salt diet

A subset of animals aged 10 weeks (N=11 per sex per treatment, 1-2 animals from each litter) was randomly allocated to receive a high salt (HS) diet (5% NaCl [wt/wt]; modified AIN 93M, SF05-023, Specialty Feeds, Glen Forest, WA, Australia). The remaining animals (N=11 per sex per treatment) were maintained on a matched control normal salt (NS) diet (0.26% NaCl [wt/wt]; AIN 93M, Specialty Feeds). Food and water consumption were monitored for the first 5 days of diet administration to ensure animals adjusted to the dietary change. Animals were maintained on the appropriate diet until post-mortem at 12 months of age.

2.4.1 Post-mortem at 4 months of age

Male offspring fed the normal salt and high salt diets were culled at 4 months of age by cervical dislocation. Body weight was measured before kidneys were dissected and immersion fixed in 4% paraformaldehyde for subsequent histological processing.

2.5 Animal physiological studies

2.5.1 Metabolic cages

Animals at 2, 4 and 12 months of age (N=9-11 per sex per treatment group) were acclimatised to individual metabolic cages for 2 hours on Day 1, and then 4 hours on Day 2. This was to limit the impact of the stress of individual housing in a non-enriched novel environment. On Day 3, animals were weighed and placed in the same metabolic cage at 1600 hours with food and water provided *ad libitum*. After 24 hours, animals were weighed and returned to home cages. Food and water consumption, body weight change and urine output over the 24h period were recorded. Urine samples were collected stored at -20 °C for further analysis. Animals fed the high salt diet at 4 (N=5) and 12 months of age (N=11) also underwent the metabolic cage protocol.

2.5.2 Water deprivation challenge

One week following initial basal urine collection, offspring aged 4 and 12 months (N = 9-11 per treatment; normal salt diet only) were subject to a 24 h water deprivation challenge in the metabolic cages. At 1600 hours, animals were placed in individual cages without access to water. Food was provided *ad libitum*. Animals were carefully monitored for signs of lethargy

(willingness to move around, alertness when handled) that are suggestive of severe dehydration every 2 hours from 0800 hours the following morning until the protocol finished at 1600 hours. Recording sheets were placed on each cage to track animal wellbeing over the final 8 hours of dehydration. Food intake, body weight change and urine output were recorded. Urine samples were stored at -20 °C for further analysis. Following the 24 h challenge, offspring were returned to their home cages, immediately offered water and body weight monitored daily over the subsequent week.

2.5.3 Urinary electrolyte excretion

Urinary sodium, chloride and potassium concentrations were measured for all urine samples by potentiometry using a COBAS Integra 400 Plus. Urine osmolarity was assessed by freezing point depression using a Micro-Osmette osmometer (Precision Systems, MA, USA).

2.5.4 Urinary albumin ELISA assay

Urinary albumin excretion under basal conditions was measured in urine samples (1:13 dilution) from 4 and 12-month-old animals using a commercially available albumin ELISA (Albuwell M, Exocell Inc., Philadelphia).

2.5.5 Urinary creatinine assay

Urinary creatinine excretion under basal conditions was measured in urine samples (1:10 dilution) from 12-month-old animals using a commercially available assay (Creatinine Companion, Exocell Inc., Philadelphia).

2.6 Blood pressure by radiotelemetry

2.6.1 Surgical preparation

Cardiovascular function was assessed in 12-month-old mice fed the normal salt diet by radiotelemetry, the current gold standard of blood pressure measurements. Animals were anaesthetised under isoflurane and radiotelemetry transmitters were implanted by Dr Tamara Paravicini, as previously described (Huetteman & Bogie, 2009). Recording of heart rate, systolic and diastolic pressure, and activity commenced 10 days post-surgery (N = 5-7 per group) in home cages placed on receiver platforms connected to Dataquest Advanced

Research Technology software (Data Sciences International). Mean arterial pressure and pulse pressure were calculated from these parameters. Data were recorded for 10 seconds every 15 minutes for three days. Blood pressure parameters are reported as the mean of three 12 h day/night cycles. Activity data was reported as the mean of every hour of the three 12 h day/night cycles.

2.6.2 Restraint stress

On the fourth day of measurements, a baseline measure was obtained from data sampled for 10 seconds, every 5 minutes, for 1 hour. Animals were immediately placed in a clear plastic container (12 x 8 x 6 cm) for 15 min, and then released back into its cage. During the restraint and 15 min recovery period, data was sampled at a rate of 10 seconds per minute.

2.7 Pressure myography

2.7.1 Mesenteric artery dissection and cannulation

Following completion of renal function measurements, animals fed both normal salt and high salt diets were euthanized by CO₂ inhalation (N=6-10 per group). The mesentery was removed and immediately pinned in an agar-filled petrie dish containing ice-cold physiological salt solution (composition in mmol/L: NaCl 118, KCl 4.65, MgSO₄ 1.18, KH₂PO₄ 1.18, CaCl₂ 2.5, NaHCO₃ 25 mM, glucose 5.5 mM, EDTA 0.026 mM). A second-order mesenteric artery was dissected from connective tissue, with care taken not to touch the vasculature. The proximal end of the vessel was cannulated in the pressure myography system (DMT, Model 110P, Denmark) containing 10 mL of PSS using two 11-0 silk sutures to secure in place to the cannula. PSS was flushed through the cannula into the lumen of the vessel to remove remaining blood or debris. The distal end of the mesenteric artery was then cannulated.

2.7.2 Vessel imaging and image capture

The stage housing the cannulated vessel was placed under the microscope (Zeiss Axio Vert.A1). Live vessel imaging (~ X100 magnification) was performed using the attached camera (The Imaging Source, Model DMK41AU02) and computer running MyoVIEW II (DMT, Denmark) for data acquisition and analysis. The MyoVIEW II software plotted and displayed vessel outer diameter (OD) and wall thickness (WT) as functions of time.

2.7.3 *Equilibration*

The chamber containing the vessel and PSS was heated to 37 °C and constantly bubbled by carbogen (95% O₂, 5% CO₂). Pressure was equalised at each cannula to ensure zero flow through the vessel. Intraluminal pressure was gradually increased in 10 mmHg to 45 mm Hg.

2.7.4 *Maximum vessel contractility using KPSS_{max}*

Maximal vessel contractility was determined using high potassium physiological salt solution (KPSS) containing equimolar substitution of KCl for NaCl. The chamber was washed 3 times with PSS and allowed 20 min to re-equilibrate.

2.7.5 *Vasoconstrictive response to phenylephrine*

Vessel contractility was assessed by cumulative concentration-response curves to phenylephrine (PE; 10⁻⁹ to 10⁻⁴ mol/L). The contractile responses were expressed as a percentage of the maximum response to KPSS (KPSS_{max}). The chamber was washed 3 times with PSS and allowed 20 min to re-equilibrate.

2.7.6 *Endothelium-dependent vasodilation*

Endothelium-dependent relaxation was assessed in vessels submaximally constricted with PE (70% of KPSS_{max}) using acetylcholine (ACh; 10⁻⁹ to 10⁻⁴ mol/L). The chamber was washed 3 times with PSS and allowed 20 min to re-equilibrate.

2.7.7 *Endothelium-independent vasodilation*

Endothelium-dependent relaxation was assessed in vessels submaximally constricted with PE (70% of KPSS_{max}) using sodium nitroprusside (SNP; 10⁻¹⁰ to 10⁻⁴ mol/L). The chamber was washed 3 times with PSS and allowed 20 min to re-equilibrate.

2.7.8 *Vascular structure and mechanics*

To measure vascular structure and mechanics, vessels were superfused with Ca²⁺-free PSS containing 1 mmol/L of ethylene glycol tetraacetic acid (EGTA), a calcium ion chelating agent, to remove intrinsic tone. Four washes (5 min duration) were performed with the Ca²⁺-

free PSS. Intraluminal pressure was increased stepwise from 3 to 140 mm Hg and lumen diameter and wall thickness measured at each pressure.

2.7.9 Data analysis

Functional studies

Relaxation responses to ACh and SNP were expressed as the percentage relaxation from the PE-induced contraction. Non-linear regression (Graphpad Prism 6) was used to determine the pEC₅₀ and maximum response (R_{max}) for each vessel.

Structural and mechanical studies

Lumen diameter (ID) was calculated from the OD and WT measurements:

$$ID = OD - (2 \times WT)$$

The media to lumen ratio was calculated from the WT and ID parameters:

$$\text{media:lumen} = (2 \times WT) / ID$$

Medial cross-sectional area (CSA) was calculated as such:

$$CSA = (\pi/4) \times (OD^2 - ID^2)$$

Circumferential stress (σ ; dyne/cm²) was given by the expression:

$$\sigma = (P \times ID) / (2 \times WT)$$

Where 'P' refers to the given intraluminal pressure (dyne/cm²).

Circumferential strain (ϵ), the deformation of the vessel at a given intraluminal pressure from the original lumen diameter at 3 mmHg (ID₀), was calculated as such:

$$\epsilon = (ID - ID_0) / ID_0$$

The elastic modulus, a determination of a material's tendency to deform elastically when force is applied, was determined by fitting stress-strain data to an exponential equation:

$$\sigma = \sigma_0 \times e^{\beta \epsilon}$$

Where σ_0 is the stress at ID_0 and β is the rate constant of the stress-strain curve.

The mean β values of each group were compared to examine differences in the incremental elastic modulus, suggestive of vascular compliance changes.

2.8 Quantitative real-time PCR

RNA was extracted from kidneys at P21 using the RNeasy minikit (QIAGEN, Chadstone Centre, VIC, Australia). All RNA was treated with deoxyribonuclease 1 and reverse transcribed into cDNA (iScript™, Bio-Rad, NSW, Australia). Amplification was performed using SBYBR Green PCR Mastermix (Applied Biosystems, VIC, Australia) in a 20 μ l reaction volume containing cDNA and 10 pmol of each primer for Aquaporin-2 (sense 5'-CTTCCTTCGAGCTGCCTTC-3'; antisense 5'-CATTGTTGTGGAGAGCATTGA C-3'). Results were normalised to expression of 18S.

2.9 Histological studies

2.9.1 Tissue collection

All tissues (kidney, heart and aorta) were fixed in 4% neutral buffered paraformaldehyde (PFA) at the time of post mortem, and either prepared for cryogenic sectioning or paraffin sections.

2.9.2 Paraffin processing and staining

Samples were thoroughly washed in running distilled water for 20 minutes and processed through increasing ethanol concentrations (70%-100%) into paraffin using a Leica ASP300S tissue processor. Paraffin blocks were exhaustively sectioned at 5 μ m and transferred to Superfrost + slides.

2.9.3 Staining

Paraffin slides were dewaxed through 3 x 2 min changes of xylene and rehydrated through decreasing concentrations of ethanol (2 x 2 min of 100% ethanol, 1x 2 min of 90% ethanol, 1x 2 min of 70 % ethanol) into distilled water.

Periodic acid-Schiff (PAS) stain

After deparaffinisation and rehydration, sections were bathed in 0.5% periodic acid for 5 minutes. Sections were washed in distilled water for 5 minutes and transferred to Schiff's reagent for 15 minutes. Excess Schiff's reagent was washed from sections until water ran clear (~ 5 min). Nuclei were stained with Mayer's haematoxylin for ~20 seconds and blued in Scott's tap water. Slides were dehydrated in ethanol and washed in xylene (3x 2 min). Slides were then mounted using DPX mounting medium (Merck, mounting medium, Darmstadt, Germany).

Masson's Trichrome stain

After deparaffinisation and rehydration, sections were bathed in freshly prepared Wiegert's haematoxylin for 10 minutes. Sections were thoroughly washed in running tap water for 5 minutes, transferred to Biebrich scarlet-acid fuchsin solution for 5 minutes and rinsed in distilled water. The stain was differentiated with phosphotungstic/phosphomolybdic acid for 10 minutes. Slides were directly transferred to Aniline blue for 5 minutes, briefly rinsed in distilled water and further differentiated in 1% acetic acid for ~30 seconds. Slides were rapidly dehydrated in 100% ethanol and washed in xylene (3x 2 min). Slides were then mounted using DPX mounting medium.

Verhoeff's van Gieson stain

After deparaffinisation and rehydration, sections were stained in freshly prepared Verhoeff's haematoxylin for 30 minutes. Sections were washed in tap water until water ran clear. Sections were differentiated in 2% ferric chloride until black fibres were clearly visible microscopically on a gray background. Sections were rinsed in distilled water, transferred to hypo for 1 minute to remove the iodine from the Verhoeff's haematoxylin and again washed in distilled water. Sections were counterstained in Van Gieson's solution for 5 minutes. Slides were rapidly dehydrated in 100% ethanol and washed in xylene (3x 2 min). Slides were then mounted using DPX mounting medium.

Histochemistry

After deparaffinisation and rehydration, endogenous peroxidase activity was blocked by incubation with 2% H₂O₂ for 10 minutes in distilled water. Slides were then incubated for 30 min at 37 °C with neuraminidase (0.1 units/ml with 1% CaCl₂ in PBS) from *Vibrio cholerae* (Sigma-Aldrich, Castle Hill, Australia). Nonspecific binding was further blocked with 2% BSA in 0.3% Triton in PBS for 30 min at room temperature. Sections were then incubated for 2 h with 20 ug/ml biotinylated peanut agglutinin (PNA; Sigma-Aldrich, Castle Hill, Australia) diluted in 2% BSA in 0.3% Triton in PBS, with 1 mM CaCl₂/MnCl₂/MgCl₂. Slides were washed, treated with avidin/biotin complex (Elite ABC Kit, Vector Laboratories, CA, USA) for 30 minutes and the reaction developed with diaminobenzidine (DAB, Vector Laboratories, CA, USA). Sections were counterstained with haematoxylin, blued in Scott's tap water and mounted with DPX mounting medium.

Immunohistochemistry

After deparaffinisation and rehydration, endogenous peroxidase activity was blocked by incubation with H₂O₂ in distilled water. Non-specific binding was blocked using 2% BSA in goat or rabbit serum in PBS for 1 h at room temperature. Slides were incubated with primary antibodies in a sealed chamber. Slides were thoroughly washed before incubated with relevant secondary antibodies (1:200 dilution; Elite ABC Kit, Vector Laboratories, CA, USA). Slides were washed, treated with avidin/biotin complex (Elite ABC Kit, Vector Laboratories, CA, USA) for 30 minutes and the reaction developed with diaminobenzidine (DAB, Vector Laboratories, CA, USA). Sections were counterstained with haematoxylin, blued in Scott's tap water and mounted with DPX mounting medium.

Image acquisition

All brightfield slides were scanned at 20x using the Aperio Scanscope XT scanning system (Aperio Technologies, Inc., Vista, CA, USA) to obtain whole-tissue fields of view. Digital slides were visualised using ImageScope software. High-power imaging was performed using an Olympus BX61 upright microscope (Olympus, Tokyo, Japan).

2.9.4 Stereology

All stereological analyses were performed by myself blinded to treatment groups.

Glomerular number estimation

A combined stereological-histochemical approach using the physical disector/fractionator method (Cullen-McEwen *et al.*, 2012) was used to determine glomerular number in P21 male (N=11 per treatment group) and female offspring kidneys (N=8 per treatment group). Nephrogenesis in the mouse is complete by P4, thereby allowing estimation of final nephron endowment in P21 kidneys (Hartman *et al.*, 2007; Brunskill *et al.*, 2011b; Rumballe *et al.*, 2011). P21 kidneys were exhaustively sectioned at 5 μm . A sampling fraction (SSF, the total number of sections advanced between sections pairs) of 100 was chosen to generate 10 section pairs across the length of the kidney (n^{th} and $n^{\text{th}+2}$, where n is the first pair). Sections were stained with peanut agglutinin (PNA) histochemistry as described in Section 2.9.3.

The entire first section (n) was projected onto a monitor. The kidney was delineated and all PNA-positive glomeruli were marked. Next, the $n^{\text{th}+2}$ section was projected onto the screen with the outline and PNA-positive markings of the nth sections still visible. PNA-positive glomeruli present in the n^{th} section but not present in the $n^{\text{th}+2}$ section were counted. Secondly, PNA-positive structures present in the $n^{\text{th}+2}$ section but not present in the n^{th} section were counted. This method was repeated for each of the 9 remaining section pairs. Total glomerular number (N_{glom}) was estimated from the following equation:

$$N_{\text{glom}} = \text{SSF} \times \left(\frac{1}{2}\right) \times \left(\frac{1}{2}\right) \times Q^{-}$$

Where Q^{-} refers to the total number of PNA-positive structures. The two $\frac{1}{2}$ terms relate to the disector pair sections and to account for two-directional counting of the section pairs.

A randomly selected kidney was counted blindly on three separate occasions throughout the counting process to determine a coefficient of variation.

Kidney volume

Kidney volume at P21 and 12 months of age was estimated using the “paint into contour feature” within StereoInvestigator Software (MBF Biosciences). Each section (10 per kidney)

was mounted on a Zeiss Axioplan 2 light microscope, viewed at 2.5x and delineated. The area (A) within the contour was determined by the StereoInvestigator software and kidney volume (V_{kid}) was estimated with the following formula:

$$V_{\text{kid}} = \text{SSF} \times \Delta \times \sum_{i=1}^n A$$

Where Δ is section thickness and $\sum A$ is the sum of the areas of all 10 kidney sections sampled.

Renal tubule lengths

Renal tubule lengths (proximal tubule [PT], thin descending limb of Henle [TDLH], distal tubule [DT] and collecting duct [CD]) at P21 and 12 months of age were assessed in control and hypoxia-exposed offspring using a combination of immunohistochemistry and unbiased stereology. This methodology is described in depth in *Chapter 5*.

In brief, 3 sets of 10 evenly spaced sections of 5 μm thickness (Δ) were collected across the length of each kidney (simultaneously with section collection for glomerular estimation). Each set of 10 sections per kidney were immunohistochemically stained with anti-Aquaporin-1 (Aqp1) to identify the PT and TDLH, anti-Tamm Horsfall-glycoprotein to identify the DT, and anti-Aquaporin-2 (Aqp2) to identify the collecting duct (described in depth in Section 2.9.3). The cycloid arcs test system within the StereoInvestigator software was used to estimate renal tubule lengths. Each section was delineated at low power (X 2.5) and then viewed at high power (X 40) using a Zeiss Axioplan 2 light microscope with X-Y-Z stage control attached to StereoInvestigator software. Each section was sampled using a systemic random sampling grid (450 μm x 450 μm), with a minimum of 30 sites sampled per kidney section. Within each grid, cycloid probes of 106.1 μm in length and associated test points were overlaid. Test points that fell on renal tissue were marked as well as the number of cycloid intersections with immuno-positive tubules. Length density (L_v) for each kidney was generated by the software using the following formula:

$$L_v = (2/\Delta) \times (p/l) \times (\sum_{i=1}^n I_i) / (\sum_{i=1}^n P_i)$$

Where p/l is test points per unit length of cycloid, I_i is the number of intersections between cycloids and immuno-positive renal tubules and P_i is the number of test points falling within the renal tubule sampling frame.

The absolute length (\hat{L}) of each tubular segment was determined by multiplying length density (L_v) with kidney volume (V_{kid}).

2.9.5 *Histomorphometric analyses*

All histomorphometric analyses were performed by a researcher blinded to treatment groups.

Determining collagen and elastin content in the aorta

Transverse aortic sections were taken at 5 μm in paraffin. Sections were stained with Masson's Trichrome to assess collagen content and Verhoeff's van Gieson elastin stain to detect elastin expression. Slides were imaged using a 20x objective on an Olympus BX61 microscope. Masson's Trichrome-stained aortic sections were graded by a blinded observer as showing 0-10% media collagen content (0), 10-25% media collagen content (1), 25-50% media collagen content (2), or 50-75% media collagen content (3).

Elastin content was evaluated by subtracting background, converting image to binary and calculating the percentage of black (elastin) and white pixels. Three fields of view were examined on three separate aorta slides for each stain. The mean value of collagen and elastin content was reported.

Semi-quantitative analysis of the kidney

Glomerular cross-sectional area was quantified in PAS-stained sections at P21, 2 months, 4 months and 12 months using ImageScope software. Tuft area was measured in 30 glomeruli per kidney in which the vascular pole was evident.

The ratio of renal cortex to renal medulla at P21, 2 months, 4 months and 12 months was determined in midline PAS-stained kidney sections. The cortex area, defined as the area superficial to the arcuate arteries and containing predominantly proximal tubules, and medulla area were measured using ImageScope software and the ratio determined.

Renal and cardiac fibrosis

Fibrosis was assessed in adult hearts and kidneys using Masson's trichrome, which stains collagen fibres a bright blue easily distinguishable from cardiac muscle and renal tubules.

Interstitial fibrosis

Sections were projected onto a screen at X 20. A 1 x 1 cm grid was projected over the section to yield ~450 points. Points that intersected with collagen in the interstitium were counted and expressed as a percentage of the total number of points falling on cardiac/renal tissue. Four fields of view were analysed per sample.

Perivascular fibrosis

Kidney and heart sections stained with Masson's trichrome were projected onto a screen. Arterioles were identified and randomly assigned a number. Two arterioles were randomly selected for analysis as described by Lim and colleagues (2006). Areas of adventitial collagen were measured using ImageScope software, and normalised to vessel lumen diameter. Values were averaged for each animal.

Histopathology of kidney and hearts sections

In addition, an expert veterinary pathologist assessed sections (PAS and Masson's trichrome for each sample) from 12-month-old mouse kidneys and hearts and provided detailed pathological reports. Each kidney/heart was graded on a four-point scale of pathology: histologically unremarkable (0), minimal (1), mild (2), moderate (3) and severe (4).

Collecting duct cell composition in the kidney

To quantify the number of principal and intercalated cells in the cortical collecting duct and medullary collecting duct, the number of cells that exhibited immunoreactivity for AQP2 and V-ATPase were counted and expressed as a percentage of the total number of cells in the different tubule segments. Twenty to 30 fields of view were selected systematically and randomly from 3 slides, and 100-250 cells were counted per animal.

Cryogenic sectioning

Kidneys were fixed in 4% PFA for 30 min to 2 hours (depending on sample size) and transferred to 30% sucrose overnight at 4 °C. A Coplin jar filled with isopentane was chilled in dry ice. A transverse cut was made to separate kidneys into two halves. The kidneys were

embedded in a mould counting Optical Cutting Temperature (OCT) compound (Ted Pelle, Redding, CA, USA) with the flat cut surface facing down. The OCT was frozen by floating the moulds on the chilled isopentane, and then stored at -80 °C. Tissue blocks were then exhaustively sectioned at 4 µm on a Thermo Cryostar NX70. Sections were transferred to Superfrost + slides and stored at -80 °C.

Immunofluorescence

Frozen sections were blocked using 10% serum in PBS for 1 h at room temperature, followed by incubation with anti-goat AQP2 (1:200, sc-9882, Santa Cruz) and anti-rabbit V-ATPase (1:200, sc-20943, Santa Cruz) for 1h at room temperature. Slides were incubated with Alexa Fluor 488 goat anti-rabbit (1:400, A11011) and Alexa Fluor 555 donkey anti-goat (1:400, cat #) for 1 h at room temperature and counterstained with DAPI for 3 min. Sections were visualised using an Olympus BX61 fluorescent microscope.

2.10 Statistical analyses

Analyses were performed using GraphPad Prism 6 software and IBM SPSS. All data is presented as mean ± SEM. Offspring body and organ weights were analysed as litter averages. Two-way analysis of variance (ANOVA) with Bonferroni *post hoc* tests with treatment and sex/postnatal diet as variables were used to analyse most data in *Chapter 3, 4* and *6* unless otherwise specified. A multivariate analysis (MANOVA) was used to examine differences between blood pressure parameters of control and hypoxia-exposed offspring, with prenatal treatment and time period as dependent variables in *Chapter 4*. A one-way ANOVA was used to compare ontogeny data of renal tubule lengths in *Chapter 5*; a Student's t test was used to compare data from 12-month-old offspring fed the normal salt and high salt diets in *Chapter 5*. A Pearson's correlation coefficient was also used to determine the relationship between collecting duct cell composition and response to a water deprivation challenge in *Chapter 6*. All data was subject to normality and variance testing and appropriate substitute test utilised when required. P<0.05 was regarded as being significant.

Chapter 3

This chapter has been published in its entirety as:

Walton, S.L., Singh, R.R., Tan, T., Paravicini, T.M., & Moritz, K.M. (2016). *Late gestational hypoxia and a postnatal high salt diet programs endothelial dysfunction and arterial stiffness in adult mouse offspring*. *The Journal of Physiology*, 594(5): 1451-63

Contributor	Statement of contribution
Walton, S.L.	Animal treatment and tissue collection (80%) Pressurised myography (50%) Histological analysis (100%) Interpreting results (70%) Writing and editing manuscript (60%) Study design (10%)
Singh, R.R.	Animal treatment and tissue collection (20%) Study design (20%) Writing and editing manuscript (10%)
Tan, T.	Pressurised myography (50%)
Paravicini, T.M.	Interpreting results (15%) Writing and editing manuscript (15%) Study design (35%)
Moritz, K.M.	Interpreting results (15%) Writing and editing manuscript (15%) Study design (35%)

Late gestational hypoxia and a postnatal high salt diet programs endothelial dysfunction and arterial stiffness in adult mouse offspring.

Sarah L Walton¹, Reetu R Singh^{1,2}, Tiffany Tan¹, Tamara M Paravicini^{1,3*} and Karen M Moritz^{1*}

*Contributed equally

¹School of Biomedical Sciences, The University of Queensland, St Lucia, Queensland, Australia

²Department of Physiology, Monash University, Clayton, Victoria, Australia

³School of Medical Sciences, RMIT University, Bundoora, Victoria, Australia

Address for correspondence:

Associate Professor Karen Moritz

School of Biomedical Sciences

University of Queensland

St Lucia, Brisbane

QLD, 4072

Email: k.moritz@uq.edu.au

Key points summary

- Maternal hypoxia is a common perturbation that leads to growth restriction and may program vascular dysfunction in adult offspring.
- An adverse prenatal environment may render offspring vulnerable to increased cardiovascular risk when challenged with a “second hit” such as high salt diet.
- We investigated whether maternal hypoxia impaired vascular function, structure and mechanics in mouse offspring, and if this was exacerbated by excess dietary salt intake in postnatal life.
- Maternal hypoxia predisposed adult male and female offspring to endothelial dysfunction.
- The combination of prenatal hypoxia and high dietary salt intake caused significant stiffening of mesenteric arteries, and altered structural characteristics of the aorta consistent with vascular stiffening.
- Our results suggest that prenatal hypoxia combined with a high salt diet in postnatal life can contribute to vascular dysfunction.

Abstract

Gestational hypoxia and high dietary salt intake have both been associated with impaired vascular function in adulthood. Using a mouse model of prenatal hypoxia, we examined whether a chronic high salt diet had an additive effect in promoting vascular dysfunction in offspring. Pregnant CD1 dams were placed in a hypoxic chamber (12% O₂) or housed under normal conditions (21% O₂) from E14.5 until birth. Gestational hypoxia resulted in reduced body weight of both male and female offspring at birth. This restriction in body weight persisted until weaning after which time the animals underwent catch-up growth. At 10 weeks of age, a subset of offspring was placed on a high salt diet (5% NaCl). Pressurised myography of mesenteric resistance arteries at 12 months of age showed that both male and female offspring exposed to maternal hypoxia had significantly impaired endothelial function as demonstrated by impaired vasodilation to acetylcholine but not sodium nitroprusside. Endothelial dysfunction caused by prenatal hypoxia was not exacerbated by postnatal consumption of a high salt diet. Prenatal hypoxia increased microvascular stiffness in male offspring. The combination of prenatal hypoxia and a postnatal high salt diet caused a leftward shift in the stress-strain relationship in both sexes. Histopathological analysis of aortic sections revealed loss of elastin integrity and increased collagen, consistent with increased vascular stiffness. These results demonstrate that prenatal hypoxia programs endothelial dysfunction in both sexes. A chronic high salt diet in postnatal life had an additive deleterious effect on vascular mechanics and structural characteristics in both sexes.

Abbreviations

C, control; CHS, control offspring fed high salt; CNS, control offspring fed normal salt; CSA, cross sectional area; CVD, cardiovascular disease; EC_{50} , half maximal effective concentration; H, hypoxia; HS, high salt; HHS, hypoxia offspring fed high salt; HNS, hypoxia offspring fed normal salt; KPSS, high potassium physiological salt solution; $KPSS_{max}$, maximum vessel contraction to KPSS; NO, nitric oxide; NS, normal salt; P, postnatal day; PE, phenylephrine; R_{max} , maximum relaxation; SNP, sodium nitroprusside.

Introduction

Cardiovascular disease (CVD) is recognised as the leading cause of global mortality. The development of CVD is associated with risk factors such as smoking, age, gender and hypertension (Mozaffarian *et al.*, 2008). Epidemiological evidence suggests that CVD can also be linked to poor development in early life (Barker, 2002). Adverse conditions during fetal life may require the fetus and placenta to make adaptations to organogenesis in order to remain viable in the short-term but these adaptations frequently lead to intrauterine growth restriction (Barker, 1998). If these adaptations occur during critical periods of development, permanent changes in organ structure and function can occur, leading to poor health outcomes and increased susceptibility to disease in adulthood. This concept is known as developmental programming (Barker, 1995, 1998).

Impaired oxygen supply to the fetus is a common clinical complication during pregnancy and can arise from living at high altitude (Giussani *et al.*, 1993), maternal smoking (Bulterys *et al.*, 1990), and poor placentation leading to reduced fetoplacental perfusion (Krebs *et al.*, 1996). Mild, acute forms of hypoxia initiate the centralisation of blood flow away from the peripheral circulations to the heart and brain (Giussani *et al.*, 1993; Baschat *et al.*, 1997). Although this adaptation is necessary for the immediate preservation of critical organs, the decreased blood flow can impair development of peripheral organs resulting in insignificant adverse consequences in later life. If the hypoxic insult is prolonged, these immediate adaptations may be sustained and result in compromised growth *in utero*. Low birth weight and brain sparing following chronic *in utero* hypoxia has been observed across all species studied including the human (Wladimiroff *et al.*, 1986; Giussani *et al.*, 2001), chick (Mulder *et al.*, 2002; Giussani *et al.*, 2007) and rat (Williams *et al.*, 2005a; Williams *et al.*, 2005b), and this is associated with increased risk of CVD later in life.

Endothelial dysfunction and arterial stiffness are both associated with CVD in adulthood (Benetos *et al.*, 2002). Interestingly, impaired peripheral vascular endothelial function has been demonstrated in low birth weight infants (Norman & Martin, 2003), children (Martin *et al.*, 2000) and young adults (Goodfellow *et al.*, 1998; Leeson *et al.*, 2001), and increased arterial stiffness has been shown to contribute to elevated blood pressure in the human population (te Velde *et al.*, 2004). There is now substantial evidence from animal models that perturbations *in utero* such as hypoxia (Williams *et al.*, 2005b), Vitamin D deficiency (Tare

et al., 2011) and undernutrition (Brawley *et al.*, 2003) can also program vascular dysfunction in adulthood. Offspring born to rats that were exposed to chronic hypoxia during late pregnancy develop endothelial dysfunction (Williams *et al.*, 2005b; Giussani *et al.*, 2012) and enhanced myogenic tone (Hemmings *et al.*, 2005). These factors may contribute to the increased arterial blood pressure observed in middle-aged rats exposed to chronic hypoxia *in utero* (Rook *et al.*, 2014). Furthermore, ventricular (Camm *et al.*, 2010) and aortic wall thickening (Rouwet *et al.*, 2002; Giussani *et al.*, 2012) and increased susceptibility to cardiac ischemia-reperfusion injury (Xu *et al.*, 2006; Xue & Zhang, 2009) have also been reported in adult rodents prenatally exposed to hypoxia. Together, these studies demonstrate that prenatal hypoxia can significantly elevate the propensity to develop CVD in adulthood.

Importantly, prenatally-programmed vulnerability to CVD may be exacerbated by a postnatal “second-hit” such as a chronic high salt diet (Ruta *et al.*, 2010), high-fat diet (Rueda-Clausen *et al.*, 2012) and aging. In a rat model of prenatal hypoxia, vascular alterations such as increased myogenic tone only arose in aged animals greater than 6 months of age (Hemmings *et al.*, 2005). In the same model, the combination of prenatal hypoxia and postnatal consumption of a high fat diet increased susceptibility to cardiac and vascular pathologies (Rueda-Clausen *et al.*, 2012). In Western societies, diets are often not only high in fat but also high in salt (Cordain *et al.*, 2005). A chronic increase in dietary sodium intake has been shown to result in increased vascular stiffness in mice (Yu *et al.*, 2004), and enhanced vasoconstrictor responsiveness in the rat (Sofola *et al.*, 2002). Whilst a high salt diet has been shown to exacerbate disease outcomes following maternal protein restriction (Woods *et al.*, 2004) and a congenital nephron deficit (Ruta *et al.*, 2010), no study has yet investigated whether the adverse vascular outcomes following prenatal hypoxia are exacerbated by a high salt diet.

In this study, we used our recently reported model of prenatal hypoxia in the mouse (Cuffe *et al.*, 2014a; Cuffe *et al.*, 2014b) to assess the impact of chronic late gestational hypoxia on microvascular structure and function in aged male and female offspring. In particular, we aimed to examine whether chronic high dietary sodium intake could exacerbate any deficits in microvascular structure and function. We hypothesised that arteries from hypoxia-exposed offspring would have endothelial dysfunction and increased vascular stiffness. In addition, we hypothesised that these alterations would be exacerbated by high dietary sodium intake.

Methods

Ethics approval

All experiments were approved in advance by the University of Queensland animal ethics committee and were conducted in accordance with the Australian Code of Practice for the Care and Use of Animals for Scientific Purposes.

Animal treatment: maternal hypoxia

At embryonic day (E) 14.5 of pregnancy, time-mated CD-1 mice were randomly allocated to normoxic room conditions (control [C]; N=21) or housed inside a hypoxic chamber continuously flushed with nitrogen gas to maintain an oxygen concentration of 12% (hypoxia [H]; N=22) for the remainder of pregnancy. Food and water was provided *ad libitum*. Body weight, food and water consumption were monitored daily throughout the experimental protocol. This experimental protocol does not result in changes in maternal food intake and weight gain, and is thus not compromised by maternal undernutrition (Cuffe *et al.*, 2014a). The dams were removed from the hypoxic chamber upon littering down (postnatal day P0). A subset of dams and offspring (C: N=10; H: N=11) were culled at P0. Pup body weight was recorded, and maternal and pup blood was collected for measurement of haematocrit. The remaining offspring remained with their mothers until weaning at P21, and were then weighed weekly for the duration of the study.

Dietary intervention: chronic high salt diet.

A subset of animals aged 10 weeks (N=11 per sex per treatment, 1-2 animals from each litter) was randomly allocated to receive a high salt (HS) diet (5% NaCl [wt/wt]; modified AIN 93M, SF05-023, Specialty Feeds). The remaining animals (N=11 per sex per treatment) were maintained on a matched control normal salt (NS) diet (0.26% NaCl [wt/wt]; AIN 93M, Specialty Feeds). Food and water consumption were monitored for the first 5 days of diet administration to ensure animals adjusted to the dietary change. Animals were maintained on the appropriate diet until post-mortem at 12 months of age.

Urinalysis

Aged offspring (12 ± 0.5 months) were housed in individual metabolic cages for 24h (food and water provided *ad libitum*) to measure urinary flow rates and electrolyte excretion. All animals were acclimatised to the metabolic cages on two consecutive days prior to the

experiment. Urine was collected and stored at -20°C for later analysis. Urinary sodium, chloride and potassium concentrations were measured using a COBAS Integra 400 Plus analyser.

Pressurized myography

Following completion of renal function measurements, animals were euthanized by CO₂ inhalation (N=6-10 per group). Second-order mesenteric arteries were dissected from connective tissue, placed in physiological salt solution (composition in mmol/L: NaCl 118, KCl 4.65, MgSO₄ 1.18, KH₂PO₄ 1.18, CaCl₂ 2.5, NaHCO₃ 25 mM, glucose 5.5 mM, EDTA 0.026 mM), mounted in a pressurised myograph and the intraluminal pressure gradually increased to 45 mm Hg. Maximal vessel contractility was determined using high potassium physiological salt solution (KPSS) containing equimolar substitution of KCl for NaCl. Vessel contractility was assessed by cumulative concentration-response curves to phenylephrine (PE; 10⁻⁹ to 10⁻⁴ mol/L). The contractile responses were expressed as a percentage of the maximum response to KPSS (KPSS_{max}). Endothelium-dependent and endothelium-independent relaxations were assessed in vessels submaximally constricted with PE (70% of KPSS_{max}), using acetylcholine (ACh; 10⁻⁹ to 10⁻⁴ mol/L) and sodium nitroprusside (SNP; 10⁻¹⁰ to 10⁻⁴ mol/L) respectively. Relaxation responses were expressed as the percentage relaxation from the PE-induced contraction. Non-linear regression (Graphpad Prism 6) was used to determine the pEC₅₀ and maximum response (R_{max}) for each vessel. To measure vascular structure and mechanics, vessels were superfused with Ca²⁺-free physiological salt solution containing 1 mmol/L of EGTA to remove intrinsic tone. Intraluminal pressure was increased stepwise from 3 to 140 mm Hg and lumen diameter and wall thickness measured at each pressure. Medial cross-sectional area (CSA), distensibility, circumferential stress and strain were calculated as previously described (Virdis *et al.*, 2002; Iglarz *et al.*, 2003).

Histomorphometric analyses of the aorta

Thoracic aortas were fixed in 4% paraformaldehyde before processing to paraffin. Transverse aortic sections were taken at 5 μm. Sections were stained with Masson's Trichrome to assess collagen content and Verhoeff's van Gieson elastin stain to detect elastin expression. Slides were imaged using a 20x objective on an Olympus BX61 microscope. Masson's Trichrome-stained aortic sections were graded by a blinded observer as showing 0-10% media collagen content (0), 10-25% media collagen content (1), 25-50% media collagen content (2), or 50-

75% media collagen content (3). Elastin content was evaluated by subtracting background, converting image to binary and calculating the percentage of black (elastin) and white pixels.

Statistical analysis

All data are presented as mean \pm SEM. Maternal haematocrit was analysed via a Student's t test. Offspring haematocrit and body weight at P0 were analysed by 2-way ANOVA examining the effects of prenatal hypoxia (P_{trt}) and sex (P_{sex}). Data for body and organ weights, urinalysis and vascular parameters of male and female offspring at 12 months of age were analysed separately. These data were analysed by 2-way ANOVA examining the effects of prenatal hypoxia (P_{trt}) and postnatal high salt diet (P_{diet}). Bonferroni post-hoc tests were used when necessary, with significance taken at $P < 0.05$.

Results

Offspring weights and growth

Maternal ($P=0.007$, Figure 1A) and pup haematocrit ($P_{\text{trt}}<0.0001$, Figure 1B) was elevated in hypoxia-exposed animals. Litter size did not differ between treatment groups (C: 14 ± 1 , H: 14 ± 1). At P0, body weights for both males and females (litter averages) were reduced by approximately 12% in animals from hypoxia-exposed dams (male C: 1.73 ± 0.5 g, male H: 1.52 ± 0.03 g, female C: 1.67 ± 0.04 g, female H: 1.46 ± 0.02 g; $P_{\text{trt}}<0.0001$; Figure 1C). Hypoxia-exposed animals remained lighter than control counterparts by approximately 7% at the weaning age of P21 (male C: 11.9 ± 0.3 g, male H: 11.0 ± 0.3 g, female C: 11.2 ± 0.3 g, female H: 10.4 ± 0.4 g; $P_{\text{trt}}=0.01$). There was no difference in body weights between treatment groups in male (Figure 2A) or female (Figure 2B) offspring from 3 to 12 months of age.

Urinalysis

Urinary excretion of electrolytes did not differ between control and hypoxic-exposed animals. However, sodium and chloride excretion was significantly elevated in male and female offspring (~3-5 fold) fed the high salt (HS) diet compared to those on the control normal salt (NS) diet (data not shown). Potassium excretion did not differ between dietary groups.

Microvascular function

The maximal contractile response to high potassium physiological salt solution (KPSS) was not affected by maternal hypoxia but was enhanced in male offspring maintained on the HS diet compared to the normal salt NS diet (CNS: 47.4 ± 1.0 ; HNS: 47.4 ± 1.0 ; CHS: 52.7 ± 0.9 ; HHS: $55.6 \pm 2.2\%$; $P_{\text{diet}}<0.0001$). The maximum contractile response to phenylephrine was unaffected by prenatal hypoxia treatment or dietary HS intake (Figure 3A). However, sensitivity to phenylephrine was increased in animals maintained on the HS diet, irrespective of the maternal treatment ($P=0.008$; Figure 3A, table 1). The maximum dilator response to acetylcholine was significantly attenuated in male hypoxia-exposed offspring (Figure 3C, table 1) whilst the sensitivity to acetylcholine was similar in all groups. The reduced response to acetylcholine indicates impairment in endothelium-dependent relaxation, as responsiveness to the nitric oxide donor sodium nitroprusside was statistically similar in all treatment groups (Figure 3E, table 1). There was a trend towards reduced maximum relaxation to SNP in male offspring fed the high-salt diet, although this was not statistically significant (Table 1, $P=0.07$). In female offspring, the maximal response to KPSS did not differ between treatment

and dietary groups (CNS: 52.2 ± 1.9 ; HNS: 50.2 ± 2.3 ; CHS: 48.4 ± 1.4 ; HHS: $51.0 \pm 1.8\%$). Arteries from female offspring showed similar responsiveness to phenylephrine, regardless of treatment or dietary groups (Figure 3B, table 1). Evidence of endothelial dysfunction was also seen in female hypoxia-exposed offspring, which had reduced maximum responses to acetylcholine (Figure 3D, table 3). Sensitivity to acetylcholine (Figure 3D, table 1) and responsiveness to sodium nitroprusside (Figure 3F, table 1) did not differ between groups.

Vascular structure

Mesenteric arteries from male offspring all had similar lumen diameters (Figure 4A) and media:lumen ratios (Figure 4E) across increasing intraluminal pressures. No differences in lumen diameters and media:lumen ratios were observed at 45 mmHg, the pressure at which the functional experiments were conducted (Table 2). Male animals fed the HS diet, had decreased medial CSA ($P_{\text{diet}} = 0.03$; Figure 4C) compared to those on a NS diet. CSA did not differ in offspring from the hypoxia and control groups. In female offspring, neither the maternal hypoxia nor the HS diet had an effect on lumen diameter (Figure 4B), medial CSA (Figure 4D) or media:lumen ratio (Figure 4F) at any pressure (Table 2).

Vascular mechanics

There was a leftward shift in the stress-strain curve in arteries from males fed the high salt diet compared to those on the NS diet, indicating increased vessel stiffness (Figure 5A). This leftward shift was greatest in male HHS mesenteric arteries compared to NS arteries (Figure 5A). The rate constant of the stress-strain curve was greater in both male offspring fed a HS diet, and hypoxia-exposed male offspring ($P_{\text{trt}}=0.03$, $P_{\text{diet}}=0.02$; Table 3). In contrast, in female offspring, the combination of hypoxia and a HS diet shifted the stress-strain curve to the left, indicating increased vessel stiffness. This was accompanied by a significant increase in the rate constant of the stress-strain curve in HHS female arteries compared to other treatment groups ($P_{\text{diet}}=0.008$, $P_{\text{trt} \times \text{diet}}=0.03$; Table 3).

Aorta histology

Representative sections of male aortas from all treatment groups stained with Masson's Trichrome to detect collagen and Verhoeff's Van Gieson to detect elastin are shown in Figure 6. Significant collagen deposition can be observed in the media of aortas taken from control male offspring fed the HS diet. Equivalent levels of collagen deposition can be seen in aortas

taken from hypoxia males fed NS and HS diets. When estimated semi-quantitatively, the aortic collagen content score was increased ~2-fold in male ($P_{\text{diet}}=0.02$, Figure 7A) and female ($P_{\text{diet}}=0.007$, Figure 7B) offspring fed the high salt diet (Figure 6). Male but not female hypoxia-exposed offspring fed a NS diet also showed increased aortic collagen content.

Aortas of male CNS offspring presented elastin fibres laid down as concentric layers, and occupying the greatest proportion of media compared to other treatment groups (Figure 6; Figure 7C). Modest degeneration of elastin fibre integrity was observed in male CHS aortas (Figure 6). Elastin content was ~30% lower in aortas from male CHS aortas compared to male CNS aortas ($P_{\text{diet}}=0.04$, Figure 7C). Prenatal hypoxia caused marked fragmentation and disorganisation of the elastin fibres (Figure 6) and reduced elastin content in male ($P_{\text{trt}}=0.03$, Figure 7C) and female offspring ($P_{\text{trt}}=0.03$, Figure 7D). Degeneration of the elastin fibres was most pronounced in aortas of the HHS male, where disorganisation and discontinuity of the elastin fibre segments can clearly be observed in Figure 6. Elastin content in aortas of male HHS offspring was ~42% lower compared to elastin content in aortas of CHS offspring (Figure 7C). The HS diet reduced aortic elastin significantly in both female control and hypoxia-exposed offspring ($P_{\text{diet}}<0.0001$; Figure 7D).

Discussion

This study examined the effects of maternal hypoxia during late gestation, and determined how this gestational insult interacted with postnatal consumption of a chronic high salt diet to affect vascular function, structure and mechanics in adult offspring. Here we show for the first time that whilst prenatal hypoxia exposure alone caused mild endothelial dysfunction in mesenteric vessels, the combined insult of prenatal hypoxia and a chronic postnatal high salt diet caused significant stiffening of the mesenteric vasculature and altered extracellular matrix composition in the aorta, most notably a loss of elastin fibre integrity. Our results suggest that whilst prenatal hypoxia may be unavoidable, consuming a healthy diet, particularly with respect to sodium intake, may prevent or at least limit adverse vascular outcomes in adulthood.

During early life suboptimal influences such as maternal low protein diet (Brawley *et al.*, 2003), maternal high fat diet (Khan *et al.*, 2004) and Vitamin D insufficiency (Tare *et al.*, 2011) can program vascular dysfunction. In particular, endothelial dysfunction due to impaired responsiveness to endothelium-dependent vasodilators such as acetylcholine is commonly reported in models of developmental programming (for review, see Mcmillen & Robinson, 2005). In our model of prenatal hypoxia there was reduced acetylcholine-induced vasodilatation in offspring of both sexes, but no differences in vasodilator responses to the NO donor sodium nitroprusside. This suggests that the impaired vascular response to acetylcholine in hypoxia-exposed offspring is due to impaired endothelial function rather than decreased vascular smooth muscle sensitivity to NO-induced relaxation. This is consistent with previous reports using a model of prenatal hypoxia in the rat that showed impaired endothelial function in the resistance vasculature of hypoxia-exposed adult offspring (Hemmings *et al.*, 2005; Williams *et al.*, 2005b; Morton *et al.*, 2011). Notably, Morton and colleagues used Sprague-Dawley rats at 12 months (the same age used in our study) to show that prenatal hypoxia impaired flow-mediated vasodilation in both sexes. Whilst in this study we did not directly determine the mechanisms underlying this endothelial dysfunction, it may be due to reduced NO bioavailability associated with increased superoxide anion production as previously reported by Williams and colleagues (2005b). Increased oxidative stress in the fetal rat vasculature has been associated with endothelial dysfunction (Giussani *et al.*, 2012), suggesting that hypoxia-induced oxidative stress during fetal development can have adverse cardiovascular outcomes in later life.

In both the human population and animal models, endothelial dysfunction is associated with low birth weight (Leeson *et al.*, 2001). Our model of chronic hypoxia in the mouse led to low birth weight, and resulted in endothelial dysfunction in aged offspring. Importantly, our model of gestational hypoxia using the mouse is not confounded by maternal undernutrition (Cuffe *et al.*, 2014a). Similar models of maternal hypoxia during late gestation in the rat have reported significant reduction in maternal food intake during the time spent inside the hypoxia chamber (Williams *et al.*, 2005b; Camm *et al.*, 2010). Undernourishment during pregnancy alone has been shown to alter vascular function (Brawley *et al.*, 2003; Torrens *et al.*, 2009). Therefore the combination of reduction in maternal oxygen supply and reduced food consumption provides a dual insult to the developing fetus. Similarly, the vascular dysfunction seen in rat models of uteroplacental insufficiency may be attributable to a reduction in both oxygen and nutrient supply to the fetus (Tare *et al.*, 2012). Our findings suggest that fetal hypoxia alone is able to result in vascular dysfunction in offspring. Growth restriction was sustained in our model during lactation but substantial catch-up growth was observed post-weaning, both of which are predictors of adult-onset cardiovascular dysfunction. Reduced body weight pre-weaning may signify an impaired lactational environment, which has previously has been reported in a model of uteroplacental insufficiency in the rat (O'Dowd *et al.*, 2008). However, in our model, absolute growth during lactation was similar in the control and prenatal hypoxia groups. Sensitivity to vasodilators and resistance artery stiffness was improved when these growth-restricted offspring were cross-fostered onto healthy mothers to improve the lactational environment (Tare *et al.*, 2012). These studies highlight the importance of a healthy diet throughout lactation for growth-restricted offspring.

Vulnerability to CVD programmed *in utero* may be exacerbated by a postnatal “second-hit”, such as a high salt (Ruta *et al.*, 2010) or high fat diet (Rueda-Clausen *et al.*, 2012). The chronic high salt diet produced modest alterations to microvascular function in aged control and hypoxia-exposed male (but not female) offspring. To our knowledge, this is the first study to examine the impact of a chronic high salt diet in the CD-1 mouse strain and importantly, to examine these effects in both sexes. Our findings therefore warrant further investigation. Dietary salt loading to assess microvascular function has overwhelmingly been performed in the rat (Liu *et al.*, 1999; Sofola *et al.*, 2002). Sprague-Dawley rats fed a high

salt diet have increased small artery reactivity to vasoconstrictors but no overall impairment in endothelial function. However, the mechanism of acetylcholine-induced dilation was altered (Sofola *et al.*, 2002). Reduced endothelium-dependent responses associated with high salt intake have been reported in skeletal muscle arterioles (Boegehold, 1995), cerebral arterioles and small feed arteries of rat gracilis muscle (Liu *et al.*, 1997). However, many of these vascular function studies were performed following exposure to extremely high levels of sodium (7-10% NaCl) in the diet over an acute period, which has limited relevance to the human population. In the present study we have employed a more modest increase in dietary sodium (from 0.26% to 5%) across the adult lifespan of the mouse, which makes our studies of greater relevance. However, we cannot discount that more overt vascular deficits may be observed with a further increase in dietary sodium.

Vascular stiffening is a major risk factor for cardiovascular dysfunction. Increased vascular stiffness is associated with low birth weight in humans but also increases with age (Martin *et al.*, 2000; te Velde *et al.*, 2004) and other cardiovascular risk factors such as hypertension, diabetes and tobacco smoking (Benetos *et al.*, 2002). A striking finding to emerge from the present study was that vascular stiffness was markedly exacerbated by the combination of prenatal hypoxia and a postnatal high salt diet. Importantly, these changes in the stress-strain relationship of the microvasculature was geometry-independent, as no changes were observed in media:lumen ratios. Prenatal hypoxia alone had a limited effect on vascular stiffness, which is consistent with observations in the aged rat that were exposed to hypoxia during late gestation (Morton *et al.*, 2011). Given that vascular stiffening occurred in the absence of geometric changes, we examined the deposition and organisation of aortic extracellular matrix proteins, particularly collagen and elastin, to determine the mechanical properties of vessel walls. We found reduced elastin content and significant disorganisation and fragmentation of the elastin layers in hypoxia-exposed offspring. The synthesis of elastin fibres responsible for vessel elasticity is restricted to fetal and early postnatal life and is therefore vulnerable to influences early in life such as chronic hypoxia (Davis, 1995). However, during the postnatal period elastin fibres are sensitive to degradation by matrix metalloproteinases and elastases produced by inflammatory cells during the pathogenesis of vascular lesions such as aneurisms and arteriosclerosis (for review, see Galis & Khatri, 2002). Although the high salt diet reduced elastin content in both treatment groups, the effect was significantly greater in hypoxia-exposed offspring, particularly males. The significant

disorganisation and loss of elastin fibres may be due to a prenatal impairment in elastin synthesis and enhanced postnatal degradation of fibres, consistent with vascular injury. Substantial collagen accumulation was observed in hypoxia-exposed male offspring, but was most prominent in offspring fed the high salt diet irrespective of prenatal treatment. Dietary salt intake is a known contributor to fibrosis in the kidney, heart and vasculature (Yu *et al.*, 2004), which in turn leads to vascular stiffening and increased cardiovascular risk. We observed slight differences between males and females in the histological changes in response to prenatal hypoxia and postnatal high salt diet. Most notably, hypoxia alone did not increase aortic collagen deposition in females, whilst it did in the male offspring. Since the female hormonal milieu contains oestrogen, a hormone with vasoprotective effects, female offspring may be protected against a mild prenatal insult such as hypoxia (Mendelsohn & Karas, 1999). The postnatal high salt diet increased aortic collagen deposition in both sexes, suggesting that the protective effects of oestrogen on the vasculature may be diminished in the ageing female mouse. This is observed in the human population where rates of CVD are higher in post-menopausal women than pre-menopausal women, associated with the declining plasma oestrogen levels with age (Khalil, 2010). As the loss of elastin fibre integrity and increased media collagen content were observed in a compliance vessel, we cannot discount that the pathophysiology could present differently in the resistance vasculature. However, these changes are indicative of vascular stiffening and are consistent with the reduced vascular compliance observed in the microvasculature of hypoxia-exposed offspring fed the high salt diet.

In conclusion, we report for the first time that vascular stiffening in aged offspring exposed to gestational hypoxia is markedly exacerbated by a postnatal high salt diet. The changes in aortic extracellular matrix composition most likely underlie the increase in vascular stiffness in hypoxia-exposed offspring fed the chronic high salt diet. Prenatal hypoxia alone impaired endothelial function in adult male and female mice, highlighting that the endothelium, a vital regulator of vascular tone, is susceptible to adverse environmental conditions *in utero*. Since high dietary salt intake is endemic in Western societies, such adverse changes in vascular function and wall stiffness may be inadvertently enhanced by suboptimal dietary choices. This may have serious consequences for individuals predisposed to CVD because of their *in utero* environments. It is advised that individuals born of low birth weight take precautions to ensure dietary sodium intake in adult life is not excessive to limit adverse cardiovascular

outcomes.

Additional information

Competing interesting

The authors declare no competing interests.

Author contributions

S.L.W., R.R.S., T.M.P. and K.M.M. were responsible for conception and design of the experiments. S.L.W. and T.T. were responsible for the collection, analysis and interpretation of data. All authors were involved in drafting the article and revising it critically for intellectual content. All authors approve the final submission.

Funding

This project was funded by the National Health and Medical Research Council (NHMRC-APP1009338) of Australia. K.M.M. was supported by fellowships provided by the NHMRC and S.L.W. was supported by an Australian Postgraduate Award.

References

- Barker DJ. (1995). Intrauterine programming of adult disease. *Mol Med Today* **1**, 418-423.
- Barker DJ. (1998). In utero programming of chronic disease. *Clin Sci* **95**, 115-128.
- Barker DJP. (2002). Fetal programming of coronary heart disease. *Trends Endocrinol Metabol* **13**, 364-368.
- Baschat AA, Gembruch U, Reiss I, Gortner L & Diedrich K. (1997). Demonstration of fetal coronary blood flow by Doppler ultrasound in relation to arterial and venous flow velocity waveforms and perinatal outcome--the 'heart-sparing effect'. *Ultrasound Obstet Gynecol* **9**, 162-172.
- Benetos A, Waeber B, Izzo J, Mitchell G, Resnick L, Asmar R & Safar M. (2002). Influence of age, risk factors, and cardiovascular and renal disease on arterial stiffness: clinical applications. *Am J Hypertens* **15**, 1101-1108.
- Boegehold MA. (1995). Flow-dependent arteriolar dilation in normotensive rats fed low- or high-salt diets. *Am J Physiol* **269**, H1407-1414.
- Brawley L, Itoh S, Torrens C, Barker A, Bertram C, Poston L & Hanson M. (2003). Dietary protein restriction in pregnancy induces hypertension and vascular defects in rat male offspring. *Pediatr Res* **54**, 83-90.
- Bulterys MG, Greenland S & Kraus JF. (1990). Chronic fetal hypoxia and sudden infant death syndrome: interaction between maternal smoking and low hematocrit during pregnancy. *Pediatrics* **86**, 535-540.
- Camm EJ, Hansell JA, Kane AD, Herrera EA, Lewis C, Wong S, Morrell NW & Giussani DA. (2010). Partial contributions of developmental hypoxia and undernutrition to prenatal alterations in somatic growth and cardiovascular structure and function. *Am J Obstetr Gynecol* **203**, 495.e424-495.e434.

Cordain L, Eaton SB, Sebastian A, Mann N, Lindeberg S, Watkins BA, O'Keefe JH & Brand-Miller J. (2005). Origins and evolution of the Western diet: health implications for the 21st century. *Am J Clin Nutr* **81**, 341-354.

Cuffe J, Walton S, Singh R, Spiers J, Bielefeldt-Ohmann H, Wilkinson L, Little M & Moritz K. (2014a). Mid-to late term hypoxia in the mouse alters placental morphology, glucocorticoid regulatory pathways and nutrient transporters in a sex-specific manner. *J Physiol* **592**, 3127-3141.

Cuffe J, Walton S, Steane S, Singh R, Simmons D & Moritz K. (2014b). The effects of gestational age and maternal hypoxia on the placental renin angiotensin system in the mouse. *Placenta* **35**, 953-961.

Davis EC. (1995). Elastic lamina growth in the developing mouse aorta. *J Histochem Cytochem* **43**, 1115-1123.

Galis ZS & Khatri JJ. (2002). Matrix metalloproteinases in vascular remodeling and atherogenesis: the good, the bad, and the ugly. *Circ Res* **90**, 251-262.

Giussani DA, Camm EJ, Niu Y, Richter HG, Blanco CE, Gottschalk R, Blake EZ, Horder KA, Thakor AS, Hansell JA, Kane AD, Wooding FBP, Cross CM & Herrera EA. (2012). Developmental programming of cardiovascular dysfunction by prenatal hypoxia and oxidative stress. *PLoS ONE* **7**, e31017.

Giussani DA, Phillips PS, Anstee S & Barker DJ. (2001). Effects of altitude versus economic status on birth weight and body shape at birth. *Pediatr Res* **49**, 490-494.

Giussani DA, Salinas CE, Villena M & Blanco CE. (2007). The role of oxygen in prenatal growth: studies in the chick embryo. *J Physiol* **585**, 911-917.

Giussani DA, Spencer JA, Moore PJ, Bennet L & Hanson MA. (1993). Afferent and efferent components of the cardiovascular reflex responses to acute hypoxia in term fetal sheep. *J Physiol* **461**, 431-449.

Goodfellow J, Bellamy MF, Gorman ST, Brownlee M, Ramsey MW, Lewis MJ, Davies DP & Henderson AH. (1998). Endothelial function is impaired in fit young adults of low birth weight. *Cardiovasc Res* **40**, 600-606.

Hemmings DG, Williams SJ & Davidge ST. (2005). Increased myogenic tone in 7-month-old adult male but not female offspring from rat dams exposed to hypoxia during pregnancy. *Am J Physiol Heart Circ Physiol* **289**, H674-H682.

Iglarz M, Touyz RM, Amiri F, Lavoie M-F, Diep QN & Schiffrin EL. (2003). Effect of peroxisome proliferator-activated receptor- α and - γ activators on vascular remodeling in endothelin-dependent hypertension. *Arterioscler Thromb Vasc Biol* **23**, 45-51.

Khalil RA. (2010). Potential approaches to enhance the effects of estrogen on senescent blood vessels and postmenopausal cardiovascular disease. *Cardiovasc Hematol Agents Med Chem* **8**, 29-46.

Khan I, Dekou V, Hanson M, Poston L & Taylor P. (2004). Predictive adaptive responses to maternal high-fat diet prevent endothelial dysfunction but not hypertension in adult rat offspring. *Circulation* **110**, 1097-1102.

Krebs C, Macara LM, Leiser R, Bowman AW, Greer IA & Kingdom JC. (1996). Intrauterine growth restriction with absent end-diastolic flow velocity in the umbilical artery is associated with maldevelopment of the placental terminal villous tree. *Am J Obstet Gynecol* **175**, 1534-1542.

Leeson C, Kattenhorn M, Morley R, Lucas A & Deanfield J. (2001). Impact of low birth weight and cardiovascular risk factors on endothelial function in early adult life. *Circulation* **103**, 1264-1268.

Liu Y, Fredricks KT, Roman RJ & Lombard JH. (1997). Response of resistance arteries to reduced PO₂ and vasodilators during hypertension and elevated salt intake. *Am J Physiol* **273**, H869-877.

Liu Y, Rusch NJ & Lombard JH. (1999). Loss of endothelium and receptor-mediated dilation in pial arterioles of rats fed a short-term high salt diet. *Hypertension* **33**, 686-688.

Martin H, Hu J, Gennser G & Norman M. (2000). Impaired endothelial function and increased carotid stiffness in 9-year-old children with low birthweight. *Circulation* **102**, 2739-2744.

McMillen IC & Robinson JS. (2005). Developmental origins of the metabolic syndrome: prediction, plasticity, and programming. *Physiol Rev* **85**, 571-633.

Mendelsohn ME & Karas RH. (1999). The protective effects of estrogen on the cardiovascular system. *N Engl J Med* **340**, 1801-1811.

Morton JS, Rueda-Clausen CF & Davidge ST. (2011). Flow-mediated vasodilation is impaired in adult rat offspring exposed to prenatal hypoxia. *J Appl Physiol* **110**, 1073-1082.

Mozaffarian D, Wilson PWF & Kannel WB. (2008). Beyond established and novel risk factors: lifestyle risk factors for cardiovascular disease. *Circulation* **117**, 3031-3038.

Mulder ALM, Miedema A, De Mey JGR, Giussani DA & Blanco CE. (2002). Sympathetic control of the cardiovascular response to acute hypoxemia in the chick embryo. *Am J Physiol Regul Integr Comp Physiol* **282**, R1156-1163

Norman M & Martin H. (2003). Preterm birth attenuates association between low birth weight and endothelial dysfunction. *Circulation* **108**, 996-1001.

O'Dowd R, Kent JC, Moseley JM & Wlodek ME. (2008). Effects of uteroplacental insufficiency and reducing litter size on maternal mammary function and postnatal offspring growth. *Am J Physiol Regul Integr Comp Physiol* **294**, R539-R548

Rook W, Johnson CD, Coney AM & Marshall JM. (2014). Prenatal hypoxia leads to increased muscle sympathetic nerve activity, sympathetic hyperinnervation, premature

blunting of neuropeptide γ signaling, and hypertension in adult life. *Hypertension* **64**, 1321-1327.

Rouwet EV, Tintu AN, Schellings MWM, van Bilsen M, Lutgens E, Hofstra L, Slaaf DW, Ramsay G & le Noble FAC. (2002). hypoxia induces aortic hypertrophic growth, left ventricular dysfunction, and sympathetic hyperinnervation of peripheral arteries in the chick embryo. *Circulation* **105**, 2791-2796.

Rueda-Clausen CF, Morton JS, Dolinsky VW, Dyck JR & Davidge ST. (2012). Synergistic effects of prenatal hypoxia and postnatal high-fat diet in the development of cardiovascular pathology in young rats. *Am J Physiol Regul Integr Comp Physiol* **303**, R418-R426.

Ruta L-AM, Dickinson H, Thomas MC, Denton KM, Anderson WP & Kett MM. (2010). High-salt diet reveals the hypertensive and renal effects of reduced nephron endowment. *Am J Physiol Regul Integr Comp Physiol* **298**, F1384-F1392.

Sofola OA, Knill A, Hainsworth R & Drinkhill M. (2002). Change in endothelial function in mesenteric arteries of sprague-dawley rats fed a high salt diet. *J Physiol* **543**, 255-260.

Tare M, Emmett SJ, Coleman HA, Skordilis C, Eyles DW, Morley R & Parkington HC. (2011). Vitamin D insufficiency is associated with impaired vascular endothelial and smooth muscle function and hypertension in young rats. *J Physiol* **589**, 4777-4786.

Tare M, Parkington HC, Bubb KJ & Wlodek ME. (2012). Uteroplacental insufficiency and lactational environment separately influence arterial stiffness and vascular function in adult male rats. *Hypertension* **60**, 378-386.

te Velde SJ, Ferreira I, Twisk JW, Stehouwer CD, van Mechelen W & Kemper HC. (2004). Birthweight and arterial stiffness and blood pressure in adulthood—Results from the Amsterdam Growth and Health Longitudinal Study. *Int J Epidemiol* **33**, 154-161.

Virdis A, Neves MF, Amiri F, Viel E, Touyz RM & Schiffrin EL. (2002). spironolactone improves angiotensin-induced vascular changes and oxidative Stress. *Hypertension* **40**, 504-510.

Williams SJ, Campbell ME, McMillen IC & Davidge ST. (2005a). Differential effects of maternal hypoxia or nutrient restriction on carotid and femoral vascular function in neonatal rats. *Am J Physiol Regul Integr Comp Physiol* **288**, R360-367.

Williams SJ, Hemmings DG, Mitchell JM, McMillen IC & Davidge ST. (2005b). Effects of maternal hypoxia or nutrient restriction during pregnancy on endothelial function in adult male rat offspring. *J Physiol* **565**, 125-135.

Wladimiroff JW, Tonge HM & Stewart PA. (1986). Doppler ultrasound assessment of cerebral blood flow in the human fetus. *Br J Obstet Gynaecol* **93**, 471-475.

Woods LL, Weeks DA & Rasch R. (2004). Programming of adult blood pressure by maternal protein restriction: Role of nephrogenesis. *Kidney Int* **65**, 1339-1348.

Xu Y, Williams SJ, O'Brien D & Davidge ST. (2006). Hypoxia or nutrient restriction during pregnancy in rats leads to progressive cardiac remodeling and impairs postischemic recovery in adult male offspring. *FASEB J* **20**, 1251-1253.

Xue Q & Zhang L. (2009). prenatal hypoxia causes a sex-dependent increase in heart susceptibility to ischemia and reperfusion injury in adult male offspring: role of protein kinase C ϵ . *J Pharmacol Exp Ther* **330**, 624-632.

Yu Q, Larson D, Slayback D, Lundeen T, Baxter J & Watson R. (2004). Characterization of high-salt and high-fat diets on cardiac and vascular function in mice. *Cardiovasc Toxicol* **4**, 37-46.

Tables

Table 1. Vascular sensitivities (expressed as pEC_{50}) and maximum responses to phenylephrine ($\%KPSS_{max}$), acetylcholine (ACh, $\%R_{max}$) and sodium nitroprusside (SNP, $\%R_{max}$).

		Normal Salt		High salt		2-way ANOVA		
		<i>Control</i>	<i>Hypoxia</i>	<i>Control</i>	<i>Hypoxia</i>	P_{trt}	P_{diet}	$P_{trt \times diet}$
Males								
<i>PE</i>	pEC_{50}	-6.2±0.2	-6.4±0.1	-6.6±0.1	-6.8±0.1	P=0.2	P=0.008	P=0.9
	$\%KPSS_{max}$	101.1±6.2	102.7±2.7	96.1±1.9	100.0±2.1	P=0.5	P=0.4	P=0.8
<i>ACh</i>	pEC_{50}	-6.6±0.2	-6.7±0.2	-6.6±0.1	-6.6±0.2	P=0.6	P=0.8	P=0.9
	$\%R_{max}$	107.3±9.2	66.3±13.2	95.4±5.0	77.2±9.5	P=0.006	P=0.96	P=0.3
<i>SNP</i>	pEC_{50}	-7.4±0.1	-6.9±0.4	-6.5±0.4	-6.6±0.3	P=0.6	P=0.09	P=0.4
	$\%R_{max}$	89.1±7.2	93.7±8.5	67.2±5.5	74.2±8.9	P=0.9	P=0.07	P=0.5
Females								
<i>PE</i>	pEC_{50}	-6.4±0.2	-6.5±0.1	-6.3±0.1	-6.7±0.1	P=0.07	P=0.7	P=0.5
	$\%KPSS_{max}$	92.9±4.3	105.2±5.1	94.1±2.2	97.6±4.5	P=0.06	P=0.4	P=0.3
<i>ACh</i>	pEC_{50}	-7.0±0.2	-6.7±0.5	-7.0±0.2	-6.4±0.2	P=0.2	P=0.6	P=0.8
	$\%R_{max}$	89.4±13.4	65.7±12.4	98.5±8.2	71.8±6.9	P=0.02	P=0.5	P=0.9
<i>SNP</i>	pEC_{50}	-7.5±0.3	-7.8±0.3	-7.7±0.1	-7.7±0.2	P=0.6	P=0.9	P=0.6
	$\%R_{max}$	70.0±6.9	76.3±4.4	66.6±5.3	68.0±6.1	P=0.5	P=0.3	P=0.7

Values are mean±SEM (N=6-10 per group). The effect of treatment (trt), diet or their interaction (trt x diet) was evaluated by two-way ANOVA.

Table 2. Structural parameters of mesenteric arteries from aged offspring when pressurised to 45 mmHg.

	Normal Salt		High salt		2-way ANOVA		
	<i>Control</i>	<i>Hypoxia</i>	<i>Control</i>	<i>Hypoxia</i>	P_{trt}	P_{diet}	$P_{trt \times diet}$
Males							
<i>Lumen</i>	212±6	237±18	207±16	232±12	P=0.1	P=0.8	P=0.97
<i>Medial CSA</i>	18666±1042	19577±1814	15962±1855	16143±752	P=0.7	P=0.03	P=0.8
<i>Media:Lumen</i>	21.5±1.0	22.5±1.0	21.8±2.4	18.1±1.2	P=0.3	P=0.1	P=0.09
Females							
<i>Lumen</i>	227±14	225±10	226±12	210±11	P=0.5	P=0.5	P=0.5
<i>Medial CSA</i>	16472±970	15992±947	18206±1123	15921±1648	P=0.3	P=0.5	P=0.5
<i>Media:Lumen</i>	19.0±1.1	18.7±1.2	21.0±1.6	21.2±3.6	P=0.98	P=0.4	P=0.9

Values are mean±SEM (N=6-10 per group). The effect of treatment (trt), diet or their interaction (trt x diet) was evaluated by two-way ANOVA.

Table 3. Rate constant, β , calculated from the exponential function fitted to stress-strain curves of mesenteric arteries from aged offspring.

β , rate	Normal Salt		High salt		Two-way ANOVA		
constant	<i>Control</i>	<i>Hypoxia</i>	<i>Control</i>	<i>Hypoxia</i>	P_{trt}	P_{diet}	$P_{trt \times diet}$
Males	4.1±0.3	4.8±0.5	4.9±0.6	6.0±0.3	P=0.03	P=0.02	P=0.6
Females	5.4±0.4	5.0±0.4	5.8±0.5	7.9±0.7*	P=0.1	P=0.008	P=0.03

Values are mean±SEM (N=6-10 per group). The effect of treatment (trt), diet or their interaction (trt x diet) was evaluated by two-way ANOVA. *P<0.01 (from Bonferroni post-hoc, compared to high salt controls).

Figures

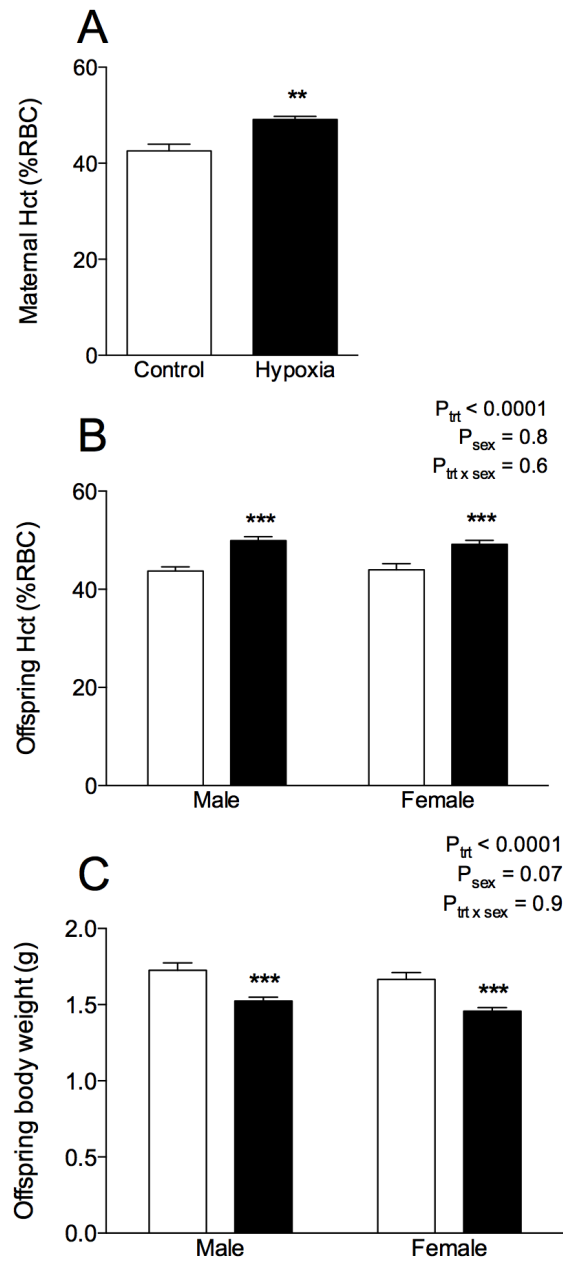


Figure 1. Maternal and offspring parameters at day of birth (P0). Maternal haematocrit (Hct, % packed red blood cell volume) (A), offspring haematocrit (B) and offspring body weight (C) were determined at P0. Control: white bars; hypoxia: black bars. Values are mean \pm SEM (N=8-10 per group). **P<0.001 from t-test, ***P<0.0001 (from Bonferroni post-hoc, compared to same sex controls).

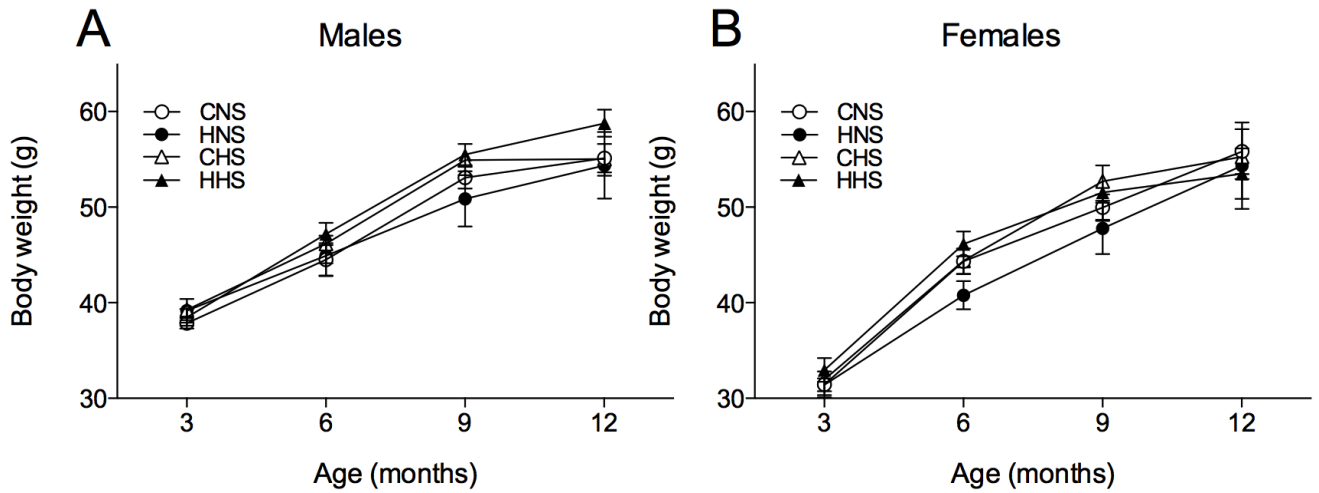


Figure 2. Growth curves of offspring either on a normal salt (0.26% NaCl) or high salt diet (5% NaCl) from the age of 3 to 12 months. Values are mean \pm SEM (of N=11 litters per group). Control: white points; hypoxia: black points. CNS, control offspring fed normal salt diet; HNS, hypoxia offspring fed normal salt diet; CHS, control offspring fed high salt diet; HHS, hypoxia offspring fed high salt diet.

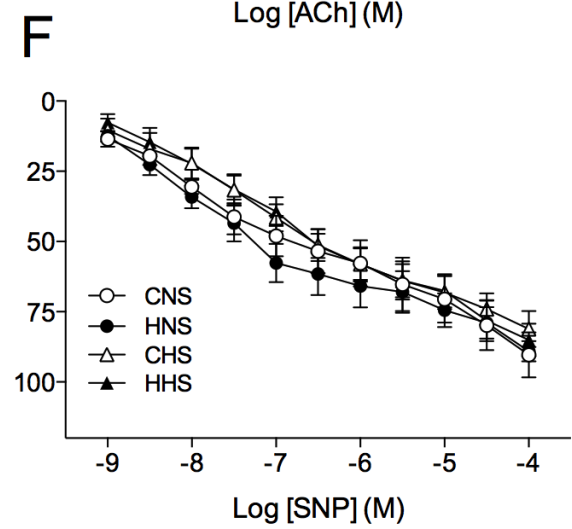
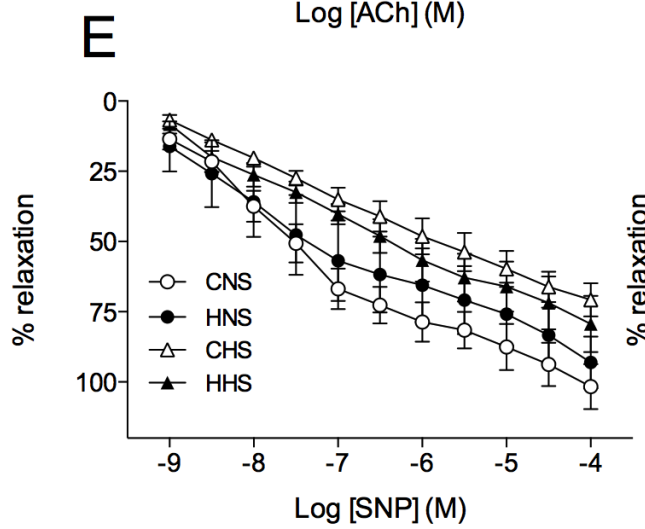
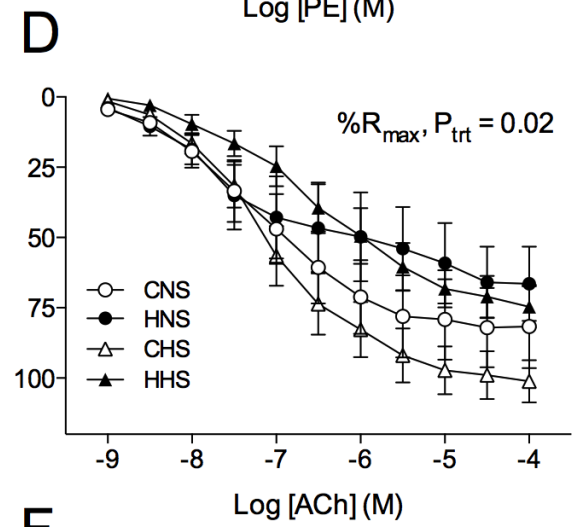
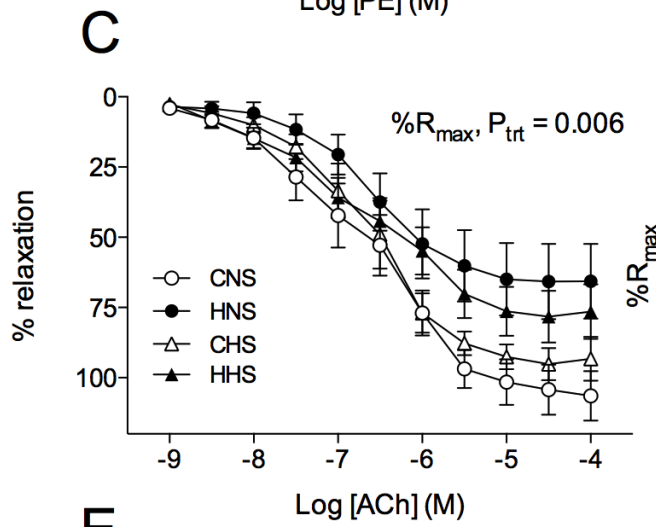
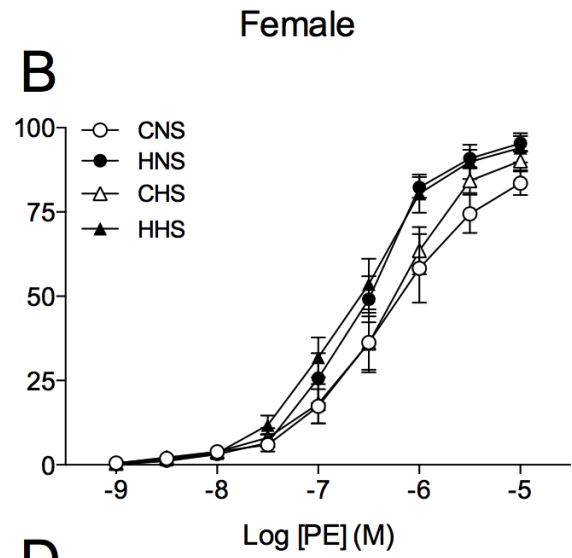
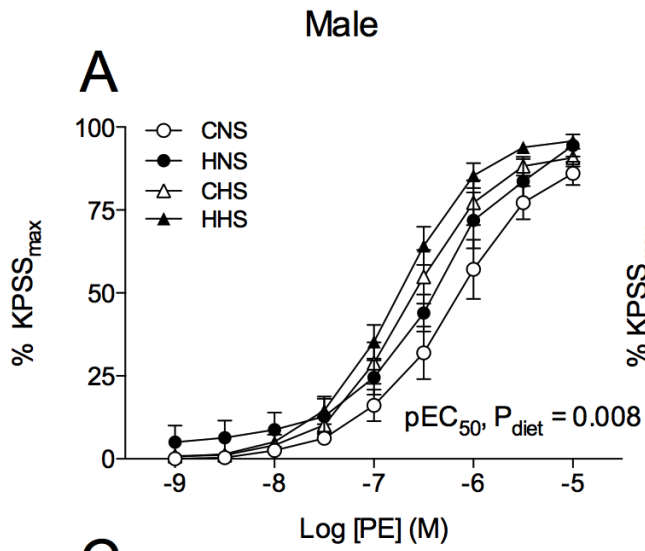


Figure 3. Mesenteric arteries were obtained from aged male (left) and female (right) control and hypoxia-exposed offspring fed a normal salt or high salt diet. Functional responses to cumulative additions of (A, B) phenylephrine, (C, D) acetylcholine and (E, F) sodium nitroprusside were measured in arteries pressurized to 45 mmHg. Data in A and B are expressed as a percentage of the maximum contraction to high-potassium physiological salt solution (KPSSmax). In C-F, vessels were contracted to ~70% of KPSSmax with phenylephrine, and relaxation responses to the vasodilator agonists expressed as a percentage of the PE-induced contraction. Values are mean±SEM (N=6-10 per group). Control: white points; hypoxia: black points. CNS, control offspring fed normal salt diet; HNS, hypoxia offspring fed normal salt diet; CHS, control offspring fed high salt diet; HHS, hypoxia offspring fed high salt diet.

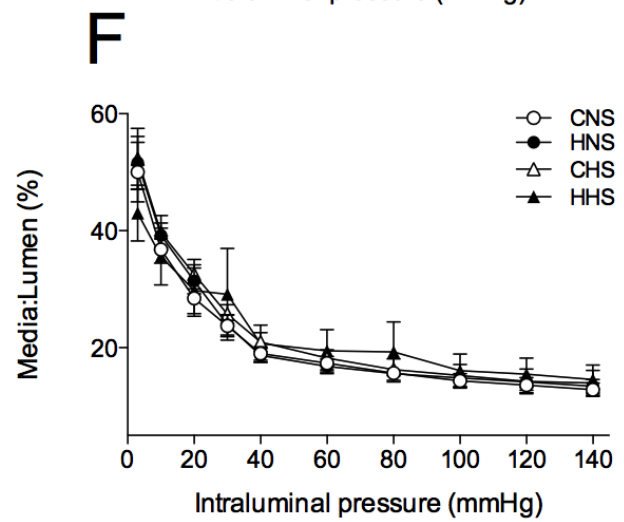
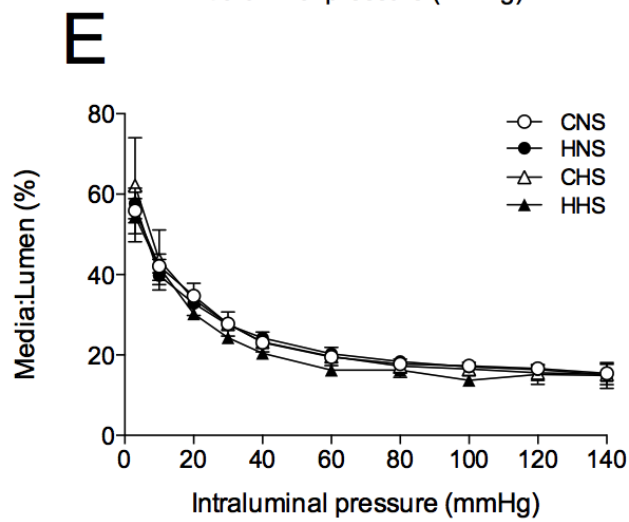
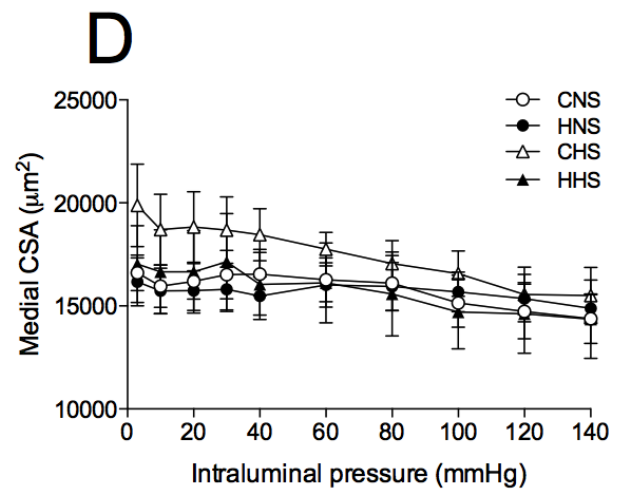
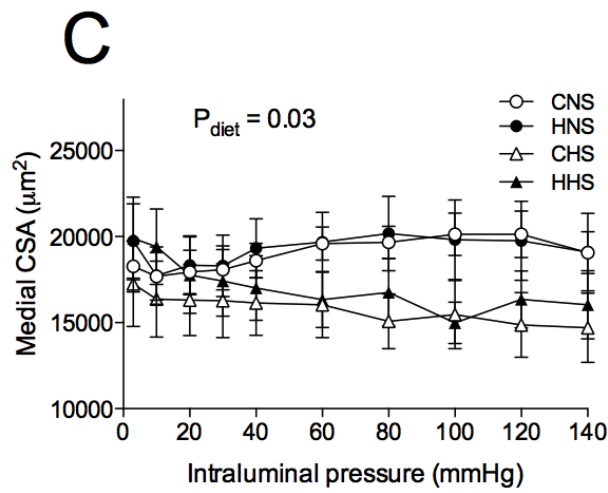
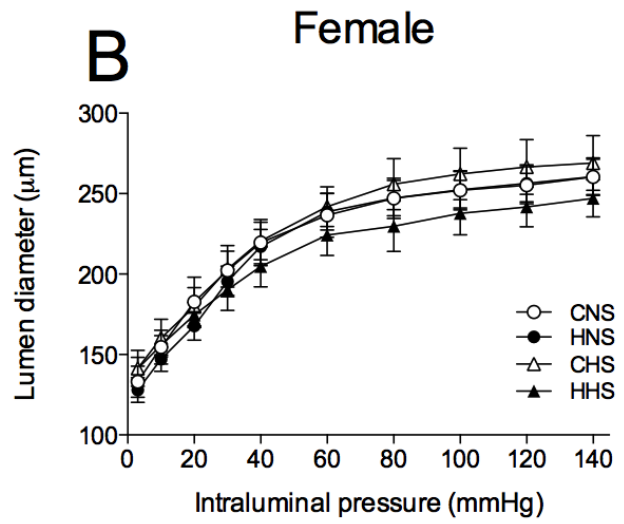
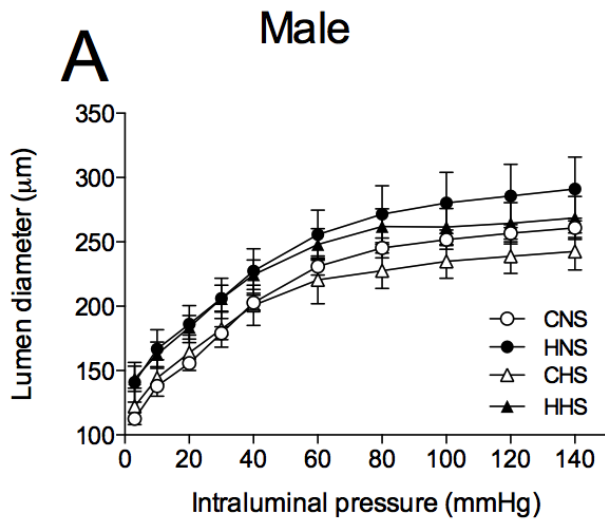


Figure 4. Mesenteric arteries were obtained from aged male (left) and female (right) control and hypoxia-exposed offspring fed a normal salt or high salt diet. Lumen diameter in male (A) and female (B) offspring, medial CSA in male (C) and female (D) offspring, and media:lumen ratio in male (E) and female (F) offspring in response to increasing intraluminal pressure in deactivated mesenteric arteries. Values are mean \pm SEM (N=6-10 per group). Control: white points; hypoxia: black points. CNS, control offspring fed normal salt diet; HNS, hypoxia offspring fed normal salt diet; CHS, control offspring fed high salt diet; HHS, hypoxia offspring fed high salt diet.

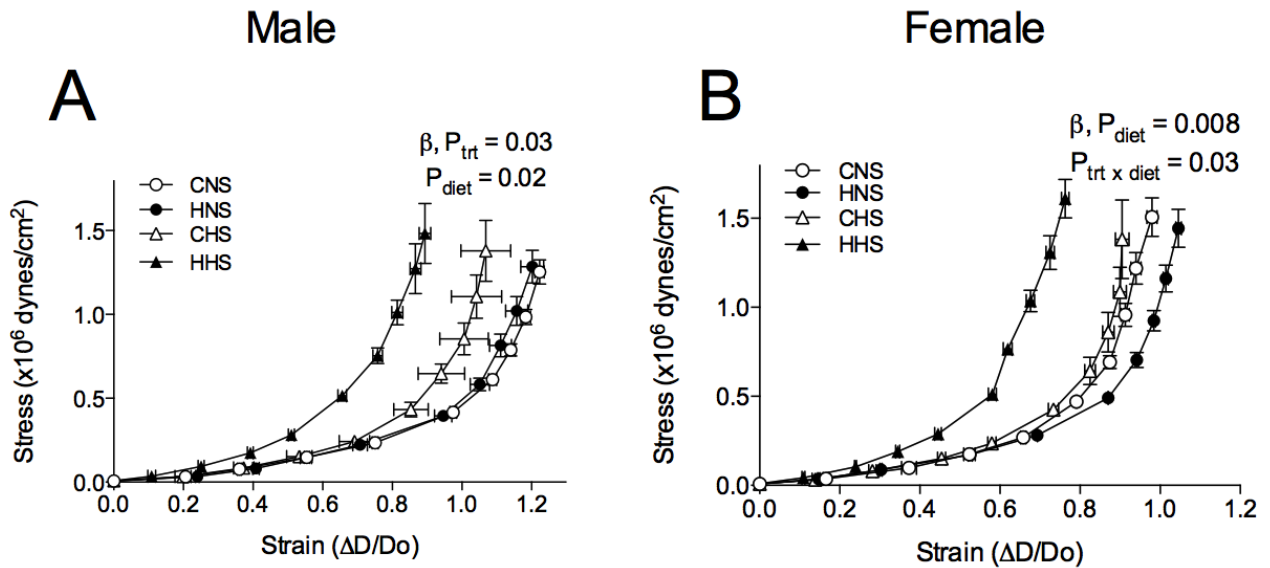


Figure 5. Deactivated mesenteric arteries were obtained from aged male (left) and female (right) control and hypoxia-exposed offspring fed a normal salt or high salt diet. Stress-strain relationship in vessels of male (A) and female (B) offspring. Values are mean±SEM (N=6-10 per group). Control: white points; hypoxia: black points. CNS, control offspring fed normal salt diet; HNS, hypoxia offspring fed normal salt diet; CHS, control offspring fed high salt diet; HHS, hypoxia offspring fed high salt diet.

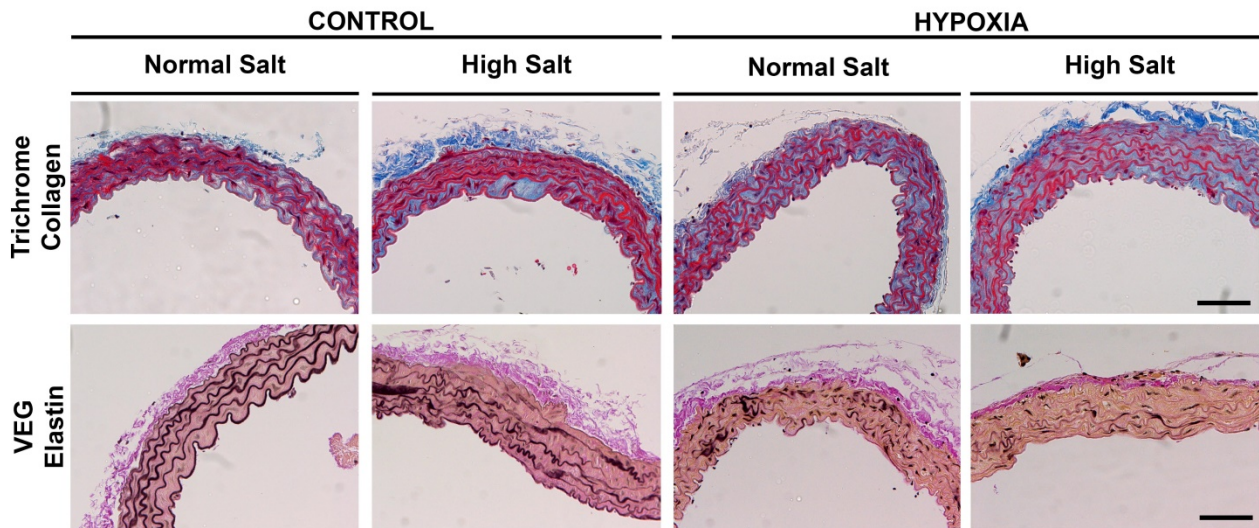


Figure 6. Microphotographs of aortic sections stained with Masson's Trichrome to detect collagen (blue) and Verhoeff's Van Gieson to detect elastin (black). Aortas were obtained from aged male hypoxia-exposed offspring fed a normal or high salt diet. Scale bar represents 50 μ m.

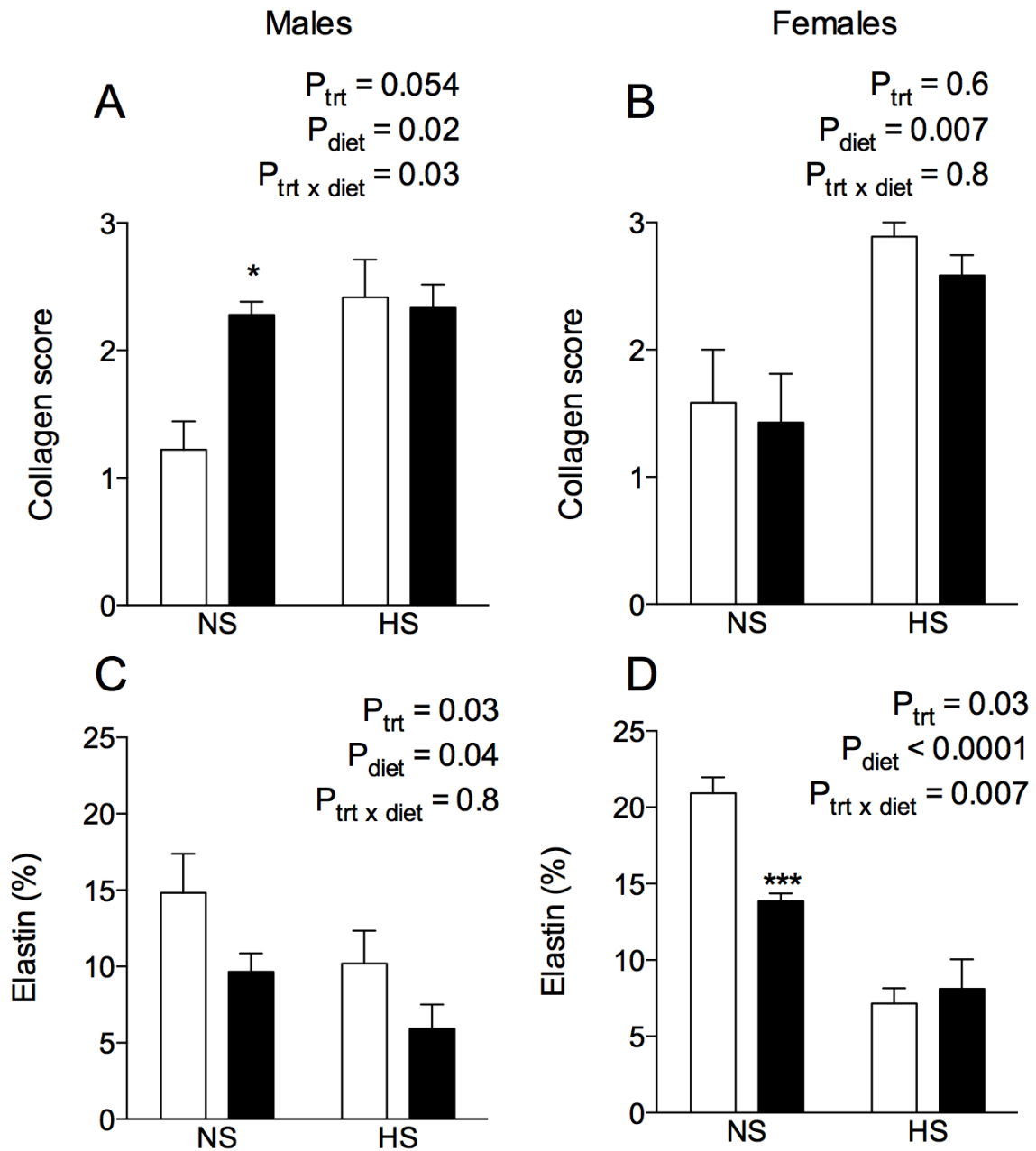


Figure 7. Semi-quantification of aortic histology. Collagen scores in aorta sections stained with Masson's Trichrome to detect collagen in male (A) and female (B) control and hypoxia exposed offspring fed a normal or high salt diet. Elastin (%) in aorta sections stained with Verhoeff's Van Gieson in male (C) and female (D) offspring. Values are mean \pm SEM (N=6-8 per group). * $P < 0.01$, *** $P < 0.0001$ (from Bonferroni post-hoc, compared to control offspring fed the normal salt diet). NS, normal salt diet; HS, high salt diet.

Chapter 4

This chapter will be submitted in its entirety for consideration for publication to The Journal of Physiology in September 2016.

Walton, S.L., Bielefeldt-Ohmann, H., Singh, R.R., Li, J., Paravicini, T.H., Little, M.H., and Moritz, K.M. (2016). *Prenatal hypoxia combined with a high-salt diet predisposes mouse offspring to renal and cardiovascular impairments.*

Incorporated as Chapter 4.

Contributor	Statement of contribution
Walton, S.L.	Animal treatment and tissue collection (80%) Metabolic cage studies (100%) Stereological analysis (100%) Histological analysis (50%) Interpreting results (65%) Study design (20%) Writing and editing manuscript (70%)
Bielefeldt-Ohmann, H.	Histological analysis (50%) Interpreting results (15%) Writing and editing manuscript (5%)
Singh, R.R.	Animal treatment and tissue collection (20%) Study design (20%) Writing and editing manuscript (5%)
Li, J.	Interpreting results (10%) Writing and editing manuscript (5%)
Paravicini, T.M.	Telemetry surgeries (100%)
Little, M.H.	Study design (10%)
Moritz, K.M.	Interpreting results (10%) Study design (50%) Writing and editing manuscript (15%)

Prenatal hypoxia combined with a high-salt diet predisposes mouse offspring to renal and cardiovascular impairments.

Walton, SL.¹, Bielefeldt-Ohmann, H², Singh, RR.³, Li, J.⁴ Paravicini, TH.², Little, MH.⁴, and Moritz, KM¹.

¹School of Biomedical Sciences, The University of Queensland, St Lucia, Queensland, Australia

²School of Veterinary Science, The University of Queensland, Gatton, Queensland, Australia

³ Department of Physiology, Monash University, Clayton, Victoria, Australia

⁴Institute for Molecular Bioscience, The University of Queensland, St Lucia, Queensland, Australia

Running title: Prenatal hypoxia and cardio-renal outcomes

Key words: hypoxia, sex differences, hypertension

Corresponding Author:

Karen M Moritz

School of Biomedical Sciences

University of Queensland

St Lucia

QLD, 4072

Phone: 61-7-3365-4598

Email: k.moritz@uq.edu.au

Key points summary

- Hypoxia is a common clinical pregnancy complication leading to growth restriction and adverse health outcomes.
- We investigated the impact of prenatal hypoxia on the cardiovascular and renal systems in mice, and whether excess dietary salt intake could exacerbate adverse health outcomes.
- Male but not female hypoxia-exposed offspring had reduced nephron number, mild albuminuria and increased renal pathology severity compared to control offspring. Prenatal hypoxia led to elevated blood pressure in both sexes.
- The combination of prenatal hypoxia and postnatal high dietary salt intake exacerbated signs of heart and kidney damage.
- Our results suggest that prenatal hypoxia increases vulnerability to cardiovascular and renal disease, particularly when the postnatal diet is high in salt.

Abstract

Prenatal hypoxia is associated with low birth weight and adverse cardiovascular outcomes in adulthood. We examined the effects of prenatal hypoxia on the kidney to determine whether renal impairments may contribute to these cardiovascular impairments. Pregnant CD1 mice were housed in a hypoxia chamber (12% O₂) or housed in normal room conditions (21% O₂) from embryonic day 14.5 until birth. Male and female offspring were raised in normal room conditions. Glomerular number in kidneys from offspring at postnatal day 21 was estimated using unbiased stereology. A subset of offspring was fed a chronic high salt diet (5% NaCl) from 10 weeks of age. Urine excretion over a 24 hours' period was assessed in offspring at 4 and 12 months of age. Blood pressure was measured using radiotelemetry in animals fed the normal-salt diet at 12 months of age, and hearts and kidneys were subsequently collected for histopathological analysis. Prenatal hypoxia caused a significant reduction in nephron number (25%, $P < 0.0001$), increased urinary albumin ($P = 0.04$), glomerular hypertrophy and increased incidence of renal fibrosis and damage in male offspring compared to control male offspring. Prenatal hypoxia led to elevated blood pressure in hypoxia-exposed male and female offspring. Hypoxia-exposed offspring were more susceptible to salt-induced cardiac damage compared to control counterparts. However, male hypoxia-exposed offspring were more susceptible to cardiac and renal damage compared to females. These results demonstrate that prenatal hypoxia programs elevated blood pressure in both sexes. However, nephron number was only reduced in male offspring suggesting there are additional factors influencing blood pressure control following exposure to prenatal hypoxia. Furthermore, the additional challenge of a high salt diet increase signs of cardiovascular and renal disease.

Glossary

E, embryonic day

DBP, diastolic blood pressure

GFR, glomerular filtration rate

HR, heart rate

HS, high salt

MANOVA, multivariate analysis of variance

MAP, mean arterial pressure

NS, normal salt

P, postnatal day

PAS, Periodic acid-Schiff

PFA, paraformaldehyde

PNA, peanut agglutinin

PP, pulse pressure

RAS, renin angiotensin system

SBP, systolic blood pressure

UACR, urinary albumin to creatinine ratio

Introduction

In utero insults such as reduced oxygen and nutrient supply to the fetus lead to growth restriction and predisposition to a range of cardiovascular, renal and metabolic diseases in later life (Barker, 1998). Growth restriction is frequently associated with impaired organ development (Moritz *et al.*, 2009), meaning offspring may be born with organs with sub-optimal function, thus lacking the robustness required to support them throughout their lifespan. Fetal hypoxia is a common clinical pregnancy complication that arises from a wide range of circumstances including, but not limited to, placental insufficiency, high altitude living and maternal factors such as smoking and pulmonary disease (Kingdom & Kaufmann, 1997; Hutter *et al.*, 2010). Frequently fetal hypoxia leads to intrauterine growth restriction and subsequent low birth weight, suggesting offspring are susceptible to disease in later life.

In the chronically hypoxic fetus, growth restriction is frequently asymmetric as blood flow is shunted towards the brain, heart and adrenal glands at the expense of peripheral organs such as the kidneys (Peeters *et al.*, 1979; Giussani *et al.*, 2001). Although the preservation of these critical organs is necessary for immediate fetal survival, the structural and functional consequences of diverting blood flow away from the periphery may become evident in later life. Cardiovascular studies in rat offspring from pregnancies complicated by hypoxia have identified ventricular and aortic wall thickening (Camm *et al.*, 2010), susceptibility to cardiac ischemia-reperfusion injury (Rueda-Clausen *et al.*, 2012) and peripheral vascular dysfunction (Williams *et al.*, 2005; Giussani *et al.*, 2012; Tare *et al.*, 2012). We have previously reported that both male and female mouse offspring exposed to prenatal hypoxia (12% O₂, reduced from 21% O₂) in late gestation are growth-restricted in late gestation with impaired placental vascularisation (Cuffe *et al.*, 2014a; Cuffe *et al.*, 2014b). Offspring of this model present with low birth weight and undergo catch-up growth after weaning (Walton *et al.*, 2016). These hypoxia-exposed offspring develop endothelial dysfunction by 12 months of age (Walton *et al.*, 2016), which in the human population is associated with increased risk of cardiovascular events (Hadi *et al.*, 2005).

Less focus has been placed on the kidney outcomes following fetal hypoxia, which is surprising given the kidney's known susceptibility to *in utero* insults as well as its role in long-term maintenance of blood pressure (Guyton *et al.*, 1972; Moritz *et al.*, 2009). Nephrogenesis, the formation of the functional filtration units of the kidney known as nephrons, is complete at 36 weeks gestation in humans (Hinchliffe *et al.*, 1991) and continues into early postnatal life in the rodent (Hartman *et al.*, 2007). After this point, no more nephrons can be formed and hence a

congenital deficit of nephrons reduces the filtration surface area of the kidney; this elevates the risk of hypertension and progressive kidney damage (Brenner & Mackenzie, 1997). A range of fetal stressors such as uteroplacental insufficiency (Wlodek *et al.*, 2007), glucocorticoid exposure (O'Sullivan *et al.*, 2015), maternal alcohol consumption (Gray *et al.*, 2010), and malnutrition (Woods *et al.*, 2004) have been shown to lead to birth of offspring with growth-restriction. These individuals also have fewer nephrons per kidney and present with altered blood pressure profiles. In the human population, low birth weight is associated with reduced glomerular number, glomerular hypertrophy, glomerulosclerosis, albuminuria and elevated blood pressure (Brenner & Mackenzie, 1997; Hughson *et al.*, 2003; Hughson *et al.*, 2006). We have previously reported that severe early-gestational hypoxia (5.5–7.5% O₂, embryonic day 9.5-10.5) and moderate mid-gestational hypoxia (12% O₂, embryonic day 12.5-14.5) in the mouse causes a reduction in nephron number and leads to similar structural phenotypes seen in patients with congenital anomalies of the kidney and urinary tract (CAKUT) (Wilkinson *et al.*, 2015). However, the consequences of prenatal hypoxia on renal and cardiovascular function have not been followed up long-term in these offspring.

The aim of our study was to utilise the mouse model of prolonged hypoxia during late gestation (12% O₂, embryonic day 14.5 – birth), previously characterised by our laboratory (Cuffe *et al.*, 2014a; Cuffe *et al.*, 2014b; Walton *et al.*, 2016), to assess blood pressure, renal function and cardiac/renal pathology in 12-month-old male and female offspring. In addition, given that evidence of predisposition to adult disease may be exacerbated by adult lifestyle (Moritz *et al.*, 2009; Giussani, 2016), such as poor diet or lack of exercise, we examined the interaction of prenatal hypoxia with a postnatal high salt diet. Previously we have reported that hypoxia-exposed mouse offspring fed a diet high in salt displayed marked stiffening of the resistance vasculature and altered extracellular matrix composition in the aorta. These changes are consistent with the pathogenesis of cardiovascular disease, and highlight that both prenatal and postnatal environments are highly influential factors in the pathogenesis of adulthood disease. We hypothesised that prenatal hypoxia would reduce nephron number in the developing kidney, thereby predisposing offspring to elevated blood pressure, renal impairments and increased susceptibility to salt-induced tissue damage in adulthood. In addition, we examined males and females separately given our previous studies have reported marked differences between the sexes (Cuffe *et al.*, 2014a; Cuffe *et al.*, 2014b; Walton *et al.*, 2016).

Methods

Maternal hypoxia

All experiments were approved by the University of Queensland Animal Ethics Committee and were conducted in accordance with the *Australian Code of Practice for the Care and Use of Animals for Scientific Purposes*. Time-mated CD1 mice at embryonic day (E) 14.5 of pregnancy, were randomly allocated to normoxic room conditions (N=19) or housed inside a hypoxic chamber continuously flushed with nitrogen gas to maintain an oxygen concentration of 12% (N=19) as described previously (Walton *et al.*, 2016). A 12 h light/dark cycle was maintained and food and water was provided *ad libitum*.

Animal handling

A subset of dams (N=8) was culled at E18.5 as described by Cuffe *et al.* (2014a). Fetal body weight, kidney, heart and brain weights were recorded. Remaining dams were removed from the hypoxic chamber upon littering down, denoted as postnatal day 0 (P0). Pup weights were monitored daily from P1 until weaning at P21. At P21, a subset of male and female offspring (1-2 of each sex per litter) was euthanized by cervical dislocation. Kidneys, hearts and brains were dissected and weighed. The left kidney was fixed in 4% paraformaldehyde (PFA) for assessment of renal pathology, glomerular number and area. The remaining offspring were aged to 12 months for renal and cardiovascular studies.

Estimation of glomerular number at P21

A combined stereological-histochemical approach was used to determine glomerular number in P21 male and female offspring kidneys (N=8 per treatment group) as previously described (Cullen McEwen *et al.*, 2012). Briefly, kidneys were processed into paraffin blocks and exhaustively sectioned at 5 μm . Ten evenly spaced section pairs were systematically sampled and stained with lectin peanut agglutinin (*Arachis hypogea*, PNA; Sigma Aldrich, Castle Hill, NSW, Australia), which stains the basement membranes of the glomerular podocytes. Glomeruli from each section pair were counted using the physical disector/fractionator combination.

Blood pressure

Animals at 12 months of age were anaesthetised under isoflurane (3-3.5% in oxygen, $\sim 125 \text{ ml min}^{-1}$) and radiotelemetry transmitters (model PA-C10; Data Sciences International, MN, USA) were implanted as described previously (O'Sullivan *et al.*, 2015). Recording of heart rate (HR), systolic (SBP) and diastolic blood pressure (DBP), and activity data commenced in conscious, unrestrained

animals 10 days post-surgery (N=5-6 per treatment group). Data were acquired for 10 seconds every 15 minutes for three days. Mean arterial pressure (MAP) and pulse pressure (PP) were calculated from these parameters.

Restraint stress

On the fourth day of measurements, animals implanted with radiotelemeters were subjected to a restraint stress challenge. Data was acquired for 10 s every 5 min for 1 h before restraint stress, and averaged to establish a baseline. Animals were immediately placed in a clear plastic container (12 x 8 x 6 cm) for 15 min, and then released to the home cage. Data was acquired continuously during the restraint and 15 min recovery period. Recovery data was sampled for 10 s every 5 min for the next hour of recovery.

High salt diet

A subset of animals aged 10 weeks (N=11 per sex per treatment, one or two animals from each litter) was randomly allocated to receive a high salt (HS) diet (5% NaCl, wt/wt; modified AIN 93M, SF05-023; Specialty Feeds, Memphis, TN, USA) or normal salt (NS) diet (0.26% NaCl, wt/wt; AIN 93M; Specialty Feeds) as previously described (Walton *et al.*, 2016). Animals were maintained on the diet until euthanasia at 12 months of age. Food and water consumption in home cages was measured over 7 days at 12 months of age and averaged per day.

Urinalysis

Male and female offspring at 2 months (normal salt animals only, N=6 per treatment group), 4 months of age (N=6-8 per treatment group) and 12 months (N=9-11 per treatment group) fed the normal salt and high salt diets, respectively, were acclimatised to individual metabolic cages prior to urine collection. Animals were then placed in individual metabolic cages for 24 h. Urine was collected and frozen at -20 °C. Urinary electrolytes (Na⁺, K⁺, Cl⁻) were measured using a COBAS Integra 400 Plus analyser. Urine osmolarity was assessed by freezing point depression using a Micro-Osmette osmometer (Precision Systems, MA, USA). Urinary excretion of albumin was determined using commercially available mouse kits (Albuwell M, Exocell, Philadelphia, USA).

Post-mortem tissue collection and histopathology

Animals were euthanized via carbon dioxide inhalation. Blood was collected via cardiac puncture and plasma separated. Body and organ weights were recorded. Hearts and kidneys were processed to paraffin as described above. Representative 5 µm midline sections from each heart and kidney were stained with Periodic Acid Schiff's (PAS) and Masson's Trichrome. Sections were assessed

by an expert veterinary pathologist blinded to treatment groups and assigned a score based on pathology severity: 0, normal; 1, minimal change; 2, mild; 3, moderate; 4, severe. Glomerular area in PAS-stained kidney sections was quantified by tracing glomerular borders when the vascular pole was evident. Twenty to 30 glomeruli were analysed per animal and measurements averaged.

To assess perivascular fibrosis in kidneys and hearts, two arterioles were selected in the Masson's trichrome-stained sections, as described in (Lim *et al.*, 2006). Area of adventitial collagen was measured and normalised to vessel lumen area, and averaged for each animal. Interstitial fibrosis was quantified by determining percentage of collagen in the interstitium in four random fields of view per animal.

Plasma analysis

Plasma cystatin C levels at 12 months of age (1:300 dilution) were determined using a commercially available kit (Mouse/Rat Cystatin C Quantikine ELISA kit, R&D Systems). Plasma electrolytes (Na⁺, Cl⁻) and triglycerides were measured using a COBAS Integra 400 Plus analyser.

Statistical analysis

Statistical analyses were performed using GraphPad Prism 5 and IBM SPSS. Data are presented as mean \pm standard error of the mean (SEM). Maternal arterial blood oxygen saturation was analysed by one-way ANOVA. A multivariate analysis of variance (MANOVA) was used to analyse basal blood pressure recordings over three days. Prenatal treatment, sex and light-dark periods were assigned as independent variables. Histology scoring was analysed using a Mann-Whitney test. All other data was analysed using two-way ANOVA examining the effects of prenatal hypoxia ($P_{\text{treatment}}$) and postnatal high salt diet (P_{diet}). Bonferroni post hoc tests comparing control and hypoxia-exposed offspring used where appropriate. $P < 0.05$ was considered significant.

Results

Body and organ weights of animals from E18.5 to 2 months of age

Body weight was reduced in hypoxia-exposed offspring by ~7% at E18.5 and P21, similar to that reported previously by Cuffe et al. (2014a) and Walton et al. (2016) (Table 1). Absolute kidney weight was reduced in both male and female hypoxia exposed offspring at E18.5 and P21 compared to controls (Table 1; $P_{\text{treatment}} = 0.04$); relative left kidney weight was similar between treatment groups. Heart weight, absolute or corrected for body weight, did not differ between treatment groups at E18.5 or P21. Brain weight did not differ between treatment groups at E18.5 (as reported previously in Cuffe et al. 2014) or at P21 (Table 1). However, brain weight corrected for body weight was elevated in hypoxia-exposed animals compared to controls at P21 (Table 1; $P_{\text{treatment}} = 0.04$, $P_{\text{sex}} = 0.03$). By 2 months of age, hypoxia-exposed offspring had the same body weight as control counterparts (control male: 35.5 ± 0.8 g, hypoxia male: 34.9 ± 0.6 g, control female: 27.6 ± 0.7 g, hypoxia female: 28.2 ± 0.7 g; $P_{\text{treatment}} = 0.98$) with females smaller than males overall ($P_{\text{sex}} < 0.0001$).

Glomerular number and urinary electrolyte excretion in young mice up to 4 months

Estimation of glomerular number revealed a significant effect of prenatal hypoxia ($P_{\text{treatment}} < 0.01$) but also an association with sex ($P_{\text{treatment} \times \text{sex}} < 0.01$). *Post hoc* analysis demonstrated that only male offspring exposed to prenatal hypoxia had significantly different nephron number to control counterparts at P21 (Table 1; 25% deficit, $P < 0.001$ by Bonferroni *post hoc*) but no differences in glomerular endowment in female offspring (Table 1). Glomerular area was equivalent between treatment groups in male and female offspring at P21 (control male: 1964 ± 130 μm^2 , hypoxia male: 2140 ± 185 μm^2 , control female: 1797 ± 72 μm^2 , hypoxia female: 1778 ± 128 μm^2). Urine output and urinary excretion of electrolytes (Na^+ , K^+ , Cl^-) did not differ between treatment groups at 2 months of age (supplementary figure 1).

At 4 months, body weight was equivalent between treatment and dietary groups in male (control NS: 40.7 ± 1.0 g, hypoxia NS: 40.9 ± 1.7 g, control HS: 42.7 ± 1.7 g, hypoxia HS: 42.9 ± 1.0 g; $P_{\text{treatment}} = 0.9$, $P_{\text{diet}} = 0.2$) and female offspring (control NS: 36.4 ± 0.9 g, hypoxia NS: 36.8 ± 1.6 g, control HS: 35.2 ± 1.9 g, hypoxia HS: 37.1 ± 2.0 g; $P_{\text{treatment}} = 0.5$, $P_{\text{diet}} = 0.8$). There were no differences between control and hypoxia exposed offspring in urine output or urinary excretion of electrolytes. However, urine output and urinary excretion of sodium and chloride were increased in 4-month-old animals fed the high salt diet, compared to the normal salt diet irrespective of prenatal

treatment (supplementary figure 1). Urinary potassium excretion and urine osmolality were equivalent between groups.

Blood pressure measurements

Body weight pre- and post-surgery did not differ between treatments groups (supplementary figure 2). MAP was elevated during the day and night cycle in male (Figure 1A, $P_{\text{treatment}} = 0.03$) and female (Figure 1B; $P_{\text{treatment}} = 0.002$) hypoxia-exposed offspring. In male offspring, this was due to an increase in DBP (Figure 1A, $P_{\text{treatment}} = 0.002$) with no change in SBP, leading to an overall narrowing of pulse pressure in hypoxia-exposed males (Figure 1A; $P_{\text{treatment}} = 0.02$). Female hypoxia-exposed offspring exhibited increases in both SBP (Figure 1B; $P_{\text{treatment}} = 0.003$) and DBP (Figure 1B; $P_{\text{treatment}} = 0.01$), with no difference in PP. Heart rate was not affected by prenatal hypoxia in male or female offspring (supplementary figure 3).

Activity in male control offspring increased during the night periods of recording (supplementary figure 4; $P_{\text{time}} < 0.0001$). However, in male hypoxia-exposed offspring, activity was blunted during the night period compared to control offspring (Figure 1C; $P_{\text{treatment}} = 0.004$, $P_{\text{treatment} \times \text{time}} = 0.03$). Female offspring activity increased during the night period, and this did not differ between treatment groups (Figure 1D; $P_{\text{treatment}} = 0.5$, $P_{\text{time}} = 0.049$).

Cardiovascular reactivity to restraint stress

MAP was elevated in both male (supplementary figure 4A; $P_{\text{treatment}} < 0.0001$) and female (supplementary figure 4B $P_{\text{treatment}} < 0.0001$) offspring compared to controls throughout the 10-minute baseline measurement before restraint stress. Restraint stress caused an immediate increase in MAP above baseline levels to ~145 mmHg in male offspring (supplementary figure 4A) and to ~125 mmHg in female offspring (supplementary figure 4B) in both treatment groups. No differences in Δ HR, PP, SBP or DBP were observed between treatment groups during restraint stress in male and female offspring (supplementary figure 4C).

Urine and plasma analysis at 12 months of age

Urinary excretion of sodium and chloride and plasma cystatin C levels did not differ between treatment groups in male (Figure 2A) and female (Figure 2B) offspring. Albumin excretion in male hypoxia-exposed offspring was elevated ~1.3-fold compared to control counterparts fed the normal salt diet (Figure 2A; $P_{\text{treatment}} = 0.04$). Albumin excretion was also elevated in hypoxia-exposed animals fed the HS diet by ~2.4-fold, compared to controls fed the high salt diet (Figure 2A;

$P_{\text{treatment}} < 0.04$; $P_{\text{diet}} = 0.8$). Overall, no differences in albumin excretion (Figure 2B) were observed in female offspring at 12 months of age.

No differences in plasma sodium, chloride or triglyceride levels were observed between treatment or dietary groups in offspring (Table 3). Plasma cystatin C levels were reduced in male offspring fed the high salt diet (Figure 2A; $P_{\text{diet}} = 0.02$) and trended towards a decrease in female offspring fed the high salt diet (Figure 2B; $P_{\text{diet}} = 0.06$), compared to offspring fed the normal salt diet. As previously reported (Walton *et al.*, 2016), the chronic high salt diet increased urinary sodium and chloride excretion in male (Figure 2A; $P_{\text{diet}} < 0.0001$) and female (Figure 2B; $P_{\text{diet}} < 0.0001$) offspring compared to counterparts fed the normal salt diet. Bonferroni post-hoc analysis revealed that hypoxia-exposed male offspring fed the high salt diet excreted ~38% more chloride than control counterparts (Figure 2A; $P < 0.05$). Potassium excretion did not differ between prenatal treatment and dietary groups (data not shown).

Offspring body and organ weights at 12 months of age

Body, kidney, heart and brain weights (absolute and corrected for body weight) were similar among prenatal treatment groups at 12 months of age (Table 2). Kidney weight was increased by ~20% in male offspring and ~15% in female offspring fed the HS diet compared to the NS diet (Table 2; $P_{\text{diet}} < 0.05$). The kidney to body weight ratio was elevated in male offspring fed the HS diet (Table 2; $P_{\text{diet}} = 0.02$). The chronic HS diet increased heart weight by ~7% in male offspring and ~14% in female offspring (Table 2; $P_{\text{diet}} < 0.05$).

Histopathology of the hearts at 12 months of age

When assessed by Masson's Trichrome staining, the degree of perivascular fibrosis in cardiac tissue was similar between (Figure 3A,C; $P=0.2$) control and hypoxia-exposed male animals. Increased perivascular fibrosis was observed in animals fed the high salt diet compared to the normal salt diet (Figure 3A,C; $P_{\text{diet}} = 0.008$). There was a trend towards increased perivascular fibrosis in the male hypoxia animals fed the high salt diet compared to controls fed the normal salt diet, although this did not reach significance (Figure 3A). Perivascular fibrosis was unaffected by prenatal hypoxia and the high salt diet in female offspring (Figure 3B). Interstitial fibrosis was significantly elevated in cardiac tissue by the high salt diet, and this effect was greatest in animals exposed to prenatal hypoxia of both sexes (Figure 3A-C; $P_{\text{treatment}} < 0.05$). Additionally, mild myocardial hypertrophy and minimal to mild interstitial leukocyte infiltration were occasionally observed in the hypoxia-exposed animals fed the normal salt and high salt diets (not shown).

Glomerular area and histopathology of adult kidneys

The nephron deficit of 25% in male-hypoxia offspring was also observed at 12 months of age (Table 2) with female hypoxia-exposed offspring having a similar number of glomeruli to their control counterparts. Male hypoxia-exposed offspring had reduced staining of PNA, the glomerular podocyte marker, compared to control counterparts (not shown). On average, cross-sectional glomerular tuft area was ~25% greater in male hypoxia-exposed offspring compared to male controls at 12 months of age (Figure 4A; $P_{\text{treatment}} = 0.03$). The chronic high salt diet increased glomerular area in control animals by 23%, and by 12% in hypoxia-exposed offspring (Figure 4A; $P_{\text{diet}} = 0.048$). Perivascular fibrosis tended to be greater in male hypoxia-exposed offspring, with no effect of postnatal diet, although this did not reach significance (Figure 4A; $P_{\text{treatment}} = 0.08$). The percentage of interstitial fibrosis in renal tissue was greatest in male hypoxia-exposed offspring compared to control animals, and there was no effect of postnatal diet (Figure 4A; $P_{\text{treatment}} = 0.01$). Prenatal treatment and the postnatal high salt diet had no effect on glomerular area, perivascular fibrosis, interstitial fibrosis or the overall histology score in female offspring (Figure 4B).

Histologically, the kidneys from hypoxia-exposed male offspring were characterized by widespread, mild to severe interstitial fibrosis, increases of mesangial matrix and glomerular basement membranes, mild to moderate thickening of the basement membrane of the Bowman's capsule, segmental thickening of tubular basement membranes, occasional regeneration of tubules and presence of hyaline, and acellular casts in tubular lumina. These changes were somewhat exacerbated in some of the animals on high salt postnatal diet (Figure 4C). In most of the affected animals there was also multifocal, mild to moderate interstitial infiltration of lymphocytes and fewer macrophages; often with a clear vasulocentric localisation.

We then examined kidneys of male offspring at 4 months of age to determine whether these pathological changes due to prenatal hypoxia or a postnatal salt were evident at a younger age. The high salt diet significantly increased perivascular fibrosis in male control and hypoxia-exposed offspring at 4 months (Figure 5A-B; $P_{\text{diet}} = 0.007$). Interstitial fibrosis was increased in hypoxia-exposed male offspring, as well as offspring fed the high salt diet (Figure 5A-B; $P_{\text{treatment}} = 0.01$, $P_{\text{diet}} = 0.007$). No signs of salt-induced glomerular hypertrophy were evident at 4 months of age (Figure 5A-B).

Discussion

Our study shows late gestation hypoxia resulted in cardiovascular and kidney dysfunction and pathology in mouse offspring. Prenatal hypoxia reduced the number of glomeruli in male offspring, leading to compensatory glomerular hypertrophy, renal fibrosis and mild albuminuria in 12-month-old offspring. In contrast, female offspring exposed to the same hypoxic insult *in utero* presented with a normal number of glomeruli and renal pathology equivalent to control animals by 12 months of age. Interestingly, both sexes developed an increase in blood pressure in later life, suggesting that gender is protective against morphological signs of kidney disease but not against the development of hypertension. We also demonstrated that a high salt diet caused an exacerbation of renal pathology after only 6 weeks in male hypoxia-exposed offspring with a nephron deficit. Maintenance of this high salt diet throughout adult life increased cardiac tissue fibrosis, particularly in male hypoxia-exposed offspring. Together this shows that the combination of prenatal hypoxia and a postnatal high salt diet predisposes offspring, particularly males, to adulthood cardiovascular disease.

Hypoxia leads to early growth restriction and subsequent catch up growth

In humans, fetal hypoxia leads to asymmetric growth restriction and subsequent low birth weight (Kingdom & Kaufmann, 1997; Giussani *et al.*, 2001), both of which are associated with hypertension as well as other cardiovascular and metabolic diseases (Barker, 1998). We have shown that both male and female hypoxia-exposed offspring are growth restricted as embryos and at birth, and remain growth restricted at weaning. The growth restriction at weaning may suggest an impaired lactational environment similar to reports in a rat model of uteroplacental insufficiency (O'Dowd *et al.*, 2008). Offspring also have an increased brain to body weight ratio at weaning, suggestive of brain sparing. This is a fetal adaptation triggered by hypoxia (acute and chronic), resulting in redistribution of cardiac output away from the peripheral tissues towards immediately essential organs such as the brain (Giussani, 2016). Persistent redistribution of blood away from the periphery may explain why the kidneys in the hypoxia-exposed animals are lighter than controls at E18.5 and P21, but heart and brain weights are maintained. Although this may increase the chance of fetal survival, this likely contributes to poor development and reduced numbers of glomeruli (nephrons) in the kidneys. As reported previously, these offspring undergo catch-up growth after weaning and by 2 months of age weigh the same as control animals (Walton *et al.*, 2016). An extensive series of epidemiological studies by David Barker and colleagues revealed that reduced fetal growth combined with accelerated postnatal growth is strongly associated with the development of hypertension (Eriksson *et al.*, 1999; Forsén *et al.*, 1999; Eriksson *et al.*, 2000). This

may be due to increased demand being placed on organs that developed sub-optimally *in utero*, and suggests these animals exposed to maternal hypoxia are at increased risk of developing elevated blood pressure.

Sex specific reductions in nephron number following prenatal hypoxia

Given kidneys from hypoxia-exposed offspring were reduced in weight from late gestation to weaning, we hypothesised that prenatal hypoxia had impaired nephrogenesis. We confirmed, using unbiased stereology, that the number of glomeruli per kidney in the male hypoxia-exposed mice was reduced by ~25%. This is an equivalent reduction in glomerular number to that seen in mice exposed to transient mid-gestational hypoxia (males and females combined) (Wilkinson *et al.*, 2015), and in males offspring following uteroplacental insufficiency in the rat (Wlodek *et al.*, 2007). However, female hypoxia-exposed offspring presented with number of glomeruli per kidney similar to that of the control offspring suggesting that gender is somewhat protective against the hypoxic insult induced throughout late gestation. Similar to our study, modest protein restriction in the pregnant rat leads to a ~25% reduction in glomerular number in male offspring (Woods *et al.*, 2001) with normal glomerular number in the female offspring (Woods *et al.*, 2005). Furthermore, sex differences in the degree of nephron deficit have been reported in a variety of models, such as maternal glucocorticoid exposure in the mouse [a nephron deficit of ~33% in male offspring compared to ~25% in female offspring (O'Sullivan *et al.*, 2015)] or alcohol exposure in rats [~20% reduction in male offspring but only ~10% in female offspring (Gray *et al.*, 2010)].

To verify our sex specific findings in juvenile animals, we performed glomerular estimation in kidneys from offspring at 12 months of age. Again, we observed the same ~25% glomerular deficit in aged male hypoxia-exposed offspring but similar glomerular number in female offspring. However, when counting glomeruli in kidneys of aged hypoxia male offspring, we observed evidence of glomerulosclerosis suggesting the congenital deficit combined with sclerotic and/or obsolescent glomeruli would result in a functional nephron deficit of >25% in aged male hypoxia-exposed offspring. This aging effect was associated with reduced PNA staining which is a marker of the plasma membrane of podocytes. No differences in PNA staining were observed at P21. Whether this implies that the glomeruli from male hypoxia-exposed offspring kidneys undergo progressive podocyte depletion with age needs to be further examined. Podocyte depletion is a cause of focal and segmental glomerulosclerosis (Puelles & Bertram, 2015). By adulthood, the kidneys from hypoxia-exposed animals attained the same weight as control animals albeit with the same nephron deficit present. This suggests that existing nephron units undergo substantial hypertrophy postnatally. This is due in part to hypertrophy of glomeruli, but may also involve

hypertrophy of renal tubular segments. It is important to note that we used simple morphometry to assess glomerular area; however, unbiased stereology in resin-embedded kidney tissue is necessary for true glomerular volume estimation. However, the increase in glomerular tuft area at 12 months of age in the prenatal hypoxia-exposed male was not observed at P21 or 4 months of age, suggesting glomerular hypertrophy occurred with age.

Impaired renal function

There was no evidence of renal dysfunction in the hypoxia exposed offspring in early life, at 2 or 4 months of age. Mild albuminuria manifested in male hypoxia-exposed offspring at 12 months, supporting our suggestion of progressive renal and cardiovascular damage in male hypoxia-exposed offspring. Albuminuria in humans is associated with cardiovascular risk factors such as vascular endothelial dysfunction (Stehouwer *et al.*, 1992; Gerstein *et al.*, 2001) which we previously reported in these animals (Walton *et al.*, 2016). Under basal conditions, hypoxia-exposed offspring were able to maintain normal urine flow and electrolyte excretion. Future studies could include introducing functional challenges to the renal system, such as a water deprivation challenge or volume loading. We did challenge the offspring with a high salt diet throughout life. In all groups of animals, the high salt diet resulted in increases in water intake and a tendency for increased 24 h urinary outputs, with increased sodium and chloride excretion. The high salt diet did not exacerbate albuminuria in offspring, which was previously reported in a genetic mouse model of low nephron number (Ruta *et al.*, 2010). However, a study using Wistar Kyoto rats shows a high salt diet elevated blood pressure and caused glomerular injury, but did not lead to proteinuria or reduced creatinine/cystatin C (Lankhorst *et al.*, 2016).

Notably creatinine measurements lack specificity and a large portion of creatinine is known to be excreted by the renal tubules rather than filtered through the glomeruli in mice (Keppler *et al.*, 2007; Eisner *et al.*, 2010). Consequently, we have used plasma cystatin C levels as a marker of renal function in mouse offspring. Reduced plasma cystatin C levels, currently the best endogenous marker of GFR in humans (Dharnidharka *et al.*, 2002), were observed in animals fed the high salt diet. This appears counterintuitive to what we would expect with salt-induced renal damage, as high plasma cystatin C levels are indicative of reduced GFR. Reduced cystatin C may indicate hyperfiltration in the high salt animals, and may reflect increased water consumption in these animals. Hyperfiltration in the setting of a nephron deficit has been reported in rats (Sanders *et al.*, 2005) and mice (Ruta *et al.*, 2010) with reduced nephron number, as well as models of early diabetes. Models of diabetes have shown that proximal tubule hypertrophy (leading to increased renal mass) increases proximal tubule sodium reabsorption, thereby reduced sodium delivery to the

distal tubule and affecting tubuloglomerular feedback in a way that leads to hyperfiltration (Thomas *et al.*, 2005). The salt-induced renal hypertrophy we have reported is likely to be predominantly tubular in origin given glomeruli occupy a relatively small proportion of the kidney (even when hypertrophied) and the renal tubules are known to have remarkable capacity to grow postnatally (for comprehensive review, see (Fong *et al.*, 2014)). Therefore, we could argue that if the increase in kidney mass is primarily due to proximal tubule hypertrophy in high salt-fed animals, hyperfiltration could ensue. GFR measurement by clearance measurements and analysis of renal tubule lengths is needed to confirm his hypothesis.

Renal pathology due to prenatal hypoxia and postnatal high salt diet

We examined kidney tissue across life and observed progressive glomerulosclerosis, tubulointerstitial fibrosis and perivascular fibrosis from P21 to 12 months of age in the male hypoxia-exposed offspring. Fibrosis is also a hallmark of aging, and is present in pathological situations such as cardiovascular and kidney disease (Liu, 2006). Renal fibrosis was widespread in most kidneys at 12 months of age, however, greatest in hypoxia-exposed male kidneys compared to control male kidneys. Although fibrosis was present in kidneys from female offspring, no effect of prenatal treatment or the high salt diet was observed. Consequently, we examined male kidneys at 4 months of age to determine whether the renal fibrosis was present at an earlier age. One of the most striking findings of our study was the significant increase in perivascular and interstitial renal fibrosis evident in hypoxia exposed male offspring on the high salt diet at 4 months of age. This was only 6 weeks after the high salt diet was introduced, suggesting the combination of two insults increases risk of organ damage. Therefore, given perivascular fibrosis was mainly influenced by diet but not prenatal treatment, consumption of a low salt diet from 2.5-12 months of age substantially attenuated cardiovascular risk factors in male hypoxia-exposed offspring. Whether intervention in early life, such as returning to a healthier diet, could ameliorate early predisposition to fibrosis is a pertinent research question given a major arm of hypertension treatment involves dietary salt reduction (Sacks *et al.*, 2001).

Prenatal hypoxia results in elevated blood pressure in both sexes

A nephron deficit is tightly associated with elevated blood pressure in the human population (Keller *et al.*, 2003) as well as in a variety of animal models (Moritz *et al.*, 2009). However, we have shown that both male and female offspring exposed to *in utero* hypoxia develop elevated blood pressure, despite female offspring not having a deficit of nephrons. The low nephron number in male offspring may contribute to elevated blood pressure, and lead to subsequent sclerosis of glomeruli and further worsening of blood pressure elevation and renal injury (Brenner & Mackenzie, 1997).

However, the nephron deficit and associated pathology that occurred with ageing is unlikely to be the sole cause of elevated blood pressure given the female offspring also presented with elevated blood pressure. Previous models of maternal hypoxia in the rat have shown that offspring develop altered vascular function/structure (Giussani *et al.*, 2012) and cardiovascular pathology (Rueda-Clausen *et al.*, 2012). We recently confirmed that modest hypoxia during pregnancy in the mouse leads to endothelial dysfunction and impaired vascular structure in both males and females (Walton *et al.*, 2016). Impaired vascular structure and function both contribute to hypertension in the human population, and could be a mechanism contributing to the elevated blood pressure in our study. It is important to note that mean arterial pressure is elevated in both sexes albeit with different origins. Diastolic blood pressure was elevated in both male and female mice, which is consistent with increased peripheral vascular resistance. The microvascular endothelial dysfunction in these offspring may be a contributing factor (Walton *et al.*, 2016). In contrast to male offspring with isolated diastolic pressure elevation, female hypoxia-exposed offspring presented with elevated systolic and diastolic blood pressure. There is controversy in the literature surrounding the relative importance of systolic and diastolic blood pressures in hypertension. However, in humans, isolated diastolic hypertension is predominant in young males and appears to be antecedent to systolic-diastolic hypertension (Franklin *et al.*, 2005). Plasma triglyceride levels, a marker of cardiovascular disease risk (Hokanson & Austin, 1996), were unaffected by prenatal hypoxia. This has previously been reported in a similar model of prenatal hypoxia in the rat, where plasma hyperlipidemia only emerged when metabolic syndrome was induced by high-fat feeding (Rueda-Clausen *et al.*, 2011).

We also examined cardiovascular reactivity to stress in offspring, as abnormal cardiovascular stress responses are strongly associated with signs of cardiovascular disease in the clinical setting, such as hypertension and left ventricular hypertrophy (Treiber *et al.*, 2003). Cardiovascular reactivity to restraint stress tended to be reduced in male and female hypoxia-exposed offspring compared to controls, although this did not reach significance. A power analysis has revealed that a sample size of 8 per treatment group would be required to detect statistical difference with the standard deviations obtained in this experiment. Unfortunately, we were only able to obtain N=4-5 animals per treatment group due to health of the offspring following surgeries and we are therefore underpowered in this study. Future studies using younger offspring less prone to surgical complications are advised in the future. The tendency towards a blunted stress response may be associated with deficits in corticosterone release during restraint stress. This has previously been reported in a mouse model deficient in corticotropin-releasing hormone receptor 1 (Timpl *et al.*, 1998). Analysis of plasma corticosterone levels from these offspring at 12 months of age could be performed in the future to examine this hypothesis. Unfortunately, we were unable to measure

blood pressure in the mice exposed to high salt due to difficulties with these animals surviving surgery.

Increased cardiac fibrosis with prenatal hypoxia and high salt

In addition to our previously reported differences in vascular function due to prenatal hypoxia and a postnatal high salt diet, we hypothesised the heart may be affected. Fibrosis can appear in the interstitium and perivascular spaces in the heart, leading to reduced myocardial and arterial compliance (Birnacka & Frangogiannis, 2011). In 12-month-old offspring, we observed that prenatal hypoxia increased interstitial cardiac fibrosis in both sexes. Pathological myocardial fibrosis is associated with diastolic dysfunction, and although we did not perform echocardiography in our study, a similar model of prenatal hypoxia (12% oxygen, E15 – birth) showed rat offspring had normal cardiac function at 4 months of age but went on to develop left ventricular diastolic dysfunction and increased ventricular collagen expression by 12 months (Rueda-Clausen *et al.*, 2008). This supports our findings in the mouse, and suggests our hypoxia-exposed animals with elevated diastolic blood pressure may be at risk of diastolic dysfunction and therefore heart failure. In addition, although we were unable to measure blood pressure in the animals fed the high salt diet, we did observe increased cardiac perivascular fibrosis in male animals on this diet. In humans, perivascular cardiac fibrosis is associated with impaired coronary blood flow (Dai *et al.*, 2012) and suggests the additional postnatal high salt diet may further increase risk of cardiovascular disease.

Conclusion

We conclude that prenatal hypoxia alone leads to elevated blood pressure and susceptibility to salt-induced cardiac injury in male and female offspring. Prenatal hypoxia impaired the process of nephrogenesis in male offspring only, leading to a reduced number of nephrons and ultimately signs of renal injury in adulthood. This suggests that the renal system in females is somehow protected from the *in utero* hypoxic insult; however, this protection does not extend to the cardiovascular system. Furthermore, male offspring were more susceptible to cardiac and renal fibrosis compared to female offspring. The mechanisms behind this sexual dichotomy remain to be elucidated. We have now shown that multiple organ systems are impaired by prenatal hypoxia, a postnatal high salt diet, or a combination of these two insults. Given our findings, we suggest that healthy dietary consumption throughout life, particularly by curtailing salt intake, can minimise progressive cardiac and renal damage for those known to have suffered from an adverse *in utero* environment. Notably, the chronic high salt diet also caused significant cardiovascular and renal tissue damage in offspring born from a normal pregnancy. This shows that adherence to the NHMRC's recommendations to reduce salt intake is relevant for the cardiovascular and renal health of all individuals in society.

Additional information

Competing interests

The authors declare no competing interests.

Author contributions

SLW, RRS, TMP and KMM were responsible for conception and design of the experiments. SLW, HBO and TMP were responsible for the collection and analysis of data. All authors were involved in data interpretation, drafting the article and revising it critically for intellectual content. All authors approved the final version of the manuscript submitted for publication.

Funding

This project was funded by the National Health and Medical Research Council of Australia (NHMRC-APP1009338). KMM was supported by fellowships provided by the NHMRC. SLW was supported by an Australian Postgraduate Award.

References

- Barker DJ. (1998). In utero programming of chronic disease. *Clin Sci* **95**, 115-128.
- Biernacka A & Frangogiannis NG. (2011). Aging and cardiac fibrosis. *Aging and Disease* **2**, 158-173.
- Brenner BM & Mackenzie HS. (1997). Nephron mass as a risk factor for progression of renal disease. *Kid Int Suppl* **63**, S124-127.
- Camm EJ, Hansell JA, Kane AD, Herrera EA, Lewis C, Wong S, Morrell NW & Giussani DA. (2010). Partial contributions of developmental hypoxia and undernutrition to prenatal alterations in somatic growth and cardiovascular structure and function. *Am J Obstet Gynecol* **203**, 495.e424-495.e434.
- Cuffe J, Walton S, Singh R, Spiers J, Bielefeldt-Ohmann H, Wilkinson L, Little M & Moritz K. (2014a). Mid-to late term hypoxia in the mouse alters placental morphology, glucocorticoid regulatory pathways and nutrient transporters in a sex-specific manner. *J Physiol* **592**, 3127-3141.
- Cuffe J, Walton S, Steane S, Singh R, Simmons D & Moritz K. (2014b). The effects of gestational age and maternal hypoxia on the placental renin angiotensin system in the mouse. *Placenta* **35**, 953-961.
- Dai Z, Aoki T, Fukumoto Y & Shimokawa H. (2012). Coronary perivascular fibrosis is associated with impairment of coronary blood flow in patients with non-ischemic heart failure. *J Cardiol* **60**, 416-421.
- Dharnidharka VR, Kwon C & Stevens G. (2002). Serum cystatin C is superior to serum creatinine as a marker of kidney function: A meta-analysis. *Am J Kidney Dis* **40**, 221-226.
- Eriksson J, Forsén T, Tuomilehto J, Osmond C & Barker D. (2000). Fetal and childhood growth and hypertension in adult life. *Hypertension* **36**, 790-794.
- Eriksson JG, Forsén T, Tuomilehto J, Winter PD, Osmond C & Barker DJP. (1999). Catch-up growth in childhood and death from coronary heart disease: longitudinal study. *BMJ* **318**, 427-431.

Fong D, Denton KM, Moritz KM, Evans R & Singh RR. (2014). Compensatory responses to nephron deficiency: adaptive or maladaptive? *Nephrology* **19**, 119-128.

Forsén T, Eriksson JG, Tuomilehto J, Osmond C & Barker DJP. (1999). Growth in utero and during childhood among women who develop coronary heart disease: longitudinal study. *BMJ* **319**, 1403-1407.

Franklin SS, Pio JR, Wong ND, Larson MG, Leip EP, Vasani RS & Levy D. (2005). Predictors of new-onset diastolic and systolic hypertension: the Framingham heart study. *Circulation* **111**, 1121-1127.

Gerstein HC, Mann JE, Yi Q & et al. (2001). ALbuminuria and risk of cardiovascular events, death, and heart failure in diabetic and nondiabetic individuals. *JAMA* **286**, 421-426.

Giussani DA. (2016). The fetal brain sparing response to hypoxia: physiological mechanisms. *J Physiol* **594**, 1215-1230.

Giussani DA, Camm EJ, Niu Y, Richter HG, Blanco CE, Gottschalk R, Blake EZ, Horder KA, Thakor AS, Hansell JA, Kane AD, Wooding FBP, Cross CM & Herrera EA. (2012). Developmental programming of cardiovascular dysfunction by prenatal hypoxia and oxidative stress. *PLoS ONE* **7**, e31017.

Giussani DA, Phillips PS, Anstee S & Barker DJP. (2001). Effects of altitude versus economic status on birth weight and body shape at birth. *Pediatr Res* **49**, 490-494.

Gray SP, Denton KM, Cullen-McEwen L, Bertram JF & Moritz KM. (2010). Prenatal exposure to alcohol reduces nephron number and raises blood pressure in progeny. *J Am Soc Nephrol* **21**, 1891-1902.

Guyton AC, Coleman TG, Cowley AW, Scheel KW, Manning RD & Norman RA. (1972). Arterial pressure regulation: overriding dominance of the kidneys in long-term regulation and in hypertension. *Am J Med* **52**, 584-594.

- Hadi HAR, Carr CS & Al Suwaidi J. (2005). Endothelial dysfunction: cardiovascular risk factors, therapy, and outcome. *Vasc Health Risk Manag* **1**, 183-198.
- Hartman HA, Lai HL & Patterson LT. (2007). Cessation of renal morphogenesis in mice. *Dev Bio* **310**, 379-387.
- Hinchliffe S, Sargent P, Howard C, Chan Y & Van Velzen D. (1991). Human intrauterine renal growth expressed in absolute number of glomeruli assessed by the disector method and Cavalieri principle. *Lab Invest* **64**, 777-784.
- Hughson M, Douglas-Denton R, Bertram J & Hoy W. (2006). Hypertension, glomerular number, and birth weight in African Americans and white subjects in the southeastern United States. *Kidney Int* **69**, 671-678.
- Hughson M, Farris AB, 3rd, Douglas-Denton R, Hoy WE & Bertram JF. (2003). Glomerular number and size in autopsy kidneys: the relationship to birth weight. *Kidney Int* **63**, 2113-2122.
- Hutter D, Kingdom J & Jaeggi E. (2010). Causes and mechanisms of intrauterine hypoxia and its impact on the fetal cardiovascular system: a review. *Int J Pediatr* **2010**, 401323.
- Keller G, Zimmer G, Mall G, Ritz E & Amann K. (2003). Nephron number in patients with primary hypertension. *N Engl J Med* **348**, 101-108.
- Kingdom JC & Kaufmann P. (1997). Oxygen and placental villous development: origins of fetal hypoxia. *Placenta* **18**, 613-621; discussion 623-616.
- Lankhorst S, Baelde HJ, Clahsen-van Groningen MC, Smedts FMM, Danser AHJ & van den Meiracker AH. (2016). Effect of high salt diet on blood pressure and renal damage during vascular endothelial growth factor inhibition with sunitinib. *Nephrol Dial Transplant* **31**, 914-921.
- Lim K, Zimanyi MA & Black MJ. (2006). Effect of maternal protein restriction in rats on cardiac fibrosis and capillarization in adulthood. *Pediatr Res* **60**, 83-87.
- Liu Y. (2006). Renal fibrosis: new insights into the pathogenesis and therapeutics. *Kidney Int* **69**, 213-217.

- Moritz KM, Singh RR, Probyn ME & Denton KM. (2009). Developmental programming of a reduced nephron endowment: more than just a baby's birth weight. *Am J Physiol Renal Physiol* **296**, F1-F9.
- O'Dowd R, Kent JC, Moseley JM & Wlodek ME. (2008). Effects of uteroplacental insufficiency and reducing litter size on maternal mammary function and postnatal offspring growth. *Am J Physiol Regul Integr Comp Physiol* **294**, R539-R548.
- O'Sullivan L, Cuffe JS, Koning A, Singh RR, Paravicini TM & Moritz KM. (2015). Excess prenatal corticosterone exposure results in albuminuria, sex-specific hypotension, and altered heart rate responses to restraint stress in aged adult mice. *Am J Physiol Renal Physiol* **308**, F1065-F1073.
- Peeters LL, Sheldon RE, Jones MD, Makowski EL & Meschia G. (1979). Blood flow to fetal organs as a function of arterial oxygen content. *Am J Obstet Gynecol* **135**, 637-646.
- Puelles VG & Bertram JF. (2015). Counting glomeruli and podocytes: rationale and methodologies. *Curr Opin Nephrol Hypertens* **24**, 224-230.
- Rueda-Clausen CF, Dolinsky VW, Morton JS, Proctor SD, Dyck JR & Davidge ST. (2011). Hypoxia-induced intrauterine growth restriction increases the susceptibility of rats to high-fat diet-induced metabolic syndrome. *Diabetes* **60**, 507-516.
- Rueda-Clausen CF, Morton JS & Davidge ST. (2008). Effects of hypoxia-induced intrauterine growth restriction on cardiopulmonary structure and function during adulthood. *Cardiovasc Res* **81**, 713-722.
- Rueda-Clausen CF, Morton JS, Dolinsky VW, Dyck JRB & Davidge ST. (2012). Synergistic effects of prenatal hypoxia and postnatal high-fat diet in the development of cardiovascular pathology in young rats. *Am J Physiol Regul Integr Comp Physiol* **303**, R418-R426.
- Ruta L-AM, Dickinson H, Thomas MC, Denton KM, Anderson WP & Kett MM. (2010). High-salt diet reveals the hypertensive and renal effects of reduced nephron endowment. *Am J Physiol Renal Physiol* **298**, F1384-F1392.

Sacks FM, Svetkey LP, Vollmer WM, Appel LJ, Bray GA, Harsha D, Obarzanek E, Conlin PR, Miller ER & Simons-Morton DG. (2001). Effects on blood pressure of reduced dietary sodium and the Dietary Approaches to Stop Hypertension (DASH) diet. *N Engl J Med* **344**, 3-10.

Sanders MW, Fazzi GE, Janssen GM, Blanco CE & De Mey JG. (2005). High sodium intake increases blood pressure and alters renal function in intrauterine growth-retarded rats. *Hypertension* **46**, 71-75.

Stehouwer CD, Nauta JJ, Zeldenrust GC, Hackeng WH, Donker AJ & den Ottolander GJ. (1992). Urinary albumin excretion, cardiovascular disease, and endothelial dysfunction in non-insulin-dependent diabetes mellitus. *Lancet* **340**, 319-323.

Tare M, Parkington HC, Bubb KJ & Wlodek ME. (2012). Uteroplacental insufficiency and lactational environment separately influence arterial stiffness and vascular function in adult male rats. *Hypertension* **60**, 378-386.

Timpl P, Spanagel R, Sillaber I, Kresse A, Reul JM, Stalla GK, Blanquet V, Steckler T, Holsboer F & Wurst W. (1998). Impaired stress response and reduced anxiety in mice lacking a functional corticotropin-releasing hormone receptor 1. *Nat Genetics* **19**, 162-166.

Thomas MC, Burns WC & Cooper ME. (2005). Tubular changes in early diabetic nephropathy. *Adv Chronic Kid Dis* **12**, 177-186.

Treiber FA, Kamarck T, Schneiderman N, Sheffield D, Kapuku G & Taylor T. (2003). Cardiovascular Reactivity and Development of Preclinical and Clinical Disease States. *Psychosomatic Med* **65**, 46-62.

Walton SL, Singh RR, Tan T, Paravicini TM & Moritz KM. (2016). Late gestational hypoxia and a postnatal high salt diet programs endothelial dysfunction and arterial stiffness in adult mouse offspring. *J Physiol* **594**, 1451-1463.

Wilkinson LJ, Neal CS, Singh RR, Sparrow DB, Kurniawan ND, Ju A, Grieve SM, Dunwoodie SL, Moritz KM & Little MH. (2015). Renal developmental defects resulting from in utero hypoxia are associated with suppression of ureteric β -catenin signaling. *Kidney Int* **87**, 975-983.

Williams SJ, Hemmings DG, Mitchell JM, McMillen IC & Davidge ST. (2005). Effects of maternal hypoxia or nutrient restriction during pregnancy on endothelial function in adult male rat offspring. *J Physiol* **565**, 125-135.

Wlodek ME, Mibus A, Tan A, Siebel AL, Owens JA & Moritz KM. (2007). Normal lactational environment restores nephron endowment and prevents hypertension after placental restriction in the rat. *J Am Soc Nephrol* **18**, 1688-1696.

Woods LL, Ingelfinger JR, Nyengaard JR & Rasch R. (2001). Maternal protein restriction suppresses the newborn renin-angiotensin system and programs adult hypertension in rats. *Pediatr Res* **49**, 460-467.

Woods LL, Ingelfinger JR & Rasch R. (2005). Modest maternal protein restriction fails to program adult hypertension in female rats. *Am J Physiol Regul Integr Comp Physiol* **289**, R1131-1136.

Woods LL, Weeks DA & Rasch R. (2004). Programming of adult blood pressure by maternal protein restriction: Role of nephrogenesis. *Kidney Int* **65**, 1339-1348.

Tables

Table 1. Offspring body/organ weights at embryonic day 18.5 and postnatal day 21, and estimated glomerular number at postnatal day 21.

	Control		Hypoxia		Two-way ANOVA		
	Male	Female	Male	Female	$P_{treatment}$	P_{sex}	$P_{treatment \times sex}$
Embryonic day 18.5							
<i>Bw (g)</i>	1.35 ± 0.04	1.34 ± 0.04	1.27 ± 0.02	1.25 ± 0.03	0.02	0.4	0.9
<i>Heart weight (mg)</i>	7.78 ± 0.4	7.90 ± 0.3	7.75 ± 0.5	6.81 ± 0.4	0.2	0.3	0.2
<i>Heart:bw</i>	5.73 ± 0.4	5.95 ± 0.3	5.94 ± 0.4	5.25 ± 0.3	0.5	0.5	0.2
<i>Kidney weight (mg)</i>	10.69 ± 0.6	10.02 ± 0.5	8.96 ± 0.5	8.8 ± 0.99	0.04	0.5	0.7
<i>Kidney:bw</i>	7.83 ± 0.5	7.48 ± 0.3	7.04 ± 0.4	6.95 ± 0.6	0.2	0.6	0.8
Postnatal day 21							
<i>Bw (g)</i>	11.86 ± 0.3	11.20 ± 0.3	10.95 ± 0.3	10.39 ± 0.4	0.01	0.08	0.9
<i>Heart weight (mg)</i>	75.2 ± 2.8	72.2 ± 1.6	72.4 ± 2.7	70.8 ± 3.3	0.4	0.4	0.8
<i>Heart:bw</i>	6.27 ± 0.1	6.42 ± 0.1	6.5 ± 0.2	6.6 ± 0.1	0.1	0.3	0.99
<i>Kidney weight (mg)</i>	83.1 ± 2.8	78.6 ± 2.8	75.9 ± 2.2	73.2 ± 3.4	0.03	0.2	0.8
<i>Kidney:bw</i>	6.94 ± 0.2	6.96 ± 0.1	6.81 ± 0.1	6.86 ± 0.1	0.3	0.7	0.9
<i>Brain weight (mg)</i>	360.9 ± 12	359.6 ± 10	357.0 ± 17	378.5 ± 9	0.5	0.4	0.4
<i>Brain:bw</i>	30.7 ± 1.4	32.5 ± 1.1	32.4 ± 1.8	37.7 ± 2.2	0.04	0.03	0.3
<i>Estimated glomerular number</i>	12888 ± 515	9782 ± 517**	9854 ± 432	9753 ± 440	0.002	0.004	0.004

Values are mean ± SEM (E18.5: N = 6-7 litters per group; P21: N = 11 litters per group). The effect of treatment, sex or their interaction (treatment x sex) was evaluated by two-way ANOVA. **P<0.001 comparing male control and hypoxia-exposed offspring with a Bonferroni's multiple comparison test.

Table 2. Offspring body and organ weights, food/water intake, urine output and estimated glomerular number at 12 months of age,

	Normal Salt		High Salt		Two-way ANOVA		
	<i>Control</i>	<i>Hypoxia</i>	<i>Control</i>	<i>Hypoxia</i>	$P_{treatment}$	P_{diet}	$P_{treatment \times diet}$
Males							
Bw (g)	55 ± 1.5	55 ± 1.8	58 ± 2.7	57 ± 2.3	0.9	0.1	0.9
Total kidney (mg)	724 ± 35	715 ± 19	841 ± 75	912 ± 26	0.5	0.002	0.4
Total kidney:bw	13.2 ± 0.6	12.7 ± 0.4	14.6 ± 1.3	16.2 ± 0.7	0.9	0.02	0.5
Heart (mg)	253 ± 5.6	245 ± 4.6	273 ± 13.5	268 ± 7.2	0.9	0.007	0.8
Heart:bw	4.5 ± 0.1	4.5 ± 0.1	4.7 ± 0.1	4.8 ± 0.2	0.8	0.2	0.9
Brain (mg)	506 ± 9	510 ± 7	517 ± 6	514 ± 9	0.9	0.3	0.7
Brain:bw	9.2 ± 0.3	9.5 ± 0.4	9.0 ± 0.5	9.2 ± 0.4	0.8	0.3	0.6
Urine output (ml/24h)	1.73 ± 0.3	1.35 ± 0.3	2.01 ± 0.4	2.19 ± 0.5	0.7	0.1	0.6
Food consumption (g/bw/24h)	0.051 ± 0.009	0.067 ± 0.01	0.067 ± 0.009	0.048 ± 0.008	0.9	0.9	0.09
Water consumption (ml/bw/24h)	0.11 ± 0.008	0.14 ± 0.03	0.26 ± 0.05	0.19 ± 0.01	0.4	0.0003	0.09
Estimated glomerular number	13750 ± 671	10561 ± 662**	-	-	-	-	-
Females							
Bw (g)	53 ± 3	53 ± 3	60 ± 3	57 ± 2	0.7	0.09	0.5
Total kidney (mg)	493 ± 10	481 ± 22	543 ± 37	582 ± 44	0.6	0.02	0.4
Total kidney:bw	9.7 ± 0.7	9.1 ± 0.4	9.0 ± 0.4	10.4 ± 1.0	0.5	0.7	0.1
Heart (mg)	194 ± 13	189 ± 8	215 ± 13	220 ± 13	0.2	0.009	0.5
Heart:bw	3.8 ± 0.4	3.6 ± 0.2	3.6 ± 0.1	3.9 ± 0.3	0.8	0.9	0.3
Brain (mg)	508 ± 21	510 ± 14	523 ± 6	535 ± 12	0.8	0.3	0.2
Brain:bw	10.1 ± 1.0	9.8 ± 0.6	8.8 ± 0.5	9.5 ± 0.5	0.8	0.3	0.5
Urine output (ml/24h)	1.50 ± 0.3	1.57 ± 0.3	2.13 ± 0.3	3.02 ± 0.7	0.7	0.1	0.6
Food consumption (g/bw/24h)	0.052 ± 0.01	0.72 ± 0.002	0.10 ± 0.02	0.045 ± 0.006	0.4	0.6	0.1
Water consumption (ml/bw/24h)	0.07 ± 0.005	0.074 ± 0.02	0.26 ± 0.05	0.18 ± 0.07	0.5	0.01	0.5
Estimated glomerular number	10326 ± 763	10864 ± 1035	-	-	-	-	-

Values are mean \pm SEM (N = 11 litters per group). The effect of treatment, diet or their interaction (treatment x diet) was evaluated by two-way ANOVA. Body weight (bw). **P<0.01 comparing male control and hypoxia-exposed offspring nephron numbers by an unpaired Student's t test.

Table 3. Plasma electrolytes and triglycerides in 12-month-old offspring.

	Normal Salt		High Salt		Two-way ANOVA		
	<i>Control</i>	<i>Hypoxia</i>	<i>Control</i>	<i>Hypoxia</i>	$P_{treatment}$	P_{diet}	$P_{treatment \times diet}$
Males							
Na^+ (mmol/L)	126.6 ± 4.9	132.6 ± 3.0	139.6 ± 10.3	137.4 ± 4.0	0.8	0.2	0.5
Cl^- (mmol/L)	92.5 ± 5.2	100.0 ± 3.6	115.8 ± 9.8	104.2 ± 2.4	0.3	0.6	0.9
Triglycerides (mmol/L)	1.95 ± 0.3	2.25 ± 0.4	1.56 ± 1.2	2.19 ± 0.6	0.5	0.7	0.8
Females							
Na^+ (mmol/L)	128.4 ± 3.8	122.8 ± 7.1	132.0 ± 3.8	130.6 ± 3.7	0.5	0.3	0.7
Cl^- (mmol/L)	107.5 ± 7.9	90.8 ± 8.2	100.1 ± 3.9	102.9 ± 2.4	0.2	0.7	0.09
Triglycerides (mmol/L)	2.42 ± 0.5	1.32 ± 0.2	1.59 ± 0.2	1.72 ± 0.3	0.2	0.6	0.1

Values are mean ± SEM (N = 5-8 animals per group). The effect of treatment, diet or their interaction (treatment x diet) was evaluated by two-way ANOVA.

Figures

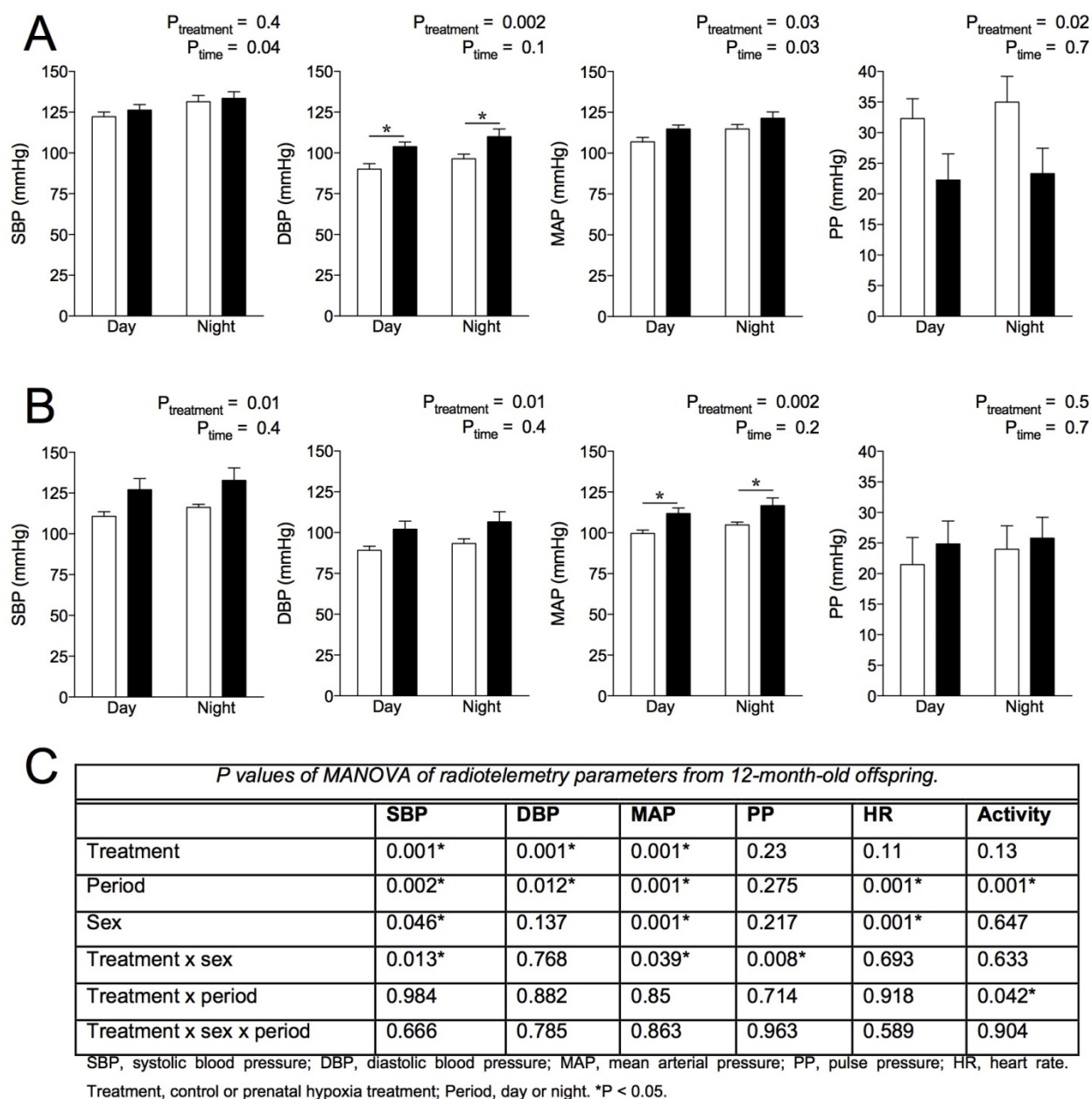


Figure 1. Effect of maternal hypoxia on the blood pressure profiles of offspring. Systolic blood pressure (SBP, mmHg), Diastolic blood pressure (DBP, mmHg), mean arterial pressure (MAP, mmHg) and pulse pressure (PP, mmHg) in male (A) and female (B) offspring. Data was analysed via two-way ANOVA and expressed as mean \pm SEM. * $P < 0.01$ comparing control and hypoxia-exposed offspring by Bonferroni *post hoc*. Control: white bars; hypoxia: black bars. P values of MANOVA of blood pressure parameters (C). N = 5-6 animals per group.

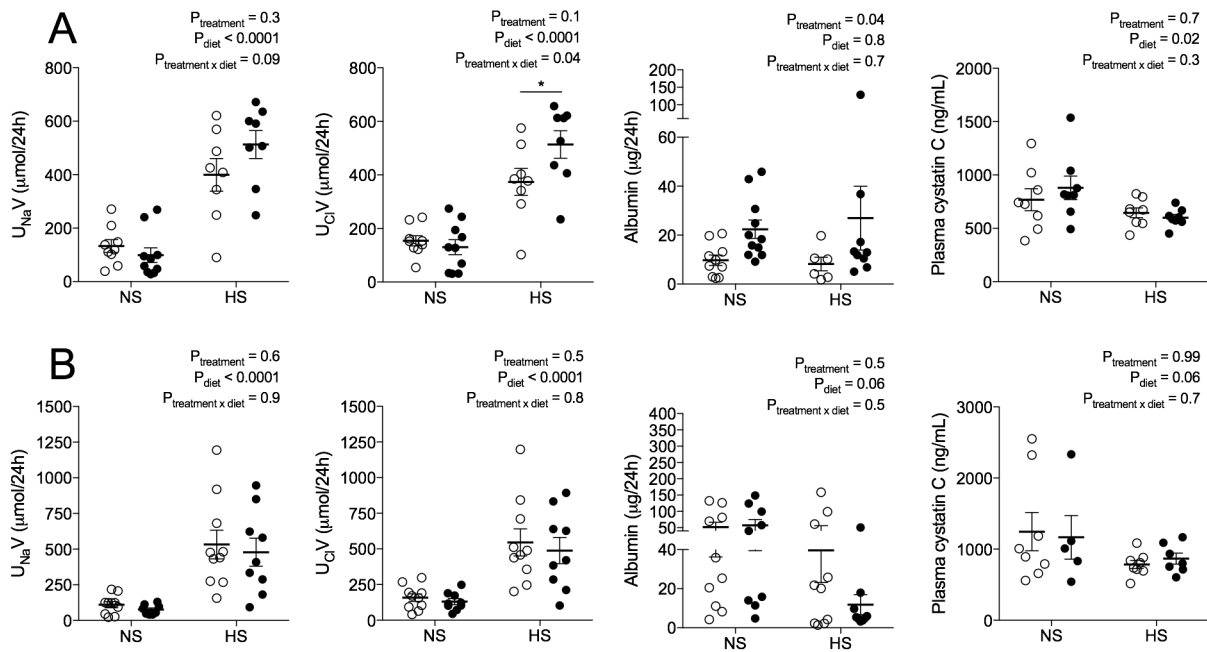


Figure 2. Effect of prenatal hypoxia on renal function in offspring aged 12 months. Urinary excretion of sodium ($\mu\text{mol}/24\text{h}$), urinary excretion of chloride ($\mu\text{mol}/24\text{h}$), urinary excretion of albumin ($\mu\text{g}/24\text{h}$) and plasma cystatin C levels (ng/mL) in male (A) and female (B) offspring. Data was analysed via two-way ANOVA and expressed as mean \pm SEM. * $P < 0.01$ comparing control and hypoxia-exposed offspring by Bonferroni *post hoc*. Control: open circles; hypoxia: black circles. Male: $N = 6-10$ animals per group; female: $N = 5-10$ animals per group.

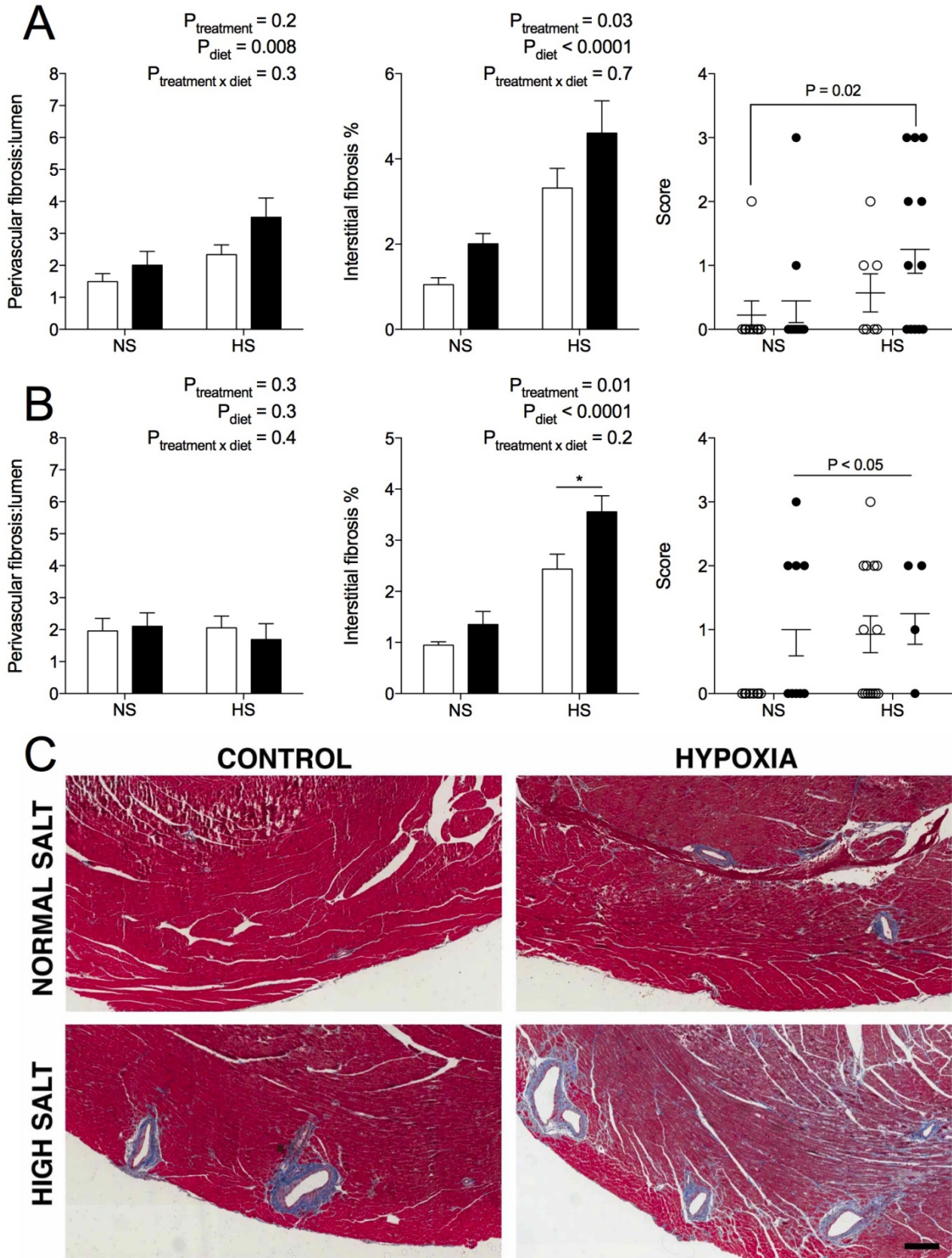


Figure 3. Histopathology of the hearts of offspring aged 12 months.

Overall histology score, perivascular fibrosis area normalised to lumen area, interstitial fibrosis expressed as a percentage of cardiac tissue in male (A) and female (B) offspring. Masson's Trichrome staining of cardiac tissue in male offspring. Blue staining marks collagen (fibrosis). (C). Scale bar represents 200 μm . Scoring was analysed via one-way ANOVA with different letters denoting statistical differences between groups. Perivascular and interstitial fibrosis were analysed via two-way ANOVA. All data expressed as mean \pm SEM. * $P < 0.01$ comparing control and hypoxia-exposed offspring by Bonferroni *post hoc*. Control: open points/bars; hypoxia: black points/bars. Male: N=5-11 animals per group; female: N=4-8 animals per group.

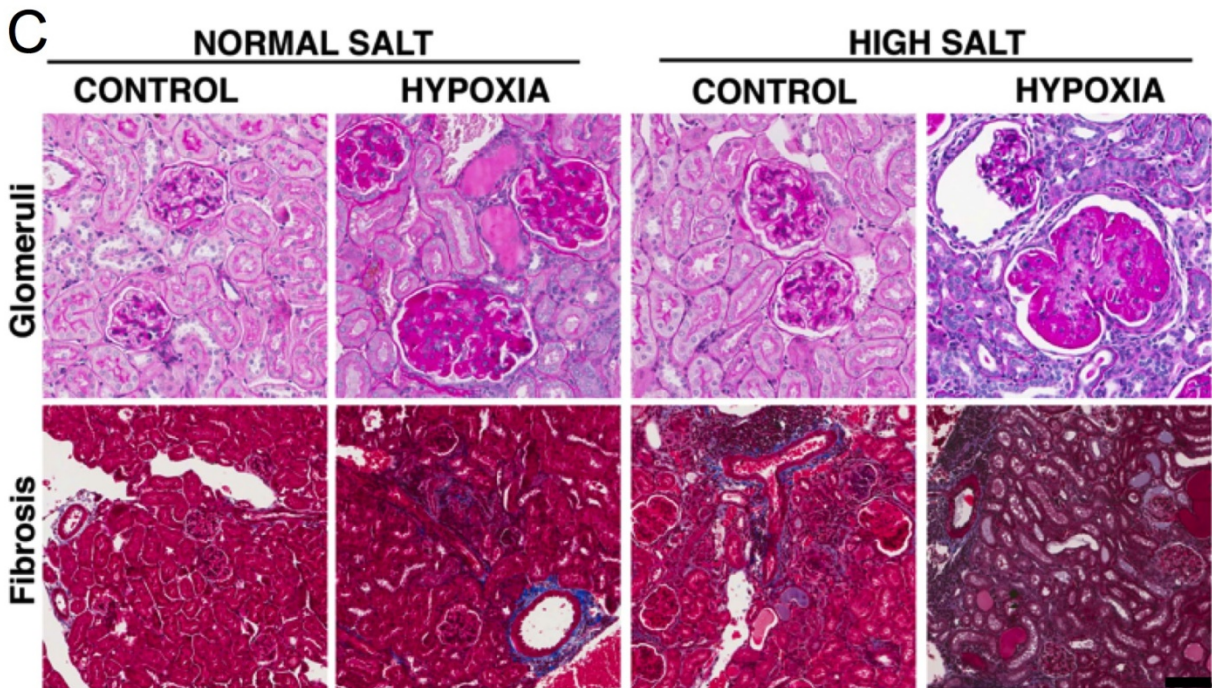
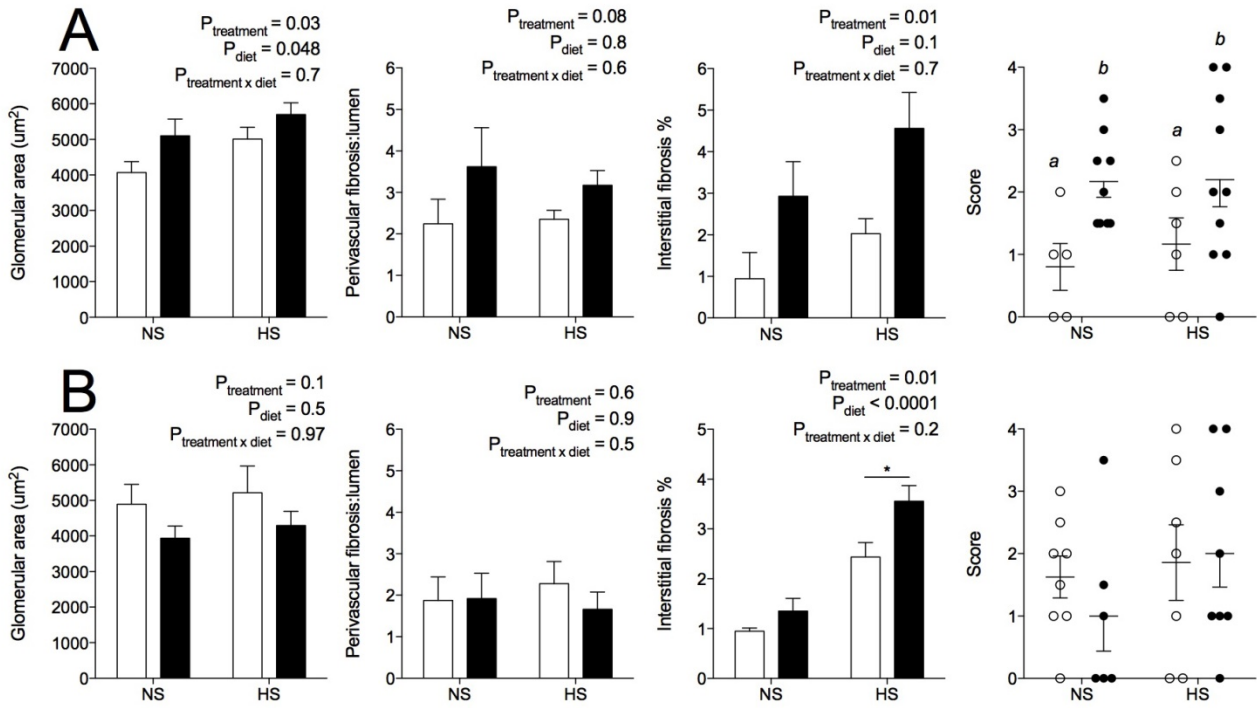


Figure 4. Renal morphometry and histopathology in male and female offspring at 12 months of age. Glomerular area, perivascular fibrosis area normalised to lumen area, interstitial fibrosis expressed as a percentage of renal tissue, and overall histopathology score in male (A) and female (B) offspring. (C) Period acid Schiff's staining of the renal cortex containing glomeruli and Masson's Trichrome staining of renal fibrosis (blue) in male offspring. Blue staining marks collagen (fibrosis). Scale bar represents 200 μm . Scoring was analysed via one-way ANOVA with different letters denoting statistical differences between groups. Perivascular and interstitial fibrosis, and glomerular area were analysed via two-way ANOVA. All data expressed as mean \pm SEM. Control: open bars; hypoxia: black bars. Male: N=5-11 animals per group.

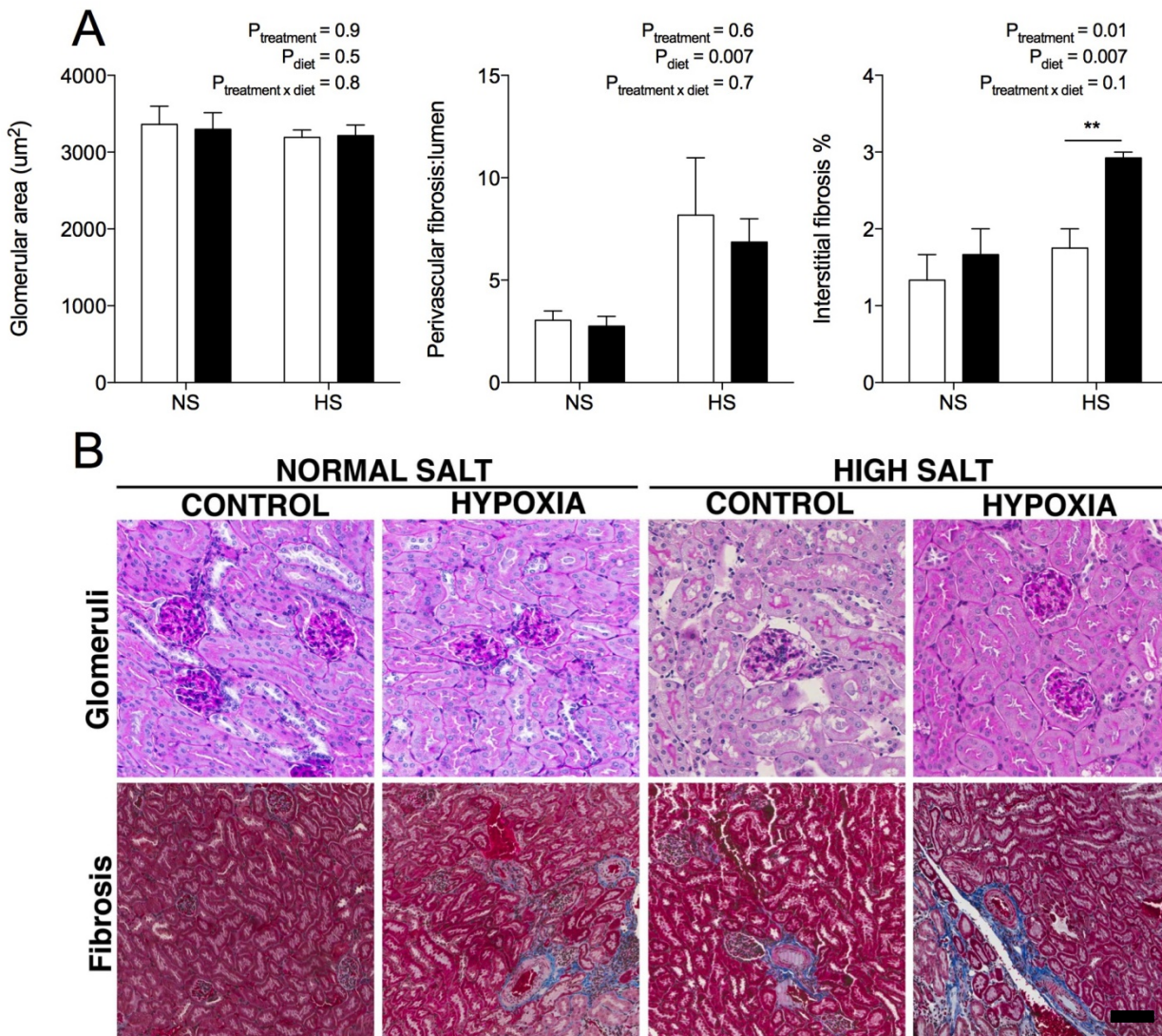
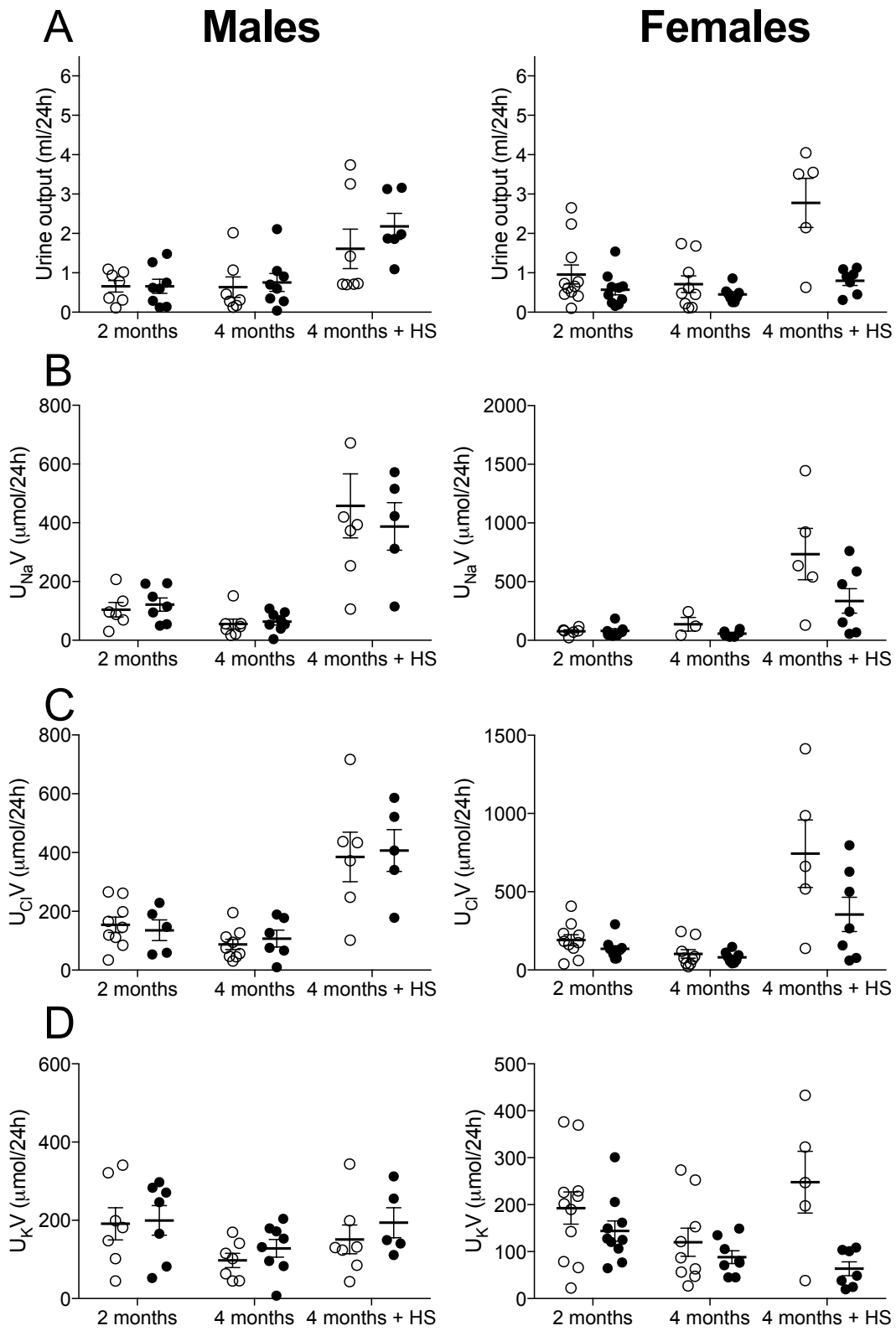


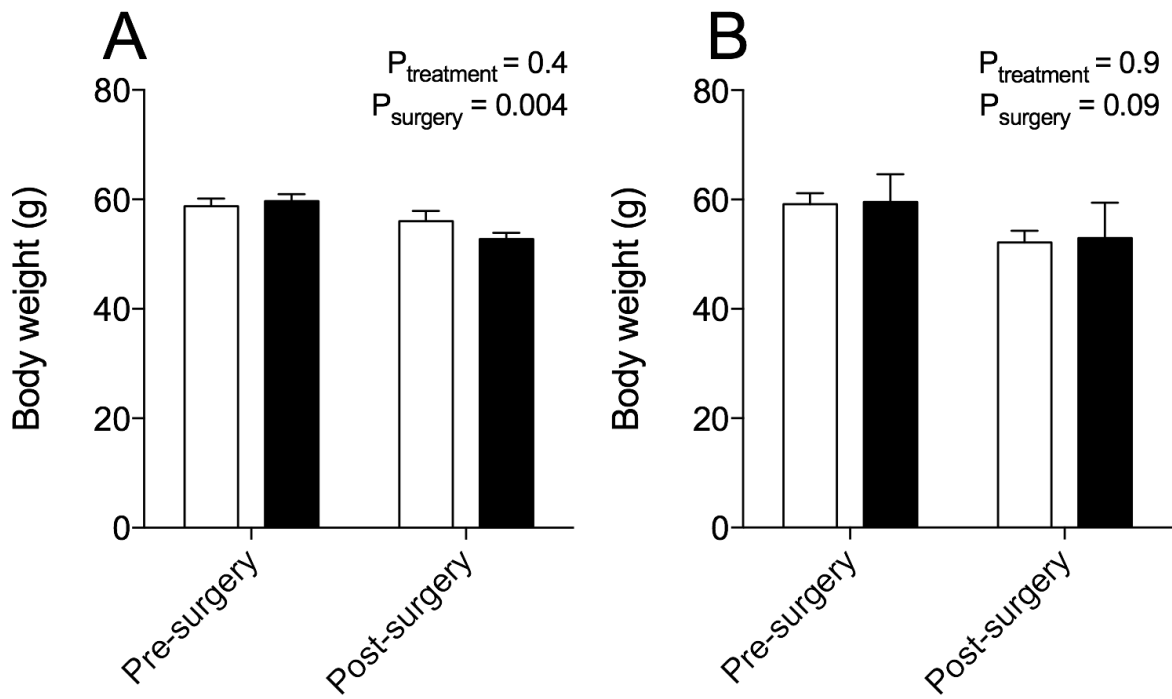
Figure 5. Renal morphometry and histopathology in male offspring at 4 months of age. (A) Glomerular area, perivascular fibrosis area normalised to lumen area, interstitial fibrosis expressed as a percentage of renal tissue, and overall histopathology score. (B) Period acid Schiff's staining of the renal cortex containing glomeruli. Masson's Trichrome staining of renal fibrosis (blue) in male offspring. Scale bar represents $200 \mu\text{m}$. Scoring was analysed via on e-way ANOVA with different letters denoting statistical differences between groups. Perivascular and interstitial fibrosis, and glomerular area were analysed via two-way ANOVA. ** $P < 0.001$ comparing control and hypoxia-exposed offspring by Bonferroni *post hoc*. All data expressed as mean \pm SEM. Control: open bars; hypoxia: black bars. Male: N=4-5 animals per group.

Supplementary figures

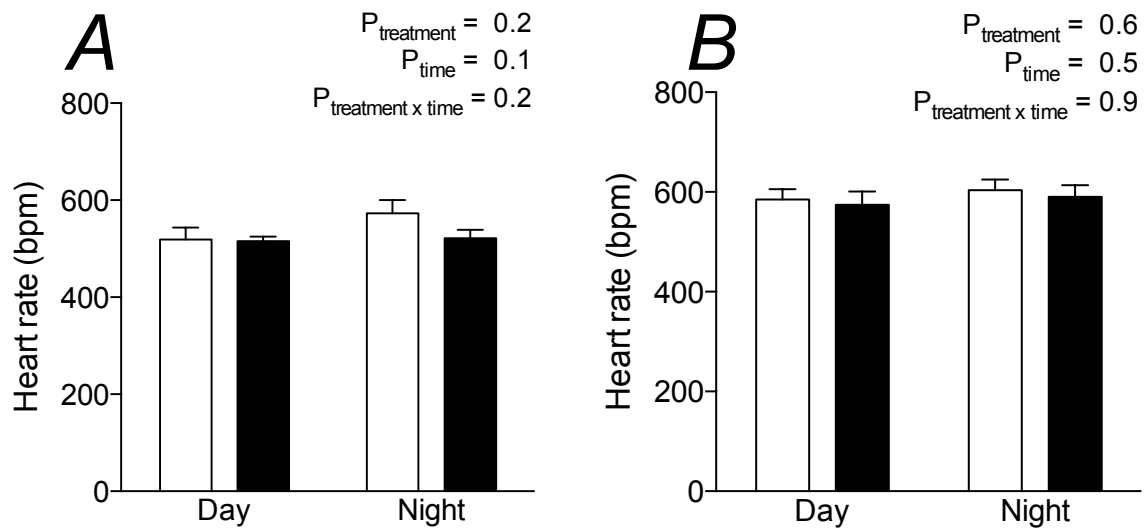


Supplementary Figure 1. Effect of prenatal hypoxia on renal function in offspring aged 2 months, and 4 months (normal salt [NS] and high salt [HS] diet).

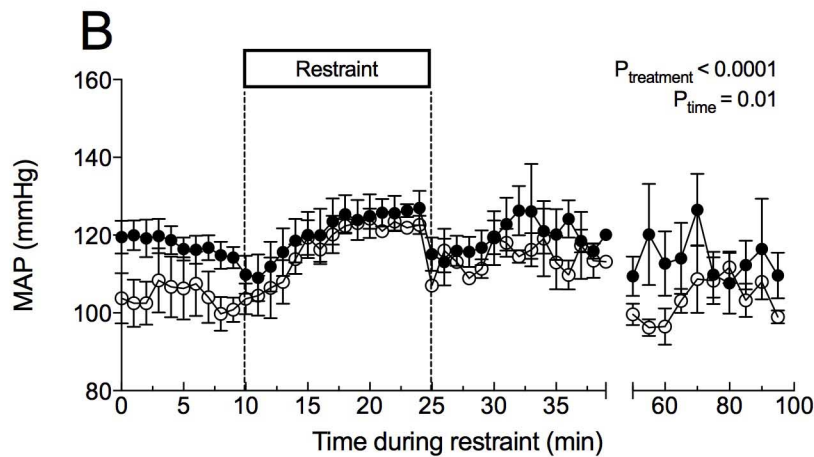
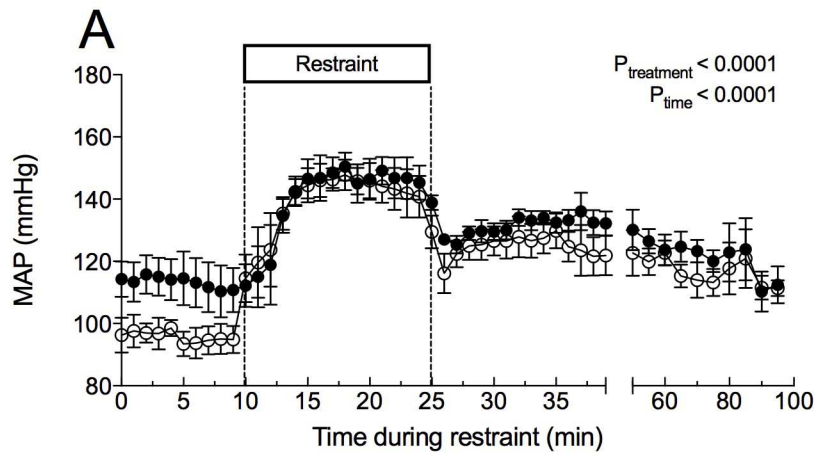
(A) Urine output (ml/24h), (B) Urinary excretion of sodium ($\mu\text{mol}/24\text{h}$), (C) urinary excretion of chloride ($\mu\text{mol}/24\text{h}$), and (D) urinary excretion of potassium ($\mu\text{mol}/24\text{h}$). Data comparing control and hypoxia-exposed offspring at 2 months of age were analysed by Student's t test. Data from 4-month-old offspring was analysed via two-way ANOVA with prenatal treatment and diet as factors. Data expressed as mean \pm SEM. Control: open circles; hypoxia: black circles. Male: N=6-10 animals per group; female: N=5-10 animals per group.



Supplementary Figure 2. Body weight before radiotelemetry surgery, and 10 days post-surgery in male (A) and female (B) offspring. Data was analysed via two-way ANOVA and expressed as mean \pm SEM. Control: white bars; hypoxia: black bars. N = 5-6 animals per group.



Supplementary Figure 3. Heart rate (bpm, beats per minute) in offspring at 12 months of age. Data was analysed via two-way ANOVA and expressed as mean \pm SEM. Control: white bars; hypoxia: black bars. N = 5-6 animals per group.



C

	Control		Hypoxia		Two-way ANOVA		
	Male	Female	Male	Female	$P_{\text{treatment}}$	P_{sex}	$P_{\text{treatment} \times \text{sex}}$
SBP (ΔAUC)	1270 \pm 175	692 \pm 429	879 \pm 216	560 \pm 139	0.3	0.06	0.6
DBP (ΔAUC)	1004 \pm 133	510 \pm 356	695 \pm 223	437 \pm 131	0.4	0.07	0.6
MAP (ΔAUC)	1147 \pm 156	561 \pm 362	783 \pm 209	499 \pm 133	0.3	0.049*	0.5
PP (ΔAUC)	313 \pm 57	216 \pm 84	199 \pm 33	259 \pm 65	0.6	0.8	0.2
HR (ΔAUC)	6438 \pm 1076	2315 \pm 511	5308 \pm 1629	2967 \pm 547	0.8	0.02*	0.5

Supplementary Figure 4. Mean arterial pressure (MAP, mmHg) response to a 15-minute restraint stress in male (A) and female (B) offspring. Stressor measurements were calculated by quantifying area under the curve (AUC) during the stressor and normalised to an equivalent amount of time during baseline (pre-stressor). Data was analysed via Student's t test and expressed as mean \pm SEM. (C) Table presenting stressor measurements of systolic blood pressure (SBP), diastolic blood pressure (DBP), MAP pulse pressure (PP) and heart rate (HR). Data was analysed via two-way ANOVA and expressed as mean \pm SEM. * $P < 0.05$. Male: $N = 5-6$ animals per group; female: $N = 3-5$ animals per group. Control: white points/white bars; hypoxia: black points/black bars. Male: $N = 5-6$ animals per group; female: $N = 3-5$ animals per group.

Chapter 5

This chapter has been submitted in its entirety for consideration for publication to the American Journal of Physiology: Renal Physiology on 5 August 2016.

Walton, S.L., Moritz, K.M., Bertram, J.F., & Singh, R.R. (2016) *Lengths of nephron tubule segments and collecting ducts in the CD-1 mouse kidney: an ontogeny study.*

Incorporated as Chapter 5.

Contributor	Statement of contribution
Walton, S.L.	Animal treatment and tissue collection (80%) Stereological analysis (100%) Interpreting results (50%) Writing and editing manuscript (60%) Study design (10%)
Moritz, K.M.	Interpreting results (15%) Writing and editing manuscript (10%) Study design (10%)
Bertram, J.F.	Interpreting results (15%) Writing and editing manuscript (10%)
Singh, R.R.	Animal treatment and tissue collection (20%) Interpreting results (20%) Writing and editing manuscript (20%) Study design (80%)

Lengths of nephron tubule segments and collecting ducts in the CD-1 mouse kidney: an ontogeny study.

Walton, Sarah L.¹, Moritz, Karen M.¹, Bertram, John F.³ and Singh Reetu R².

¹School of Biomedical Sciences, The University of Queensland, St Lucia, Queensland, Australia

²Department of Physiology, Monash University, Clayton, Victoria, Australia

³Cardiovascular Program, Monash Biomedicine Discovery Institute and Department of Anatomy and Developmental Biology, Monash University, Melbourne, Victoria, Australia;

Running head: Estimating tubule lengths in the kidney

Address for correspondence:

Reetu R Singh (PhD)

Department of Physiology, 26 Innovation Walk

Monash University

Clayton

VIC, 3800

Email: reetu.singh@monash.edu

Facsimile: 03-99029500

Telephone: 03-99052285

Abstract

The kidney continues to mature postnatally, with significant elongation of nephron tubules and collecting ducts to maintain fluid/electrolyte homeostasis. The aim of this project was to develop methodology to estimate lengths of specific segments of nephron tubules and collecting ducts in the CD-1 mouse kidney using a combination of immunohistochemistry and design-based stereology (vertical uniform random sections with cycloid arc test system). Lengths of tubules were determined at postnatal day 21 (P21), 2 and 12 months of age and also in mice fed a high salt diet throughout adulthood. Immunohistochemistry was performed to identify individual tubule segments (aquaporin-1: proximal tubules and thin descending limbs of Henle; uromodulin: distal tubules; aquaporin-2: collecting ducts). All tubular segments increased significantly in length between P21 and 2 months of age (proximal tubule: 602% increase, distal tubule: 200% increase, thin descending limb of Henle: 35% increase, collecting duct: 53% increase). However, between 2 and 12 months, a significant increase in length was only observed for the proximal tubule (76% increase in length). At 12 months of age, kidneys of mice on a high salt diet demonstrated a 27% greater length of the thin descending limb of Henle and a tendency for increased lengths of the proximal and distal tubule compared with the normal-salt group. Collecting duct length was unaffected by high salt intake. Our study demonstrates an efficient method of estimating lengths of specific segments of the renal tubular system. This technique can be applied to examine structure of the renal tubules in combination with the number of glomeruli in the kidney in models of altered renal phenotype.

Keywords

Stereology, proximal tubule, collecting duct, loop of Henle, distal tubule

Glossary

ΣP , number of test points per kidney

A , area

$a(p)$, area associated with each test point

CD, collecting duct

DT, distal tubule

GFR, glomerular filtration rate

HS, high salt

I_i , number of intersections between cycloid and tubules

l , unit length of cycloid

\hat{L} , length (m)

L_v , length density ($\times 10^{-4} \mu\text{m}^{-2}$)

P, postnatal day

P_i , number of test points per section

PT, proximal tubule

SSF, section sampling fraction

TDLH, thin descending limb of Henle

$U_{\text{Na}} V$, urinary sodium excretion ($\mu\text{mol}/24\text{h}$)

V_{kid} , volume of kidney

VUR, vertical uniform random

Introduction

The placenta regulates much of the extracellular fluid homeostasis of the fetus but upon birth, the neonatal kidney is forced into maintaining the body's fluid homeostasis (5). Within a few hours after birth, mean arterial pressure increases and renal vascular resistance decreases significantly, which contribute to the postnatal increase in renal blood flow and glomerular filtration rate (GFR). In response to the increase in filtered load, tubular reabsorption of sodium also increases significantly (2, 25). In contrast to the newborn/infant where distal tubules have been shown to modulate sodium reabsorption, proximal tubules in the adult kidney are the primary site for reabsorption of sodium (25). These functional adaptations are supported overtime by structural changes in nephron tubules.

Nephrogenesis (the formation of new nephrons) is complete before term in humans and in early postnatal life in rodents (17, 20). Although no new nephrons form after term birth in humans, an increase in size of glomeruli (hypertrophy) supports the increase in GFR during postnatal maturation of the kidney. Additionally, the significant increase in reabsorption of sodium from infancy into adulthood is associated with a significant increase in diameter and length of proximal tubules and, to a lesser extent, distal tubules which maximises reabsorptive area (4, 14, 24, 29). This process of postnatal tubular maturation allows the adult kidney to cope with daily fluctuations in fluid and sodium intake and maintain body fluid homeostasis (15).

Suboptimal kidney development has been implicated in the development of chronic kidney disease, with low numbers of functional glomeruli (a surrogate marker for nephron number) strongly associated with hypertension and renal disease (28). However, the development of the renal tubule system has not been studied in detail, which is surprising given its primary role in sodium reabsorption and the known capacity for compensatory growth following unilateral nephrectomy (12, 35). Although postnatal maturation of the glomerulus and proximal tubule has been well described (14), an analysis of the postnatal growth of the loop of Henle, distal tubule and collecting duct is lacking. This is partly due to technical limitations of assessing the structural characteristics of the nephron and collecting duct, with traditional light microscopy suitable for easy identification of the proximal tubule and glomerulus but more difficult for the loop of Henle, distal tubule and collecting duct.

The primary aim of this study was to quantify the postnatal morphological maturation of nephron segments and collecting ducts in the mouse kidney using a combination of immunohistochemistry and stereology. In order to determine lengths of all major tubular segments of the nephron and

collecting ducts, we used immunohistochemistry to unambiguously identify proximal tubules, thin descending limbs of loop of Henle, distal tubules and collecting ducts. Some segments of the nephron, as well as collecting ducts, exhibit marked anisotropy meaning the lineal structures are not identical in all orientations (49). This presents difficulties in terms of traditional stereology. To combat this, we have used thin vertical uniform random (VUR) sections in combination with the cycloid arcs test system to determine tubule length density (length per volume, or L_v) as well as the estimation of the absolute length of renal tubules (\hat{L}) in an unbiased manner as previously described (7, 16). Tubule lengths were determined in mice at postnatal day 21 (P21), 2 months and 12 months. In addition, we measured tubule lengths in 12-month-old mice fed a chronic high salt diet from 10 weeks of age, as high salt diets are known to cause renal hypertrophy. We hypothesised that all nephron tubule segments as well as collecting ducts would elongate between P21, 2 months and 12 months of age and indicate postnatal maturation of the kidney. We also hypothesised that a chronic high salt diet may increase lengths of tubules as an adaptation to an initial increase in filtered load of sodium (26) and this may account for some of the renal hypertrophy associated with increased dietary salt intake observed in the rodent.

Methods

Animals

All experiments were approved in advance by the University of Queensland animal ethics committee and were conducted in accordance with the Australian Code of Practice for the Care and Use of Animals for Scientific Purposes. Male CD1 mice from 9 separate litters were weaned at P21, humanely killed and their left kidneys were excised, decapsulated, weighed and fixed in 4% paraformaldehyde (PFA) for further analysis.

Urinary electrolyte excretion was assessed in animals at 2 months of age (N=6) by housing in individual metabolic cages for 24 h, with food and water provided *ad libitum*. Urine was collected and stored at -20 °C for future analysis of sodium concentration and osmolality. These animals were killed humanely and left kidneys were excised, decapsulated, weighed and fixed in 4% PFA.

In another group of mice, the effect of chronic high salt intake was examined. For these experiments, mice (N=8) aged 10 weeks were randomly allocated to receive a high salt diet (5% NaCl (wt/wt); modified AIN 93M, SF05-023, Specialty Feeds, Glen Forrest, WA) or maintained on a matched control diet (N=9, AIN 93M, Specialty Feeds, Glen Forrest, WA) (47). The animals were maintained on their respective diets until 12 months of age when renal function was assessed in both groups as described earlier, following which the animals were humanely killed and their left kidneys collected. Urinary sodium concentration was measured for all urine samples using a COBAS Integra 400 Plus. Urinary excretion rate of sodium ($U_{Na}V$; $\mu\text{mol}/24\text{h}$) was calculated from urine flow x urine sodium concentration over 24 hours. Urine osmolality was assessed by freezing point depression using a Micro-Osmette osmometer (Precision Systems, MA, USA).

Tissue sectioning

Whole kidneys were prepared for paraffin processing but prior to embedding, the kidneys were laid down flat on the laboratory bench and rotated along an arbitrary vertical axis, then embedded in paraffin in this final orientation. Then beginning at a random start (n), the entire kidney was exhaustively sectioned at 5 μm . Sections at intervals (section sampling fraction, *SSF*) of 100, 170, 200 and 210 for kidneys from offspring aged P21, 2 months, 12 months and 12 months + high salt diet respectively were collected to provide 3 sets of 10 evenly spaced sections across the entire length of each kidney.

Immunohistochemistry

Each set of 10 sections per kidney were immunohistochemically stained with either anti-Aquaporin-1 (Aqp1) to identify proximal tubules (PT, Figure 1A) and thin descending limbs of Henle (TDLH) (Figure 1B), anti-Tamm Horsfall-glycoprotein (also referred to as Uromodulin, Umod) to identify distal tubules (DT, Figure 1C) or anti-Aquaporin-2 (Aqp2) to identify collecting ducts (CD, Figure 1D). Antibodies were observed to be specific and reliable, with strong expression in the desired segments with minimal background staining (Figure 1). The PT was distinguished from the TDLH based on the presence of a brush border and location within the renal cortex.

Kidney sections were dewaxed and rehydrated in xylene and a series of ethanol washes. Endogenous peroxidase activity was blocked using 0.9% H₂O₂ in distilled water for 30 minutes. Non-specific binding was blocked using 2% bovine serum albumin (BSA) in goat serum in phosphate buffer (PB) or rabbit serum in PB for 1 h at 37 °C. Slides were incubated with primary antibodies at a 1:1000 dilution (anti-Aqp1 and anti-Aqp2, Millipore; and anti-Umod, Chemicon International) at room temperature for 1 h in a sealed, humidified chamber. Slides were washed in PB and incubated with a biotinylated anti-rabbit secondary antibody (anti-Aqp1 and anti-Aqp2) or a biotinylated anti-sheep secondary antibody (anti-Umod) for 30 min at 37 °C. Following PB washes, slides were incubated in avidin/biotin ABC enzyme complex (VECTOR Laboratories VECTA-STAIN Elite ABC Reagent, PK-6101 or PK-6106) for 30 min at 37 °C. Slides were then washed in PB and colour developed with ImmPACT DAB peroxidase substrate solution (VECTOR Laboratories). Slides were counterstained in Mayer's haematoxylin for 30 s, blued in Scott's tap water and mounted.

Estimation of kidney volume

Kidney volume was estimated using Stereo Investigator's (MBF Bioscience, Vermont, USA) "paint into contour" feature for Cavalieri point counting. Each section (10 per kidney) was mounted on a Zeiss Axioplan 2 light microscope viewed at 2.5x. The kidney section profile was delineated using the "contour" function and the area was provided by the Stereo Investigator program. Kidney volume (V_{kid}) was calculated from the above area estimate:

$$V_{kid} = SSF \times \Delta \times \sum_{i=1}^n A$$

where SSF is the section sampling fraction, Δ is section thickness, and $\sum A$ is the sum of the areas of all 10 kidney sections sampled.

Estimation of lengths of renal tubules

The principles of the cycloid test system for determination of lengths of linear structures (16) were utilised in the present study. Stereological analysis was carried out by one researcher on a computer-controlled, motorised Zeiss Axioplan 2 light microscope using Stereo Investigator software (Version 5, MBF Bioscience). The “cycloids for L_v ” probe was selected which enables the determination of total line length per unit reference volume. Each section (10 per kidney; N=6-9 animals per age) was delineated using the two-dimensional area function at low power (2.5x objective, Figure 2B) and then switched to 40x objective. The systematic random sampling (“SRS”) grid layout was defined manually as X: 450 μm and Y: 450 μm . This yielded on average, 40, 80, 130 and 140 frames on each kidney section at ages P21, 2 months, 12 months and 12 months + high salt diet, respectively, spaced 295 μm apart (Figure 2C). Following this, the section thickness (5 μm) and width of cycloid (106.1 μm) were specified and the software then overlaid a test grid of cycloids and angles on the image projected. The vertical axis was defined (under “define vertical axis” prompt) to align with the vertical axis of the tissue. The dimensions of the sampling sites and the cycloid probe were determined in a pilot study to reduce the coefficient of variation to below 5% and this sampling regime yielded a minimum of ~200 intersections per kidney between immunohistochemically stained renal tubules and cycloids. To estimate length density (L_v), the “count objects” prompt was followed and wherever the cycloids crossed the ‘backbone’ of the tubule segments (tubule segments stained positively for their respective antibodies) was marked as intersections (I); intersections were marked in all focal planes (by focusing up and down through the section) of the tissue and angles (P) that fell on all renal tissue were marked as well (Figure 2D). If one arc crossed more than one tubule, its intersections with these additional tubules were marked. Similarly, if one arc crossed the ‘backbone’ of one tubule X number of times, then X number of intersections was marked. This process was repeated for each of the 10 sections per kidney and the final results for L_v for each kidney were generated by the software using the following formula (Stereo Investigator, MBF Bioscience):

$$L_v = \frac{2}{\Delta} \left(\frac{p}{l} \right) \frac{\sum_{i=1}^n I_i}{\sum_{i=1}^n P_i}$$

Where: Δ is section thickness, $\frac{p}{l}$ is test points per unit length of cycloid, I_i is number of intersections between cycloids and immunostained renal segments and P_i is the number of angles (points) falling on the renal tissue sampling frame.

The absolute length (\hat{L}) of each tubular segment (length of tubule segment for entire kidney) was determined by multiplying L_v with V_{kid} .

Statistical analysis

All data are presented as mean \pm SEM. Multiple comparisons were made using one-way analysis of variance (ANOVA) in conjunction with a post-hoc Tukey's test (Graphpad Prism 6.0c). In addition, data from 12 month-old mice fed the normal salt and high salt diets were analysed by unpaired Student's t-tests. The level of significance was taken as $P \leq 0.05$.

Results

Body and organ weights, and electrolyte excretion

Body weight increased significantly with age ($P < 0.0001$ comparing P21 to 2 months and $P < 0.0001$ comparing 2 months to 12 months), However, a high salt diet had no significant effect on body weight compared to normal-salt control animals (Figure 3A). With age, a significant increase was also observed for kidney weight ($P < 0.0001$ for both, comparing P21 to 2 months and for 2 months to 12 months, Figure 3B) and kidney volume ($P < 0.0001$ comparing P21 to 2 months and $P = 0.0001$ comparing 2 months to 12 months, Figure 3D). Kidney weight normalised to body weight was not different between P21 and 12 months of age (Figure 3C). Although kidney weight and kidney weight normalised to body weight was not significantly affected by a high salt diet, kidney volume was significantly increased in animals on a high salt diet compared to their normal salt counterparts ($P = 0.02$, Figure 3D). Animals fed the high salt diet showed elevated urinary sodium excretion ($U_{Na}V$, $P = 0.0007$, Figure 3E) compared to animals fed the normal salt diet. Urine osmolality was greatest at 2 months of age ($P = 0.03$, Figure 3F) but was similar in mice fed the normal salt and high salt diet at 12 months of age (Figure 3F).

Length density and absolute length of tubules at postnatal day 21, 2 months and 12 months of age

The length density of PT was similar at all ages studied (Table 1). However, there was a significant increase in the absolute length of proximal tubule at 2 and 12 months of age compared with P21 (proximal tubule length (m): P21: 30.2 ± 4.7 , 2 months: 211.8 ± 13.0 , 12 months: 372.5 ± 30.5 , $P < 0.0001$ for both 2 and 12 months compared to P21; $P < 0.0001$ comparing 2 months to 12 months, Figure 4A). This reflected an increase in proximal tubule length of 602% between P21 and 2 months and an increase of 76% between 2 and 12 months of age. In contrast to proximal tubules, the length densities of the thin descending limb of Henle, distal tubules and collecting ducts were

greatest at P21 ($P < 0.0001$; Table 1); length densities were not different for any of the aforementioned segments between 2 and 12 months of age. The absolute length of the thin descending limb of Henle was greater at 2 and 12 months compared with P21 (the thin descending limb of Henle length (m): P21; 12.6 ± 1.1 , 2 months: 17.1 ± 1.3 , 12 months: 17.3 ± 1.5 , $P = 0.04$ comparing P21 and 2 months, $P = 0.03$ comparing P21 and 12 months, Figure 4B). This reflected an increase of 35% between P21 and 2 months but there was no further increase in length of the thin descending limb of Henle after 2 months of age. Compared to P21, the length of the distal tubule was significantly greater at 2 and 12 months of age reflecting a 3-fold increase between P21 and 2 months, but no significant increase in length was observed between 2 and 12 months of age (distal tubule length (m); P21: 33.8 ± 1.5 , 2 months: 101.2 ± 4.5 , 12 months: 108.1 ± 7.9 , $P < 0.0001$ for both 2 and 12 months compared to P21; Figure 4C). Total collecting duct length increased by 53% from P21 to 2 months of age ($P < 0.05$, Figure 4A), with no further elongation between 2 and 12 months of age.

Tubule lengths in kidneys from mice fed high salt diet

Although not statistically significant, a chronic high salt diet increased proximal tubule length to $452 \text{ m} \pm 24 \text{ m}$, an increase of 20% compared to age-matched controls on a normal salt diet ($P = 0.06$; Figure 4A). Similarly, a tendency for an increase in length density (20%) of the proximal tubule was observed in kidneys from mice fed the high salt diet compared to mice fed a normal salt diet ($P = 0.06$; Table 1). There was a significant increase in the thin descending limb of Henle length (27%, $P = 0.02$, Figure 4B) and length density (28%, $P = 0.02$, Table 1) in the kidneys from animals fed a high salt diet compared with their normal-salt counterparts. Distal tubule length tended to increase in animals fed the high salt diet compared to the normal-salt diet ($P = 0.09$; Figure 4C) but distal tubule length density did not differ between dietary groups at 12 months of age (Table 1). Collecting duct length (Figure 4D) and length density (Table 1) were the same between kidneys from animals fed the normal salt and high salt diet.

Discussion

The present study demonstrates that simultaneous measurement of length of nephron tubular segments and collecting ducts is feasible in a single kidney of the mouse across the lifespan. Importantly, it provides additional evidence that tubular elongation of the nephron persists into adulthood. Our primary finding is that in the CD-1 mouse kidney, there is a substantial increase in lengths of the proximal tubule, thin descending limb of Henle, distal tubule and collecting duct between P21 (juvenile) and 2 months of age (early adulthood), but the proximal tubule is the only nephron segment to lengthen from 2 to 12 months of age, likely contributing to increased renal mass in late adulthood. Our second major finding is that a chronic high salt diet increased the length of the thin descending limb of Henle and tended to increase the length of the proximal tubule. This suggests that tubular elongation may contribute to some of the renal hypertrophy previously observed with chronic salt-intake (19).

Several stereological methods to estimate renal tubule lengths have been described in detail (31). Although these methods have been used to estimate the length of a particular tubule segment, very few studies have examined more than one tubule type within a single kidney (21), with most studies focusing only on the renal cortex (34, 41, 42). Our aim was to optimise a method allowing for analysis of the major renal tubule segments in a single kidney in a way that would also allow for simultaneous determination of glomerular (and thus nephron) endowment. Tissue used in this study was simultaneously collected for determination of nephron number (data not shown) using previously described stereological methodology (10). In the present study in order to unambiguously identify the different tubular compartments we performed immunohistochemistry using specific markers for proximal tubule, thin descending limb of Henle, distal tubule and collecting duct. This combined immunohistochemical/stereological approach can be modified to estimate lengths of other tubules or tubular structures in the kidney, such as the ascending limb of Henle or the vasculature, simply by substituting appropriate immunohistochemical markers. For the method to be feasible for a wide range of studies, it was essential that it was relatively quick and easy to perform. We have used an automated system (Stereo Investigator, MBF Bioscience) to increase the speed of analysis, with volume estimation taking less than 10 minutes per kidney and length estimation of a tubule segment within a kidney possible in 1-2 hours. The cycloids test system can be used without a specialised stereology microscope and software, however this would increase analysis time significantly. A caveat to our approach was that it necessitated the use of paraffin embedded tissues and thus our estimates of length are most likely underestimated given that paraffin processing results in significant tissue shrinkage. However, all samples were manually

processed at the same time and treated identically so comparisons between groups are unlikely to be significantly affected. It should also be emphasised that tubule identification in the present study relied on identification using immunohistochemistry. In settings of pathology, expression of markers may be diminished to an undetectable level, reducing the validity of this method of tubule identification.

Comparing our estimates of tubule lengths in the rodent kidney with those of previous studies, we have identified some similarities and some distinct differences. Hoseini and colleagues (21) reported lengths of renal tubules in female BALB-C- mice where the orientator method was used to generate isotropic uniform random sections and renal tubule lengths were determined by point-counting. In mice weighing 30 g with kidney weights of ~139 mg (half the kidney mass of our 2 month old mice), Hoseini (21) reported most tubules were similar in length to our present values (proximal tubule ~30 m, loop of Henle ~23 m, distal tubule ~ 26 m), but the length of collecting ducts (~36 m) was greater than the proximal tubule segment. Our estimates of lengths of all tubular segments in the P21 CD-1 mouse kidney (~33 m for the distal tubule, ~13 m for the thin descending limb of Henle and ~ 21 m for the collecting duct) compare well with that study. However, our estimate of proximal tubule length at 2 months of age was almost 7-fold greater than the estimate of Hoseini and colleagues (21). This discrepancy could be a result of several factors, including greater kidney to body weight ratio in 2 month old CD-1 mice compared to the BALB-C mice (21). Furthermore, we counted ~400-500 sites per kidney compared to their 10-14 sites per kidney and our study was performed in males. In a more recent study by the same group (36), in male mice weighing 30g they found lengths of the collecting duct to be similar to our study (~20-40 m) but lengths for proximal tubules (40-60 m), distal tubules (5-15 m) and loop of Henle (0.2-0.8 m) were all significantly shorter than those obtained in our 2 month old mice. Additionally, their estimates for lengths of distal tubules and loop of Henle were also significantly less than their estimates in the previous study (21). Very large standard deviations were observed in that study. This may reflect differences in animal strains and sexes. Additionally, our study examined considerably more fields of view, which may have decreased the variance observed. Using point-counting to estimate tubule lengths in the renal cortex of the male Wistar rat, Pfaller *et al.* (34) reported lengths of proximal tubules (~500 m), distal tubules (~75 m) and collecting ducts (~13 m) in a ~1200 mg kidney. Relative to kidney size, based on these estimates in the Wistar rat, our estimates of proximal tubule length in the kidneys of 21 day old mouse are ~11% lesser and ~40 greater in the 2 month old mouse with estimates of distal tubules and collecting ducts significantly greater. These differences may be accounted for by the fact that Pfaller *et al.* (34) only sampled the renal cortex. Furthermore, it is unclear whether that study used isotropic sections to estimate tubule lengths. The

orientator/point-counting method was also used recently to estimate tubule lengths in the kidneys of Persian squirrels (1). The Persian squirrel kidney was ~ 2.5 x larger than the CD-1 mice kidney at 12 months of age, however the overall length of the proximal tubule was approximately the same in the two species. Notably the total length of the collecting duct in the Persian squirrel kidney is equivalent to the total length of the proximal tubule, suggesting these animals have a larger cortex/medulla ratio than CD-1 mice and likely increased capacity to concentrate urine given their arid habitat. Overall, there appears to be significant variation between species and strains in the lengths of various renal tubules. Given the extensive use of the mouse in developmental biology, further studies in this species under a variety of genetic and environmental manipulations will assist in more clearly defining how tubule lengths vary with age and disease.

In the present study we have demonstrated that kidney weight/volume in the mouse increased from P21 to 2 months of age. Over this period, although all tubule segments increased in length, the proximal tubule underwent the greatest increase ($\sim 600\%$), followed by the distal tubule ($\sim 200\%$). This finding in the mouse is consistent with previous documentation of proximal and distal tubule growth during early postnatal life in the rat and human (4, 14). Over the first few months of postnatal life, the proximal tubule rapidly increases in length and volume (14) and supports marked increases in GFR and tubular reabsorption of sodium (3, 39, 44). The postnatal increase in GFR is rapid, occurring within a few hours after birth in the sheep (25), rodent (22) and human (38), but structural changes in the kidney occur over a longer period of time, and consequently sodium reabsorption in the infant is lower than the adult. Studies in the newborn puppy (6) and late gestation sheep fetus (25) demonstrate that both the proximal and distal tubule contribute to glomerulotubular balance, but the proximal tubule becomes the primary site of tubular sodium reabsorption in the adult. This corroborates with our structural findings that the proximal and distal tubule are of similar lengths in the early juvenile mice, however the proximal tubule overwhelmingly increases in length and becomes the longest tubule segment in the adult mouse. Our data show that the thin descending limb of Henle and collecting duct both increase in length from P21 to 2 months of age. The kidney rapidly increases the ability to concentrate urine during the postnatal period and this occurs in parallel with elongation of the loop of Henle and collecting duct within the renal medulla and papilla (46) which are responsible for urine concentration (45). In the rat, this process occurs rapidly during weaning (37) and involves rapid elongation of the loops of Henle by cellular proliferation (8) and apoptosis (23). The cells of the collecting duct undergo substantial postnatal proliferation and differentiation into principal cells (Aqp2-positive), which influence the fine-tuning of fluid and electrolyte balance, and intercalated cells, which are responsible for acid-base balance (27). Therefore, our data demonstrating the increase in lengths of

both the TDLH and collecting duct suggest mice develop an increased capacity to concentrate urine between weaning at P21 and 2 months of age.

Between 2 and 12 months of age, there were further increases in the weight and volume of the kidney but this was associated only with lengthening of the proximal tubule, which doubled in length over this time. Whether the further increase in proximal tubule length observed in this 10-month period occurred to maintain the body's extracellular fluid volume (which would now be greater relative to kidney size) is unknown and needs further examination. The increase in kidney weight and volume are likely not only driven by an increase in tubular growth but by growth of glomeruli, vessels and the interstitium. The thin descending limb of Henle and collecting ducts did not elongate from 2 to 12 months of age and no change in osmolar excretion was observed. Interestingly, however, when mice consumed a high salt diet, an increase in lengths of all nephron segments was observed, albeit only statistically significant for the thin descending limb of Henle, with a tendency for an increase in proximal and distal tubule lengths. This suggests that with pathological renal tubule hypertrophy, tubules other than proximal can increase their length. Although the kidney has a great capacity to cope with changing physiological conditions, high dietary sodium intake in modern Western society presents a challenge to the adult kidney, with consumption higher than that of our ancestors (9). Evidence from animal and epidemiological studies have shown excess sodium intake leads to progressive renal damage marked by hypertension, proteinuria and altered renal outcomes including glomerular hypertrophy, glomerulosclerosis, fibrosis, hyperfiltration, and whole-kidney hypertrophy (40, 48, 50). Other adverse health outcomes are also associated with compensatory renal growth reported in adult rodent models of reduced renal mass such as uninephrectomy (18, 35) and diabetic nephropathy (30). Growth of the proximal tubule appears to increase disproportionately in cases of renal hypertrophy compared to other nephron segments. *Hayslett et al.* (18) reported an increase of ~35% and 17% length in the proximal and distal tubule segments respectively in remnant kidneys of uninephrectomised rats. Similarly, *Pollock et al.* (35) reported an increase of ~72% length in the proximal tubule segment in rats following uninephrectomy. Disproportionate growth of the proximal segment has also been reported in a model of diabetes mellitus, where stereological analysis revealed that whole kidney hypertrophy was associated with increased total number and volume of primarily the proximal cells but also distal cells (30). Uniquely, we have also shown a modest increase in the length of the thin descending limb of Henle in mice fed the high salt diet, compared to the normal salt diet. To our knowledge this has not been reported in the literature, previously. Interestingly, the only tubule examined that was not affected by the high salt diet was collecting duct. Given this is the final tubular component before the calyceal system, where only a

small proportion (~7%) of the water and sodium is reabsorbed, it may be that compensatory adaptations in the earlier segments are sufficient to compensate for the increased filtered load.

In conclusion, the present study demonstrates a robust method to determine lengths of three nephron tubule segments and collecting ducts in a single mouse kidney. It will be of interest to examine if, or indeed how, the renal tubules may adapt to an insult to the developing kidney. Many prenatal insults leading to a congenital nephron deficit (32, 43), or perturbations during postnatal kidney maturation such as acute kidney injury (13) or nephrotoxic drug administration (33) are associated with increased risk of cardiovascular and kidney disease, which may involve alterations to the renal tubules which perform the bulk of fluid homeostasis. This is a pertinent topic to pursue as postnatal development of the kidney, particularly the papilla, is poorly understood, and a reduced nephron number cannot fully explain the increased prevalence of CKD and hypertension (11).

Funding

This work was funded by the National Health and Medical Research Council of Australia (NHMRC-APP1009338). K.M.M. was supported by a fellowship provided by the NHMRC and S.L.W. was supported by an Australian postgraduate award.

Tables

Table 1. Estimated length density of renal tubule compartments in kidneys of male CD1 mice using a cycloid arcs test system.

	Length density (μm^{-2}) $\times 10^{-4}$				One-way ANOVA
	P21	2 months	12 months	12 months + high salt	
Proximal tubule	16.54 \pm 2.8 ^a	14.35 \pm 1.0 ^a	17.56 \pm 1.6 ^a	21.17 \pm 0.8 ^a	ns
Thin descending limb of Henle	6.77 \pm 0.46 ^a	1.15 \pm 0.10 ^b	0.81 \pm 0.07 ^b	1.04 \pm 0.06 ^{b*}	P < 0.0001
Distal tubule	18.91 \pm 0.80 ^a	6.83 \pm 0.34 ^b	5.08 \pm 0.42 ^b	6.67 \pm 0.78 ^b	P < 0.0001
Collecting ducts	11.66 \pm 1.18 ^a	2.06 \pm 0.17 ^b	1.68 \pm 0.14 ^b	1.60 \pm 0.09 ^b	P < 0.0001

Data are presented as mean \pm SEM and analysed via one-way ANOVA with a Tukey multiple comparisons test. In addition, a Student's t-test was performed between the two groups at 12 months of age to examine the effect of a high-salt diet. N = 6-11 mice, with 1-2 mice per litter. Letters represent statistical differences by ANOVA when comparing data from offspring aged P21, 2 months and 12 months. * represents $P \leq 0.05$ when comparing 12 month mice fed normal salt or high salt diet.

Figures

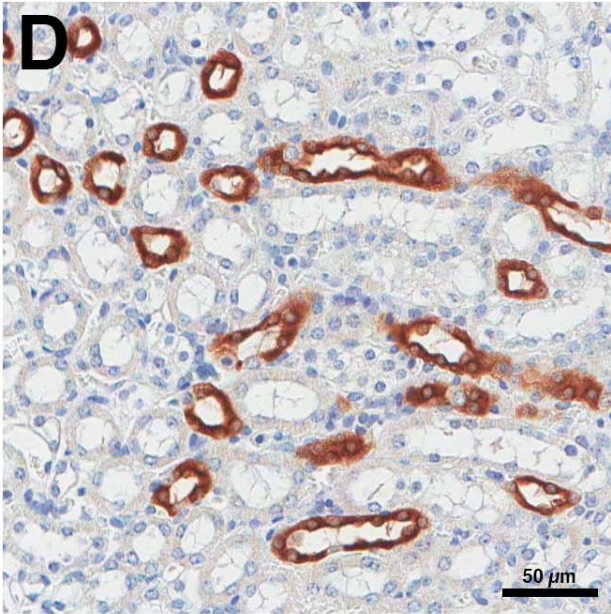
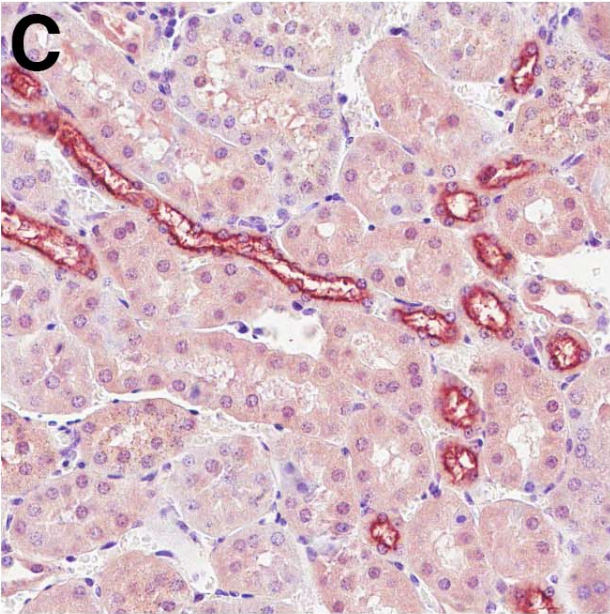
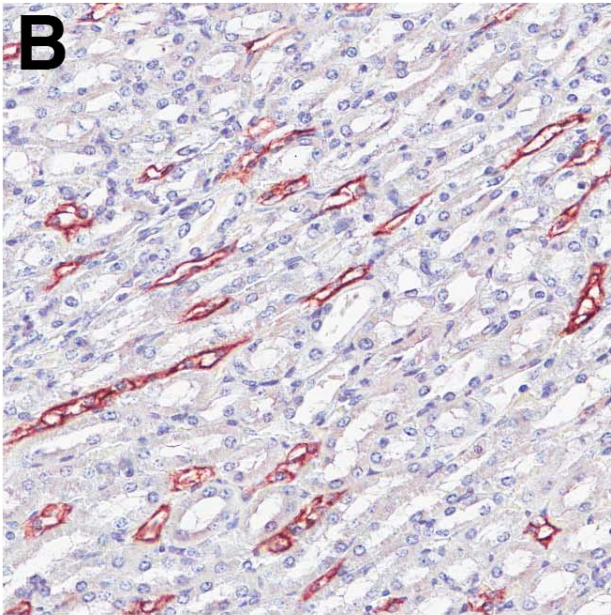
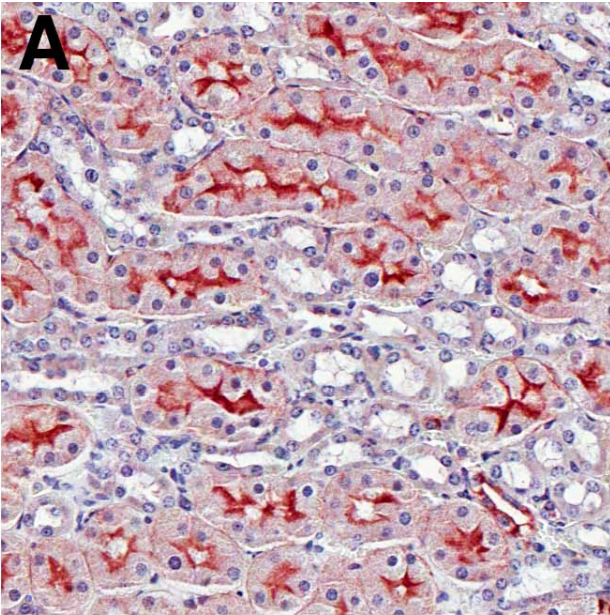


Figure 1. Nephron tubular segments and collecting ducts in P21 mouse kidneys identified using immunohistochemical markers.

(A) Proximal tubules identified using antibodies to Aqp1. (B) Thin descending limbs of the loop of Henle identified using antibodies to Aqp1. (C) Distal tubules identified using antibodies to Uromodulin. (D) Collecting ducts identified using antibodies to Aqp2. Scale bar represents 50 μm .

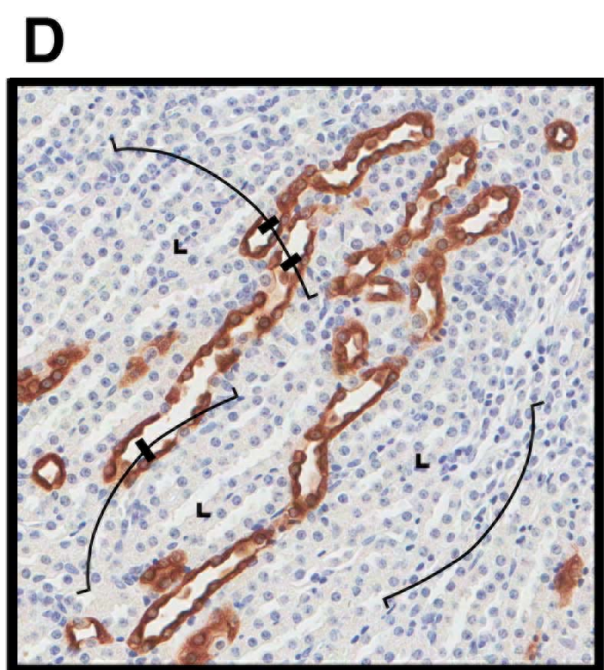
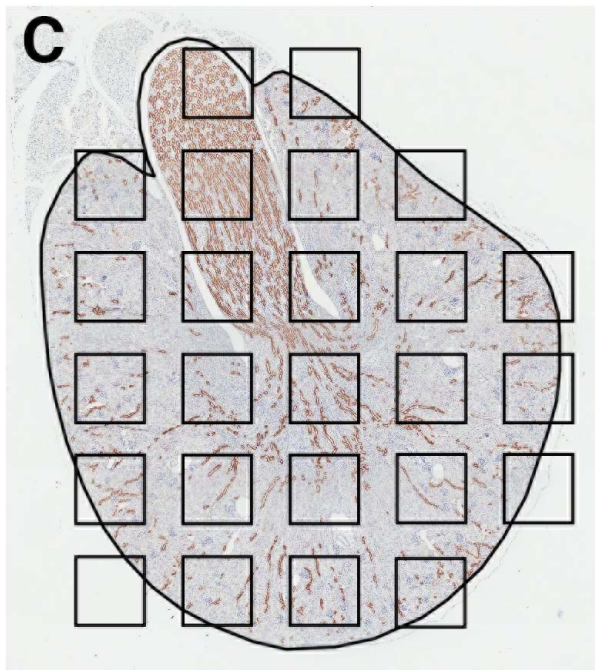


Figure 2. Diagrammatic representation of cycloid arcs test system to estimate lengths of renal tubules.

(A) Immunostained kidney sections (10 sections per kidney; Aqp2 staining of collecting ducts shown) are projected onto a screen at low power (2.5x objective). (B) Kidney sections were delineated using the Stereo Investigator program. (C) The total kidney section area was sampled using unbiased counting frames of known area ($450 \times 450 \mu\text{m}$) spaced $295 \mu\text{m}$ apart. (D) Sampling is performed at high magnification (40x objective). Cycloid probes (black arcs) are projected onto the tissue. Intersections between immunopositive tubules are marked (3 intersections visible) and test points (black 'L' symbols) that fall on renal tissue are marked (3 test points visible). Note diagram is not to scale.

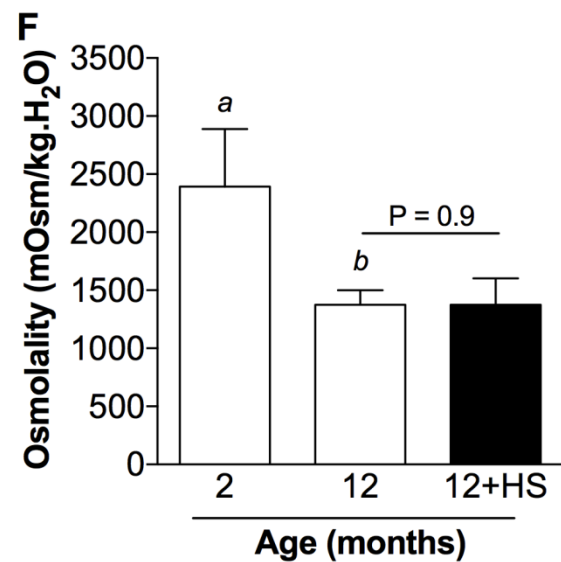
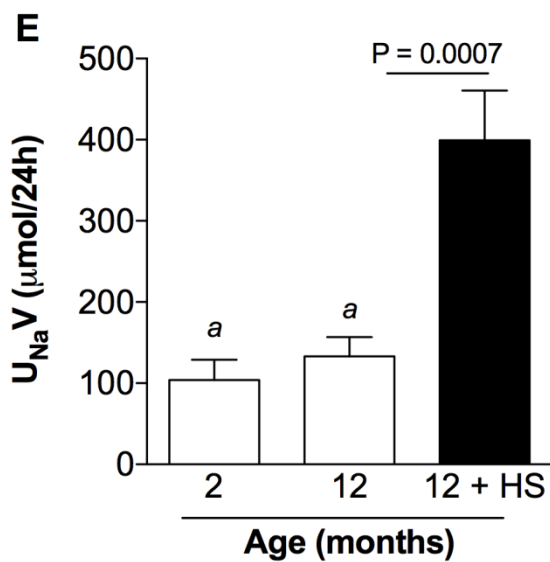
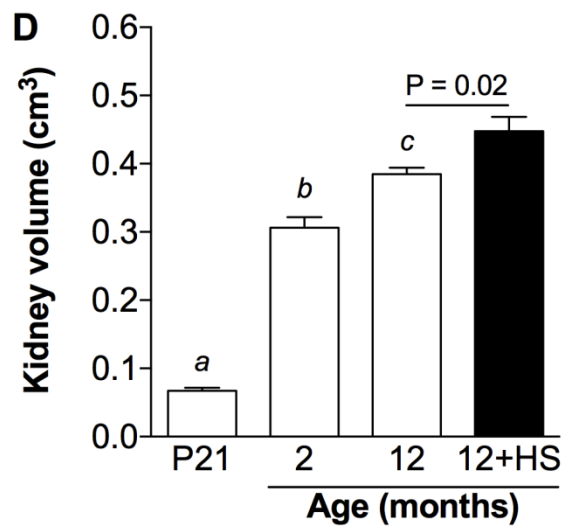
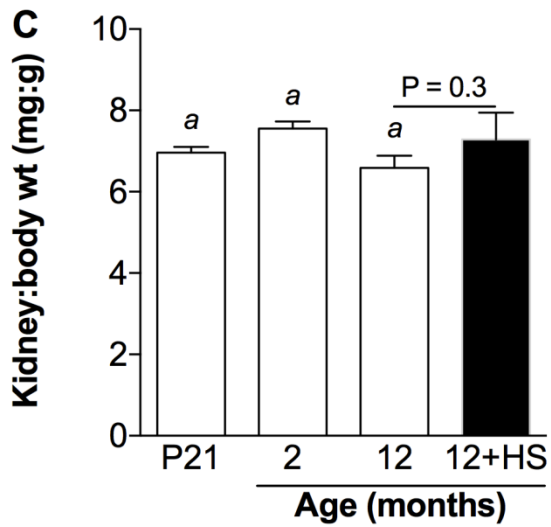
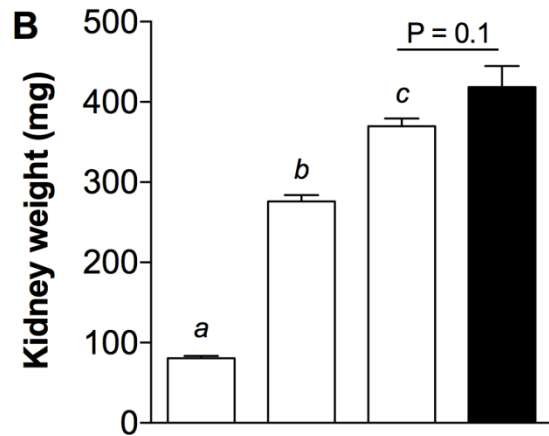
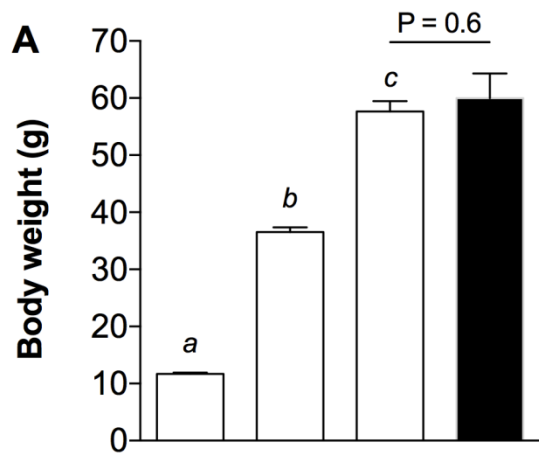


Figure 3. (A) Body weight, (B) kidney weight, (C) kidney to body weight ratio and (D) estimated kidney volume in CD1 male mice aged 21 days (P21), 2 months, 12 months and 12 month old mice that consumed a chronic high-salt (HS) diet. (E) Urinary excretion of sodium ($U_{Na}V$; $\mu\text{mol}/24\text{h}$) and (F) Urine osmolality ($\text{mOsm}/\text{kg.H}_2\text{O}$) in mice at 2 and 12 months of age. Data are presented as mean \pm SEM and analysed via one-way ANOVA comparing groups at P21, 2 months and 12 months (on a normal salt diet) followed by a Tukey's multiple comparisons test. N = 6-11 mice, with 1-2 mice per litter. Letters represent statistical differences by ANOVA when comparing data from offspring aged P21, 2 months and 12 months. The effect of diet was examined by a t-test comparing mice from the normal and high-salt diet groups at 12 months of age. For (E) and (F), a t-test was performed comparing urinary sodium excretion and osmolality at 2 and 12 months (normal salt group). Values (bars) signified by the same letter are not significantly different.

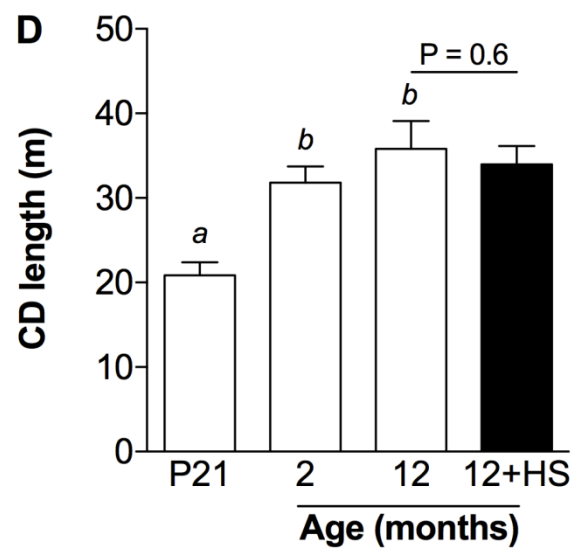
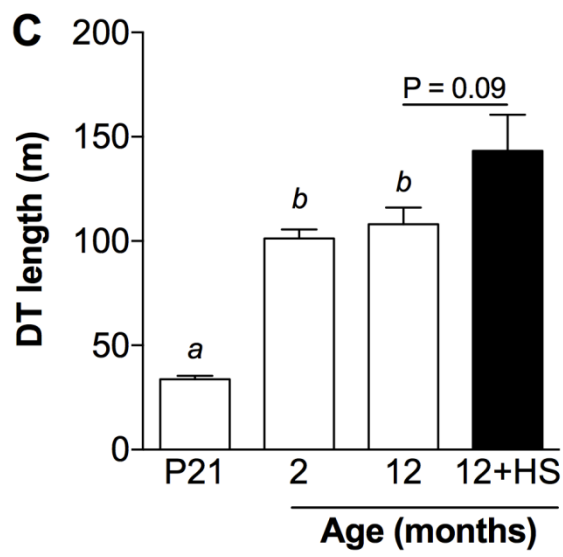
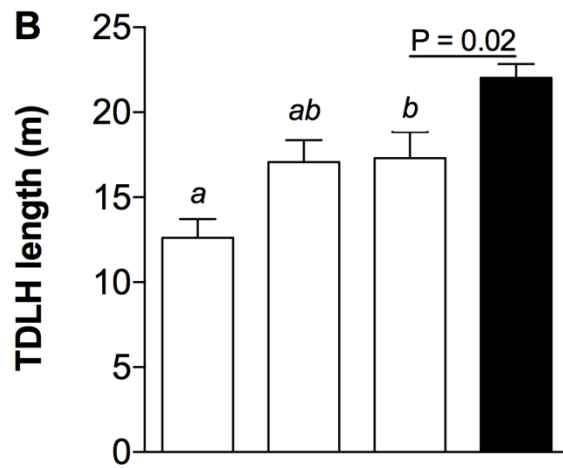
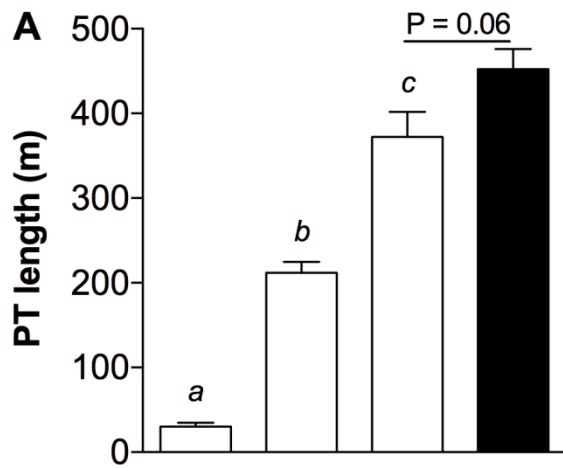


Figure 4. Estimated lengths of renal tubule compartments in kidneys of male CD1 mice aged 21 days (P21), 2 and 12 months and mice that consumed a high-salt diet from 10 weeks of age (12+HS). (A) Proximal tubule (PT) length, (B) Thin descending loop of Henle (TDLH) length, (C) Distal tubule (DT) length, (D) Collecting duct (CD) length. Data are presented as mean \pm SEM. Data at P21, 2 and 12 months (normal salt) were analysed via one-way ANOVA with a Tukey's multiple comparisons test. Differences between 12 month-old mice fed a normal salt or HS diet were analysed by t-test. N = 6-11 mice, with 1-2 mice per litter. Letters represent statistical differences by ANOVA when comparing data from offspring aged P21, 2 months and 12 months. Note differences in y-axis scale between tubule segments.

References

1. **Akbari M, Goodarzi N, and Tavafi M.** Stereological assessment of normal Persian squirrels (*Sciurus anomalus*) kidney. *Anat Sci Int* 1-8, 2016.
2. **Aperia A, Broberger O, Elinder G, Herin P, and Zetterstrom R.** Postnatal development of renal function in pre-term and full-term infants. *Acta Paediatr* 70: 183-187, 1981.
3. **Aperia A, Broberger O, Herin P, and Joelsson I.** Renal hemodynamics in the perinatal period. *Acta Physiol Scand* 99: 261-269, 1977.
4. **Aperia A, and Larsson L.** Correlation between fluid reabsorption and proximal tubule ultrastructure during development of the rat kidney. *Acta Physiol Scand* 105: 11-22, 1979.
5. **Arant BS.** Developmental patterns of renal functional maturation compared in the human neonate. *J Pediatr* 92: 705-712, 1978.
6. **Arant BS, Edelmann CM, and Nash MA.** The renal reabsorption of glucose in the developing canine kidney: a study of glomerulotubular balance. *Pediatr Res* 8: 638-646, 1974.
7. **Baddeley A, Gundersen H-JG, and Cruz-Orive LM.** Estimation of surface area from vertical sections. *J Microsc* 142: 259-276, 1986.
8. **Cha J-H, Kim Y-H, Jung J-Y, Han K-H, Madsen KM, and Kim J.** Cell proliferation in the loop of henle in the developing rat kidney. *J Am Soc Nephrol* 12: 1410-1421, 2001.
9. **Cordain L, Eaton SB, Sebastian A, Mann N, Lindeberg S, Watkins BA, O'Keefe JH, and Brand-Miller J.** Origins and evolution of the Western diet: health implications for the 21st century. *Am J Clin Nutr* 81: 341-354, 2005.
10. **Cullen-McEwen LA, Armitage JA, Nyengaard JR, Moritz KM, and Bertram JF.** A design-based method for estimating glomerular number in the developing kidney. *Am J Physiol Renal Physiol* 300: F1448-F1453, 2011.
11. **Dorey ES, Pantaleon M, Weir KA, and Moritz KM.** Adverse prenatal environment and kidney development: implications for programming of adult disease. *Reproduction* 147: R189-R198, 2014.
12. **Douglas-Denton R, Moritz KM, Bertram JF, and Wintour EM.** Compensatory renal growth after unilateral nephrectomy in the ovine fetus. *Clin J Am Soc Nephrol* 13: 406-410, 2002.
13. **Ellery SJ, Ireland Z, Kett MM, Snow R, Walker DW, and Dickinson H.** Creatine pretreatment prevents birth asphyxia-induced injury of the newborn spiny mouse kidney. *Pediatr Res* 73: 201-208, 2013.
14. **Fetterman GH, Shuplock NA, Philipp FJ, and Gregg HS.** The growth and maturation of human glomeruli and proximal convolutions from term to adulthood studies by microdissection. *Pediatrics* 35: 601-619, 1965.

15. **Fong D, Denton KM, Moritz KM, Evans R, and Singh RR.** Compensatory responses to nephron deficiency: adaptive or maladaptive? *Nephrology* 19: 119-128, 2014.
16. **Gokhale A.** Unbiased estimation of curve length in 3D using vertical slices. *J Microsc* 159: 133-141, 1990.
17. **Hartman HA, Lai HL, and Patterson LT.** Cessation of renal morphogenesis in mice. *Dev Biol* 310: 379-387, 2007.
18. **Hayslett JP, Kashgarian M, and Epstein FH.** Functional correlates of compensatory renal hypertrophy. *J Clin Invest* 47: 774, 1968.
19. **Henry C, Burrell LM, Black MJ, Wu LL, Dilley RJ, Cooper ME, and Johnston CI.** Salt induces myocardial and renal fibrosis in normotensive and hypertensive rats. *Circulation* 98: 2621-2628, 1998.
20. **Hinchliffe S, Sargent P, Howard C, Chan Y, and Van Velzen D.** Human intrauterine renal growth expressed in absolute number of glomeruli assessed by the disector method and Cavalieri principle. *Lab Invest* 64: 777-784, 1991.
21. **Hoseini L, Roozbeh J, Sagheb M, Karbalay-Doust S, and Noorafshan A.** Nandrolone decanoate increases the volume but not the length of the proximal and distal convoluted tubules of the mouse kidney. *Micron* 40: 226-230, 2009.
22. **Kavlock R, and Gray J.** Evaluation of renal function in neonatal rats. *Neonatology* 41: 279-288, 1982.
23. **Kim J, Lee G, Tisher CC, and Madsen KM.** Role of apoptosis in development of the ascending thin limb of the loop of Henle in rat kidney. *Am J Physiol Renal Physiol* 271: F831-F845, 1996.
24. **Larsson L, and Horster M.** Ultrastructure and net fluid transport in isolated perfused developing proximal tubules. *J Ultrastruct Res* 54: 276-285, 1976.
25. **Lumbers ER, Hill KJ, and Bennett VJ.** Proximal and distal tubular activity in chronically catheterized fetal sheep compared with the adult. *Can J Physiol Pharmacol* 66: 697-702, 1988.
26. **Mallamaci F, Leonardis D, Bellizzi V, and Zoccali C.** Does high salt intake cause hyperfiltration in patients with essential hypertension? *J Hum Hypertens* 10: 157-161, 1996.
27. **Matsumoto T, Fejes-Toth G, and Schwartz GJ.** Postnatal Differentiation of Rabbit Collecting Duct Intercalated Cells¹. *Pediatr Res* 39: 1-12, 1996.
28. **Moritz KM, Dodic M, and Wintour EM.** Kidney development and the fetal programming of adult disease. *Bioessays* 25: 212-220, 2003.
29. **Neiss WF, and Klehn KL.** The postnatal development of the rat kidney, with special reference to the chemodifferentiation of the proximal tubule. *Histochemistry* 73: 251-268, 1981.

30. **Nyengaard J, Flyvbjerg A, and Rasch R.** The impact of renal growth, regression and regrowth in experimental diabetes mellitus on number and size of proximal and distal tubular cells in the rat kidney. *Diabetologia* 36: 1126-1131, 1993.
31. **Nyengaard JR.** Stereologic Methods and Their Application in Kidney Research. *J Am Soc Nephrol* 10: 1100-1123, 1999.
32. **O'Sullivan L, Cuffe JS, Koning A, Singh RR, Paravicini TM, and Moritz KM.** Excess prenatal corticosterone exposure results in albuminuria, sex-specific hypotension, and altered heart rate responses to restraint stress in aged adult mice. *Am J Physiol Renal Physiol* 308: F1065-F1073, 2015.
33. **Patzer L.** Nephrotoxicity as a cause of acute kidney injury in children. *Pediatr Nephrol* 23: 2159-2173, 2008.
34. **Pfaller W, Seppi T, Ohno A, Giebisch G, and Beck FX.** Quantitative Morphology of Renal Cortical Structures during Compensatory Hypertrophy. *Nephron* 6: 308-319, 1998.
35. **Pollock CA, Bostrom TE, Dyne M, Györy AZ, and Field MJ.** Tubular sodium handling and tubuloglomerular feedback in compensatory renal hypertrophy. *Pflügers Archiv* 420: 159-166, 1992.
36. **Rafati A, Hoseini L, Babai A, Noorafshan A, Haghbin H, and Karbalay-Doust S.** Mitigating Effect of Resveratrol on the Structural Changes of Mice Liver and Kidney Induced by Cadmium; A Stereological Study. *Prev Nutr Food Sci* 20: 266-275, 2015.
37. **Rane S, Aperia A, Eneroth P, and Lundin S.** Development of urinary concentrating capacity in weaning rats. *Pediatr Res* 19: 472-475, 1985.
38. **Rhodin MM, Anderson BJ, Peters AM, Coulthard MG, Wilkins B, Cole M, Chatelut E, Grubb A, Veal GJ, Keir MJ, and Holford NHG.** Human renal function maturation: a quantitative description using weight and postmenstrual age. *Pediatr Nephrol* 24: 67-76, 2008.
39. **Robillard JE, and Weitzman RE.** Developmental aspects of the fetal renal response to exogenous arginine vasopressin. *Am J Physiol Renal Physiol* 238: F407-F414, 1980.
40. **Sacks FM, Svetkey LP, Vollmer WM, Appel LJ, Bray GA, Harsha D, Obarzanek E, Conlin PR, Miller ER, Simons-Morton DG, Karanja N, Lin P-H, Aickin M, Most-Windhauser MM, Moore TJ, Proschan MA, and Cutler JA.** Effects on Blood Pressure of Reduced Dietary Sodium and the Dietary Approaches to Stop Hypertension (DASH) Diet. *N Engl J Med* 344: 3-10, 2001.
41. **Seyer-Hansen K, Gundersen H, and Østerby R.** Stereology of the rat kidney during compensatory renal hypertrophy. *Acta Path Micro Scand* 93: 9-12, 1985.
42. **Seyer-Hansen K, Hansen J, and Gundersen HJG.** Renal hypertrophy in experimental diabetes. *Diabetologia* 18: 501-505, 1980.

43. **Singh RR, Cullen-McEwen LA, Kett MM, Boon WM, Dowling J, Bertram JF, and Moritz KM.** Prenatal corticosterone exposure results in altered AT1/AT2, nephron deficit and hypertension in the rat offspring. *J Physiol* 579: 503-513, 2007.
44. **Smith FG, and Lumbers ER.** Effects of maternal hyperglycemia on fetal renal function in sheep. *Am J Physiol Renal Physiol* 255: F11-F14, 1988.
45. **Song R, and Yosypiv IV.** Development of the kidney medulla. *Organogenesis* 8: 10-17, 2012.
46. **Stephenson JL.** Models of the urinary concentrating mechanism. *Kidney Int* 31: 648-661, 1987.
47. **Walton SL, Singh RR, Tan T, Paravicini TM, and Moritz KM.** Late gestational hypoxia and a postnatal high salt diet programs endothelial dysfunction and arterial stiffness in adult mouse offspring. *J Physiol* 594: 1451-1463, 2016.
48. **Weinberger MH, and Fineberg NS.** Sodium and volume sensitivity of blood pressure. Age and pressure change over time. *Hypertension* 18: 67-71, 1991.
49. **Wreford NG.** Theory and practice of stereological techniques applied to the estimation of cell number and nuclear volume in the testis. *Microsc Res Tech* 32: 423-436, 1995.
50. **Yu Q, Larson D, Slayback D, Lundeen T, Baxter J, and Watson R.** Characterization of high-salt and high-fat diets on cardiac and vascular function in mice. *Cardiovasc Toxicol* 4: 37-46, 2004.

Chapter 6

The impact of prenatal hypoxia on renal medulla and papilla structure and functional maturation in the mouse.

Abstract

Prenatal hypoxia is a common perturbation to arise during pregnancy, and can lead to adverse health outcomes in later life. Previously we have reported male hypoxia-exposed mice offspring have reduced glomerular number and signs of renal injury by 12 months of age. In the present study, we examined the impact of prenatal hypoxia on renal medulla and papilla structure, and functional maturation in mouse offspring. Pregnant CD1 mice were housed in a hypoxia chamber (12% O₂) or housed in normal room conditions (21% O₂) from embryonic day 14.5 until birth. Male and female offspring were raised in normal room conditions. Urine excretion under basal conditions and also in response to a 24-hour water deprivation challenge was assessed in offspring at 4 and 12 months of age. A subset of offspring was culled at postnatal day (P) 6, P21 and 12 months of age and kidneys collected for histopathological analysis. Renal tubules lengths in male and female kidneys at P21 were estimated using unbiased stereology, and collecting duct cell composition in male kidneys was determined at all ages. The kidneys of juvenile male hypoxia-exposed mice (P6 and P21) had altered collecting duct cell composition and expression of Aquaporin-2 compared to controls. Total proximal tubule and distal tubule lengths were increased in kidneys from male hypoxia-exposed offspring at P21 compared to controls, reflected by increased cortex-to-medulla ratio. At 12 months of age, male hypoxia-exposed offspring exhibited minor defects in their ability to concentrate urine when deprived of water for 24 hours. This was accompanied by altered cellular composition of the collecting duct, diminished expression of AQP2 and tubular dilation in male hypoxia-exposed offspring compared to controls at 12 months of age. No differences in renal structure or function were observed between female control and hypoxia-exposed offspring at any age. Together, this study highlights the importance of considering the impact of *in utero* perturbations on the structure of the renal tubules and collecting duct system, as well as nephron number and sex of the offspring.

Introduction

Kidney disease in Australia

Kidney disease is highly prevalent in Australian society, placing a tremendous health burden for patients and health services (Chadban *et al.*, 2003). One in 10 Australians have clinical signs of chronic kidney disease (CKD) and this rate is doubled in Aboriginal and Torres Strait Islander people (Australian Bureau of Statistics, 2013). Kidney disease is frequently asymptomatic, meaning kidney disease can progress without symptoms until a substantial functional capacity is lost (Chadban *et al.*, 2003; Sarnak *et al.*, 2003). Consequently, the initial cause of kidney disease in an individual can be difficult to determine. However, a range of risk factors for developing kidney disease has been identified, including low birth weight, hypertension, diabetes mellitus, obesity and age (Brenner & Mackenzie, 1997; Levey *et al.*, 2003).

Developmental programming of kidney disease

Low birth weight is a clinical marker of a poor intrauterine environment and is associated with impaired kidney development (Moritz *et al.*, 2009). Nephrogenesis begins in fetal life and is complete by 36 weeks gestation in humans; after this point, no new nephrons can be formed. Therefore, impaired kidney development frequently manifests as low nephron number that will remain with the individual throughout life (Hinchliffe *et al.*, 1991). An extensive body of literature has shown that reduced nephron number compromises functional renal capacity and therefore increases vulnerability to hypertension and kidney disease in both humans (Brenner & Mackenzie, 1997; Hoy *et al.*, 1999; Hughson *et al.*, 2003; Keller *et al.*, 2003; Hughson *et al.*, 2006) and animal models (Langley-Evans *et al.*, 1999; Moritz *et al.*, 2002; Moritz *et al.*, 2003; Cullen-McEwen *et al.*, 2012). Indeed, this thesis demonstrated in *Chapter 4* that prenatal hypoxia reduces nephron number by 25% and leads to signs of renal disease in adult offspring. Importantly, fluid and electrolyte balance is maintained by a fine interplay between glomerular filtration and sodium and water reabsorption in the renal tubules. As such, alterations to tubular structure and function can have a profound impact on body fluid homeostasis. It is highly likely that impaired renal tubule development and/or inappropriate compensatory growth, in conjunction with reduced nephron number, contribute to the risk of developing kidney disease in adult life. Surprisingly, tubule development has yet to be explored in depth in any model of prenatal insult resulting in a reduced nephron endowment.

Development of the renal medulla and papilla

Unlike nephrogenesis, renal tubule development begins during embryogenesis and persists into postnatal life. The ureteric bud penetrates the metanephric mesenchyme and initiates reciprocal induction to form nephron segments including proximal tubules, the loop of Henle and distal tubules; branching of the uretic bud gives rise to the collecting duct system (Little & McMahon, 2012). Significant postnatal tubular maturation occurs following birth to support the new functional requirements of the neonatal kidney (*Chapter 5*). At birth in the rodent and human, the renal papillary lobe(s) are short and underdeveloped; rapid elongation occurs during the first two weeks of life by extension of papillary tubules (Wilkinson *et al.*, 2012; *Chapter 5*). Establishment of an osmotic gradient from the cortico-medullary boundary to the papillary tip by countercurrent multiplication (Layton *et al.*, 2009) allows full urine concentration capacity to be achieved 12 months after birth in humans (Atiyeh *et al.*, 1996). All filtration units of the nephron drain through the collecting ducts of the papillary lobe(s), which are responsible for the final control of water excretion and therefore urine concentration. This is achieved by the presence of principal cells in the collecting duct, which express aquaporin 2 (AQP2) and are the site of sodium reabsorption and aldosterone and vasopressin action.

Structure of the renal medulla and papilla

Comparative animal studies have shown that urine-concentrating capacity is tightly associated with medulla and papilla size. Desert dwelling rodents such as the spiny mouse and kangaroo rat have very long papillae, providing a greater surface area to generate a higher osmotic gradient to produce more concentrated urine (Dickinson *et al.*, 2007). In contrast, the beaver, a semiaquatic species, lacks an inner stripe of the medulla (Schmidt-Nielsen & O'Dell, 1961). These structural differences confer a functional advantage, allowing these animals to adapt to suit different environment conditions (namely, ease of access to water). Poor fetal and neonatal kidney development could therefore reduce functional renal capacity in a way that might compromise their adaptation to particular environments.

Impaired function of the renal medulla and papilla

The functional capacity of the medulla and papilla is also reduced with the ageing process, within urine concentrating capacity known to decline with age in both humans and rodents (Donahue & Lowenthal, 1997). Reduced urine concentrating capacity is also used as clinical marker of early

renal failure as it is observed in patients with reduced GFR (Nieto *et al.*, 2008). This has previously been attributed to progressive loss of glomeruli, impaired vasopressin secretion or responsiveness (Beck & Yu, 1982), and decreased AQP2 expression in the collecting ducts (Tian *et al.*, 2004). Interestingly in children, reduced urine concentrating capacity has been strongly associated with reduced GFR and is used as maker of early renal failure (Nieto *et al.*, 2008). It is likely that structural deficits due to perturbed fetal kidney development may also contribute to impaired urine concentration early in life however it remains difficult to directly correlate renal structure and function in living neonates in the human population. Renal function studies in neonates have shown the incidence of acute kidney injury in asphyxiated neonates is high, and is associated with poor renal outcomes including renal failure (Karlłowicz & Adelman, 1995; Gupta *et al.*, 2005). In addition, renal concentrating capacity is lowered in asphyxiated neonates compared to healthy term neonates (Svenningsen & Aronson, 1974). Together these studies suggest structural deficits may underlie impaired neonatal renal function. Animal studies have allowed researchers to implicate adverse early life influences in impaired medullary structure and function. A urine-concentrating deficit was shown to emerge with age in sheep with low nephron number following fetal uninephrectomy (Singh *et al.*, 2011). Neonatal ureteral obstruction in the rat resulted in decreased expression of sodium transporters and aquaporins and impaired urinary concentrating capacity (Shi *et al.*, 2004). Furthermore, delayed medullary tubule development and structural damage to the medulla and papilla has been reported in a model of birth asphyxia in the spiny mouse (Ellery *et al.*, 2013). Therefore, it is likely that poor kidney development may affect the medulla and papilla, as well as the number of functional nephrons, ultimately increasing vulnerability to kidney disease.

Experimental rationale

The aims of this study were to further characterise renal impairment in our model of late gestational maternal hypoxia by examining the structure and functional capacity of the renal medulla and papilla. First, the structure of the renal medulla was examined histologically in young offspring (P6 and P21). Secondly, the ability to concentrate urine in response to a water deprivation challenge was determined in offspring at a young age (4 months) and then in aged offspring (12 months). Finally, immunohistochemistry combined with stereology/morphometry was used to elucidate whether the prenatal hypoxia insult permanently altered the structural integrity of the renal medulla and papilla. The physiological measurements were carried out in both sexes but only the renal medulla and papilla from kidneys from male offspring were further examined in this study, given males but not females exposed to prenatal hypoxia displayed signs of chronic kidney disease at 12 months of age (*Chapter 4*). We hypothesised that *in utero* hypoxia during late gestation would

impair development of the renal medulla and papilla, leading to an impaired ability to concentrate urine under a water deprivation challenge.

Materials and methods

A detailed description of the methodologies relating to animal handling experiments in this thesis chapter can be found in *Chapter 2: Materials and Methods*. Additional information related to the experiments described in this chapter can be found below.

Animals

Ethical approval was obtained from the University of Queensland animal ethics committee prior to commencement of animal work for this study. Pregnant CD1 mice were either housed in normoxic room conditions (21% oxygen; N = 11) or in a hypoxia chamber (12% oxygen; N = 11) from embryonic day (E) 14.5 until birth (P0), as previously described in this thesis. Offspring were subsequently housed in normoxic room conditions with their mothers until weaning at P21.

Maternal arterial oxygen saturation

Peripheral capillary oxygen saturation (SpO₂) was measured using a pulse oximeter contained within a collar sensor, designed for measurements on conscious mice (Mouse Ox system, STARR Life Sciences, Oakmont, Philadelphia). Average SpO₂ measurements were collected for 10 minutes prior to housing in chamber at E14.5, 10 minutes after housing in chamber for 1 hour at E14.5 and again at E18.5 (N = 3 dams).

Tissue collection in fetuses and young offspring

A subset of dams (N = 5 per treatment) was culled at E18.5 by cervical dislocation as previously described in *Chapter 2: Materials and Methods*. Fetuses were removed from the uterine horn, swiftly decapitated and kidneys were either snap-frozen in liquid nitrogen or fixed in 4% PFA. Fixed tissues were processed into OCT or paraffin and exhaustively sectioned at 5 μ m.

Remaining dams littered down naturally. A subset of male offspring was culled at P6 (N = 3-4) by decapitation. Additional male and female offspring were culled at P21 (N = 11 per sex per treatment

group) by cervical dislocation. Kidneys were removed, immersion fixed in 4% PFA and processed into OCT or paraffin. Kidneys were exhaustively sectioned at 5 μm .

Basal metabolic cage urine collection

Offspring aged 2, 4 and 12 months (male: N = 7-11 per treatment group; female: N = 5-10 per treatment group) were acclimatised to individual metabolic cages two days prior to collection. Animals were then placed in individual metabolic cages for 24 h, with food and water consumption, body weight change and urine flow over 24 hour recorded. Urine samples were collected stored at -20 °C for further analysis.

Water deprivation challenge

One week following initial basal urine collection, offspring aged 4 and 12 months were subject to a 24-hour water deprivation challenge in the metabolic cages. At 1600 hours, animals were placed in individual cages without access to water. Food was provided *ad libitum*. Animals were carefully monitored for signs of lethargy (willingness to move around, alertness when handled) that are suggestive of severe dehydration every 2 hours from 0800 hours the following morning until the protocol finished at 1600 hours. Recording sheets were placed on each cage to track animal wellbeing over the final 8 hours of dehydration. Food intake, body weight change and urine output were recorded. Urine samples were stored at -20 °C for further analysis. Following the 24-hour challenge, offspring were returned to their home cages, immediately offered water and body weight monitored daily over the subsequent week. Animals were then killed for collection of the kidneys (as described above).

Urinalysis

Urinary sodium, chloride and potassium concentrations were measured for all urine samples by potentiometry using a COBAS Integra 400 Plus. Urine osmolality was assessed by freezing point depression using a Micro-Osmette osmometer (Precision Systems, MA, USA). Note basal urine output and sodium excretion have previously been reported in Chapter 4.

Stereology

Renal tubule lengths (proximal tubule [PT], thin descending limb of Henle [TDLH], distal tubule [DT] and collecting duct [CD]) from control and hypoxia-exposed offspring at age P21 were estimated using unbiased stereology, as described in *Chapter 5*. Note the renal tubule lengths for control offspring at P21 have previously been reported in *Chapter 5*.

Morphometry and pathology

Median transverse sections from kidneys were stained with periodic acid-Schiff to assess tubular morphology by a researcher blinder to treatment groups. The width of the cortex and medulla were measured in midline kidney sections at all ages (Figure 1). The cortex thickness was defined as the area superficial to the arcuate arteries and containing predominantly proximal tubules, distal tubules and glomeruli. The medulla region was defined from the border of the cortex to the papillary tip.

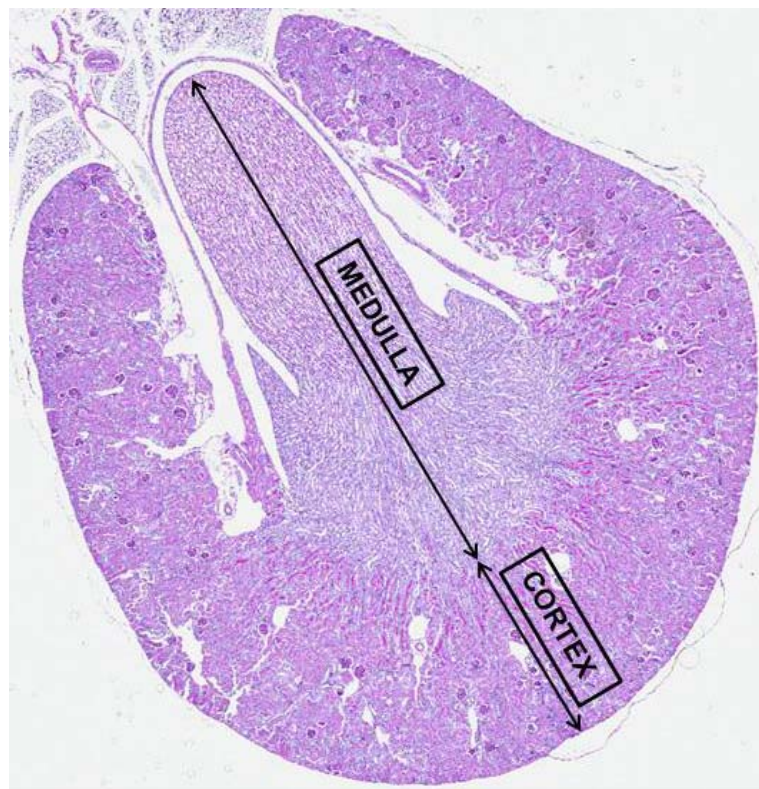


Figure 1. Measurement of cortex and medulla thickness in kidney sections

A representative image of a median transverse kidney section, stained with periodic acid-Schiff, from a P21 control male mouse. The thickness of the cortex was measured and compared to the length of medulla/papilla visible in the section.

Single labelling with immunohistochemistry

Kidney sections from offspring at P21 and 12 months of age were dewaxed and rehydrated in xylene and a series of ethanol washes. Endogenous peroxidase activity was blocked using 0.9% H₂O₂ in distilled water for 30 minutes. Non-specific binding was blocked using 2% bovine serum albumin (BSA) in serum in phosphate buffer (PB) for 1 h. Sequential sections were incubated with anti-goat AQP2 (1:200, sc-9882, Santa Cruz) and anti-rabbit V-ATPase (1:200, sc-20943, Santa Cruz) at room temperature for 1 hour in a sealed, humidified chamber. Slides were washed in PB and incubated with a biotinylated secondary antibody for 30 min at 37 °C. Following PB washes, slides were incubated in avidin/biotin ABC enzyme complex (VECTOR Laboratories VECTA-STAIN Elite ABC Reagent, PK-6101 or PK-6106) for 30 min. Slides were then washed in PB. Colour was developed with ImmPACT DAB peroxidase substrate solution (VECTOR Laboratories, SK-4805). Slides were counterstained in Mayer's haematoxylin for 30 s, blued in Scott's tap water and mounted.

Double labelling with immunofluorescence

Sections from kidneys collected at P6 and P21 were blocked using 10% serum in PBS for 1 hour at room temperature, followed by incubation with anti-goat AQP2 (1:200, sc-9882, Santa Cruz) and anti-rabbit V-ATPase (1:200, sc-20943, Santa Cruz) for 1h at room temperature. Slides were incubated with Alexa Fluor 488 goat anti-rabbit (1:400, A11011) and Alexa Fluor 555 donkey anti-goat (1:400, cat # A21432) for 1h at room temperature and counterstained with DAPI for 3 min. Sections were visualised using an Olympus BX61 fluorescent microscope.

Quantification of collecting duct composition

Twenty to 30 fields of view (X 40 magnification) within the renal cortex and medulla (Figure 2) were selected systematically and randomly from 3-5 slides per kidney. The renal papilla tip was excluded from the counting process. To quantify the number of principal and intercalated cells in the cortical collecting duct and medullary collecting duct, the number of cells that exhibited immunoreactivity for AQP2 and V-ATPase were counted and expressed as a percentage of the total number of cells in the tubule segments. One hundred to 250 cells were counted per kidney and location within the cortex or medulla was noted.

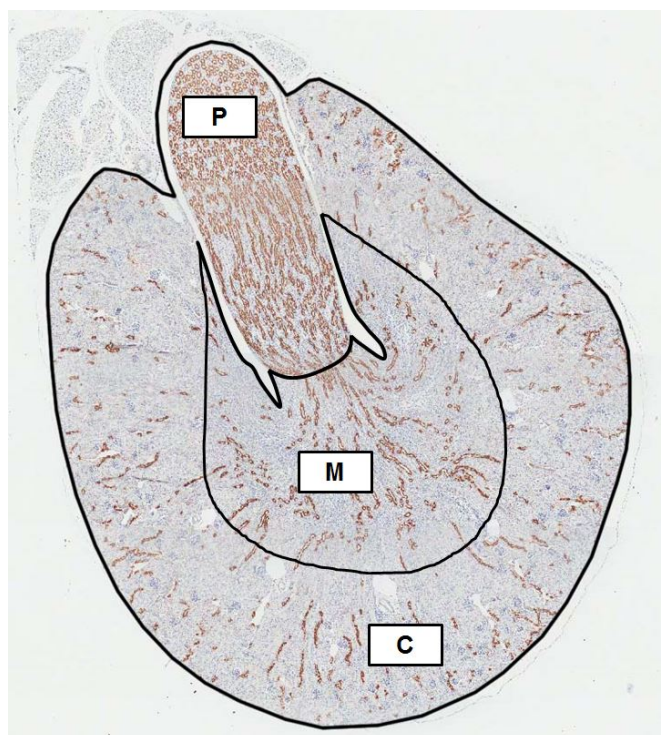


Figure 2. Sampling of the renal cortex and medulla to quantify collecting duct cell composition.

A representative image of a median transverse kidney section, stained with AQP2 using immunohistochemistry, from a P21 control male mouse. Twenty to 30 sampling sites were evenly distributed systematically and randomly throughout the cortex (C) and medulla (M). The renal papilla (P) was excluded from the counting process. Counting was performed at X 40 magnification. Note diagram is not to scale.

Tubular dilation in the renal papilla

Kidney sections (5 μ m) were stained with periodic acid-Schiff's and examined by an expert pathologist blinded to treatment groups.

Quantitative real-time PCR

RNA was extracted from kidneys at P21 using the RNeasy minikit (QIAGEN, Chadstone Centre, VIC, Australia). All RNA was treated with deoxyribonuclease 1 and reverse transcribed into cDNA (iScriptTM, Bio-Rad, NSW, Australia). Amplification was performed using SBYBR Green PCR Mastermix (Applied Biosystems, VIC, Australia) in a 20 μ l reaction volume containing cDNA and 10 pmol of each primer for aquaporin-2 (sense 5'-CTTCCTTCGAGCTGCCTTC-3'; antisense 5'-CATTGTTGTGGAGAGCATTGA C-3'). Results were normalised to 18S expression.

Statistics

All values are expressed as mean \pm SEM. Data were analysed using two-way ANOVA with treatment and age, renal tubule type or kidney region as factors. Bonferroni post-hoc tests were used when appropriate. A Pearson correlation coefficient was computed to assess the relationship between collecting duct cell composition and urine concentration capacity. All other data was analysed using two-way ANOVA examining the effects of prenatal hypoxia ($P_{\text{treatment}}$), and offspring age (P_{age}), renal tubule type (P_{tubule}) or region of kidney analysed (P_{region}). Bonferroni post hoc tests comparing control and hypoxia-exposed offspring used where appropriate. The level of significance was taken as $P < 0.05$.

Results

Maternal arterial oxygen saturation

Mean maternal arterial oxygen saturation under normal room conditions was $98.7 \% \pm 0.2 \%$ (Figure 3). This decreased to $77.8 \% \pm 0.5 \%$ following relocation to the hypoxia chamber at E14.5, and remained at this level at E18.5 (Figure 3, $P = 0.0004$).

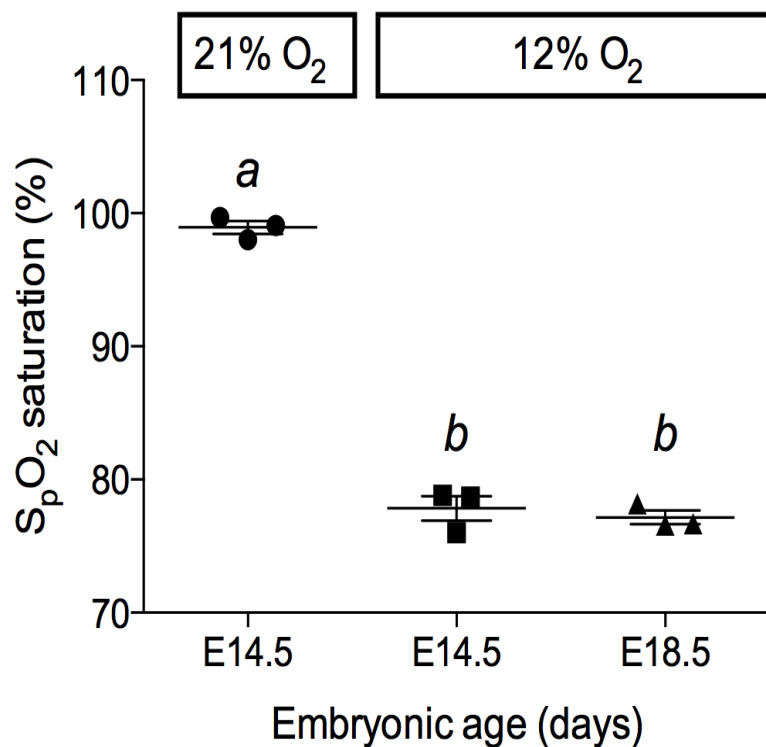


Figure 3. Maternal peripheral capillary oxygen saturation (SpO₂, %) at embryonic day 14.5 at standard room conditions (21% O₂), following an hour of hypoxia (E14.5) and after 4 days in the hypoxia chamber at 12% O₂ (E18.5). N = 3 dams. Different letters between groups indicate statistical significance from a one-way ANOVA ($P < 0.05$). Data are mean \pm SEM.

Urinalysis under basal conditions

Male offspring

Urine output over 24 hours did not differ between treatment groups of male offspring 4 and 12 months of age (Figure 4A). Urinary sodium concentration ($U_{Na}V$, mmol/L) tended to be reduced in 12-month-old mice compared to 4-month-old mice (Figure 4B; $P_{age} = 0.058$). Two-way ANOVA revealed a significant effect of age on urine osmolality (Figure 4C; $P_{age} = 0.01$). Urine osmolality also showed a significant interaction between treatment and age (Figure 4C; $P_{treatment \times age} = 0.03$).

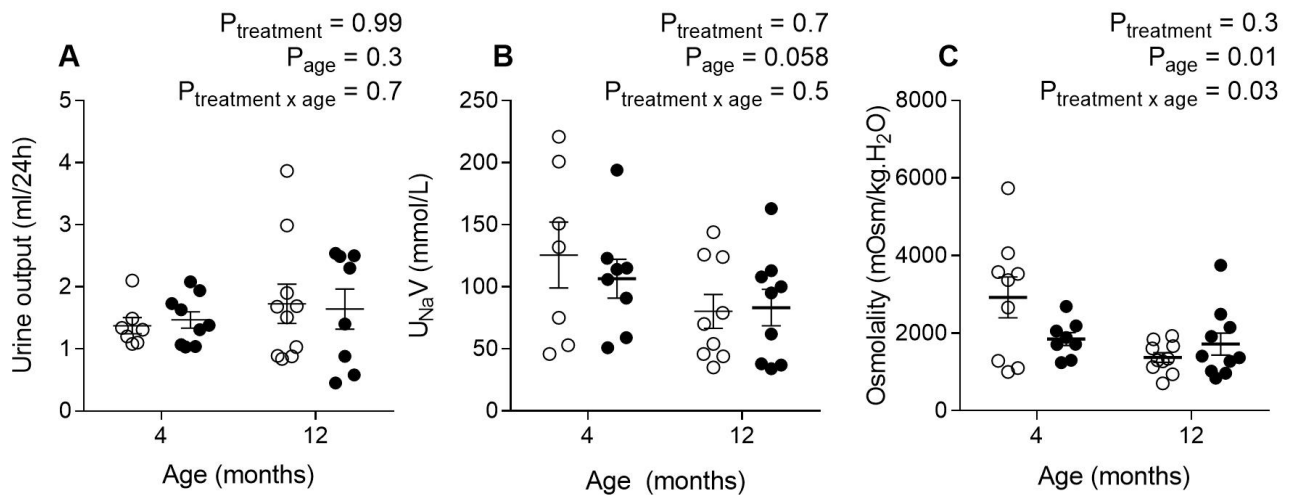


Figure 4. Urinalysis of male offspring aged 4 and 12 months.

(A) Urine output (ml/ 24h). (B) Urinary excretion of sodium (mmol/L). (C) Urinary osmolality (mOsm/kg.H₂O). Data was analysed via two-way ANOVA and expressed as mean \pm SEM. Control: open circles; hypoxia: black circles. Male: N=7-11 animals per group.

Female offspring

Urine output over 24 hours was greater in control female offspring at 12 months of age compared to 4 months of age (Figure 5A; $P_{\text{age}} = 0.001$). There was a tendency towards reduced urine output in hypoxia-exposed female offspring at 12 months of age, compared to control female offspring at 12 months of age (Figure 5A; $P_{\text{treatment}} = 0.09$, $P_{\text{treatment} \times \text{age}} = 0.07$). Urinary sodium concentration did not differ between treatment groups, and was unaffected by age (Figure 5B). Urine osmolality tended to be reduced in 12-month-old female offspring, compared to 4-month female offspring (Figure 4C; $P_{\text{age}} = 0.05$).

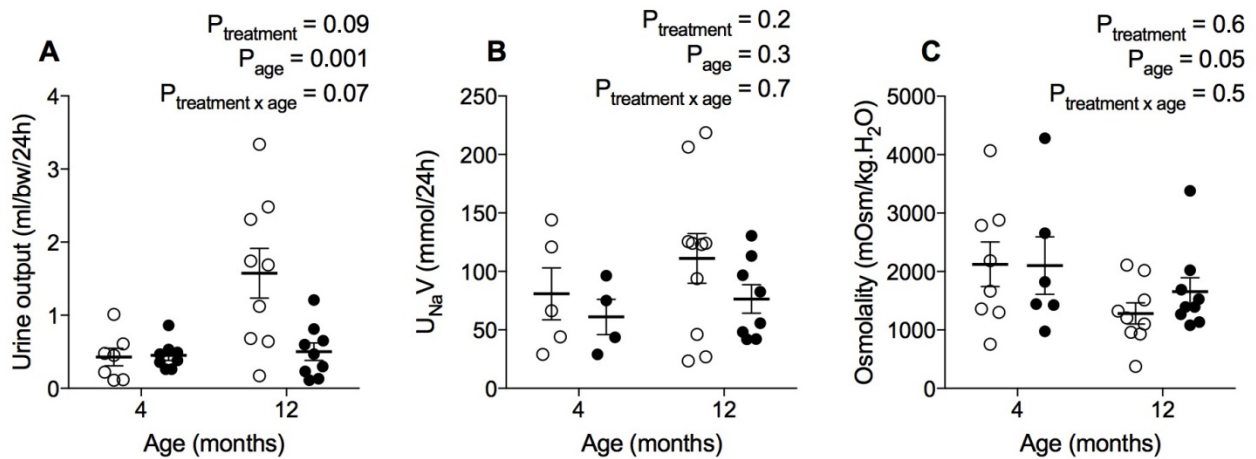


Figure 5. Urinalysis of female offspring aged 4 and 12 months.

(A) Urine output (ml/24h). (B) Urinary excretion of sodium (mmol/L). (C) Urinary osmolality (mOsm/kg.H₂O). Data was analysed via two-way ANOVA and expressed as mean \pm SEM. Control: open circles; hypoxia: black circles. N=5-10 animals per group.

Water deprivation challenge

Male offspring

No difference in urine flow reduction or urinary sodium excretion in response to 24h water deprivation was observed between control and hypoxia-exposed offspring at 4 months of age (Figure 6). When subjected to 24h water deprivation at 12 months of age, control offspring reduced urine flow by ~50% (Figure 6) compared to basal urine output. A subset of hypoxia-exposed offspring at 12 months of age increased urine flow and urinary sodium excretion under water deprivation conditions, leading to an overall significant difference to controls when analysed by Bonferroni post-hoc test (Figure 6A-B; $P < 0.05$ from a Bonferroni *post-hoc* analysis). Urine osmolality increased from a basal to water-deprived state at 4 and 12 months of age, and was not different between ages or treatment groups (Figure 6C).

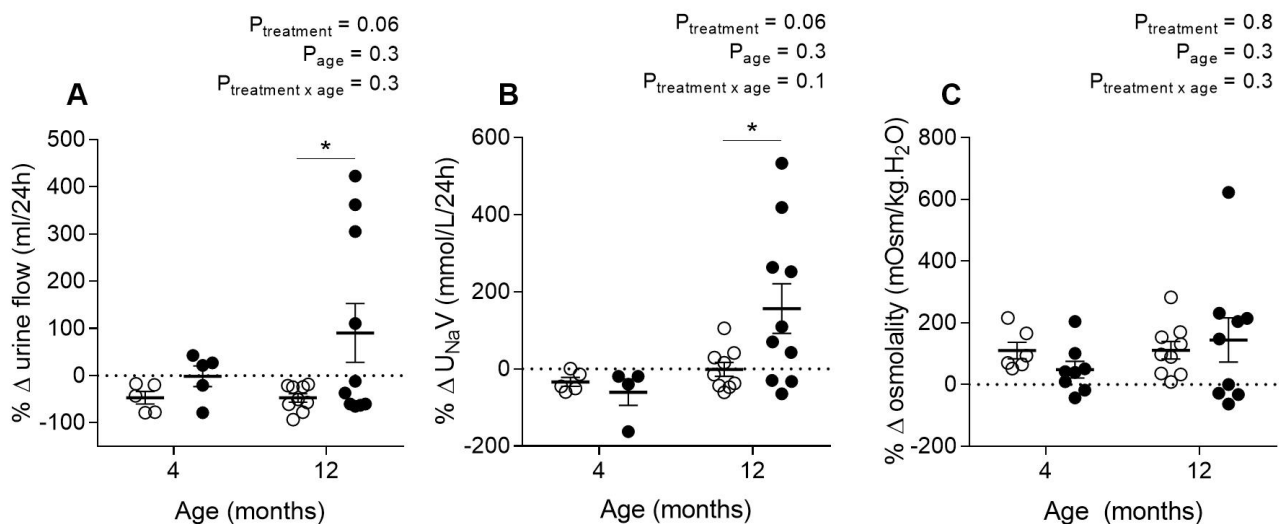


Figure 6. Response to a 24-hour water deprivation challenge in male offspring at 4 and 12 months of age.

(A) Percentage change in urine flow (ml/24h) from a basal to water-deprived state. (B) Percentage change in urinary sodium excretion (mmol/L/24h) from a basal to water-deprived state. (C) Percentage change in urine osmolality (mOsm/kg.H₂O) from a basal to water-deprived state.

Data was analysed via two-way ANOVA and expressed as mean \pm SEM. Control: open circles; hypoxia: black circles. N=6-10 animals per group. * $P < 0.05$ by Bonferroni post-hoc.

Female offspring

No difference in urine flow reduction, urinary sodium excretion in response to 24h water deprivation was observed between control and hypoxia-exposed offspring at 4 and 12 months of age in female offspring (Figure 7A-C).

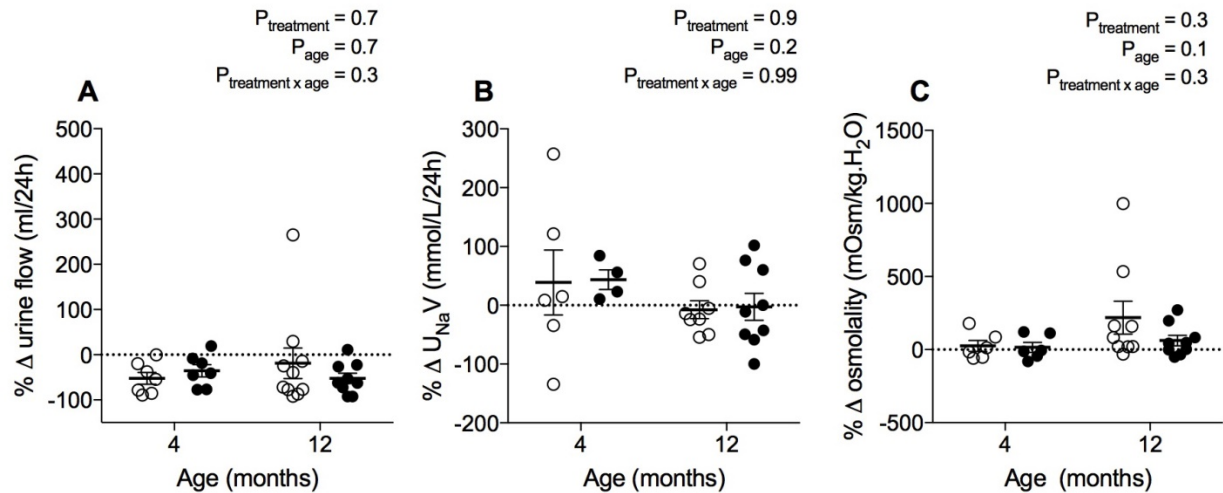


Figure 7. Response to a 24-hour water deprivation challenge in female offspring at 4 and 12 months of age.

(A) Percentage change in urine flow (ml/24h) from a basal to water-deprived state. (B) Percentage change in urinary sodium excretion (mmol/L/24h) from a basal to water-deprived state. (C) Percentage change in urine osmolality (mOsm/kg.H₂O) from a basal to water-deprived state.

Data was analysed via two-way ANOVA and expressed as mean \pm SEM. Control: open circles; hypoxia: black circles. N=5-10 animals per group. * P < 0.05 by Bonferroni post-hoc.

Renal morphometry at postnatal day 21

Male offspring

The proportion of renal cortex to renal medulla was significantly increased in kidneys from male hypoxia-exposed offspring, compared to controls (Figure 8A; $P < 0.05$). This was associated with an increase in total proximal (Figure 8B; $P < 0.01$) and distal tubule lengths (Figure 8B; $P < 0.01$), the predominant tubules of the renal cortex, and a trend towards decreased collecting duct length, located primarily in the renal medulla, compared to control counterparts (Figure 8B; $P = 0.07$ comparing control and hypoxia-exposed collecting duct lengths using an unpaired Student's t test).

Intense AQP2 expression was concentrated on the apical surface of the CD epithelial cells in the male hypoxia-exposed offspring kidneys at P21; in contrast, kidneys from control offspring at P21 showed more diffuse AQP2 expression in CD cells (Figure 8D). Relative *Aqp2* mRNA expression was increased by 3-fold in the male hypoxia-exposed kidneys compared to control kidneys (Figure 8C; $P < 0.0001$).

Female offspring

No differences in total proximal tubule length (control: 111.3 ± 3 m, hypoxia: 112.2 ± 11 m), thin descending limb of Henle length (control: 27.4 ± 2 , hypoxia: 20.4 ± 3 m), distal tubule length (control: 77.9 ± 4 m, hypoxia: 86.9 ± 12 m), or collecting duct lengths (control: 39.4 ± 2 , hypoxia: 32.9 ± 1 m) were observed between kidneys of female control and hypoxia-exposed offspring at P21.

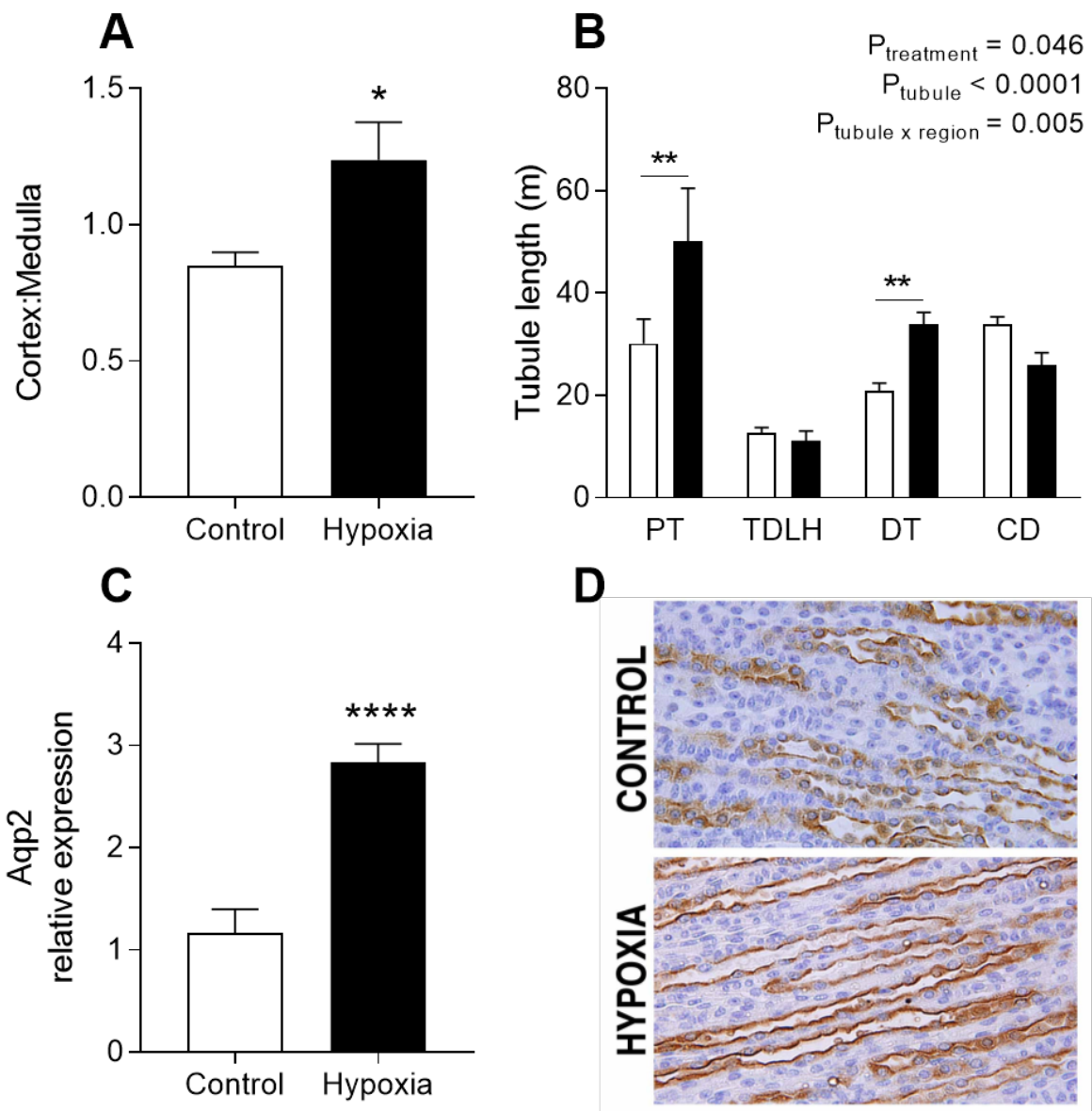


Figure 8. Male kidney morphometry and Aquaporin 2 expression at postnatal day 21.

(A) Ratio of cortex to medulla in kidneys. (B) Lengths of renal tubules in kidneys from offspring (PT, proximal tubule. TDLH, thin descending limb of Henle. DT, distal tubule. CD, collecting duct). (C) Relative *Aqp2* mRNA expression in the kidney. (D) AQP2 distribution in the collecting duct. Data was analysed via two-way ANOVA and expressed as mean \pm SEM. Control: open bars; hypoxia: black bars. Male: N=6-10 animals per group. * $P < 0.05$, **** $P < 0.0001$ from an unpaired Student's t test. ** $P < 0.01$ from Bonferroni post-hoc.

Cellular collecting duct composition across life in male offspring

A higher proportion of AQP2-positive cells were observed in the renal medulla compared to the renal cortex at P6 (Figure 9A; $P_{\text{region}} = 0.05$), P21 (Figure 9B; $P_{\text{region}} = 0.001$) and 12 months of age (Figure 9C; $P_{\text{region}} = 0.001$). The ratio of principal to intercalated cells in the kidney was elevated in hypoxia-exposed offspring compared to controls at P6 (Figure 9A; $P_{\text{treatment}} = 0.01$) and P21 (Figure 9B; $P_{\text{treatment}} = 0.03$). Bonferroni *post-hoc* analysis revealed that hypoxia-exposed animals had a greater proportion of V-ATPase positive cells in medullary collecting ducts compared to control kidneys (Figure 9C; $P < 0.05$).

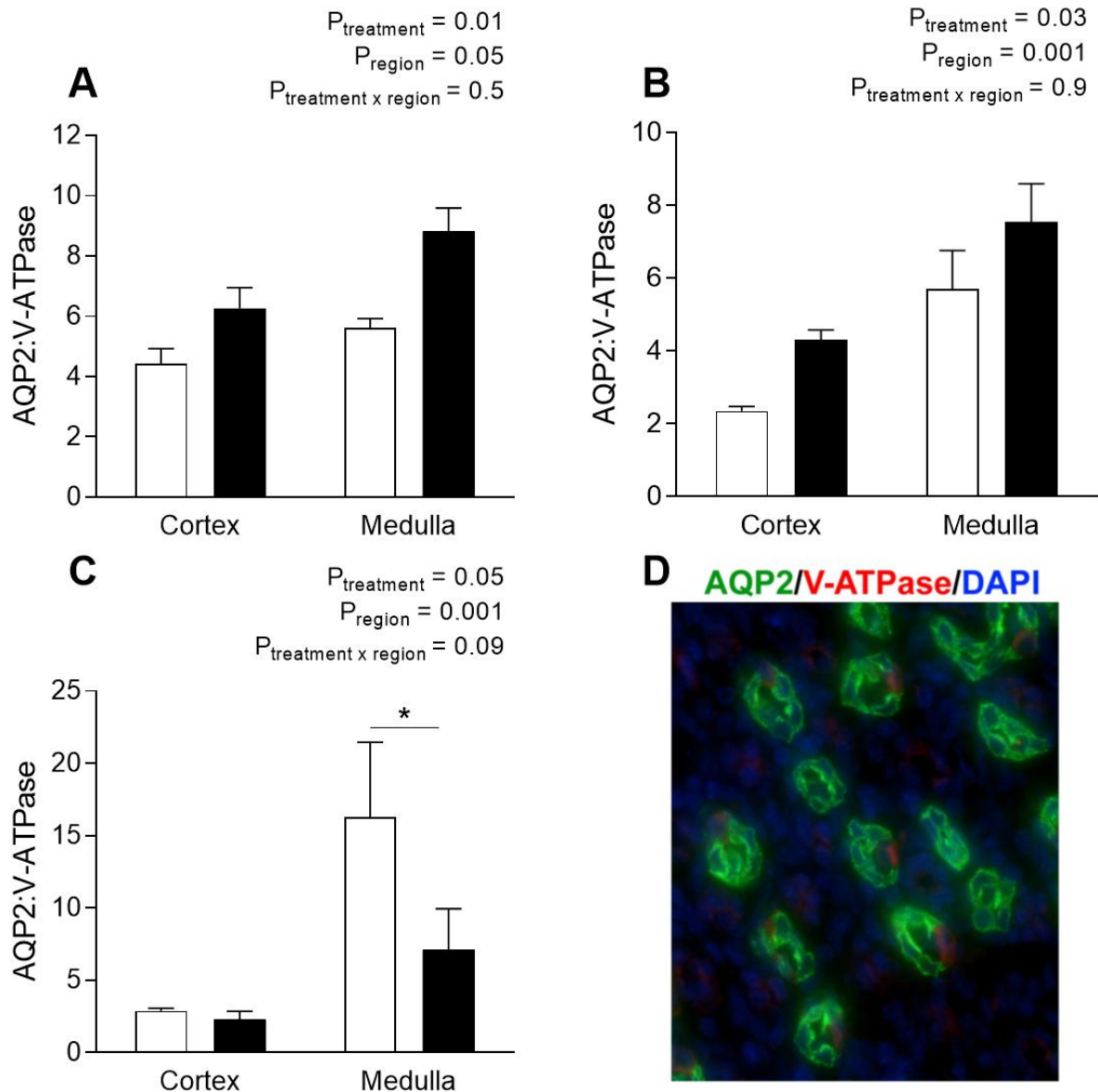


Figure 9. Cellular composition of the collecting duct in male offspring

Ratio of AQP2-positive to V-ATPase-positive cells in the collecting duct from kidneys of offspring at postnatal day 6 (A), postnatal day 21 (B) and 12 months of age (C). Immunofluorescent staining (D) of Aqp2 and V-ATPase expression in the medullary collecting ducts of the kidney. Data was analysed via two-way ANOVA and expressed as mean \pm SEM. Control: open bars; hypoxia: black bars. Male: N=4-9 animals per group (P6, 12 months). * $P < 0.05$ by Bonferroni post hoc.

Correlation between urine concentration capacity and collecting duct composition in male offspring

Immunohistochemistry revealed that AQP2 expression was decreased and also more diffusely distributed in the collecting duct cytoplasm in kidneys from hypoxia-exposed animals compared to controls at 12 months of age (Figure 10). Intense V-ATPase staining was observed in cortical collecting ducts from a subset of hypoxia-exposed kidneys, with a greater proportion of cortical collecting duct cells staining for V-ATPase compared to AQP2.

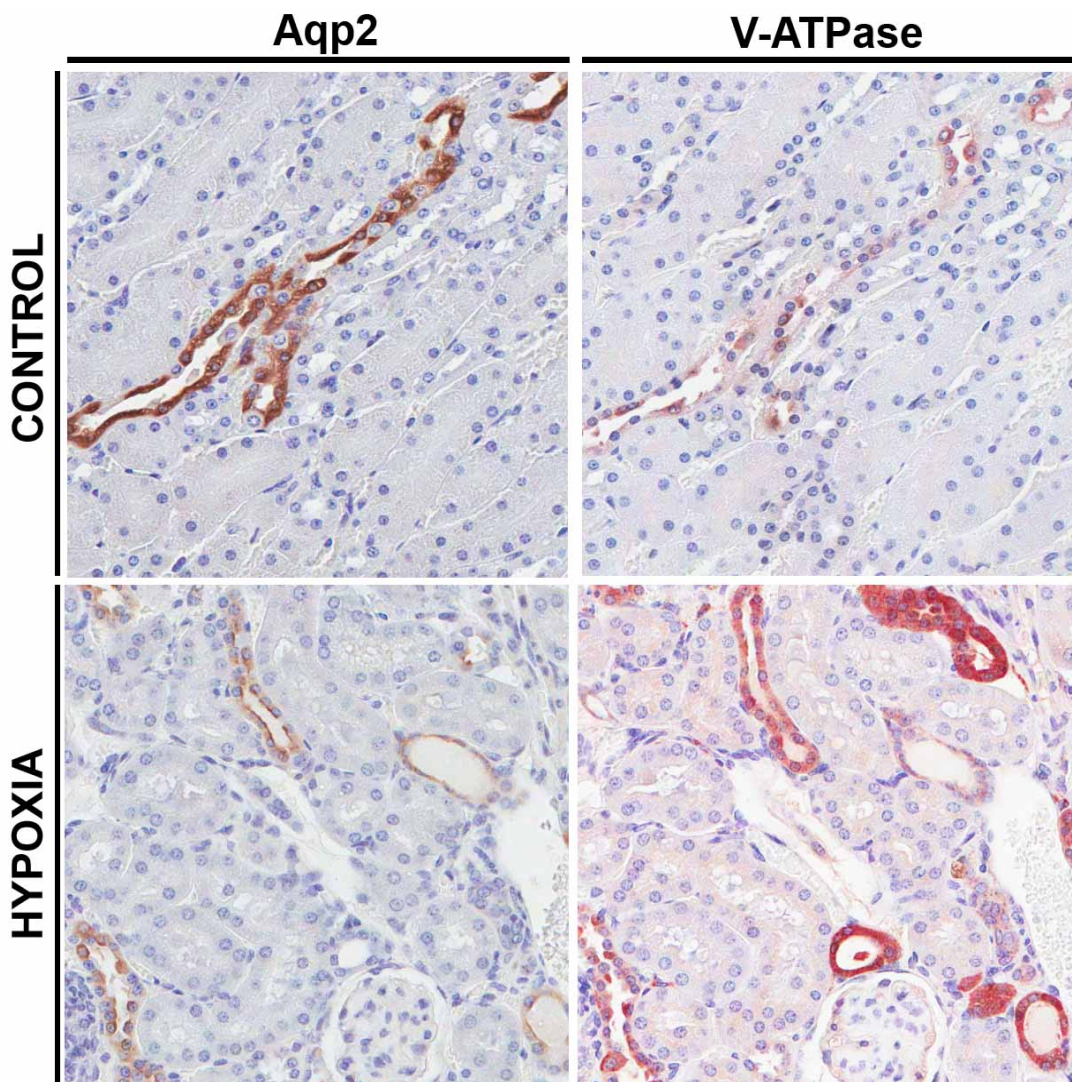


Figure 10. Collecting duct cell composition in kidneys from 12-month-old male offspring. Sequential sections were stained for AQP2 (principal cells, in brown staining) and V-ATPase (intercalated cells, in red staining) in the collecting duct. Nuclei are stained with haematoxylin.

The renal cortical collecting duct consisted of about 72% principal cells and 28% intercalated cells in control animals at 12 months of age ($72.45\% \pm 1.54\%$ principal cells vs. $27.55\% \pm 1.54\%$ intercalated cells). Two-way ANOVA revealed a trend towards an interaction between treatment and cell type ($P = 0.06$), with a reduction in AQP2-expressing principal cells and increased V-ATPase-expressing intercalated cells in the cortical collecting duct of hypoxia-exposed kidneys ($58.46\% \pm 8.26\%$ principal cells vs. $41.54\% \pm 8.26\%$ intercalated cells). Notably there was much greater variation within this group compared to controls, with half of the samples presenting with a greater proportion of V-ATPase-expressing intercalated cells compared to AQP2-expressing principal cells in the cortical collecting duct. Fewer intercalated cells were present in medullary collecting ducts compared to cortical collecting ducts in control ($89.47\% \pm 2.81\%$ principal cells vs. $10.54\% \pm 2.81\%$ intercalated cells) and hypoxia-exposed kidneys ($88.03\% \pm 3.43\%$ principal cells vs. $11.97\% \pm 3.43\%$ intercalated cells). When expressed as a ratio, hypoxia-exposed kidneys had a reduced proportion of AQP2-expressing principal cells within medullary cortical collecting ducts (Figure 11; $P_{\text{treatment}} = 0.051$).

A Pearson's correlation coefficient was computed to assess whether the hypoxia-exposed offspring with impaired urine concentration ability might be associated with an altered cellular composition in the renal collecting duct. Overall, there was a strong, negative correlation between the percentage of AQP2-expressing cells in the cortical collecting duct (CCD) and urine concentrating ability in kidneys of hypoxia-exposed animals [$r = -0.872$, $n = 8$, $p = 0.002$, with $r^2 = 0.760$]. Similarly, the percentage of AQP2-expressing cells in the medullary collecting duct (MCD) correlated with urine concentrating ability in hypoxia-exposed offspring [$r = -0.897$, $n = 8$, $p = 0.001$].

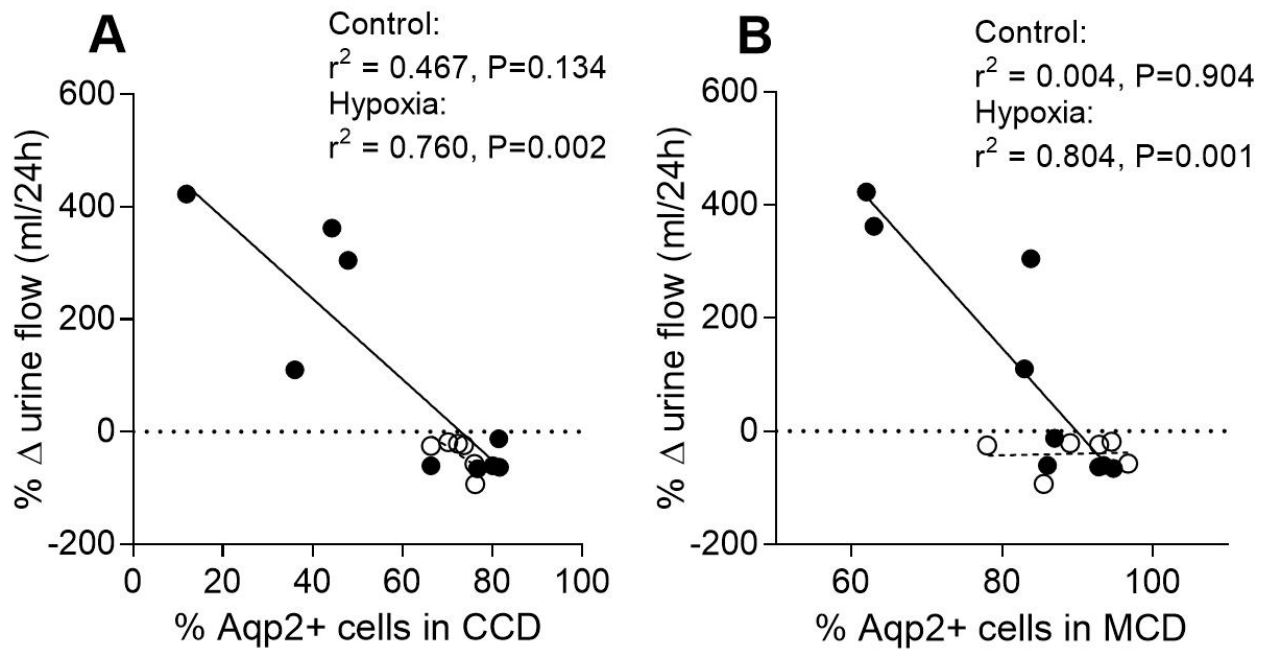


Figure 11. Correlation between cortical collecting duct composition and urine concentrating capacity in male offspring at 12 months of age. A Pearson's correlation was performed to correlate the number of AQP2-positive cells in the (A) cortical collecting duct (CCD) and (B) medullary collecting duct (MCD) to urine flow reduction in response to water deprivation over 24h. Control: open points; hypoxia: black points. Male: N=5-8 animals per group.

Tubular dilation in the renal papilla of male hypoxia-exposed offspring

Tubular dilation in the renal papilla was not evident at P21, 2 months, or 4 months of age (not shown). Microscopically, discernible tubular dilation appeared in the renal papilla of most male hypoxia-exposed offspring at 12 months of age (Figure 12).

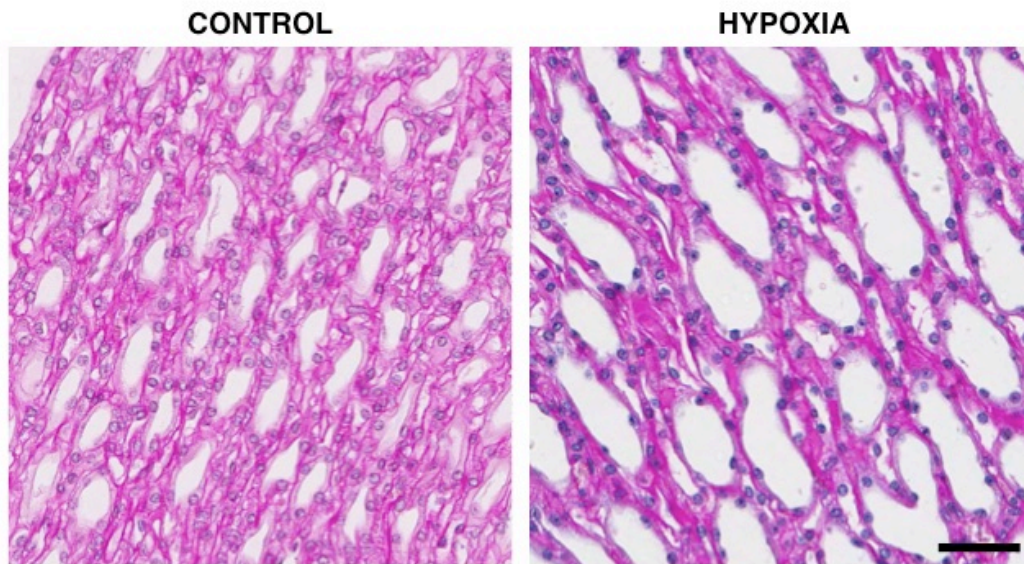


Figure 12. Periodic acid-Schiff staining of the renal papilla of 12-month-old male offspring. Scale bar represents 50 μm .

Discussion

This study provides compelling evidence that prenatal hypoxia has impacted the development of the renal tubules and collecting duct system in male offspring only, as well as reducing the number of glomeruli. Changes were evident in young male mice exposed to prenatal hypoxia, with increased AQP2 expression in the collecting duct and evidence of disproportionate growth of the renal cortex due to proximal and distal tubule elongation. Basal excretion of water and electrolytes was maintained in male hypoxia-exposed offspring throughout life; however, a subset of aged animals was unable to reduce urine flow in response to a 24 hour water deprivation challenge at 12 months of age. This was accompanied by altered cellular composition of the collecting duct, diminished expression of AQP2 and tubular dilation in male hypoxia-exposed offspring at 12 months of age. Hypoxia-exposed female offspring exhibited normal urine output, sodium excretion and osmolality under basal and water-deprived conditions compared to control females. In-depth structural analyses of the kidney were performed in male offspring only, as no functional or structural phenotypes were observed in female hypoxia-exposed offspring. Together, this study highlights the importance of considering the impact of *in utero* perturbations on the structure of the renal tubules and collecting duct system, as well as nephron number and sex of the offspring.

Maternal hypoxia reduces renal mass and alters renal structure in male offspring

As reported in *Chapters 3 and 4*, prenatal hypoxia led to growth restriction at E18.5, with catch-up growth observed by 2-3 months of age. Male hypoxia-exposed offspring had a 25% nephron deficit compared to male controls (*Chapter 4*) despite the kidney attaining the same mass at 12 months of age. This suggests that the existing nephron units underwent hypertrophy postnatally to produce a kidney of equal mass, albeit with 75% of the typical number of nephrons of CD1 mice. Indeed, when we examined the lengths of the renal tubules and collecting ducts of the kidneys at postnatal day 21, we observed marked elongation of the proximal and distal tubules in kidneys of hypoxia-exposed offspring compared to controls. Compensatory renal growth is a characteristic adaptation to reduced renal mass, which requires the remaining renal tissue to perform fluid and electrolyte homeostasis. In models of nephrectomy, the remnant kidney has been shown to increase single nephron glomerular filtration rate, which stimulates renal tubule hypertrophy and hyperplasia as well as glomerular hypertrophy (Hayslett *et al.*, 1968; Pollock *et al.*, 1992; Fong *et al.*, 2014). This growth likely allows the animals to maintain normal excretory function throughout adult life. Notably it has been suggested that increased proximal tubule growth may be maladaptive, leading to sodium retention and contributing to hypertension observed in models of a nephron deficiency (Fong *et al.*, 2014). However, this increase in proximal tubule length at P21 was only observed in

male hypoxia-exposed offspring, but not female offspring. It is important to note that female hypoxia-exposed offspring had normal nephron endowment compared to control female counterparts (*Chapter 4*), however mean arterial pressure was elevated. Therefore, increased proximal tubule length is unlikely to be the direct cause of hypertension as it was observed in both sexes as reported in *Chapter 4*.

Increased AQP2 expression in young male hypoxia-exposed mice

Interestingly, the collecting duct length in kidneys of male hypoxia-exposed offspring appeared to be shorter compared to control at P21. The development of the collecting ducts and loop of Henle that comprise the renal medulla and papilla has not been described in great detail in the literature. It is important to note that the kidneys of mice have a single papilla that extends into the renal pelvis, compared to multiple papillary lobes in the human kidney. However, we know that postnatal maturation of the collecting ducts and loop of Henle by tubule elongation occurs postnatally in both species (Evan *et al.*, 1991; Song & Yosypiv, 2012). Thus, reduced collecting duct length may indicate delayed or impaired collecting duct elongation. There was marked increase in apical AQP2 expression on the apical surface of collecting duct epithelial cells in the kidneys of male hypoxia-exposed offspring at P21. This appears to be a shift towards a more mature phenotype, as the expression level and distribution of AQP2 is shown to change from infancy to adulthood in line with increased capacity to concentrate urine (Yasui *et al.*, 1996). Therefore, increased AQP2 expression may be a sign of accelerated functional maturation, allowing maintenance of fluid and electrolyte homeostasis with reduced collecting duct surface area in the male hypoxia-exposed offspring.

We have also reported an increase in the proportion of AQP2-expressing principal cells compared to V-ATPase-expressing intercalated cells in the collecting duct in young mice (P6 and P21), indicating further compensation for reduced nephron number. This may render hypoxia-exposed offspring more susceptible to disturbances in acid/base balance, given this process is regulated by intercalated cells of the collecting duct. The neonatal kidney has a limited ability to mediate H^+/HCO_3^- homeostasis due to functional immaturity of the collecting duct, and is therefore more sensitive to acid/base disturbances (Matsumoto *et al.*, 1996). Furthermore, the neonatal cortical collecting duct has fewer differentiated intercalated cells compared to the adult, and no intercalated cells are present in the collecting ducts within the superficial renal cortex that contains the nephrogenic zone (Evan *et al.*, 1991; Matsumoto *et al.*, 1996). Throughout the first month of life, intercalated cells undergo significant postnatal proliferation and differentiation. Type A intercalated cells are thought to differentiate earlier than Type B cells, and studies in the newborn rabbit show

this is associated with low secretion of HCO_3^- compared to the adult (Mehrgut *et al.*, 1990). A study of maternal acidosis saw a reduced proportion of B-type intercalated cells, showing initial differentiation of intercalated cells can be modulated by maternal disturbances (Narbaitz *et al.*, 1993). Therefore, these observed changes might be attributed in an acid-base imbalance caused by maternal hypoxia. An in-depth examination of the maternal physiology in response to hypoxia is therefore warranted, as well as differentiation between intercalated cell types in the neonatal collecting duct.

Together these data suggest that overall kidney maturation is significantly delayed in male hypoxia-exposed offspring. Interestingly, this reduction in the proportion of intercalated cells compared to principal cells remained at 3 weeks of age. Metabolic cage studies could not be performed in the 3-week-old mice due to their young age; however, future studies may aim to collect spot urine to assess urine osmolality and pH. Susceptibility to fluctuations in acid/base balance in these hypoxia-exposed animals could be examined by acid and alkali loading in the maternal diet as previously studied in the rat (Narbaitz *et al.*, 1993).

Urinary excretion under basal conditions

Urine excretion under basal conditions was largely similar between control and hypoxia-exposed offspring, from 2 months of age until late adulthood in both sexes. Control male and female animals had lower urine osmolality at 12 months of age compared to 2-4 months, suggesting urine-concentrating capacity had declined with age. Declining urine concentrating capacity has been observed in elderly humans (Rowe *et al.*, 1976; Phillips *et al.*, 1984) as well as studies of ageing animals (Bengele *et al.*, 1981; Perucca *et al.*, 2007; Singh *et al.*, 2011). This decline is multifactorial, linked to progressive loss of functional glomeruli, reduced secretion of vasopressin (Tian *et al.*, 2004), impaired cellular response to vasopressin (Beck & Yu, 1982; Corman *et al.*, 1992; Geelen & Corman, 1992) and reduced GFR (Levinsky *et al.*, 1959). As urine osmolality tended to be lower in 4-month-old male hypoxia-exposed offspring compared to control counterparts, an early onset decline in urine concentrating capacity may have occurred in these animals.

Male hypoxia-exposed offspring have an altered response to a water deprivation challenge

A subset of male hypoxia-exposed animals was unable to respond appropriately to a water deprivation challenge at 12 months of age. There was a strong correlation between the inability to reduce urine flow during water deprivation in male offspring and a reduced proportion of AQP2-expressing principal cells in the collecting duct at this age. Furthermore, staining for AQP2 revealed diffuse, cytoplasmic staining of the principal collecting duct cells in animals that did not reduce

urine flow, compared to intense apical staining in control animals. When blood plasma osmolality is increased, such as the case of water deprivation, vasopressin is secreted and acts to increase water permeability by stimulating translocation of aquaporin 2 (AQP2) into the apical plasma membrane of principal collecting duct cells. Thus, the inability to reduce urine flow combined with reduced apical AQP2 expression in the collecting duct may suggest impairment in vasopressin action, possibly due to reduced vasopressin secretion or renal insensitivity to vasopressin. However, as observed in our model, declining urine concentration capacity as a result to altered responsiveness to vasopressin was likely due to decreased AQP2 abundance. In the future we aim to address this hypothesis by assessing circulating vasopressin levels at 12 months of age using archived plasma samples. However, ageing rat models have shown that impaired urine concentrating capacity can be present despite normal vasopressin secretion (Combet *et al.*, 2001; Tian *et al.*, 2004). Furthermore, age-associated decreased in renal expression of the vasopressin receptor V2R have been implicated in reduced renal concentrating capacity (Tian *et al.*, 2004), which suggests another avenue for this project to explore in the future.

Notably the phenotype we observe is mild, and the animals appeared to maintain urine osmolality during the water deprivation period. Other groups have created more severe models of total water dehydration by depriving animals of water for 2-4 days to yield a urine-concentrating deficit (Beck & Yu, 1982; Steiner & Phillips, 1988; Geelen & Corman, 1992; Terashima *et al.*, 1998). However this is associated with substantial body weight loss, hypovolemia and hypernatremia. Thus, total dehydration is unlikely to be representative of common physiological situations.

Female hypoxia-exposed offspring respond normally to water deprivation

Unlike males, female control and hypoxia-exposed offspring reduced urine flow in response to the water deprivation challenge. As previously reported in *Chapter 4*, female hypoxia-exposed offspring have similar glomerular endowment to control female offspring and no signs of worsened renal pathology at 12 months of age. Consequently, in our study, kidneys of female offspring appear to be protected from a late-gestational hypoxic insult and subsequently do not present with renal impairments observed in males. Sex differences have been reported in urine concentration capacity in ageing humans (Perucca *et al.*, 2007). Males have a greater tendency to concentrate urine, which may contribute to increased susceptibility to CKD and hypertension. To our knowledge, no study has reported sex differences in urine concentration capacity in response to a congenital nephron deficit. However, female offspring are frequently not studied in models of developmental programming given males are thought to be more susceptible to an *in utero* insult. For example, male sheep that were uninephrectomised in fetal life develop a urine concentrating

deficit, however the females were not examined. Thus, our study may encourage future research to consider both sexes, particularly when examining renal function.

Altered collecting duct cellular composition at 12 months of age

We turned our attention to the cellular composition of the collecting duct of male offspring, given this is the final site of water reabsorption in the kidney. There was disruption of the typical ‘salt and pepper’ distribution of the principal and intercalated cells within the collecting duct in kidneys from male hypoxia-exposed offspring. The predominant cell type in the collecting duct is the principal cell, comprising 70% of the cortical collecting duct. However, at 12 months of age we observed cases of entire tubules stained for the intercalated cell marker V-ATPase in the renal cortex. This was not observed in young animals. Interestingly, although tubular cells in the adult kidney are generally quiescent under normal conditions, this alteration in collecting duct composition suggests postnatal remodelling occurred at some point between weaning and old age. Indeed, postnatal remodelling of the collecting duct has been reported in a model of nephrogenic diabetes insipidus (Kim *et al.*, 2003; Christensen *et al.*, 2006). Collecting duct remodelling was associated with increased proliferation, but greater turnover, of principal cells (Christensen *et al.*, 2006). It was also suggested that adult principal cells may have biopotential, capable of differentiation into intercalated cells in responses to changes in acid-base balance or potassium depletion; this was not elucidated in the aforementioned study. Notably, a putative stem cell niche is thought to exist in the renal papilla, with renal stem cells entering the cell cycle during renal repair in the adult (Oliver *et al.*, 2004; Li *et al.*, 2015) and may be implicated in collecting duct remodelling. Future studies should measure blood acid-base parameters in the offspring from our model of prenatal hypoxia to examine signs of acidosis, and examine if proliferation or de-differentiation of collecting duct cell types may be associated with the increased proportion of intercalated cells observed within the kidneys of male hypoxia-exposed offspring.

Variability in the male hypoxia-exposed offspring

Importantly, prenatal hypoxia did not lead to renal deficits and structural alterations in every animal and this produced large variability in the study. Indeed, approximately 50% of the hypoxia-exposed kidneys appeared histologically similar to controls. Similar findings are observed in the human population, where individuals with reduced renal mass can survive without adverse renal or cardiovascular function. Children with congenital solitary kidney, for example, have an increased risk of renal damage compared to the average population, although are not guaranteed to develop renal insufficiency in their lifetime (Dursun *et al.*, 2005; Wasilewska *et al.*, 2006). Furthermore, the majority of adult kidney donors have stable renal function and blood pressure across life despite the

50% loss in kidney filtration surface area. However, some develop renal dysfunction, as well as moderate to overt hypertension (Hakim *et al.*, 1984; Talseth *et al.*, 1986; Fehrman-Ekholm *et al.*, 2001; Gossmann *et al.*, 2005). Thus, it is important to recognise that impaired kidney structure (such as a nephron deficit) does not always lead to renal dysfunction and signs of kidney. Therefore, it is plausible that the individuals with reduced renal mass who develop renal and cardiovascular dysfunction may have an underlying abnormality of the remaining kidney, or even a lower nephron number than average.

Study limitations and future directions

While this study has shown that prenatal hypoxia predisposes offspring to abnormalities in the renal medulla and papilla, many questions remain regarding the mechanisms regulating and potentially responsible for impaired medulla and papilla development. We have used simple morphometry to analyse the proportion of renal cortex to the medulla/papilla, but we aim to further characterise the altered kidney morphology for publication by estimating volume of the medulla (further categorised into the inner and outer stripe) and the papilla using unbiased stereology as described in *Chapter 5* in animals at P6, P21, 2 months and 12 months of age. Collecting duct cell composition will be examined in kidneys at 2 months of age, as collecting duct elongation is complete by this time point in control mouse offspring (*Chapter 5*) and markers of kidney injury and impaired renal function were not yet evident hypoxia-exposed offspring. Additionally, we will complete estimation of renal tubule lengths in offspring at 2 and 12 months of age; however, an additional collecting duct marker is required given the expression of AQP2 was greater diminished in hypoxia-exposed offspring.

Conclusions

This study has provided compelling preliminary evidence that prenatal hypoxia perturbed development of the renal tubule and collecting duct system, as well as reducing glomerular number. The kidneys of juvenile hypoxia-exposed mice had an increased proportion of renal cortex to medulla, due to elongation of the proximal and distal tubules compared to control animals. At 12 months of age, hypoxia-exposed offspring were capable of maintaining basal fluid and electrolyte excretion; however, offspring displayed a compromised response when subjected to a 24-hour water deprivation challenge. Animals that did not reduce urine flow in response to water deprivation had decreased renal AQP2 expression and altered cellular composition of the collecting duct. Together these data suggest that the renal tubule and collecting duct system had adapted to a nephron deficit, however a renal phenotype was unmasked when presented with a functional challenge. The mechanisms remain to be elucidated, but overall this study highlights that the renal tubules should be considered in conjunction with the number of glomeruli in future studies.

References

- Atiyeh BA, Dabbagh SS & Gruskin AB. (1996). Evaluation of renal function during childhood. *Pediatr Rev* **17**, 175-180.
- Australian Bureau of Statistics. (2013). Australian Health Survey: Biomedical Results for Chronic Diseases, 2011-12. Canberra.
- Beck N & Yu BP. (1982). Effect of aging on urinary concentrating mechanism and vasopressin-dependent cAMP in rats. *Am J Physiol Renal Physiol* **243**, F121-F125.
- Bengele HH, Mathias RS, Perkins JH & Alexander EA. (1981). Urinary concentrating defect in the aged rat. *Am J Physiol Renal Physiol* **240**, F147-F150.
- Brenner BM & Mackenzie HS. (1997). Nephron mass as a risk factor for progression of renal disease. *Kidney Int Suppl* **63**, S124-127.
- Chadban SJ, Briganti EM, Kerr PG, Dunstan DW, Welborn TA, Zimmet PZ & Atkins RC. (2003). Prevalence of Kidney Damage in Australian Adults: The AusDiab Kidney Study. *J Am Soc Nephrol* **14**, S131-S138.
- Christensen BM, Kim YH, Kwon TH & Nielsen S. (2006). Lithium treatment induces a marked proliferation of primarily principal cells in rat kidney inner medullary collecting duct. *Am J Physiol Renal Physiol* **291**, F39-48.
- Combet S, Teillet L, Geelen G, Pitrat B, Gobin R, Nielsen S, Trinh-Trang-Tan M-M, Corman B & Verbavatz J-M. (2001). Food restriction prevents age-related polyuria by vasopressin-dependent recruitment of aquaporin-2. *Am J Physiol Renal Physiol Physiology* **281**, F1123-F1131.
- Corman B, Roinel N & Geelen G. (1992). Plasma vasopressin and cortical nephron function in aging rats. *Mech Ageing Dev* **62**, 263-277.
- Cullen-McEwen LA, Douglas-Denton RN & Bertram JF. (2012). Estimating total nephron number in the adult kidney using the physical disector/fractionator combination. *Methods Mol Biol* **886**, 333-350.
- Dickinson H, Moritz K, Wintour EM, Walker DW & Kett MM. (2007). A comparative study of renal function in the desert-adapted spiny mouse and the laboratory-adapted C57BL/6 mouse: response to dietary salt load. *Am J Physiol Renal Physiol* **293**, F1093-1098.

- Donahue JL & Lowenthal DT. (1997). Nocturnal polyuria in the elderly person. *Am J Med Sci* **314**, 232-238.
- Dursun H, Bayazit AK, Büyükçelik M, Soran M, Noyan A & Anarat A. (2005). Associated anomalies in children with congenital solitary functioning kidney. *Pediatr Surg Int* **21**, 456-459.
- Ellery SJ, Ireland Z, Kett MM, Snow R, Walker DW & Dickinson H. (2013). Creatine pretreatment prevents birth asphyxia-induced injury of the newborn spiny mouse kidney. *Pediatr Res* **73**, 201-208.
- Evan AP, Satlin LM, Gattone VH, 2nd, Connors B & Schwartz GJ. (1991). Postnatal maturation of rabbit renal collecting duct. II. Morphological observations. *Am J Physiol* **261**, F91-107.
- Fehrman-Ekholm I, Dunér F, Brink B, Tydén G & Elinder C-G. (2001). No Evidence of Accelerated Loss of Kidney Function in Living Kidney Donors: Results From A Cross-Sectional Follow-Up1. *Transplantation* **72**, 444-449.
- Fong D, Denton KM, Moritz KM, Evans R & Singh RR. (2014). Compensatory responses to nephron deficiency: adaptive or maladaptive? *Nephrology* **19**, 119-128.
- Geelen G & Corman B. (1992). Relationship between vasopressin and renal concentrating ability in aging rats. *Am J Physiol Regul Integr Comp Physiol* **262**, R826-R833.
- Gossmann J, Wilhelm A, Kachel HG, Jordan J, Sann U, Geiger H, Kramer W & Scheuermann EH. (2005). Long-Term Consequences of Live Kidney Donation Follow-Up in 93% of Living Kidney Donors in a Single Transplant Center. *Am J Transplan* **5**, 2417-2424.
- Gupta BD, Sharma P, Bagla J, Parakh M & Soni JP. (2005). Renal failure in asphyxiated neonates. *Indian Pediatr* **42**, 928-934.
- Hakim RM, Goldszer RC & Brenner BM. (1984). Hypertension and proteinuria: long-term sequelae of uninephrectomy in humans. *Kidney Int* **25**, 930-936.
- Hayslett JP, Kashgarian M & Epstein FH. (1968). Functional correlates of compensatory renal hypertrophy. *J Clin Invest* **47**, 774.
- Hinchliffe S, Sargent P, Howard C, Chan Y & Van Velzen D. (1991). Human intrauterine renal growth expressed in absolute number of glomeruli assessed by the disector method and Cavalieri principle. *Lab Invest* **64**, 777-784.

Hoy WE, Rees M, Kile E, Mathews JD & Wang Z. (1999). A new dimension to the Barker hypothesis: low birthweight and susceptibility to renal disease. *Kidney Int* **56**, 1072-1077.

Hughson M, Douglas-Denton R, Bertram J & Hoy W. (2006). Hypertension, glomerular number, and birth weight in African Americans and white subjects in the southeastern United States. *Kidney Int* **69**, 671-678.

Hughson M, Farris AB, 3rd, Douglas-Denton R, Hoy WE & Bertram JF. (2003). Glomerular number and size in autopsy kidneys: the relationship to birth weight. *Kidney Int* **63**, 2113-2122.

Karlowicz MG & Adelman RD. (1995). Nonoliguric and oliguric acute renal failure in asphyxiated term neonates. *Pediatr Nephrol* **9**, 718-722.

Keller G, Zimmer G, Mall G, Ritz E & Amann K. (2003). Nephron number in patients with primary hypertension. *N Engl J Med* **348**, 101-108.

Kim Y-H, Kwon T-H, Christensen BM, Nielsen J, Wall SM, Madsen KM, Frøkiær J & Nielsen S. (2003). Altered expression of renal acid-base transporters in rats with lithium-induced NDI. *Am J Physiol Renal Physiol* **285**, F1244-F1257.

Langley-Evans SC, Welham SJ & Jackson AA. (1999). Fetal exposure to a maternal low protein diet impairs nephrogenesis and promotes hypertension in the rat. *Life Sci* **64**, 965-974.

Layton AT, Layton HE, Dantzler WH & Pannabecker TL. (2009). The Mammalian Urine Concentrating Mechanism: Hypotheses and Uncertainties. *Physiology* **24**, 250-256.

Levey AS, Coresh J, Balk E, Kausz AT, Levin A, Steffes MW, Hogg RJ, Perrone RD, Lau J & Eknoyan G. (2003). National Kidney Foundation practice guidelines for chronic kidney disease: evaluation, classification, and stratification. *Ann Intern Med* **139**, 137-147.

Levinsky NG, Davidson DG & Berliner RW. (1959). Effects of reduced glomerular filtration on urine concentration in the presence of antidiuretic hormone. *J Clin Invest* **38**, 730.

Li J, Ariunbold U, Suhaimi N, Sunn N, Guo J, McMahon JA, McMahon AP & Little M. (2015). Collecting Duct-Derived Cells Display Mesenchymal Stem Cell Properties and Retain Selective In Vitro and In Vivo Epithelial Capacity. *J Am Soc Nephrol* **26**, 81-94.

- Little MH & McMahon AP. (2012). Mammalian kidney development: principles, progress, and projections. *Cold Spring Harbor perspectives in biology* **4**, a008300.
- Matsumoto T, Fejes-Toth G & Schwartz GJ. (1996). Postnatal Differentiation of Rabbit Collecting Duct Intercalated Cells. *Pediatr Res* **39**, 1-12.
- Mehrgut FM, Satlin LM & Schwartz GJ. (1990). Maturation of HCO₃⁻ transport in rabbit collecting duct. *Am J Physiol* **259**, F801-808.
- Moritz KM, Dodic M & Wintour EM. (2003). Kidney development and the fetal programming of adult disease. *Bioessays* **25**, 212-220.
- Moritz KM, Singh RR, Probyn ME & Denton KM. (2009). Developmental programming of a reduced nephron endowment: more than just a baby's birth weight. *Am J Physiol Renal Physiol* **296**, F1-9.
- Moritz KM, Wintour EM & Dodic M. (2002). Fetal uninephrectomy leads to postnatal hypertension and compromised renal function. *Hypertension* **39**, 1071-1076.
- Narbaitz R, Kapal VK & Levine DZ. (1993). Induction of intercalated cell changes in rat pups from acid- and alkali-loaded mothers. *Am J Physiol* **264**, F415-420.
- Nieto VMG, Yanes MIL, Zamorano MM, González MJH, Aros CP & Garin EH. (2008). Renal concentrating capacity as a marker for glomerular filtration rate. *Acta Paediatr* **97**, 96-99.
- Oliver JA, Maarouf O, Cheema FH, Martens TP & Al-Awqati Q. (2004). The renal papilla is a niche for adult kidney stem cells. *J Clin Invest* **114**, 795-804.
- Perucca J, Bouby N, Valeix P & Bankir L. (2007). Sex difference in urine concentration across differing ages, sodium intake, and level of kidney disease. *Am J Physiol Regul Integr Comp Physiol* **292**, R700-R705.
- Phillips PA, Rolls BJ, Ledingham JG, Forsling ML, Morton JJ, Crowe MJ & Wollner L. (1984). Reduced thirst after water deprivation in healthy elderly men. *N Engl J Med* **311**, 753-759.
- Pollock CA, Bostrom TE, Dyne M, Györy AZ & Field MJ. (1992). Tubular sodium handling and tubuloglomerular feedback in compensatory renal hypertrophy. *Pflügers Archiv* **420**, 159-166.
- Rowe J, Shock N & DeFronzo R. (1976). The influence of age on the renal response to water deprivation in man. *Nephron* **17**, 270-278.

Sarnak MJ, Levey AS, Schoolwerth AC, Coresh J, Culeton B, Hamm LL, McCullough PA, Kasiske BL, Kelepouris E, Klag MJ, Parfrey P, Pfeffer M, Raij L, Spinosa DJ & Wilson PW. (2003). Kidney Disease as a Risk Factor for Development of Cardiovascular Disease. *A Statement From the American Heart Association Councils on Kidney in Cardiovascular Disease, High Blood Pressure Research, Clinical Cardiology, and Epidemiology and Prevention* **108**, 2154-2169.

Schmidt-Nielsen B & O'Dell R. (1961). Structure and concentrating mechanism in the mammalian kidney. *Am J Physiol* **200**, 1119-1124.

Shi Y, Li C, Thomsen K, Jørgensen TM, Knepper MA, Nielsen S, Djurhuus JC & Frøkiær J. (2004). Neonatal ureteral obstruction alters expression of renal sodium transporters and aquaporin water channels. *Kidney Int* **66**, 203-215.

Singh RR, Denton KM, Bertram JF, Dowling J & Moritz KM. (2011). Urine-concentrating defects exacerbate with age in male offspring with a low-nephron endowment. *Am J Physiol Renal Physiol* **301**, F1168-1176.

Song R & Yosypiv IV. (2012). Development of the kidney medulla. *Organogenesis* **8**, 10-17.

Steiner M & Phillips MI. (1988). Renal tubular vasopressin receptors downregulated by dehydration. *Am J Physiol Cell Physiol* **254**, C404-C410.

Svenningsen NW & Aronson AS. (1974). Postnatal development of renal concentration capacity as estimated by DDAVP-Test in normal and asphyxiated neonates. *Neonatology* **25**, 230-241.

Talseth T, Fauchald P, Skrede S, Djøseland O, Berg KJ, Stenstrøm J, Heilo A, Brodwall EK & Flatmark A. (1986). Long-term blood pressure and renal function in kidney donors. *Kidney Int* **29**, 1072-1076.

Terashima Y, Kondo K, Inagaki A, Yokoi H, Arima H, Murase T, Iwasaki Y & Oiso Y. (1998). Age-associated decrease in response of rat aquaporin-2 gene expression to dehydration. *Life Sci* **62**, 873-882.

Tian Y, Serino R & Verbalis JG. (2004). Downregulation of renal vasopressin V2 receptor and aquaporin-2 expression parallels age-associated defects in urine concentration. *Am J Physiol Regul Integr Comp Physiol* **287**, F797-F805.

Wasilewska A, Zoch-Zwierz W, Jadeszko I, Porowski T, Biernacka A, Niewiarowska A & Korzeniecka-Kozerska A. (2006). Assessment of serum cystatin C in children with congenital solitary kidney. *Pediatr Nephrol* **21**, 688-693.

Wilkinson L, Kurniawan ND, Phua YL, Nguyen MJ, Li J, Galloway GJ, Hashitani H, Lang RJ & Little MH. (2012). Association between congenital defects in papillary outgrowth and functional obstruction in Crim1 mutant mice. *J Pathol* **227**, 499-510.

Yasui M, Marples D, Belusa R, Eklof A, Celsi G, Nielsen S & Aperia A. (1996). Development of urinary concentrating capacity: role of aquaporin-2. *Am J Physiol Regul Integr Comp Physiol* **271**, F461-F468.

Chapter 7: General Discussion

7.1 Thesis summary

This thesis has investigated the impact of maternal hypoxia during late gestation on susceptibility of offspring to cardiovascular and renal impairments in adulthood. Our first aim was to establish a model of maternal hypoxia in the mouse and examine growth of offspring from late gestation to weaning. We then focussed on the effects of maternal hypoxia on renal function and structure in offspring throughout life. Following this, we examined blood pressure and microvascular function, structure and mechanics in offspring at 12 months of age. The combined effects of prenatal hypoxia and a postnatal diet high in salt, common in society were also assessed. Finally, we have developed a design-based stereological method to estimate lengths of nephron segments and collecting ducts in the kidney. We applied this method to our model of maternal hypoxia to examine nephron tubule and collecting duct lengths in offspring. This methodology can be readily utilised in any future studies examining changes to renal tubule architecture. The major findings of our studies show that all hypoxic offspring are born growth-restricted but undergo catch-up growth after weaning. Male but not female hypoxia-exposed offspring have reduced glomerular endowment and increased susceptibility to renal impairments throughout life. Notably, both sexes are vulnerable to hypertension, endothelial dysfunction and salt-induced microvascular stiffening and cardiac damage. This suggests that although prenatal hypoxia may, in many cases, be a non-modifiable risk factor for later renal and cardiovascular impairments, consuming a healthy diet may reduce the risk of developing these diseases in later life. This chapter will summarise the findings of this thesis and place our research in context with the literature and other work performed by our laboratory.

Summary of results

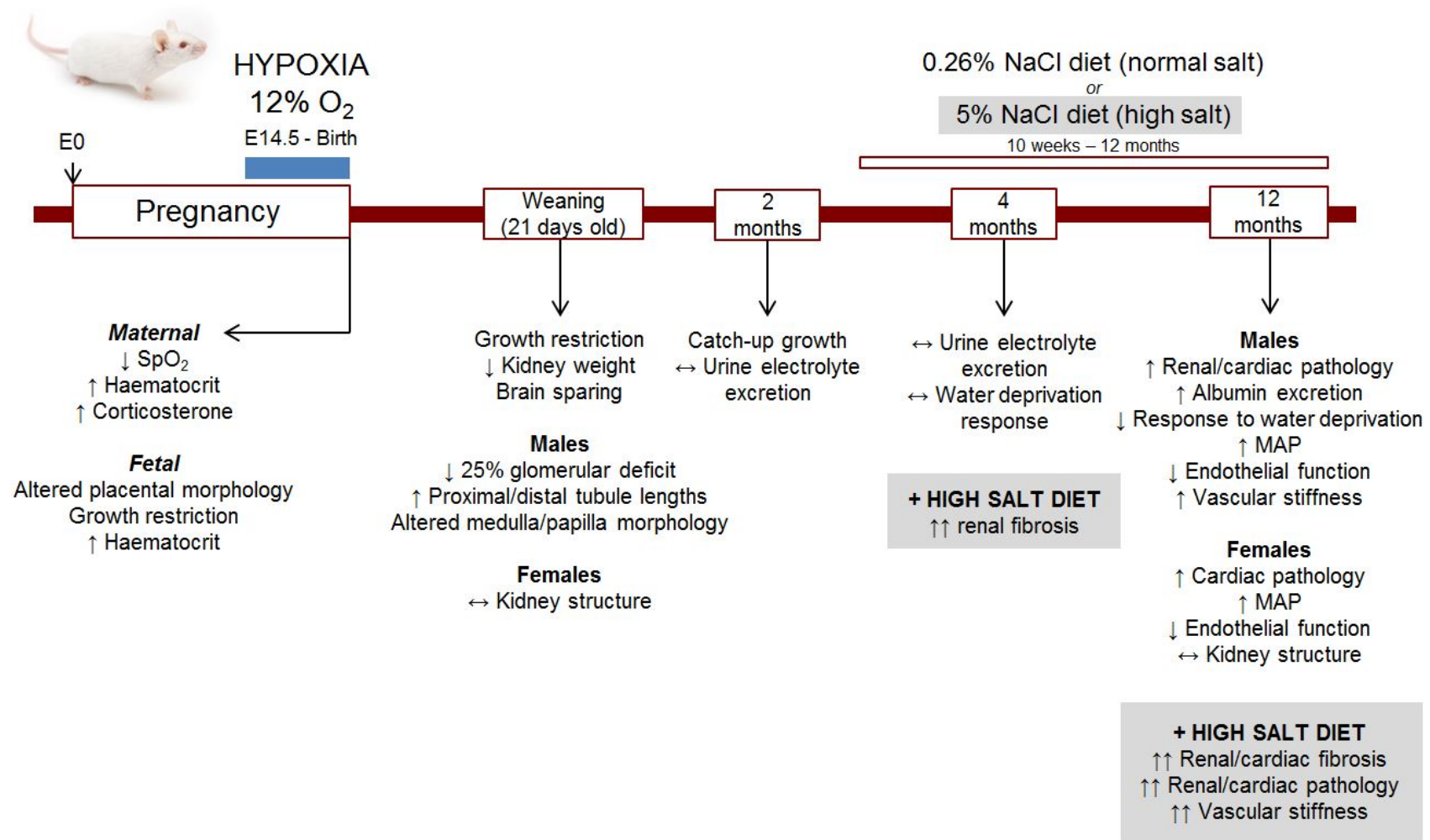


Figure 7.1. A summary of the major time points within this model and long-term health outcomes of offspring exposed to maternal hypoxia during late gestation.

Abbreviations: SpO₂, peripheral capillary oxygen saturation. MAP, mean arterial pressure.

7.2 Modelling prenatal hypoxia in the mouse

The first aim of this study was to develop a model of late gestational hypoxia in the mouse, as displayed in Figure 7.1. As can be seen in Table 1.3, the effects of prenatal hypoxia have been well characterised in the rat, chicken and sheep but the mouse has been comparatively understudied. This is not surprising as physiological measurements in the mouse are more challenging than in larger animals, although completely feasible as reported in this thesis. However, the mouse is currently the best tool to examine development of organs across life with an array of molecular tools available. In particular, the development of the murine kidney, the primary focus of this thesis, has been extensively documented in the GUDMAP database (Harding *et al.*, 2011), a molecular atlas of gene expression within the genitourinary tract. Therefore, now we have established a physiological model of late gestational hypoxia in the mouse, future studies in our laboratory will be able to take advantage of the molecular tools available to examine murine development.

The kidney is known to develop in a relatively hypoxic environment, however further reduction in oxygen tension leads to detrimental renal outcomes dependent on timing, duration and severity of the insult. Severe (5.5%-6.5% O₂) acute (8 h) hypoxia during early gestation (E9.5-10.5), for example, results in duplex kidneys whereas as more moderate exposure to hypoxia (12% O₂) during midgestation (E12.5-14.5) causes renal hypoplasia (Wilkinson *et al.*, 2015). Functional outcomes have not been assessed in these animals. Both phenotypes fall within the congenital abnormalities of the kidney and urinary tract (CAKUT) spectrum, one of the most prevalent birth defects in humans (Schedl, 2007). Instead, we have examined moderate, chronic hypoxia exposure throughout late gestation (12% O₂; E14.5 – birth). Approximately 80 glomeruli are estimated to be present at E14.5, but this number increased to ~8000 in the newborn mouse (Cebrian *et al.*, 2004). Therefore, the timing of hypoxia exposure in this thesis is designed to coincide with the rapid process of nephrogenesis in the fetal murine kidney. This hypoxic insult also covers the definitive configuration of the heart, and modification of coronary vasculature and atrioventricular valve leaflets (Savolainen *et al.*, 2009).

The following section will integrate the outcomes following prenatal hypoxia across the life span, firstly focussing on the effects on maternal physiology, the developing fetus and placenta and then offspring growth. This will involve discussion of two publications during my candidature (Cuffe *et al.*, 2014a; Cuffe *et al.*, 2014b), not included in the thesis, in which I made significant contributions by performing all of the animal experiments and tissue collection, and some of the histological analyses of the placenta. Renal and cardiovascular outcomes following prenatal hypoxia (*Chapter*

3, 4 and 6) will be discussed, and finally the combined effects of prenatal hypoxia and a postnatal diet high in salt. Commentary on developing a method to estimate tubule lengths in the mouse kidney (*Chapter 5*) will be provided at the end of this discussion chapter.

7.3 Quantifying fetal, placental and maternal hypoxia

Quantifying the degree of hypoxia in the mouse presents greater challenges compared to larger animals such as the sheep where blood gas measurements via chronic instrumentation of both the mother and fetus is possible (Allison *et al.*, 2016). Instead, a pulse oximeter designed for rodents and protein analysis was used to assess the degree of hypoxia in the mother and fetus. Using this technology, a sustained reduction of maternal peripheral capillary oxygen saturation to a mean level of 77% was observed. This occurred without affecting maternal food or water intake during habitation in the hypoxia chamber (Cuffe *et al.*, 2014a). Prior to this thesis, we have also shown increased expression of pimonidazole adducts which binds to thiol groups at oxygen tensions below 10 mmHg, in placentae at E18.5. Additionally, increased HIF1A staining was observed in the fetal liver (Cuffe *et al.*, 2014a) and both maternal and fetal haematocrit were elevated at E18.5. The increased HIF1A staining in the liver may suggest shunting of oxygenation blood through the ductus venosus away from the liver to organs of higher priority, such as the heart and brain. Elevated haematocrit is a typical physiologic response to reduced cellular oxygenation and frequently observed at high altitude (Graber & Krantz, 1978; León-Velarde *et al.*, 2010). Together, these data suggest that maternal hypoxia has translated into both placental and fetal hypoxia in our mouse model.

7.4 Fetal and early offspring growth following prenatal hypoxia

Table 7.1 summarises the impact of prenatal hypoxia on body and organ weight at late gestation (E18.5) and weaning (P21). Prenatal hypoxia led to growth restriction and specific reduction in kidney weight at E18.5 and P21. In comparison, there was no effect of prenatal hypoxia on heart weight or absolute brain weight at either age. Interestingly there was a significant increase in the brain-to-body weight ratio at P21, meaning brain size was maintained despite overall reduced body size. This is known as ‘brain sparing’, a form of asymmetric growth restriction commonly observed in models of prenatal hypoxia (Giussani, 2016). It suggests that blood flow, and thus oxygenation, is maintained to the brain. Given the finding of increased HIF1A in the fetal liver following maternal hypoxia, it will be of interest to directly compare the degree of HIF1A staining between fetal tissues, particularly the fetal brain and kidney given we observed brain sparing and a specific reduction in kidney weight.

Table 7.1. Summary of the effects of maternal hypoxia on body and organ weights compared to control offspring at late gestation (E18.5) and weaning (P21)

	E18.5		P21	
	Male	Female	Male	Female
Body weight	↓	↓	↓	↓
Kidney weight	↓	↓	↓	↓
Kidney:body weight	↔	↔	↔	↔
Heart weight	↔	↔	↔	↔
Heart:body weight	↔	↔	↔	↔
Brain weight	↔	↔	↔	↔
Brain:body weight	↔	↔	↑	↑

7.5 Responses to maternal hypoxia

Having ascertained this model of maternal hypoxia in the mouse results in growth restriction, it is important to consider the potential mechanisms and compensatory adaptations made by the dam and placenta. In conjunction with the studies within my thesis, many aspects of maternal and placental physiology were examined (Cuffe *et al.*, 2014a; Cuffe *et al.*, 2014b). These studies provide insight into the contribution of altered maternal physiology and placentation to growth restriction and subsequent susceptibility to renal and cardiovascular dysfunction in adult offspring.

a) Excess maternal glucocorticoids

Many perturbations throughout pregnancy are associated with stress, or are known to mediate effects via stress-responsive pathways (Edwards & McMillen, 2001; Ramadoss *et al.*, 2008; Moritz *et al.*, 2011; O'Sullivan *et al.*, 2015). Indeed, we have previously reported that pregnant dams exposed to our model of hypoxia from E14.5 to E18.5 have a 40% increase in plasma corticosterone concentrations and a similar increase in plasma glucose concentrations (Cuffe *et al.*, 2014a). This suggests a sustained stress response to housing in the hypoxia chamber. The placenta expresses a glucocorticoid-inactivating enzyme, HSD11B2, to protect the fetus from excess maternal glucocorticoids. However, our model of maternal hypoxia reduced expression of HSD11B2 in the late term placenta (Cuffe *et al.*, 2014a), increasing the potential for increased placental transfer to glucocorticoids to the developing fetus. Similar findings have been observed in babies of mothers with uncontrolled asthma, where there is a reduction in birth weight, increased fetal cortisol and

reduced placental HSD11B2 activity (Murphy *et al.*, 2002). Consequently, excess glucocorticoid exposure may contribute to adverse offspring outcomes in combination with hypoxia.

b) Maternal nutritional adaptations to hypoxia

As previously mentioned, maternal undernutrition was not a confounding factor in our study. Many studies have reported decreased appetite in pregnant animals exposed to maternal hypoxia, thus requiring a pair-fed group (de Grauw *et al.*, 1986; Gleed & Mortola, 1991; Williams *et al.*, 2005a; Williams *et al.*, 2005b; Camm *et al.*, 2010). Marked appetite loss is often observed in humans in high-altitude expeditions (Westerterp-Plantenga *et al.*, 1999) or even those exposed to simulated high altitude in a hypobaric chamber (Westerterp-Plantenga, 1999). These aforementioned animal studies of maternal hypoxia may accurately reflect high altitude populations which are often impoverished, and can discern the relative contributions of fetal hypoxia and undernutrition to disease outcomes. In contrast, our model allows us to examine the effects of prenatal hypoxia independent of maternal undernutrition. The reasons for this difference to other species are unknown; however, in a more severe model of maternal hypoxia (8% O₂, 24 h) in the mouse, food consumption decreased by 88% after 24 hours of hypoxia (Ream *et al.*, 2008). This reduction in food intake was associated with high rates of embryonic lethality (89% and 51% lethality after 24 h of hypoxia at E13.5 and E17.5 respectively) (Ream *et al.*, 2008). No embryonic lethality was observed in our model, and hypoxia-exposed dams had litter sizes equivalent to control dams (Cuffe *et al.*, 2014a). This suggests timing and severity of the hypoxic insult as well as species differences may affect nutritional status. We speculate that leptin, a neuroendocrine regulator of satiety, may contribute to the differences in hypoxia-associated decline in food consumption between species, given suppressed appetite at high altitude has been associated with increased serum leptin levels in humans (Tschöp *et al.*, 1999).

c) Placental adaptations to hypoxia

Importantly, the placenta facilitates nutrient transport to the fetus and produces growth factors to regulate fetal growth. Therefore, perturbations to the placenta as a result of maternal hypoxia may contribute to growth restriction, possibly due to decreased nutrient and oxygen transfer to the fetus. Unlike maternal glucose, we have shown that fetal blood glucose levels were unaffected by maternal hypoxia (Cuffe *et al.*, 2014a). This suggests placental glucose transporter activity prevented fetal hyperglycaemia. It is important to note that fetal blood glucose levels were measured in pooled male and female plasma samples due to limited sample volume, and thus sex differences could not be considered. We have reported reduced mRNA/protein levels of *Slc2a1*/GLUT1 in placentae of female hypoxia-exposed offspring, a glucose transporter in the

placenta (Cuffe *et al.*, 2014a). Reduced GLUT1 protein expression has also been shown in placentae from high altitude pregnancies which result in growth restriction (Zamudio *et al.*, 2006). Therefore, glucose transfer capacity may be related to poor fetal growth in pregnancies. Maternal hypoxia also decreased mRNA expression of the VEGF receptor (*Kdr*) and *Igf2*, two factors that are largely responsible for regulating growth of the placental vascular network (Carmeliet & Collen, 1998; Sibley *et al.*, 2004). These gene expression changes associated with vascular branching may be underlying the increased branching of the placental labyrinth vasculature, although further research into this is required to elucidate the role of placental vasculogenesis in our mouse model of prenatal hypoxia. Undoubtedly, maternal hypoxia has translated into altered placental formation in a sex-specific manner in this model. A wealth of studies have revealed placental insufficiency (Wlodek *et al.*, 2005; Burke *et al.*, 2006; Wlodek *et al.*, 2007; O'Dowd *et al.*, 2008; Moritz *et al.*, 2009a; Black *et al.*, 2012) is associated with adverse health outcomes in offspring, and it is therefore likely that impaired placentation may underlie many of the disease outcomes to be outlined further on in this discussion.

7.6 Catch-up growth

The degree of growth restriction observed in hypoxia-exposed offspring at late gestation was sustained throughout lactation. Reduced body weight pre-weaning may suggest an impaired lactational environment, which we have not addressed in the present thesis. Similarly, a study by Moore and Price in 1948 revealed rats at high altitude were growth-restricted until weaning, suggested impaired lactation in mothers at high altitude. A model of uteroplacental insufficiency in the rat has reported that the procedure impairs lactation and contributes to growth restriction (O'Dowd *et al.*, 2008). Cigarette smoking, which can lead to fetal hypoxia, is associated with reduced breast-milk volume in the human population (Vio *et al.*, 1991). Aside from these studies, literature considering lactation and maternal hypoxia, even at high altitude, is scarce and warrants further investigation. However, substantial catch-up growth was observed in the hypoxic exposed offspring post-weaning. Catch-up growth is observed in children following delayed growth, such as intrauterine growth restriction or illness. It is frequently observed within the first 2 years of life in humans. Growth restriction and subsequent catch-up growth are both accurate predictors of adult-onset disease (Barker, 1998). Increased rate of weight gain within the first 2 years of life has been associated with obesity by 5 years of age, and the development of hypertension (Eriksson *et al.*, 1999; Forsén *et al.*, 1999; Ong *et al.*, 2000). This suggests that hypoxia-exposed offspring are at increased risk of cardiovascular disease in later life.

7.7 Effect of maternal hypoxia on early postnatal kidney structure and function

7.7.1 *Reduced nephron number and proximal/distal tubule hypertrophy in male offspring*

One of the most interesting findings from *Chapter 4* was the 25% nephron deficiency in male but not female hypoxia-exposed offspring (Table 7.2). This is an unusual finding, although as discussed in *Chapter 1*, male offspring tend to have a greater reduction in nephron number and increased risk of disease in adulthood. Furthermore, a male-specific reduction in nephron number has previously been reported in studies of protein restriction in the rat (Woods *et al.*, 2001; Woods *et al.*, 2004; Woods *et al.*, 2005) so our findings are not unprecedented. This reduction in nephron number was accompanied by an increase in the relative proportion of renal cortex compared to medulla at P21. Using our methodology to estimate tube lengths, we determined this increase was driven by increased proximal and distal tubule lengths (*Chapter 6*; Table 7.2). This is the first study to report altered renal tubule lengths in a developmental programming model and highlights that prenatal insults are likely to affect other aspects of renal development apart from glomerular number. Increased proximal and distal tubule lengths are characteristic of compensatory renal hypertrophy, reported frequently in reduced renal mass such as nephrectomy (Hayslett *et al.*, 1968; Pollock *et al.*, 1992; Douglas-Denton *et al.*, 2002) but also in pathological cases of diabetes mellitus (Nyengaard *et al.*, 1993). The proximal tubule in our study underwent the greatest increase in length, with a more modest increase in length occurring in the distal tubules as previously reported (Hayslett *et al.*, 1968). This growth in compensatory renal hypertrophy mirrors the normal growth pattern of the kidney in early postnatal life, as reported in *Chapter 5*. It is thought that increased single nephron GFR associated with a nephron deficiency may promote proximal tubule hypertrophy and tubular reabsorption of sodium, due in part to increased sodium channel and transport expression and tentatively linked to increased renal sympathetic nerve activity (Furukawa *et al.*, 1997; Fong *et al.*, 2014). This allows the remaining renal mass to perform fluid and electrolyte homeostasis. Indeed, urine flow and electrolyte excretion remained unperturbed from 2 to 12 months of age. Proximal tubule hypertrophy may become maladaptive by leading to a rightward shift in the pressure-natriuresis curve, resulting in further sodium and water retention and hypertension (Figure 7.2) (Guyton *et al.*, 1972). We have not yet performed tubule length estimations in kidneys at 12 months of age to confirm this hypothesis, although the same findings are likely given the kidneys have similar mass to controls despite the 25% reduction in glomerular number present at this age.

Not surprisingly, reduced nephron number in male hypoxia-exposed offspring was associated with glomerular hypertrophy, a slight increase in urinary albumin excretion, increased incidence of

glomerulosclerosis and elevated arterial pressure at 12 months of age. This is in striking accordance with the Brenner hypothesis (Figure 1.2), where a congenital nephron deficiency leads to an increase in single nephron GFR and ultimately progressive glomerular scarring and arterial hypertension (Brenner *et al.*, 1988; Brenner & Mackenzie, 1997). However, this may be an oversimplification of our study as female offspring also develop elevated mean arterial pressure in the absence of a nephron deficit. Therefore, a reduced nephron number may contribute to elevated arterial pressure in male offspring, but is unlikely to be the direct cause. Our novel data on changes in tubule lengths is likely to be important. On the other hand, elevated arterial pressure in female offspring may have different origins to male offspring although this is speculative at the present time. Blood pressure will be discussed in detail in the following section of this discussion.

Table 7.2. Summary of renal outcomes in young and aged mice.

Arrows represent changes in renal function/structure in hypoxia-exposed offspring relative to age-matched control counterparts.

	Hypoxia-exposed young mice		Hypoxia-exposed mice at 12 months	
	Male	Female	Male	Female
<i>Kidney structure</i>				
Nephron number*	↓	↔	↓	↔
Proximal tubule length*	↑	↔		
TDLH length*	↔	↔		
Distal tubule length*	↑	↔		
CD length*	↔	↔		
Aqp2:V-ATPase in CD*#	↑		↓	
<i>Basal urinalysis</i>				
Urine flow [^]	↔	↔	↔	↑
Urinary sodium [^]	↔	↔	↔	↔
Urine osmolality [^]	↓	↔	↔	↓
<i>Urinalysis under water deprivation</i>				
Urine flow [^]	↔	↔	↑	↔
Urinary sodium [^]	↔	↔	↑	↔
Urine osmolality [^]	↔	↔	↔	↔

TDLH, thin descending limb of Henle. CD, collecting duct.

Ages of young mice: *postnatal day 21, # postnatal day 6, [^] 4 months of age

7.7.2 Mechanisms of the sex-specific reduction in nephron number

Why males but not females have a nephron deficit remains an interesting question which we wish to elucidate. We have several hypotheses to explain this phenomenon. Firstly, it is vital to note that female CD1 mice have 25% fewer glomeruli than males (*Chapter 4*; Schlegel et al., 2016), similar to few numbers of nephrons in human females compared to males. Therefore, hypoxia-exposed male offspring have the same number of glomeruli as female control and hypoxia-exposed offspring. This may suggest that the hypoxic insult impaired development of the final 25% of nephrons formed in the control male CD1 mouse, and would therefore not affect female hypoxia-exposed offspring. This could be attributed to timing of the hypoxic insult. Indeed, a study in our laboratory investigating prenatal hypoxia in mid-gestation (12% O₂) showed a similar reduction in glomerular number in both male and female (unpublished) offspring (Wilkinson *et al.*, 2015). Note that glomerular numbers of both sexes were pooled for publication. From about E11-12 in the mouse, differentiation of the metanephric kidney is evident although mesonephros is still present. Early nephrons in the developing renal cortex are recognisable from about E13-14; therefore, the hypoxic insult from E12-14 will affect the first nephrons to form in the kidney, but is unlikely to affect the final wave of nephrogenesis post-birth or the process of cessation. In the present study, the dams were housed in the hypoxia chamber from E14.5 until birth. This means that the hypoxia exposure will affect not only nephron formation *in utero*, but possibly nephrogenesis persisting postnatally.

Currently the mechanisms controlling nephron number are unclear, particularly in humans. It is known that multi-potential nephron progenitors surrounding the branching ureteric bud are induced to differentiate into nephrons. These progenitors have a finite lifespan. Therefore, nephron endowment is determined by the balance between nephron progenitor renewal and rate of differentiation. In the mouse, a burst of nephrogenesis from P2 to P4 is followed by cessation, where all remaining mesenchyme is converted to nephrons (Hartman *et al.*, 2007; Rumballe *et al.*, 2011). A study by Brunskill and colleagues (2011) has suggested increased oxygen availability post-birth in the rodent may trigger differentiation of nephron progenitors into nephrons. The fetuses from this study were delivered by Caesarean section at E18.5, resuscitated and cross-fostered, so the effects of parturition were not considered. Additionally, preterm birth (Gubhaju *et al.*, 2011) and cross-fostering (Wlodek *et al.*, 2007) are known to affect renal development. A study by Cebrian and colleagues (2014) addressed the cessation of nephrogenesis using the DTA mouse, a genetic mouse model of renal hypoplasia. They revealed the number of nephron progenitors within the kidney determines final nephron number. This suggests that investigation into the number of nephron progenitors and molecular analyses of genes controlling nephron endowment is warranted.

An intriguing finding by Wlodek and colleagues (2007) was that reduced nephron number in growth-restricted rat pups (born to mothers with poor lactation) was restored simply by cross-fostering onto a healthy mother. This highlights that nephron endowment can be modulated by the early postnatal environment when, in the rodent, nephrogenesis is still occurring. Similarly, extension of the nephrogenic period has also been reported in a sheep model of unilateral fetal nephrectomy (Douglas-Denton *et al.*, 2002). It is possible that female hypoxia-exposed offspring may have improved nutrition relative to males throughout late nephrogenesis, which may prevent nephron number reduction or even restore a currently undetected nephron deficit at an early gestational age. Indeed, our placental studies using this model show placentae from female offspring have made vascular adaptations as well as altered growth factor and nutrient transporter expression. This may improve their nutritional status and oxygen levels *in utero* compared to males. It is important to be reminded that nephrogenesis is complete before birth in humans (Hinchliffe *et al.*, 1991), so studies in rodents may appear to have limited translational applications. However, the question may be asked: can nephrogenesis be stimulated in the immediate postnatal period to improve nephron endowment, particularly in the preterm infant? Improved lactation, for example, would be tempting to consider as a therapy given the findings from Wlodek and colleagues (2007). A growing body of evidence has suggested retinoic acid treatment (the active metabolite of vitamin A) may stimulate nephrogenesis (Vilar *et al.*, 1996; Makrakis *et al.*, 2007), although this is currently of experimental focus only given retinoic acid is teratogenic at high doses.

Disruption to the renin angiotensin system (RAS) have been reported in many developmental programming models (Woods *et al.*, 2001; Moritz *et al.*, 2003; Woods *et al.*, 2005; Grigore *et al.*, 2007; Ojeda *et al.*, 2007a; Cuffe *et al.*, 2014b). Interestingly, perturbations to the RAS are thought to be sex-specific. Indeed, we have previously reported altered mRNA expression of various components of the placental RAS in hypoxia-exposed offspring, but to a greater extent in females compared to males. Similar findings have been reported in a more severe hypoxic insult (10% O₂) from E15.5 to E17.5 in the mouse (Goyal *et al.*, 2011). An altered placental RAS during late gestation may contribute to fetal growth restriction and suboptimal organ development. In the studies by Woods and colleagues, discussed above, the nephron deficit and programmed hypertension in male but not female growth-restricted offspring was associated with suppression of the intrarenal RAS in newborns (Woods *et al.*, 2001; Woods *et al.*, 2005). The intrarenal RAS in the developing kidney warrants investigation in our studies to ascertain whether it is implicated in the sex-related difference in nephron number.

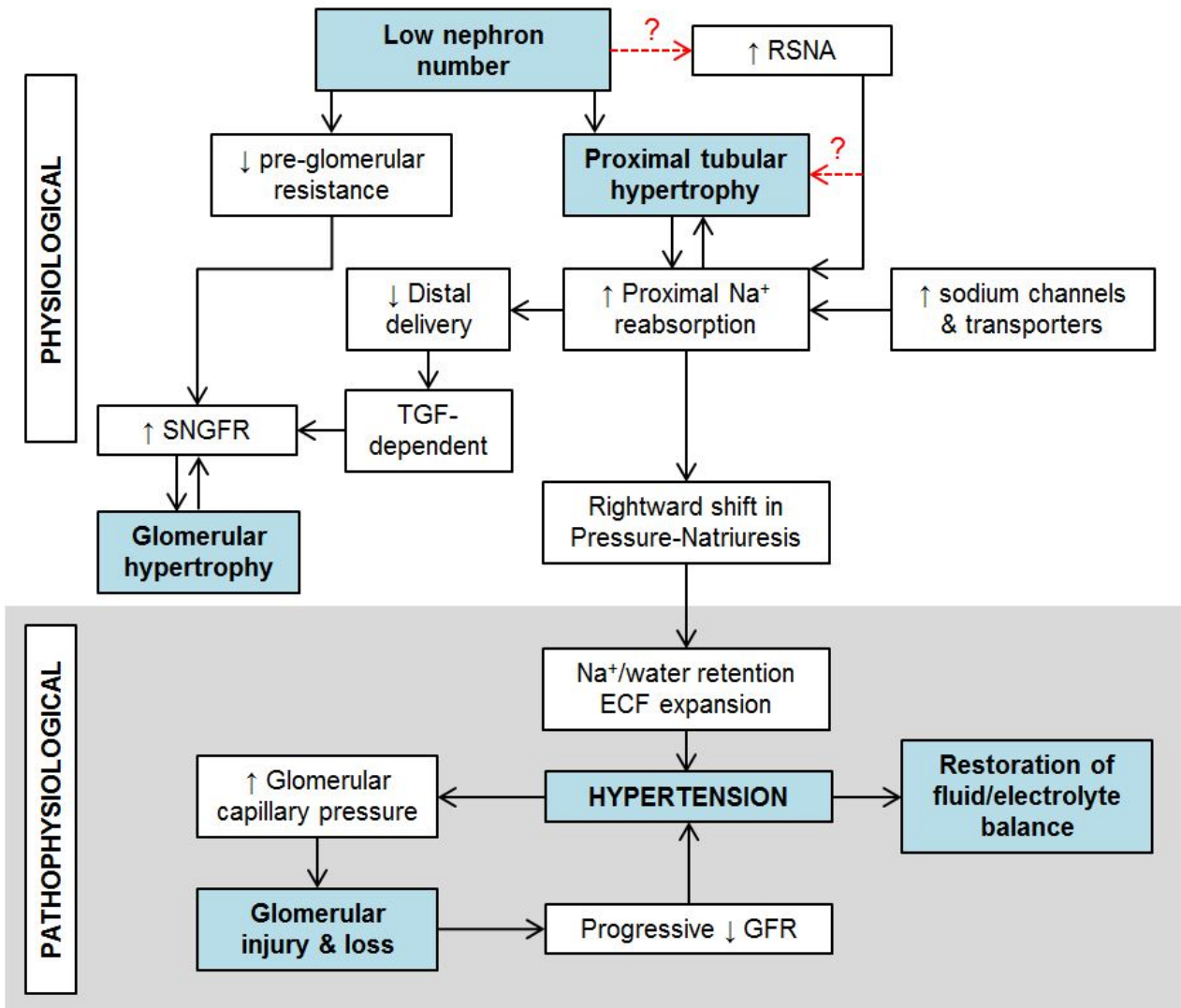


Figure 7.2. Potential mechanisms that may drive increased blood pressure following reduced renal mass.

Concepts in blue represent findings in male hypoxia-exposed offspring in the present study. The physiological adaptations to reduced renal mass (in the present study, a 25% congenital nephron deficit) are an increase in single nephron glomerular filtration rate (SNGFR), driven by decreased pre-glomerular vascular resistance, and proximal tubule hypertrophy. This promotes increased proximal tubule reabsorption of sodium (Na⁺), decreasing sodium delivery to the distal tubule. Tubuloglomerular feedback leads to a further increase in SNGFR, glomerular hypertrophy and ultimately hyperfiltration. Proximal tubule sodium reabsorption may be driven by increased expression of sodium channels and transporters in the proximal tubule and increased renal sympathetic nerve activity (RSNA). This leads to a rightward shift in the pressure-natriuresis curve, expanded extracellular fluid (ECF) volume and elevated mean arterial pressure (hypertension). As described in the Brenner hypothesis, this leads to a vicious cycle of progressive glomerular loss and further worsening of hypertension. Adapted from Fong *et al.*, 2014.

7.7.3 Examining renal function under a water deprivation challenge

The nephron deficiency of 25% in the male hypoxia-exposed offspring is comparatively mild, given many kidney donors continue through life with minimal (or no) signs of renal dysfunction (Fehrman-Ekholm *et al.*, 2001). Therefore, it is unsurprising that urine flow and urinary electrolyte excretion was maintained under basal conditions in these animals. Consequently, we sought to challenge the kidney with water deprivation over a 24-hour period to examine renal concentrating capacity. As observed in Table 7.2, male hypoxia-exposed offspring had a slight reduction in urine osmolality at 4 months of age, which was not present at 2 months. This possibly suggests the age-related decline in urine osmolality observed in control offspring occurred early in the hypoxia-exposed males. Interestingly a subset of male hypoxia-exposed offspring did not reduce urine flow and experienced sodium loss when deprived of water for 24 hours. This is an intriguing finding given the female offspring responded normally to the water deprivation challenge, once again highlighting the susceptibility of male offspring to renal impairments. We have also shown this altered response to a water deprivation challenge was correlated with reduced numbers of AQP2-expressing principal cells in the collecting duct at 12 months of age. Interestingly we observed structural abnormalities of the renal medulla/papilla in juvenile mice, including reduced size and low immunohistochemical expression of AQP2 in hypoxia-exposed male offspring at P21. Referring back to Figure 7.2, it is evident that low nephron number and proximal tubule hypertrophy may contribute to hypertension and signs of CKD. However, our research in *Chapter 6* has shown significant changes in the renal medulla/papilla, which is promising evidence that the renal tubules and collecting ducts can be programmed by developmental insults. We suggest that abnormal development of the renal medulla/papilla may, in conjunction with low nephron number, contribute to increased risk of CKD in later life. The direction of this research into the future will be discussed in detail in the following section.

7.7.4 Measuring renal function in mice

As yet, we have not directly measured GFR in these animals. Traditional techniques to monitor GFR are invasive and can require multiple blood collections in conscious animals. Plasma creatinine, measured using the colorimetric Jaffé method, is routinely used as a marker of renal function. However, this method is known to lack specificity and a large portion of creatinine is known to be excreted by the renal tubules rather than filtered through the glomeruli in mice (Keppler *et al.*, 2007; Eisner *et al.*, 2010). High-performance liquid chromatography (HPLC) is considered a more precise method of creatinine measurement (Keppler *et al.*, 2007), however the process is costly and time consuming.

To examine aspects of renal function, urinary albumin and plasma cystatin C were measured. These are both recognised as predictors of renal function in humans and mice (Dharnidharka *et al.*, 2002; Song *et al.*, 2009), particularly in diabetes (Deckert *et al.*, 1989; Ninomiya *et al.*, 2009). However, prenatal hypoxia had no effect on plasma cystatin C levels. This may suggest GFR is not perturbed in male hypoxia-exposed offspring, although it is possible that renal damage is not severe enough to be detected. This was surprising given the stark glomerulosclerosis and renal injury in these male hypoxia-exposed offspring compared to control counterparts. Recently a transcutaneous method to measure GFR has been developed and validated for use in conscious mice (Schreiber *et al.*, 2012). This technique has several advantages including repeated GFR measurements and ability to be performed in old mice (Schock-Kusch *et al.*, 2013) and could be readily applied to this model in the future.

7.8 Effect of maternal hypoxia on cardiovascular function and structure

7.8.1 Elevated mean arterial pressure

Cardiovascular outcomes at 12 months of age can be observed in Table 7.3. Prenatal hypoxia led to elevated mean arterial pressure in both male and female offspring. In male offspring this was driven by increased diastolic blood pressure, which in turn reduced pulse pressure. In contrast, females had elevations in systolic and diastolic blood pressures, once again highlighting the sexual dimorphic response to prenatal hypoxia in our study. Diastolic blood pressure was elevated in both male and female mice, which is consistent with increased peripheral vascular resistance. The microvascular endothelial dysfunction in these offspring may be a contributing factor (Walton *et al.*, 2016). In contrast to male offspring with isolated diastolic pressure elevation, female hypoxia-exposed offspring presented with elevated systolic and diastolic blood pressure. There is controversy in the literature surrounding the relative importance of systolic and diastolic blood pressures in hypertension. However, in humans, isolated diastolic hypertension is predominant in young males and appears to be antecedent to systolic-diastolic hypertension (Franklin *et al.*, 2005). It is important to note that, while female hypoxia-exposed offspring had higher mean arterial pressure elevated blood pressure compared to control females, male hypoxia-exposed offspring had the greatest elevation in mean arterial pressure when comparing all groups. Based on our studies, we cannot comment on whether a particular sex is at greater risk of cardiovascular events and we suggest further cardiovascular analyses such as echocardiography or the myocardial response to ischaemia-reperfusion injury may shed light on the subject.

To our knowledge we are the first study to examine blood pressure in a prenatal hypoxia model using radiotelemetry, the gold standard of blood pressure measurements in rodents. A study of prenatal hypoxia throughout most of gestation in the rat (E5-20) revealed offspring were normotensive under basal conditions however mean arterial pressure increased under stress (Peyronnet *et al.*, 2002). It is important to note that this study only considered male offspring, and systolic/diastolic blood pressures were not reported. Additionally, blood pressure measurements were performed using aortic cannulas at a relatively young age of 4 months compared to 12 months of age in this thesis. Previously, progressive signs of cardiovascular dysfunction have been reported in rat offspring exposed to prenatal hypoxia, with diastolic dysfunction and pulmonary hypertension emerging between 4 and 12 months of age (Rueda-Clausen *et al.*, 2008). We observed no signs of renal injury in hypoxia-exposed offspring at 4 months of age despite significant pathology present at 12 months, which suggest that ageing is an additional stressor in animals exposed to prenatal hypoxia. An additional cohort of animals is required to assess blood pressure at a younger age to determine if the hypertensive phenotype is present in the juvenile mouse, or only develops with age as previously described in the rat.

Table 7.3. Summary of cardiovascular outcomes in 12-month-old hypoxia-exposed offspring fed the normal-salt and high salt diet. Arrows represent changes in renal function/structure in hypoxia-exposed offspring relative to age-matched control counterparts on the matching normal or high salt diet.

	Hypoxia + Normal Salt		Hypoxia + High Salt	
	Male	Female	Male	Female
<i>Heart pathology</i>				
Pathology score	↑	↑	↑↑	↑
Perivascular fibrosis	↑	↔	↑↑	↔
Interstitial fibrosis	↑	↑	↑↑	↑↑
<i>Blood pressure</i>				
Mean arterial pressure	↑	↑		
Systolic blood pressure	↔	↑		
Diastolic blood pressure	↑	↑		
Pulse pressure	↓	↔		
Heart rate	↔	↔		
Locomotor activity	↓	↔		
Restraint stress response	↔	↔		
<i>Plasma analysis</i>				
Sodium	↔	↔	↔	↔
Chloride	↔	↔	↔	↔
Triglycerides	↔	↔	↔	↔
<i>Microvascular function</i>				
Vasoconstriction to PE	↔	↔	↔	↔
Endothelium-dependent vasodilation (ACh)	↓	↓	↓	↓
Endothelium-independent vasodilation (SNP)	↔	↔	↔	↔
<i>Microvascular structure</i>				
Lumen diameter	↔	↔	↔	↔
Medial CSA	↔	↔	↓	↔
Media:lumen	↔	↔	↔	↔
<i>Microvascular mechanics</i>				
Vascular stiffness	↑	↔	↑↑	↑
<i>Aorta structure</i>				
Elastin content	↓	↓	↓↓	↓↓
Collagen deposition	↑	↔	↑	↑

7.8.2 Vascular function

Impaired endothelium-dependent vasodilation in the mesenteric arteries was observed in both male and female hypoxia-exposed offspring, demonstrating that the endothelium, a vital regulator of vascular tone, is susceptible to *in utero* hypoxia. Endothelial dysfunction is a well-recognised precursor to elevated blood pressure and atherosclerosis in humans, and consequently may be an underlying mechanism for elevated mean arterial pressure in our hypoxia-exposed offspring. Vascular dysfunction is often amplified with ageing, as reported in a similar model of hypoxia in the rat. We have not performed an ontogeny study of microvasculature function as our primary focus was kidney structure and function across life, although it would be an interesting point to consider in future studies. We did not observe any changes in myogenic tone, unlike previous reports in the rat (Hemmings *et al.*, 2005). Notably, vascular outcomes in developmental programming models have been shown to be dependent on the vascular bed studied. Due to the limitation of only one myography in our laboratory, we could only process one artery per animal at once. Consequently, examination of the function and structure of multiple vascular beds per animal was not possible but is a point of consideration in future studies. We did not directly elucidate the mechanisms underlying endothelial dysfunction in this study, but it is possibly due to reduced nitric oxide bioavailability associated with enhanced vascular generation of reactive oxygen species, as previously reported in the rat (Williams *et al.*, 2005b; Giussani *et al.*, 2012).

7.8.3 Vascular stiffening

Vascular stiffening is a major risk factor for cardiovascular dysfunction, and is also associated with low birth weight in humans (Martin *et al.*, 2000; te Velde *et al.*, 2004). The proportion of elastin and collagen content in vessels determines vascular stiffness. We observed a slight decrease in microvascular compliance in male hypoxia-exposed offspring in the absence of vascular remodelling. Furthermore, the aortas of hypoxia-exposed males had increased collagen deposition, and both males and females had reduced elastin content and significant disorganisation of the elastin fibres when examined histologically. This change in elastin content may be developmentally programmed, given synthesis of elastin fibres primarily occurs during fetal and early postnatal life, and is minimal in the adult (Davis, 1995). Elastin content can also be degraded in age by matrix metalloproteinases and elastases produced by inflammatory cells in cardiovascular diseases (Galis & Khatri, 2002).

7.8.4 Role of sex hormones in mediating offspring outcomes

A multitude of developmental programming studies have reported sex differences in renal and cardiovascular outcomes. Commonly, male rodent offspring are more susceptible to developmentally programmed cardiovascular deficits than female offspring when the sexes are directly compared (Dodic *et al.*, 2002; Hemmings *et al.*, 2005; Woods *et al.*, 2005; Ojeda *et al.*, 2007a; Ojeda *et al.*, 2007b). Few, however, have elucidated the mechanisms leading to sex differences. Sex hormones have been highlighted as a critical determinant of blood pressure outcomes, in part through both testosterone (Ojeda *et al.*, 2007b) and estradiol/estrogen modulating the RAS. Estradiol has appears to be protective against hypertension in adult female growth-restricted offspring, in part through increased expression of *Ace2* mRNA (Ojeda *et al.*, 2007a), a RAS component which generates vasoactive peptide angiotensin (1-7) to negatively regulate vasoconstrictor effects of angiotensin II (Ferrario & Chappell, 2004). However, female hypoxia-exposed mice exhibited similar elevations in mean arterial pressure compared to males in the present study. It is possible that this is a function of ageing, as cycle irregularity begins at about 9-12 months of age in female rodents (Lu *et al.*, 1994; Chakraborty & Gore, 2004). After 12 months of age, when we performed blood pressure measurements using radiotelemetry, female rodents become acyclic and enter 'estropause'. Ovulation eventually ceases and estrogen levels decline from this point onwards. This differs to women in the human population, where menopause is associated with a rapid decline in estrogen and loss of ovarian follicles. We did not measure sex hormones or determine cycles in female mice in this thesis, but it would be interesting to see if estropause or declining estrogen levels may be associated with elevated blood pressure in the female hypoxia-exposed offspring. Furthermore, blood pressure and vascular function could be assessed in younger offspring with sex hormones and cyclicity assayed to consider their contributions to observed hypertension and endothelial dysfunction. An alternative approach to understanding the role of androgens in mediating sex differences could involve gonadectomy in hypoxia-exposed offspring as previously performed in IUGR male and female offspring (Ojeda *et al.*, 2007a; Ojeda *et al.*, 2007b).

7.8.5 Renal nerves

Figure 7.2 shows that changes in renal sympathetic activity can affect pressure natriuresis, leading to long-term changes in arterial pressure. We have not examined the role of renal nerves in hypertension in the present studies, however prenatal hypoxia has been associated with sympathetic hyperinnervation in the chick embryo (Rouwet *et al.*, 2002; Tintu *et al.*, 2007). Additionally, hypertension associated with placental insufficiency has been successfully prevented with renal

denervation (Alexander *et al.*, 2005; Ojeda *et al.*, 2007c). This is thought to involve increased sodium transporter expression (Manning *et al.*, 2002b; Dagan *et al.*, 2008), as shown in Figure 7.2. The renal nerves are oft forgotten in developmental programming studies, but constitute a promising pathway for future research in the field.

7.9 The impact of high dietary salt intake

As expected, the high salt diet caused widespread pathological fibrosis in the aorta, heart and kidney in all animals, as previously reported (Henry *et al.*, 1998), and whole-organ hypertrophy of both the heart and kidneys. The kidneys were the most severely affected organ system in male offspring, with moderate to severe interstitial fibrosis, tubular injury and glomerular damage (Table 7.4). These changes were somewhat exacerbated in male hypoxia-exposed offspring fed the high salt diet. Fibrosis in the kidney can lead to renal impairment, which may lead to elevated blood pressure as seen in Figure 7.2. Surprisingly, despite striking renal pathology, the high salt diet did not lead to overt albuminuria in offspring. We did observe reduced cystatin C levels in plasma of all offspring fed the high salt diet compared to the normal salt diet, irrespective of prenatal treatment or sex. This may be indicative of hyperfiltration as previously reported in models of diabetes (Thomas *et al.*, 2005). Notably, salt-induced renal hypertrophy was due in part to elongation of the proximal tubule (*Chapter 5*), which is also a hallmark of diabetes-induced renal hypertrophy. As shown in Figure 7.2, increased proximal tubule surface area increases proximal tubule sodium reabsorption, thereby reducing sodium delivery to the distal tubule. This affects tubuloglomerular feedback in a way that leads to hyperfiltration (Thomas *et al.*, 2005). It is plausible that this is also observed in animals fed the high salt diet, although confirmation using measurements of GFR in these animals is required to confirm this hypothesis.

Table 7.4. Summary of renal outcomes in offspring fed normal salt and high salt diets at 12 months of age

Arrows represent changes in renal function/structure in hypoxia-exposed offspring relative to age-matched control counterparts on the normal or high salt diet.

	Hypoxia + Normal Salt		Hypoxia + High Salt	
	Male	Female	Male	Female
<i>Kidney structure</i>				
Pathology score	↑	↔	↑↑	↔
Perivascular fibrosis	↔	↔	↔	↔
Interstitial fibrosis	↑	↔	↑	↔
Glomerular area	↑	↔	↑↑	↔
<i>Markers of renal function</i>				
Urine flow	↔	↔	↔	↔
Albuminuria	↑	↔	↑	↔
Urinary sodium	↔	↔	↑*	↑*
Urinary chloride	↔	↔	↑↑*	↑*
Urinary potassium	↔	↔	↔	↔
Plasma Cystatin C	↔	↔	↓	↓

* comparing animals fed the normal salt and high salt diet within each sex.

Mild myocardial hypertrophy and salt-induced cardiac interstitial fibrosis was substantially elevated in aged hypoxia-exposed offspring of both sexes, which suggests stiffening and reduced contractility of the myocardium (Biernacka & Frangogiannis, 2011). Substantial fibrosis surrounding intramyocardial arteries was also observed in male offspring fed the high salt diet, which in humans is thought to impair flow through the coronary arteries (Dai *et al.*, 2012). Although microvascular function was unaffected by the high salt diet, marked stiffening of the mesenteric arteries were observed in both male and female offspring exposed to prenatal hypoxia and subsequently fed the high salt diet. Furthermore, increased collagen deposition and substantial degradation of elastin fibres in the aorta in these animals suggests the combination of prenatal hypoxia and a postnatal high salt diet may have tremendous impact on cardiovascular function. Unfortunately we were unable to perform blood pressure measurements in these animals fed the high salt diet due to high mortality from ~10-12 months of age, so we cannot comment on whether the chronic high salt diet exacerbated hypertension in hypoxia-exposed offspring. However, the substantial aggravation of renal and cardiac pathology in these animals, particularly males, suggests this is likely. Future studies should aim to perform telemetry implantation surgeries at a younger age in the CD1 mouse strain. Echocardiography or *ex vivo* measurements of heart function using an isolated perfused heart preparation could be used to determine the impact of salt-induced myocardial hypertrophy and fibrosis.

7.10 Methodology to determine tubule and collecting duct lengths in the mouse kidney

This project arose from a need to examine architecture of renal tubules in response to a congenital nephron deficit, however no method of unbiased stereology had been reported. Furthermore, a systematic analysis of lengths of multiple nephron segments and collecting ducts was lacking. Consequently, a large component of this thesis involved developing a methodology to estimate the lengths of renal tubules and collecting ducts in the mouse kidney. Firstly, length estimation can be performed on thin (~3-5 μm) or thick (~15-30 μm) tissue section. We chose to use thin paraffin sections as this allowed immunohistochemical detection of specific tubule segments and simultaneous estimation of glomerular number in the same kidney using the current gold standard (Cullen-McEwen *et al.*, 2011; Cullen-McEwen *et al.*, 2012). As thin sections are not isotropic, a vertical uniform random sectioning protocol was required (Baddeley *et al.*, 1986; Gokhale, 1990; Wreford, 1995). Thick sections allow the use of isotropic stereology probes, meaning tissue does not have to be randomly oriented. However, time saved by avoiding vertical uniform random sectioning would be lost during the counting procedure as the antibodies used to detect tubule segments were not effective in thick sections. This method has since been applied to estimate

lengths in the rat and sheep kidney (unpublished), although antibodies and the sectioning protocol had to be modified for the larger kidney of the sheep.

This protocol is feasible in terms of time, with volume estimation taking less than 10 minutes per kidney and length estimation of a tubule segment within a kidney possible in 1-2 hours. Tubule lengths in kidneys from younger animals are substantially faster to count than adults due to smaller size. The cycloids test system can be used without a specialised stereology microscope and software, however this would increase analysis time significantly. A caveat to our approach was that it necessitated the use of paraffin embedded tissues and thus our estimates of length are most likely underestimated given that paraffin processing results in significant tissue shrinkage. However, all samples were manually processed at the same time and treated identically so comparisons between groups are unlikely to be significantly affected. It should also be emphasised that tubule identification in the present study relied on identification using immunohistochemistry. In settings of pathology, expression of markers may be diminished to an undetectable level, reducing the validity of this method of tubule identification.

Using this method, we have shown that total distal tubule length in the P21 kidney was similar to total proximal tubule length, which is likely due to both the proximal and distal tubule contributing to glomerulotubular balance in the neonate (Lumbers *et al.*, 1988). The proximal tubule underwent overwhelming elongation from P21 to 12 months of age to become the longest tubule segment in the adult mouse. For the first time in the rodent, we have shown the thin descending limb of Henle and collecting duct both increase in length from P21 to 2 months of age. This occurs in line with progressively increased capacity to concentrate urine during the postnatal period (Stephenson, 1987; Song & Yosypiv, 2012). Unlike the proximal tubule which doubled in length, no growth of the distal tubule, thin descending limb of Henle or collecting duct were observed from 2 to 12 months of age. Whether the further increase in proximal tubule length observed in this 10-month period occurred to maintain the body's extracellular fluid volume (which would now be greater respective to kidney size) is unknown and needs further examination.

Interestingly, however, when mice consumed a high salt diet, an increase in lengths of all nephron segments was observed, albeit only statistically significant for the thin descending limb of Henle, with a tendency for an increase in proximal and distal tubule lengths. As discussed above, proximal tubule hypertrophy is frequently reported in compensatory renal hypertrophy and diabetes-induced renal hypertrophy (Hayslett *et al.*, 1968; Nyengaard *et al.*, 1993). Our data suggests that with pathological renal tubule hypertrophy, tubules other than proximal can increase their length. To our

knowledge, this has not been reported in the literature previously. Interestingly, the only tubule examined that was not affected by the high salt diet was the collecting duct. Given this is the final tubular component before the calyceal system, where only a small proportion (~7%) of the water and sodium is reabsorbed, it may be that compensatory adaptations in the earlier segments are sufficient to compensate for the increased filtered load.

To conclude, this is a robust method to examine renal tubule and collecting duct architecture in the rodent, but also other species. We have successfully applied this methodology to a model of a congenital deficiency of nephrons to reveal increased growth of the proximal and distal tubules.

Scope remains for investigation of other tubule segments, such as the ascending limb of Henle. Lengths of specific components of nephron segments, for example the S1 segment of the proximal tubule, could be estimated if desired, as well as lengths of vasculature within the kidney.

7.11 Limitations and future directions

Our current studies have investigated several aspects regarding maternal hypoxia throughout late gestation on the developmental programming of cardiovascular and renal dysfunction. However, there are many questions that still remain unanswered regarding these studies. The following criticisms and refinements of these studies will assist in directing future projects regarding maternal hypoxia exposure and its effect on disease susceptibility in later life, particularly with regards to the kidney.

7.11.1 Cardiovascular and renal measurements

The animals used for this thesis were raised for multiple experiments and therefore we were unable to perform multiple invasive measures of renal and cardiovascular function. With the advent of the transcutaneous measure of GFR, we are now equipped to perform an ontogeny of GFR across life in combination with 24-hour metabolic cages to collect urine. Unfortunately, a significant limitation in the study is the lack of blood pressure measurements in animals fed the high salt diet. We had an unprecedented number of spontaneous deaths in the CD1 mice beyond ~10 months of age. All animals were sent for analysis by expert pathologist, Dr Helle Bielefeldt-Ohmann, who determined an array of pathologies including, but not limited to, multiple cases of leukaemia, hepatocellular adenomas and nephropathies. Our laboratory had successfully raised C57BL/6 mice to this age, suggesting this is a strain-specific phenomenon. In the future, we suggest an earlier time point for

blood pressure measurements would be optimal for surgical recovery (< 10 months of age). An interesting outcome means our study has examined the ‘survivors’.

7.11.2 Developmental programming of the renal medulla and papilla

Chapter 6 describing the impact of prenatal hypoxia on the structure and function of the renal tubules and collecting ducts has yielded novel and exciting findings. To date, the field of developmental programming has focussed almost entirely on congenital nephron deficits with little thought to the associated nephrons and collecting ducts. We have shown promising preliminary evidence that the renal medulla and papilla too may contribute to increased susceptibility to chronic kidney and cardiovascular disease. However, a set of clearly defined experimental questions, as listed below, need to be addressed before publication:

1. Assessment of renal medulla and papilla volume using unbiased stereology as described in *Chapter 5*. This will be performed in animals at P6, P21, 2 months and 12 months of age using archived samples.
2. Collecting duct cell composition will be examined in kidneys at 2 months of age after postnatal collecting duct elongation has been completed. This will complement cell counts performed in the early postnatal kidney (P6, P21) and the ageing kidney (12 months of age).
3. Estimation of renal tubule lengths in kidneys of hypoxia-exposed offspring at 12 months of age is required to determine whether proximal tubule elongation observed at P21 in hypoxia-exposed male offspring is present at an older age.
4. Using kidneys collected from the aforementioned ages, protein will be extracted from the renal medulla and papilla for Western blot analysis of water, acid-base and electrolyte channels (AQP2, V-ATPase, NKCC2, and NCC). This will determine functional maturity of the kidney in younger animals, and quantify observations made using immunohistochemistry in 12-month-old offspring.
5. Kidneys from juvenile offspring at P6 and P21 will be used for molecular analysis of factors regulating renal papilla development.

The overall outcome of this research will determine, for the first time, whether postnatal renal papilla development can be affected by a common *in utero* perturbation. This study will be enhanced by molecular analyses of factors regulating renal papilla development. Involvement of Wnt/ β -catenin signalling will be of particular interest given its known role in postnatal papilla development (Yu *et al.*, 2009; Li *et al.*, 2014). This is of great interest as our laboratory has previously shown suppression of β -catenin signalling in the kidney following short-term hypoxia exposure at mid-gestation (Wilkinson *et al.*, 2015). The renin-angiotensin system is also important in the development of renal morphology, with disruption of this system leading to impaired kidney development (Niimura *et al.*, 1995; Guron *et al.*, 1998) and, in severe cases, hypoplastic medulla/papilla and an inability to concentrate urine (Tsuchida *et al.*, 1998; Saez *et al.*, 2007). Interaction between Wnt/ β -catenin signalling and the renin-angiotensin system in chronic disease (Zhou & Liu, 2016) further strengthen the rationale to investigate these molecular pathways prior to publication.

One of the advantages of moving to the mouse as a model of developmental programming is the vast array of tools available to help discern molecular mechanisms involved. The GUDMAP database, for example, maps the molecular anatomy of murine kidney development and can be used as a resource to identify potential genes sensitive to changes in renal oxygen tension (Harding *et al.*, 2011). This may help us identify specific targets affected by prenatal hypoxia exposure, contributing to reduced nephron endowment in males, or conversely renal protection in females. We can extend our research further, and examine potential gene-environment interactions which are known to be critical in CAKUT, for example, by using a transgenic mouse model of renal hypoplasia combined with *in utero* hypoxia. The use of GUDMAP, which also details novel transgenic mouse strains, will be highly useful for developing future research (Harding *et al.*, 2011). Our research into programming of the renal tubules and collecting ducts may be extended beyond preclinical animal models to investigate renal papilla development in neonates. This would be possible using pre-acquired ultrasound images, and archived kidney and urine samples. To date focus has been placed almost exclusively on nephrogenesis and final nephron endowment. Very little is known about renal papillae in humans, and no systematic analysis of papillae development has been performed. This research is vital to understand whether common complications during pregnancy, such as hypoxia, may affect renal papilla remodelling and maturation into postnatal life. It is highly likely that perturbed papilla development may contribute to renal dysfunction in adulthood, as does reduced nephron endowment.

7.12 Conclusion

Adequate oxygen tension in the developing fetus is vital for optimal organ development. Episodes of hypoxia during gestation are common, but may have profound implications for fetal growth and adult health outcomes. This thesis has comprehensively shown that prenatal hypoxia exposure in the mouse markedly increased vulnerability to adverse cardiovascular outcomes in adulthood, including elevated mean arterial pressure, vascular endothelial dysfunction and cardiac fibrosis. Prenatal hypoxia also led to reduced glomerular endowment, albuminuria and increased renal pathology severity in male offspring in adulthood. In addition, prenatal hypoxia perturbed the structure of the collecting duct system, possibly contributing to an impaired response to a water deprivation challenge. Notably, female offspring exposed to hypoxia were protected from these adverse renal outcomes. This highlights that sex is an important consideration in models of developmental programming, particularly with regards to the kidney. A postnatal high salt diet combined with prenatal hypoxia exposure led to increased fibrosis in multiple organ systems (kidney, heart and vasculature) and caused marked stiffening of the microvasculature. As high dietary sodium intake is endemic in Western societies, programmed changes to organs in response to *in utero* environments may inadvertently exacerbated by suboptimal dietary choices. Finally, our new methodology to estimate tubule lengths in the kidney can be readily used in future studies examining renal architecture. We encourage future research to consider the importance of the renal tubules and collecting ducts in conjunction with glomerular endowment.

References

- Adelman DM, Gertsenstein M, Nagy A, Simon MC & Maltepe E. (2000). Placental cell fates are regulated in vivo by HIF-mediated hypoxia responses. *Genes Dev* **14**, 3191-3203.
- Al-Odat I, Chen H, Chan YL, Amgad S, Wong MG, Gill A, Pollock C & Saad S. (2014). The impact of maternal cigarette smoke exposure in a rodent model on renal development in the offspring. *PLoS ONE* **9**, e103443.
- Al Rifai M, Silverman MG, Nasir K, Budoff MJ, Blankstein R, Szklo M, Katz R, Blumenthal RS & Blaha MJ. (2015). The association of nonalcoholic fatty liver disease, obesity, and metabolic syndrome, with systemic inflammation and subclinical atherosclerosis: the Multi-Ethnic Study of Atherosclerosis (MESA). *Atherosclerosis* **239**, 629-633.
- Alexander BT, Hendon AE, Ferril G & Dwyer TM. (2005). Renal denervation abolishes hypertension in low-birth-weight offspring from pregnant rats with reduced uterine perfusion. *Hypertension* **45**, 754-758.
- Allison BJ, Brain KL, Niu Y, Kane AD, Herrera EA, Thakor AS, Botting KJ, Cross CM, Itani N, Skeffington KL, Beck C & Giussani DA. (2016). Fetal in vivo continuous cardiovascular function during chronic hypoxia. *J Physiol* **594**, 1247-1264.
- Alwaseel SH & Ashton N. (2009). Prenatal programming of renal sodium handling in the rat. *Clin Sci* **117**, 75-84.
- Alwaseel SH, Barker DJ & Ashton N. (2012). Prenatal programming of renal salt wasting resets postnatal salt appetite, which drives food intake in the rat. *Clin Sci* **122**, 281-288.
- Amri K, Freund N, Vilar J, Merlet-Benichou C & Lelievre-Pegorier M. (1999). Adverse effects of hyperglycemia on kidney development in rats: in vivo and in vitro studies. *Diabetes* **48**, 2240-2245.
- Anderson EA, Sinkey CA, Lawton WJ & Mark AL. (1989). Elevated sympathetic nerve activity in borderline hypertensive humans. Evidence from direct intraneural recordings. *Hypertension* **14**, 177-183.

- Aperia A, Broberger O, Elinder G, Herin P & Zetterstrom R. (1981). Postnatal development of renal function in pre-term and full-term infants. *Acta Paediatr* **70**, 183-187.
- Aperia A, Broberger O, Wikstad I & Wilton P. (1977). Renal growth and function in patients nephrectomized in childhood. *Acta Paediatr* **66**, 185-192.
- Aperia A & Larsson L. (1979). Correlation between fluid reabsorption and proximal tubule ultrastructure during development of the rat kidney. *Acta Physiol Scand* **105**, 11-22.
- Arant BS. (1978). Developmental patterns of renal functional maturation compared in the human neonate. *J Pediatr* **92**, 705-712.
- Armitage JA, Lakasing L, Taylor PD, Balachandran AA, Jensen RI, Dekou V, Ashton N, Nyengaard JR & Poston L. (2005). Developmental programming of aortic and renal structure in offspring of rats fed fat-rich diets in pregnancy. *J Physiol* **565**, 171-184.
- Athukorala C, Rumbold AR, Willson KJ & Crowther CA. (2010). The risk of adverse pregnancy outcomes in women who are overweight or obese. *BMC Pregnancy Childbirth* **10**, 56.
- Atiyeh BA, Dabbagh SS & Gruskin AB. (1996). Evaluation of renal function during childhood. *Pediatr Rev* **17**, 175-180.
- Atkins RC. (2005). The epidemiology of chronic kidney disease. *Kidney Int* **67**, S14-S18.
- Baddeley A, Gundersen H-JG & Cruz-Orive LM. (1986). Estimation of surface area from vertical sections. *J Microsc* **142**, 259-276.
- Bae S, Xiao Y, Li G, Casiano CA & Zhang L. (2003). Effect of maternal chronic hypoxic exposure during gestation on apoptosis in fetal rat heart. *Am J Physiol Heart Circ Physiol* **285**, H983-H990.
- Bagby SP. (2007). Maternal nutrition, low nephron number, and hypertension in later life: pathways of nutritional programming. *J Nutr* **137**, 1066-1072.

- Barcroft J, Barron DH, Cowie AT & Forsham PH. (1940). The oxygen supply of the foetal brain of the sheep and the effect of asphyxia on foetal respiratory movement. *J Physiol* **97**, 338.
- Barker DJ. (1998). In utero programming of chronic disease. *Clin Sci* **95**, 115-128.
- Barker DJ. (2007). The origins of the developmental origins theory. *J Intern Med* **261**, 412-417.
- Barker DJ & Osmond C. (1986). Diet and coronary heart disease in England and Wales during and after the second world war. *J Epidemiol Community Health* **40**, 37-44.
- Barker DJ, Osmond C, Forsen TJ, Kajantie E & Eriksson JG. (2007). Maternal and social origins of hypertension. *Hypertension* **50**, 565-571.
- Barker DJ, Osmond C, Golding J, Kuh D & Wadsworth ME. (1989). Growth in utero, blood pressure in childhood and adult life, and mortality from cardiovascular disease. *BMJ* **298**, 564-567.
- Barker DJP, Gelow J, Thornburg K, Osmond C, Kajantie E & Eriksson JG. (2010). The early origins of chronic heart failure: impaired placental growth and initiation of insulin resistance in childhood. *Eur J Heart Fail* **12**, 819-825.
- Bartelds B, Bel FV, Teitel DF & Rudolph AM. (1993). Carotid, not aortic, chemoreceptors mediate the fetal cardiovascular response to acute hypoxemia in lambs. *Pediatr Res* **34**, 51-55.
- Baum M, Quigley R & Satlin L. (2003). Maturation changes in renal tubular transport. *Curr Opin Nephrol Hypertens* **12**, 521-526.
- Bertino M, Beauchamp GK & Engelman K. (1982). Long-term reduction in dietary sodium alters the taste of salt. *Am J Clin Nutr* **36**, 1134-1144.
- Bianchi G, Fox U, Di Francesco GF, Giovanetti AM & Pagetti D. (1974). Blood pressure changes produced by kidney cross-transplantation between spontaneously hypertensive rats and normotensive rats. *Clin Sci Mol Med* **47**, 435-448.
- Biernacka A & Frangogiannis NG. (2011). Aging and cardiac fibrosis. *Aging Dis* **2**, 158-173.

- Bigham AW, Mao X, Mei R, Brutsaert T, Wilson MJ, Julian CG, Parra EJ, Akey JM, Moore LG & Shriver MD. (2009). Identifying positive selection candidate loci for high-altitude adaptation in Andean populations. *Human genomics* **4**, 79-90.
- Bigham AW, Wilson MJ, Julian CG, Kiyamu M, Vargas E, Leon-Velarde F, Rivera-Chira M, Rodriquez C, Browne VA, Parra E, Brutsaert TD, Moore LG & Shriver MD. (2013). Andean and Tibetan patterns of adaptation to high altitude. *American J Hum Bio* **25**, 190-197.
- Black MJ, Siebel AL, Gezmish O, Moritz KM & Wlodek ME. (2012). Normal lactational environment restores cardiomyocyte number after uteroplacental insufficiency: implications for the preterm neonate. *Am J Physiol Regul Integr Comp Physiol* **302**, R1101-1110.
- Black RE, Allen LH, Bhutta ZA, Caulfield LE, de Onis M, Ezzati M, Mathers C & Rivera J. (2008). Maternal and child undernutrition: global and regional exposures and health consequences. *The Lancet* **371**, 243-260.
- Blackmore HL & Ozanne SE. (2013). Maternal diet-induced obesity and offspring cardiovascular health. *J Dev Orig Health Dis* **4**, 338-347.
- Boorman J, Cunningham J & Mackerras D. (2008). Salt intake from processed food and discretionary use in Australia. *FSANZ*. Australia.
- Boulware LE, Jaar BG, Tarver-Carr ME, Brancati FL & Powe NR. (2003). Screening for proteinuria in US adults: a cost-effectiveness analysis. *JAMA* **290**, 3101-3114.
- Brenner BM & Chertow GM. (1994). Congenital oligonephropathy and the etiology of adult hypertension and progressive renal injury. *Am J Kidney Dis* **23**, 171-175.
- Brenner BM, Garcia DL & Anderson S. (1988). Glomeruli and blood pressure. Less of one, more the other? *Am J Hypertens* **1**, 335-347.
- Brenner BM & Mackenzie HS. (1997). Nephron mass as a risk factor for progression of renal disease. *Kidney Int Suppl* **63**, S124-127.

- Bridgewater D, Cox B, Cain J, Lau A, Athaide V, Gill PS, Kuure S, Sainio K & Rosenblum ND. (2008). Canonical WNT/beta-catenin signaling is required for ureteric branching. *Dev Biol* **317**, 83-94.
- Brunskill EW, Lai HL, Jamison DC, Potter SS & Patterson LT. (2011a). Microarrays and RNA-Seq identify molecular mechanisms driving the end of nephron production. *BMC Dev Biol* **11**, 1-12.
- Burke C, Sinclair K, Cowin G, Rose S, Pat B, Gobe G & Colditz P. (2006). Intrauterine growth restriction due to uteroplacental vascular insufficiency leads to increased hypoxia-induced cerebral apoptosis in newborn piglets. *Brain Res* **1098**, 19-25.
- Burton GJ, Reshetnikova OS, Milovanov AP & Teleshova OV. (1996). Stereological evaluation of vascular adaptations in human placental villi to differing forms of hypoxic stress. *Placenta* **17**, 49-55.
- Camm EJ, Hansell JA, Kane AD, Herrera EA, Lewis C, Wong S, Morrell NW & Giussani DA. (2010). Partial contributions of developmental hypoxia and undernutrition to prenatal alterations in somatic growth and cardiovascular structure and function. *Am J Obstet Gynecol* **203**, 495.e424-495.e434.
- Camm EJ, Martin-Gronert MS, Wright NL, Hansell JA, Ozanne SE & Giussani DA. (2011). Prenatal hypoxia independent of undernutrition promotes molecular markers of insulin resistance in adult offspring. *FASEB J* **25**, 420-427.
- Cannata DJ, Ireland Z, Dickinson H, Snow RJ, Russell AP, West JM & Walker DW. (2010). Maternal creatine supplementation from mid-pregnancy protects the diaphragm of the newborn spiny mouse from intrapartum hypoxia-induced damage. *Pediatr Res* **68**, 393-398.
- Carmeliet P & Collen D. (1998). Vascular development and disorders: molecular analysis and pathogenic insights. *Kidney Int* **53**, 1519-1549.

- Casari G, Barlassina C, Cusi D, Zagato L, Muirhead R, Righetti M, Nembri P, Amar K, Gatti M & Macciardi F. (1995). Association of the α -adducin locus with essential hypertension. *Hypertension* **25**, 320-326.
- Cebrian C, Asai N, D'Agati V & Costantini F. (2014). The number of fetal nephron progenitor cells limits ureteric branching and adult nephron endowment. *Cell Reports* **7**, 127-137.
- Cebrian C, Borodo K, Charles N & Herzlinger DA. (2004). Morphometric index of the developing murine kidney. *Dev Dyn* **231**, 601-608.
- Chadban SJ, Briganti EM, Kerr PG, Dunstan DW, Welborn TA, Zimmet PZ & Atkins RC. (2003). Prevalence of kidney damage in Australian adults: the AusDiab kidney study. *J Am Soc Nephrol* **14**, S131-S138.
- Chakraborty TR & Gore AC. (2004). Aging-related changes in ovarian hormones, their receptors, and neuroendocrine function. *Exp Biol Med* **229**, 977-987.
- Chen W, Chen W, Wang H, Dong X, Liu Q, Mao H, Tan J, Lin J, Zhou F & Luo N. (2009). Prevalence and risk factors associated with chronic kidney disease in an adult population from southern China. *Nephrol Dial Transplant* **24**, 1205-1212.
- Chen YW, Chenier I, Tran S, Scotcher M, Chang SY & Zhang SL. (2010). Maternal diabetes programs hypertension and kidney injury in offspring. *Pediatr Nephrol* **25**, 1319-1329.
- Chin HJ, Ahn JM, Na KY, Chae D-w, Lee TW, Heo NJ & Kim S. (2010). The effect of the World Kidney Day campaign on the awareness of chronic kidney disease and the status of risk factors for cardiovascular disease and renal progression. *Nephrol Dial Transplant* **25**, 413-419.
- Chow C, Cardona M, Raju PK, Iyengar S, Sukumar A, Raju R, Colman S, Madhav P, Raju R & Reddy KS. (2007). Cardiovascular disease and risk factors among 345 adults in rural India—the Andhra Pradesh Rural Health Initiative. *Int J Cardiol* **116**, 180-185.

- Clifton VL, Engel P, Smith R, Gibson P, Brinsmead M & Giles WB. (2009). Maternal and neonatal outcomes of pregnancies complicated by asthma in an Australian population. *Aust NZ J Obstet Gynaecol* **49**, 619-626.
- Cohen WR, Piasecki GJ & Jackson BT. (1982). Plasma catecholamines during hypoxemia in fetal lamb. *Am J Physiol Regul Integr Comp Physiol* **243**, R520-R525.
- Cohn HE, Sacks EJ, Heymann MA & Rudolph AM. (1974). Cardiovascular responses to hypoxemia and acidemia in fetal lambs. *Am J Obstet Gynecol* **120**, 817-824.
- Corstius HB, Zimanyi MA, Maka N, Herath T, Thomas W, van der Laarse A, Wreford NG & Black MJ. (2005). Effect of intrauterine growth restriction on the number of cardiomyocytes in rat hearts. *Pediatr Res* **57**, 796-800.
- Cousins L. (1999). Fetal oxygenation, assessment of fetal well-being, and obstetric management of the pregnant patient with asthma. *J Allergy Clin Immunol* **103**, S343-349.
- Cowley AW. (1992). Long-term control of arterial blood pressure. *Physiol Rev* **72**, 231-300.
- Crowe C, Dandekar P, Fox M, Dhingra K, Bennet L & Hanson MA. (1995). The effects of anaemia on heart, placenta and body weight, and blood pressure in fetal and neonatal rats. *J Physiol* **488**, 515-519.
- Cuffe J, Walton S, Singh R, Spiers J, Bielefeldt-Ohmann H, Wilkinson L, Little M & Moritz K. (2014a). Mid-to late term hypoxia in the mouse alters placental morphology, glucocorticoid regulatory pathways and nutrient transporters in a sex-specific manner. *J Physiol* **592**, 3127-3141.
- Cuffe J, Walton S, Steane S, Singh R, Simmons D & Moritz K. (2014b). The effects of gestational age and maternal hypoxia on the placental renin angiotensin system in the mouse. *Placenta* **35**, 953-961.
- Cuffe, J.S.M., Walton, S.L., & Moritz, K.M. (2015). The developmental origins of renal dysfunction. Editor: Rosenfeld C. In *The Epigenome and Developmental Origins of Health and Disease*, pp. 291-314. Academic Press, Elsevier, USA.

- Cullen-McEwen L, Sutherland MR & Black MJ. (2016). The Human Kidney: Parallels in Structure, Spatial Development, and Timing of Nephrogenesis. Editor: Little, MH. In *Kidney Development, Disease, Repair and Regeneration*, pp. 27-40. Academic Press, Elsevier, USA.
- Cullen-McEwen LA, Armitage JA, Nyengaard JR, Moritz KM & Bertram JF. (2011). A design-based method for estimating glomerular number in the developing kidney. *Am J Physiol Renal Physiol* **300**, F1448-1453.
- Cullen-McEwen LA, Douglas-Denton RN & Bertram JF. (2012). Estimating total nephron number in the adult kidney using the physical disector/fractionator combination. *Methods Mol Biol* **886**, 333-350.
- Cullen-McEwen LA, Kett MM, Dowling J, Anderson WP & Bertram JF. (2003). Nephron number, renal function, and arterial pressure in aged GDNF heterozygous mice. *Hypertension* **41**, 335-340.
- Curtis JJ, Luke RG, Dustan HP, Kashgarian M, Whelchel JD, Jones P & Diethelm AG. (1983). Remission of essential hypertension after renal transplantation. *N Engl J Med* **309**, 1009-1015.
- Dagan A, Gattineni J, Cook V & Baum M. (2007). Prenatal programming of rat proximal tubule Na⁺/H⁺ exchanger by dexamethasone. *Am J Physiol Regul Integr Comp Physiol* **292**, R1230-R1235.
- Dagan A, Kwon HM, Dwarakanath V & Baum M. (2008). Effect of renal denervation on prenatal programming of hypertension and renal tubular transporter abundance. *Am J Physiol Renal Physiol* **295**, F29-34.
- Dahl LK, Heine M & Thompson K. (1974). Genetic influence of the kidneys on blood pressure. Evidence from chronic renal homografts in rats with opposite predispositions to hypertension. *Circ Res* **40**, 94-101.

- Dai Z, Aoki T, Fukumoto Y & Shimokawa H. (2012). Coronary perivascular fibrosis is associated with impairment of coronary blood flow in patients with non-ischemic heart failure. *J Cardiol* **60**, 416-421.
- Danaei G, Ding EL, Mozaffarian D, Taylor B, Rehm J, Murray CJL & Ezzati M. (2009). The preventable causes of death in the United States: comparative risk assessment of dietary, lifestyle, and metabolic risk factors. *PLoS Med* **6**, e1000058.
- Davis EC. (1995). Elastic lamina growth in the developing mouse aorta. *J Histochem Cytochem* **43**, 1115-1123.
- de Grauw TJ, Myers RE & Scott WJ. (1986). Fetal growth retardation in rats from different levels of hypoxia. *Biol Neonate* **49**, 85-89.
- de Jong JC, van der Vliet WA, van den Heuvel LP, Willems PH, Knoers NV & Bindels RJ. (2002). Functional expression of mutations in the human NaCl cotransporter: evidence for impaired routing mechanisms in Gitelman's syndrome. *J Am Soc Nephrol* **13**, 1442-1448.
- De Rooij S, Painter R, Roseboom T, Phillips D, Osmond C, Barker D, Tanck M, Michels R, Bossuyt P & Bleker O. (2006). Glucose tolerance at age 58 and the decline of glucose tolerance in comparison with age 50 in people prenatally exposed to the Dutch famine. *Diabetologia* **49**, 637-643.
- Deane HW & Masson GMC. (1951). Adrenal cortical changes in rats with various types of experimental hypertension. *J Clin Endocrinol Metab* **11**, 193-208.
- Deckert T, Feldt-Rasmussen B, Borch-Johnsen K, Jensen T & Kofoed-Enevoldsen A. (1989). Albuminuria reflects widespread vascular damage. *Diabetologia* **32**, 219-226.
- Dharnidharka VR, Kwon C & Stevens G. (2002). Serum cystatin C is superior to serum creatinine as a marker of kidney function: a meta-analysis. *Am J Kidney Dis* **40**, 221-226.
- Dickinson H, Walker DW, Cullen-McEwen L, Wintour EM & Moritz K. (2005). The spiny mouse (*Acomys cahirinus*) completes nephrogenesis before birth. *Am J Physiol Renal Physiol* **289**, F273-279.

- Dickinson H, Walker DW, Wintour EM & Moritz K. (2007). Maternal dexamethasone treatment at midgestation reduces nephron number and alters renal gene expression in the fetal spiny mouse. *Am J Physiol Regul Integr Comp Physiol* **292**, R453-461.
- Ding XX, Wu YL, Xu SJ, Zhang SF, Jia XM, Zhu RP, Hao JH & Tao FB. (2014). A systematic review and quantitative assessment of sleep-disordered breathing during pregnancy and perinatal outcomes. *Sleep Breath* **18**, 703-713.
- Dodic M, Abouantoun T, O'Connor A, Wintour EM & Moritz KM. (2002). Programming effects of short prenatal exposure to dexamethasone in sheep. *Hypertension* **40**, 729-734.
- Domingo C, Latorre E, Mirapeix RM & Abad J. Snoring, obstructive sleep apnea syndrome, and pregnancy. *Int J Gynaecol Obstet* **93**, 57-59.
- Douglas-Denton R, Moritz KM, Bertram JF & Wintour EM. (2002). Compensatory renal growth after unilateral nephrectomy in the ovine fetus. *J Am Soc Nephrol* **13**, 406-410.
- Du Cailar G, Ribstein J, Daures JP & Mimran A. (1992). Sodium and left ventricular mass in untreated hypertensive and normotensive subjects. *Am J Physiol* **263**, H177-181.
- Edelstone DI., Rudolph AM & Heymann MA. (1980). Effects of hypoxemia and decreasing umbilical flow liver and ductus venosus blood flows in fetal lambs. *Am J Phys Heart Circ Phys* **238**, H656-H663.
- Edwards LJ & McMillen IC. (2001). Maternal undernutrition increases arterial blood pressure in the sheep fetus during late gestation. *J Physiol* **533**, 561-570.
- Eisner C, Faulhaber-Walter R, Wang Y, Leelahavanichkul A, Yuen PS, Mizel D, Star RA, Briggs JP, Levine M & Schnermann J. (2010). Major contribution of tubular secretion to creatinine clearance in mice. *Kidney Int* **77**, 519-526.
- Ellery SJ, Ireland Z, Kett MM, Snow R, Walker DW & Dickinson H. (2013). Creatine pretreatment prevents birth asphyxia-induced injury of the newborn spiny mouse kidney. *Pediatr Res* **73**, 201-208.

- Eriksson J, Forsén T, Tuomilehto J, Osmond C & Barker D. (2000). Fetal and childhood growth and hypertension in adult life. *Hypertension* **36**, 790-794.
- Eriksson JG, Forsen T, Tuomilehto J, Osmond C & Barker DJ. (2001). Early growth and coronary heart disease in later life: longitudinal study. *BMJ* **322**, 949-953.
- Eriksson JG, Forsén T, Tuomilehto J, Winter PD, Osmond C & Barker DJP. (1999). Catch-up growth in childhood and death from coronary heart disease: longitudinal study. *BMJ* **318**, 427-431.
- Evans LC, Liu H, Pinkas GA & Thompson LP. (2012). Chronic hypoxia increases peroxynitrite, MMP9 expression, and collagen accumulation in fetal guinea pig hearts. *Pediatr Res* **71**, 25-31.
- Ezzati M, Lopez AD, Rodgers A, Vander Hoorn S & Murray CJL. (2002). Selected major risk factors and global and regional burden of disease. *Lancet* **360**, 1347-1360.
- Ezzati M & Riboli E. (2013). Behavioral and dietary risk factors for noncommunicable diseases. *N Engl J Med* **369**, 954-964.
- Fehrman-Ekholm I, Dunér F, Brink B, Tydén G & Elinder C-G. (2001). No evidence of accelerated loss of kidney function in living kidney donors: results from a cross-sectional follow-up. *Transplantation* **72**, 444-449.
- Feldser D, Agani F, Iyer NV, Pak B, Ferreira G & Semenza GL. (1999). Reciprocal positive regulation of hypoxia-inducible factor 1alpha and insulin-like growth factor 2. *Cancer Res* **59**, 3915-3918.
- Ferrario CM & Chappell MC. (2004). Novel angiotensin peptides. *Cell Mol Life Sci* **61**, 2720-2727.
- Fields NG, Yuan BX & Leenen FH. (1991). Sodium-induced cardiac hypertrophy. Cardiac sympathetic activity versus volume load. *Circ Res* **68**, 745-755.

- Foley RN, Parfrey PS, Harnett JD, Kent GM, Martin CJ, Murray DC & Barre PE. (1995). Clinical and echocardiographic disease in patients starting end-stage renal disease therapy. *Kidney Int* **47**, 186-192.
- Foley RN, Parfrey PS & Sarnak MJ. (1998). Clinical epidemiology of cardiovascular disease in chronic renal disease. *Am J Kidney Dis* **32**, S112-119.
- Fong D, Denton KM, Moritz KM, Evans R & Singh RR. (2014). Compensatory responses to nephron deficiency: adaptive or maladaptive? *Nephrology* **19**, 119-128.
- Forsén T, Eriksson JG, Tuomilehto J, Osmond C & Barker DJP. (1999). Growth in utero and during childhood among women who develop coronary heart disease: longitudinal study. *BMJ* **319**, 1403-1407.
- Franklin SS, Pio JR, Wong ND, Larson MG, Leip EP, Vasan RS & Levy D. (2005). Predictors of new-onset diastolic and systolic hypertension: the Framingham heart study. *Circulation* **111**, 1121-1127.
- Fung AM, Wilson DL, Lappas M, Howard M, Barnes M, O'Donoghue F, Tong S, Esdale H, Fleming G & Walker SP. (2013). Effects of maternal obstructive sleep apnoea on fetal growth: a prospective cohort study. *PLoS ONE* **8**, e68057.
- Furukawa K, Ninomiya I, Shimizu J, Wada T & Matsuura Y. (1997). Renal sympathetic nerve activity and the weight of the remaining kidney in unilateral nephrectomized rats. *J Auton Nerv Syst* **63**, 91-100.
- Galandrin S, Denis C, Boularan C, Marie J, M'Kadmi C, Pilette C, Dubroca C, Nicaise Y, Seguelas M-H & N'Guyen D. (2016). Cardioprotective Angiotensin-(1-7) Peptide Acts as a Natural-Biased Ligand at the Angiotensin II Type 1 Receptor. *Hypertension*, DOI:116.08118.
- Galis ZS & Khatri JJ. (2002). Matrix metalloproteinases in vascular remodeling and atherogenesis: the good, the bad, and the ugly. *Circ Res* **90**, 251-262.

- Gezmish O, Tare M, Parkington HC, Morley R, Porrello ER, Bubb KJ & Black MJ. (2010). Maternal vitamin D deficiency leads to cardiac hypertrophy in rat offspring. *Reprod Sci* **17**, 168-176.
- Gilbert JS & Nijland MJ. (2008). Sex differences in the developmental origins of hypertension and cardiorenal disease. *Am J Physiol Regul Integr Comp Physiol* **295**, R1941-R1952.
- Gimonet V, Bussieres L, Medjebeur AA, Gasser B, Lelongt B & Laborde K. (1998). Nephrogenesis and angiotensin II receptor subtypes gene expression in the fetal lamb. *Am J Physiol Renal Physiol* **274**, F1062-F1069.
- Girgis S, Neal B, Prescott J, Prendergast J, Dumbrell S, Turner C & Woodward M. (2003). A one-quarter reduction in the salt content of bread can be made without detection. *Eur J Clin Nutr* **57**, 616-620.
- Giussani DA. (2016). The fetal brain sparing response to hypoxia: physiological mechanisms. *J Physiol* **594**, 1215-1230.
- Giussani DA, Camm EJ, Niu Y, Richter HG, Blanco CE, Gottschalk R, Blake EZ, Horder KA, Thakor AS & Hansell JA. (2012). Developmental programming of cardiovascular dysfunction by prenatal hypoxia and oxidative stress. *PLoS one* **7**, e31017.
- Giussani DA, Phillips PS, Anstee S & Barker DJ. (2001). Effects of altitude versus economic status on birth weight and body shape at birth. *Pediatr Res* **49**, 490-494.
- Giussani DA, Salinas CE, Villena M & Blanco CE. (2007). The role of oxygen in prenatal growth: studies in the chick embryo. *J Physiol* **585**, 911-917.
- Gleed RD & Mortola JP. (1991). Ventilation in newborn rats after gestation at simulated high altitude. *J Appl Physiol* **70**, 1146-1151.
- Gluckman PD & Hanson MA. (2006). The developmental origins of health and disease. In *Early Life Origins of Health and Disease*, pp. 1-7. Springer.

- Godfrey KM, Redman CW, Barker DJ & Osmond C. (1991). The effect of maternal anaemia and iron deficiency on the ratio of fetal weight to placental weight. *Br J Obstet Gynaecol* **98**, 886-891.
- Gokhale A. (1990). Unbiased estimation of curve length in 3-D using vertical slices. *J Microsc* **159**, 133-141.
- Gonzalez-Rodriguez P, Jr., Tong W, Xue Q, Li Y, Hu S & Zhang L. (2013). Fetal hypoxia results in programming of aberrant angiotensin ii receptor expression patterns and kidney development. *Int J Med Sci* **10**, 532-538.
- Goyal R, Lister R, Leitzke A, Goyal D, Gheorghe CP & Longo LD. (2011). Antenatal maternal hypoxic stress: adaptations of the placental renin-angiotensin system in the mouse. *Placenta* **32**, 134-139.
- Gray SP, Cullen-McEwen LA, Bertram JF & Moritz KM. (2012). Mechanism of alcohol-induced impairment in renal development: Could it be reduced by retinoic acid? *Clin Exp Pharmacol Physiol* **39**, 807-813.
- Gray SP, Denton KM, Cullen-McEwen L, Bertram JF & Moritz KM. (2010). Prenatal exposure to alcohol reduces nephron number and raises blood pressure in progeny. *J Am Soc Nephrol* **21**, 1891-1902.
- Gray SP, Kenna K, Bertram JF, Hoy WE, Yan EB, Bocking AD, Brien JF, Walker DW, Harding R & Moritz KM. (2008). Repeated ethanol exposure during late gestation decreases nephron endowment in fetal sheep. *Am J Physiol Regul Integr Comp Physiol* **295**, R568-574.
- Grigore D, Ojeda NB, Robertson EB, Dawson AS, Huffman CA, Bourassa EA, Speth RC, Brosnihan KB & Alexander BT. (2007). Placental insufficiency results in temporal alterations in the renin angiotensin system in male hypertensive growth restricted offspring. *Am J Physiol Regul Integr Comp Physiol* **293**, R804-811.
- Gubhaju L, Sutherland MR & Black MJ. (2011). Preterm birth and the kidney: implications for long-term renal health. *Reprod Sci* **18**, 322-333.

- Gurich RW & Beach RE. (1994). Abnormal regulation of renal proximal tubule Na (+)-K (+)-ATPase by G proteins in spontaneously hypertensive rats. *Am J Physiol Renal Physiol* **267**, F1069-F1075.
- Guron G, Sundelin B, Wickman A & Friberg P. (1998). Angiotensin-converting enzyme inhibition in piglets induces persistent renal abnormalities. *Clin Exp Pharmacol Physiol* **25**, 88-91.
- Guyton AC. (1990). The surprising kidney-fluid mechanism for pressure control – its infinite gain! *Hypertension* **16**, 725-730.
- Guyton AC, Coleman TG, Cowley AW, Scheel KW, Manning RD & Norman RA. (1972). Arterial pressure regulation: overriding dominance of the kidneys in long-term regulation and in hypertension. *Am J Med* **52**, 584-594.
- Hadi HA, Carr CS & Suwaidi JA. (2005). Endothelial dysfunction: cardiovascular risk factors, therapy, and outcome. *Vasc Health Risk Manag* **1**, 183.
- Hadi MW, Thengker A, Marwali K, Lim H & Lukito AA. (2015). Correlation between Types of Left Ventricular Hypertrophy and Chronic Kidney Disease in Hypertensive Heart Disease. *J Hypertension* **33**, e42-e43.
- Hajjar, I., et al. (2016). "Roles of arterial stiffness and blood pressure in hypertension-associated cognitive decline in healthy adults." *Hypertension* **67**(1): 171-175.
- Halliwell B & Gutteridge JM. (1999). *Free radicals in biology and medicine*. Oxford University Press, USA.
- Harding SD, Armit C, Armstrong J, Brennan J, Cheng Y, Haggarty B, Houghton D, Lloyd-MacGilp S, Pi X, Roochun Y, Sharghi M, Tindal C, McMahon AP, Gottesman B, Little MH, Georgas K, Aronow BJ, Potter SS, Brunskill EW, Southard-Smith EM, Mendelsohn C, Baldock RA, Davies JA & Davidson D. (2011). The GUDMAP database--an online resource for genitourinary research. *Development* **138**, 2845-2853.
- Hartman HA, Lai HL & Patterson LT. (2007). Cessation of renal morphogenesis in mice. *Dev Biol* **310**, 379-387.

- Hayslett JP, Kashgarian M & Epstein FH. (1968). Functional correlates of compensatory renal hypertrophy. *J Clin Invest* **47**, 774.
- Hemmings DG, Williams SJ & Davidge ST. (2005). Increased myogenic tone in 7-month-old adult male but not female offspring from rat dams exposed to hypoxia during pregnancy. *Am J Physiol Heart Circ Physiol* **289**, H674-H682.
- Henry C, Burrell LM, Black MJ, Wu LL, Dilley RJ, Cooper ME & Johnston CI. (1998). Salt induces myocardial and renal fibrosis in normotensive and hypertensive rats. *Circulation* **98**, 2621-2628.
- Herzog CA, Ma JZ & Collins AJ. (1998). Poor long-term survival after acute myocardial infarction among patients on long-term dialysis. *N Engl J Med* **339**, 799-805.
- Hinchliffe S, Sargent P, Howard C, Chan Y & Van Velzen D. (1991). Human intrauterine renal growth expressed in absolute number of glomeruli assessed by the disector method and Cavalieri principle. *Lab Invest* **64**, 777-784.
- Hokanson JE & Austin MA. (1996). Plasma triglyceride level is a risk factor for cardiovascular disease independent of high-density lipoprotein cholesterol level: a meta-analysis of population-based prospective studies. *J Cardiovasc Risk* **3**, 213-219.
- Hoppe CC, Evans RG, Bertram JF & Moritz KM. (2007a). Effects of dietary protein restriction on nephron number in the mouse. *Am J Physiol Regul Integr Comp Physiol* **292**, R1768-1774.
- Hoppe CC, Evans RG, Moritz KM, Cullen-McEwen LA, Fitzgerald SM, Dowling J & Bertram JF. (2007b). Combined prenatal and postnatal protein restriction influences adult kidney structure, function, and arterial pressure. *Am J Physiol Regul Integr Comp Physiol* **292**, R462-469.
- Hornbein T & Schoene R. (2001). *High Altitude: An Exploration of Human Adaptation*. Taylor & Francis, USA.

- Hoy WE, Hughson MD, Singh GR, Douglas-Denton R & Bertram JF. (2006). Reduced nephron number and glomerulomegaly in Australian Aborigines: a group at high risk for renal disease and hypertension. *Kidney Int* **70**, 104-110.
- Hoy WE, Rees M, Kile E, Mathews JD & Wang Z. (1999). A new dimension to the Barker hypothesis: low birthweight and susceptibility to renal disease. *Kidney Int* **56**, 1072-1077.
- Hoy WE, White AV, Tipiloura B, Singh GR, Sharma S, Bloomfield H, Swanson CE, Dowling A & McCredie DA. (2016). The influence of birthweight, past poststreptococcal glomerulonephritis and current body mass index on levels of albuminuria in young adults: the multideterminant model of renal disease in a remote Australian Aboriginal population with high rates of renal disease and renal failure. *Nephrol Dial Transplant* **31**, 971-977.
- Huch A, Huch R, Schneider H & Rooth G. (1977). Continuous transcutaneous monitoring of fetal oxygen tension during labour. *Br J Obstet Gynaecol* **84 Suppl 1**, 1-39.
- Huetteman DA & Bogie H. (2009). Direct blood pressure monitoring in laboratory rodents via implantable radio telemetry. *Methods Mol Biol* **573**, 57-73.
- Hughson M, Douglas-Denton R, Bertram J & Hoy W. (2006). Hypertension, glomerular number, and birth weight in African Americans and white subjects in the southeastern United States. *Kidney Int* **69**, 671-678.
- Hughson M, Farris AB, 3rd, Douglas-Denton R, Hoy WE & Bertram JF. (2003). Glomerular number and size in autopsy kidneys: the relationship to birth weight. *Kidney Int* **63**, 2113-2122.
- Hutter D, Kingdom J & Jaeggi E. (2010). Causes and mechanisms of intrauterine hypoxia and its impact on the fetal cardiovascular system: a review. *Int J Pediatr* **2010**, 401323.
- Ireland Z, Castillo-Melendez M, Dickinson H, Snow R & Walker DW. (2011). A maternal diet supplemented with creatine from mid-pregnancy protects the newborn spiny mouse brain from birth hypoxia. *Neuroscience* **194**, 372-379.

- Ireland Z, Dickinson H, Snow R & Walker DW. (2008). Maternal creatine: does it reach the fetus and improve survival after an acute hypoxic episode in the spiny mouse (*Acomys cahirinus*)? *Am J Obstet Gynecol* **198**, 431 e431-436.
- Iulita MF & Girouard H. (2016). Treating Hypertension to Prevent Cognitive Decline and Dementia: Re-Opening the Debate. p. 1-27. Springer US, Boston, MA.
- Iwamoto HS & Rudolph AM. (1985). Metabolic responses of the kidney in fetal sheep: effect of acute and spontaneous hypoxemia. *Am J Physiol Renal Physiol* **249**, F836-F841.
- Iwamoto HS, Rudolph AM, Mirkin BL & Keil LC. (1983). Circulatory and humoral responses of sympathectomized fetal sheep to hypoxemia. *Am J Physiol Heart Circ Physiol* **245**, H767-H772.
- Izci B, Martin SE, Dundas KC, Liston WA, Calder AA & Douglas NJ. (2005). Sleep complaints: snoring and daytime sleepiness in pregnant and pre-eclamptic women. *Sleep Medicine* **6**, 163-169.
- Jackson CM, Alexander BT, Roach L, Haggerty D, Marbury DC, Hutchens ZM, Flynn ER & Maric-Bilkan C. (2012). Exposure to maternal overnutrition and a high-fat diet during early postnatal development increases susceptibility to renal and metabolic injury later in life. *Am J Physiol Renal Physiol* **302**, 7.
- Jensen A, Garnier Y & Berger R. (1999). Dynamics of fetal circulatory responses to hypoxia and asphyxia. *Eur J Obstet Gynaecol Reprod Biol* **84**, 155-172.
- Jha V, Garcia-Garcia G, Iseki K, Li Z, Naicker S, Plattner B, Saran R, Wang AY-M & Yang C-W. (2013). Chronic kidney disease: global dimension and perspectives. *Lancet* **382**, 260-272.
- Julian CG, Vargas E, Armaza JF, Wilson MJ, Niermeyer S & Moore LG. (2007). High-altitude ancestry protects against hypoxia-associated reductions in fetal growth. *Arch Dis Child Fetal Neonatal Ed* **92**, F372-377.

- Kadyrov M, Schmitz C, Black S, Kaufmann P & Huppertz B. (2003). Pre-eclampsia and maternal anaemia display reduced apoptosis and opposite invasive phenotypes of extravillous trophoblast. *Placenta* **24**, 540-548.
- Kadyrov N, Kosanke G, Kingdom J & Kaufmann P. (1998). Increased fetoplacental angiogenesis during first trimester in anaemic women. *The Lancet* **352**, 1747-1749.
- Kamitomo M, Alonso JG, Okai T, Longo LD & Gilbert RD. (1993). Effects of long-term, high-altitude hypoxemia on ovine fetal cardiac output and blood flow distribution. *Am J Obstet Gynaecol* **169**, 701-707.
- Kawasaki T, Delea CS, Bartter FC & Smith H. (1978). The effect of high-sodium and low-sodium intakes on blood pressure and other related variables in human subjects with idiopathic hypertension. *Am J Med* **64**, 193-198.
- KDIGO. (2013). KDIGO 2012 clinical practice guidelines for the evaluation and management of chronic kidney disease. *Kidney Int Suppl* **3**, 1-150.
- Keller G, Zimmer G, Mall G, Ritz E & Amann K. (2003). Nephron number in patients with primary hypertension. *N Engl J Med* **348**, 101-108.
- Keppler A, Gretz N, Schmidt R, Kloetzer HM, Groene HJ, Lelongt B, Meyer M, Sadick M & Pill J. (2007). Plasma creatinine determination in mice and rats: an enzymatic method compares favorably with a high-performance liquid chromatography assay. *Kidney Int* **71**, 74-78.
- Kingdom JCP & Kaufmann P. (1997). Oxygen and placental villous development: Origins of fetal hypoxia. *Placenta* **18**, 613-621.
- Kobori H, Nangaku M, Navar LG & Nishiyama A. (2007). The intrarenal renin-angiotensin system: from physiology to the pathobiology of hypertension and kidney disease. *Pharmacol Rev* **59**, 251-287.
- Krampl E, Lees C, Bland JM, Espinoza Dorado J, Moscoso G & Campbell S. (2000). Fetal biometry at 4300 m compared to sea level in Peru. *Ultrasound Obstet Gynecol* **16**, 9-18.

- Lal A, Veinot JP & Leenen FHH. (2003). Prevention of high salt diet-induced cardiac hypertrophy and fibrosis by spironolactone*. *Am J Hypertens* **16**, 319-323.
- Langley-Evans SC, Welham SJ & Jackson AA. (1999). Fetal exposure to a maternal low protein diet impairs nephrogenesis and promotes hypertension in the rat. *Life Sci* **64**, 965-974.
- Lawler JM, Barnes WS, Wu G, Song W & Demaree S. (2002). Direct antioxidant properties of creatine. *Biochem Biophys Res Commun* **290**, 47-52.
- Layton AT, Layton HE, Dantzler WH & Pannabecker TL. (2009). The mammalian urine concentrating mechanism: hypotheses and uncertainties. *Physiology* **24**, 250-256.
- Leeson CP, Kattenhorn M, Morley R, Lucas A & Deanfield JE. (2001). Impact of low birth weight and cardiovascular risk factors on endothelial function in early adult life. *Circulation* **103**, 1264-1268.
- Lelièvre-Pégorier M, Vilar J, Ferrier M-L, Moreau E, Freund N, Gilbert T & Merlet-Bénichou C. (1998). Mild vitamin A deficiency leads to inborn nephron deficit in the rat. *Kidney Int* **54**, 1455-1462.
- León-Velarde F, Villafuerte FC & Richalet J-P. (2010). Chronic mountain sickness and the heart. *Prog Cardiovasc Dis* **52**, 540-549.
- Levey AS, Coresh J, Balk E, Kausz AT, Levin A, Steffes MW, Hogg RJ, Perrone RD, Lau J & Eknoyan G. (2003). National Kidney Foundation practice guidelines for chronic kidney disease: evaluation, classification, and stratification. *Ann Intern Med* **139**, 137-147.
- Lewis RM, Forhead AJ, Petry CJ, Ozanne SE & Hales CN. (2002). Long-term programming of blood pressure by maternal dietary iron restriction in the rat. *Br J Nutr* **88**, 283-290.
- Li G, Xiao Y, Estrella JL, Ducsay CA, Gilbert RD & Zhang L. (2003). Effect of fetal hypoxia on heart susceptibility to ischemia and reperfusion injury in the adult rat. *J Soc Gynecol Investig* **10**, 265-274.

- Li J, Ariunbold U, Suhaimi N, Sunn N, Guo J, McMahon JA, McMahon AP & Little M. (2014). Collecting duct-derived cells display mesenchymal stem cell properties and retain selective in vitro and in vivo epithelial capacity. *J Am Soc Nephrol*.
- Li J, LaMarca B & Reckelhoff JF. (2012). A model of preeclampsia in rats: the reduced uterine perfusion pressure (RUPP) model. *Am J Physiol Heart Circ Physiol* **303**, H1-H8.
- Li S, Sloboda DM, Moss TJ, Nitsos I, Polglase GR, Doherty DA, Newnham JP, Challis JR & Braun T. (2013). Effects of glucocorticoid treatment given in early or late gestation on growth and development in sheep. *J Dev Orig Health Dis* **4**, 146-156.
- Li Y, He Y, Qi L, Jaddoe VW, Feskens EJ, Yang X, Ma G & Hu FB. (2010). Exposure to the Chinese famine in early life and the risk of hyperglycemia and type 2 diabetes in adulthood. *Diabetes* **59**, 2400-2406.
- Li Y, Jaddoe VW, Qi L, He Y, Lai J, Wang J, Zhang J, Hu Y, Ding EL & Yang X. (2011). Exposure to the Chinese famine in early life and the risk of hypertension in adulthood. *J Hypertens* **29**, 1085-1092.
- Lim K, Zimanyi MA & Black MJ. (2006). Effect of maternal protein restriction in rats on cardiac fibrosis and capillarization in adulthood. *Pediatr Res* **60**, 83-87.
- Lim SS, Vos T, Flaxman AD & *al. e.* (2012). A comparative risk assessment of burden of disease and injury attributable to 67 risk factors and risk factor clusters in 21 regions, 1990-2010: a systematic analysis for the Global Burden of Disease Study 2010. *The Lancet* **380**, 2224-2260.
- Lone FW, Qureshi RN & Emanuel F. (2004). Maternal anaemia and its impact on perinatal outcome. *Trop Med Int Health* **9**, 486-490.
- Low JA. (2004a). Determining the contribution of asphyxia to brain damage in the neonate. *J Obstet Gynaecol Res* **30**, 276-286.
- Low JA. (2004b). Reflections on the occurrence and significance of antepartum fetal asphyxia. *Best Pract Res Clin Obstet Gynaecol* **18**, 375-382.

- Lu JKH, Anzalone CR & LaPolt PS. (1994). Relation of neuroendocrine function to reproductive decline during aging in the female rat. *Neurobiol Aging* **15**, 541-544.
- Lueder FL, Kim S-B, Buroker CA, Bangalore SA & Ogata ES. (1995). Chronic maternal hypoxia retards fetal growth and increases glucose utilization of select fetal tissues in the rat. *Metabolism* **44**, 532-537.
- Lumbers ER, Hill KJ & Bennett VJ. (1988). Proximal and distal tubular activity in chronically catheterized fetal sheep compared with the adult. *Can J Physiol Pharmacol* **66**, 697-702.
- Lumey LH. (1992). Decreased birthweights in infants after maternal in utero exposure to the Dutch famine of 1944–1945. *Paediatr Perinat Epidemiol* **6**, 240-253.
- Luyckx VA, Bertram JF, Brenner BM, Fall C, Hoy WE, Ozanne SE & Vikse BE. (2013). Effect of fetal and child health on kidney development and long-term risk of hypertension and kidney disease. *Lancet* **382**, 273-283.
- Maasilta P, Bachour A, Teramo K, Polo O & Laitinen LA. (2001). Sleep-related disordered breathing during pregnancy in obese women. *Chest* **120**, 1448-1454.
- Machnik A, Neuhofer W, Jantsch J, Dahlmann A, Tammela T, Machura K, Park J-K, Beck F-X, Muller DN, Derer W, Goss J, Ziomber A, Dietsch P, Wagner H, van Rooijen N, Kurtz A, Hilgers KF, Alitalo K, Eckardt K-U, Luft FC, Kerjaschki D & Titze J. (2009). Macrophages regulate salt-dependent volume and blood pressure by a vascular endothelial growth factor-C-dependent buffering mechanism. *Nat Med* **15**, 545-552.
- Maka N, Makrakis J, Parkington HC, Tare M, Morley R & Black MJ. (2008). Vitamin D deficiency during pregnancy and lactation stimulates nephrogenesis in rat offspring. *Pediatr Nephrol* **23**, 55-61.
- Makrakis J, Zimanyi MA & Black MJ. (2007). Retinoic acid enhances nephron endowment in rats exposed to maternal protein restriction. *Pediatr Nephrol* **22**, 1861-1867.

- Manning J, Beutler K, Knepper MA & Vehaskari VM. (2002). Upregulation of renal BSC1 and TSC in prenatally programmed hypertension. *Am J Physiol Renal Physiol* **283**, F202-206.
- Marose TD, Merkel CE, McMahon AP & Carroll TJ. (2008). Beta-catenin is necessary to keep cells of ureteric bud/Wolffian duct epithelium in a precursor state. *Dev Biol* **314**, 112-126.
- Martin H, Hu J, Gennser G & Norman M. (2000). Impaired endothelial function and increased carotid stiffness in 9-year-old children with low birthweight. *Circulation* **102**, 2739-2744.
- Matsuzawa Y, Guddeti RR, Kwon T-G, Lerman LO & Lerman A. (2015). Treating coronary disease and the impact of endothelial dysfunction. *Prog Cardiovasc Dis* **57**, 431-442.
- McMullen S, Gardner DS & Langley-Evans SC. (2004). Prenatal programming of angiotensin II type 2 receptor expression in the rat. *Br J Nutr* **91**, 133-140.
- Minutolo R, De Nicola L, Mazzaglia G, Postorino M, Cricelli C, Mantovani LG, Conte G & Cianciaruso B. (2008). Detection and awareness of moderate to advanced CKD by primary care practitioners: a cross-sectional study from Italy. *Am J Kidney Dis* **52**, 444-453.
- Mohri T, Emoto N, Nonaka H, Fukuya H, Yagita K, Okamura H & Yokoyama M. (2003). Alterations of circadian expressions of clock genes in Dahl salt-sensitive rats fed a high-salt diet. *Hypertension* **42**, 189-194.
- Moore CR & Price D. (1948). A study at high altitude of reproduction, growth, sexual maturity, and organ weights. *J Exp Zool* **108**, 171-216.
- Moore LG. (2003). Fetal growth restriction and maternal oxygen transport during high altitude pregnancy. *High Alt Med Biol* **4**, 141-156.
- Moore LG, Shriver M, Bemis L, Hickler B, Wilson M, Brutsaert T, Parra E & Vargas E. (2004). Maternal Adaptation to High-altitude Pregnancy: An Experiment of Nature—A Review. *Placenta* **25**, Supplement, S60-S71.
- Moore LG, Charles SM & Julian CG. (2011). Humans at high altitude: hypoxia and fetal growth. *Respir Physiol Neurobiol* **178**, 181-190.

- Moore LG, Young D, McCullough RE, Droma T & Zamudio S. (2001). Tibetan protection from intrauterine growth restriction (IUGR) and reproductive loss at high altitude. *Am J Hum Biol* **13**, 635-644.
- Moritz K, Wintour-Coghlan EM, Black MJ, Bertram JF & Caruana G. (2008a). *Factors Influencing Mammalian Kidney Development: Implications for Health in Adult Life*. Springer, Berlin Heidelberg.
- Moritz KM, Cuffe JS, Wilson LB, Dickinson H, Wlodek ME, Simmons DG & Denton KM. (2010). Review: Sex specific programming: a critical role for the renal renin-angiotensin system. *Placenta* **31 Suppl**, S40-46.
- Moritz KM, De Matteo R, Dodic M, Jefferies AJ, Arena D, Wintour EM, Probyn ME, Bertram JF, Singh RR, Zanini S & Evans RG. (2011). Prenatal glucocorticoid exposure in the sheep alters renal development in utero: implications for adult renal function and blood pressure control. *Am J Physiol Regul Integr Comp Physiol* **301**, R500-509.
- Moritz KM, Dodic M & Wintour EM. (2003). Kidney development and the fetal programming of adult disease. *Bioessays* **25**, 212-220.
- Moritz KM, Johnson K, Douglas-Denton R, Wintour EM & Dodic M. (2002). Maternal glucocorticoid treatment programs alterations in the renin-angiotensin system of the ovine fetal kidney. *Endocrinology* **143**, 4455-4463.
- Moritz KM, Mazzuca MQ, Siebel AL, Mibus A, Arena D, Tare M, Owens JA & Wlodek ME. (2009a). Uteroplacental insufficiency causes a nephron deficit, modest renal insufficiency but no hypertension with ageing in female rats. *J Physiol* **587**, 2635-2646.
- Moritz KM, Singh RR, Probyn ME & Denton KM. (2009b). Developmental programming of a reduced nephron endowment: more than just a baby's birth weight. *Am J Physiol Renal Physiol* **296**, F1-9.

- Moritz KM, Wintour EM, Black MJ, Bertram JF & Caruana G. (2008b). Factors influencing mammalian kidney development: implications for health in adult life. *Adv Anat Embryol Cell Biol* **196**, 1-78.
- Morrison JL. (2008). Sheep models of intrauterine growth restriction: fetal adaptations and consequences. *Clin Exp Pharmacol Physiol* **35**, 730-743.
- Morrison JL, Botting KJ, Dyer JL, Williams SJ, Thornburg KL & McMillen IC. (2007). Restriction of placental function alters heart development in the sheep fetus. *Am J Physiol Regul Integr Comp Physiol* **293**, R306-R313.
- Murphy VE, Zakar T, Smith R, Giles WB, Gibson PG & Clifton VL. (2002). Reduced 11beta-hydroxysteroid dehydrogenase type 2 activity is associated with decreased birth weight centile in pregnancies complicated by asthma. *J Clin Endocrinol Metab* **87**, 1660-1668.
- National Health and Medical Research Council. (2006). Nutrient reference values for Australia and New Zealand. Australian Government, Australia.
- National Kidney Foundation. (2002). K/DOQI clinical practice guidelines for chronic kidney disease: evaluation, classification, and stratification. *Am J Kidney Dis* **39**, S1-266.
- Nieto VMG, Yanes MIL, Zamorano MM, González MJH, Aros CP & Garin EH. (2008). Renal concentrating capacity as a marker for glomerular filtration rate. *Acta Paediatr* **97**, 96-99.
- Niimura F, Labosky PA, Kakuchi J, Okubo S, Yoshida H, Oikawa T, Ichiki T, Naftilan AJ, Fogo A, Inagami T & et al. (1995). Gene targeting in mice reveals a requirement for angiotensin in the development and maintenance of kidney morphology and growth factor regulation. *J Clin Invest* **96**, 2947-2954.
- Ninomiya T, Perkovic V, de Galan BE, Zoungas S, Pillai A, Jardine M, Patel A, Cass A, Neal B, Poulter N, Mogensen C-E, Cooper M, Marre M, Williams B, Hamet P, Mancia G, Woodward M, MacMahon S & Chalmers J. (2009). Albuminuria and kidney function independently predict cardiovascular and renal outcomes in diabetes. *J Am Soc Nephrol* **20**, 1813-1821.

- Nyengaard J, Flyvbjerg A & Rasch R. (1993). The impact of renal growth, regression and regrowth in experimental diabetes mellitus on number and size of proximal and distal tubular cells in the rat kidney. *Diabetologia* **36**, 1126-1131.
- Nyengaard JR & Bendtsen TF. (1992). Glomerular number and size in relation to age, kidney weight, and body surface in normal man. *Anat Rec* **232**, 194-201.
- O'Dowd R, Kent JC, Moseley JM & Wlodek ME. (2008). Effects of uteroplacental insufficiency and reducing litter size on maternal mammary function and postnatal offspring growth. *Am J Physiol Regul Integr Comp Physiol* **294**, R539-R548.
- O'Sullivan L, Cuffe JS, Koning A, Singh RR, Paravicini TM & Moritz KM. (2015). Excess prenatal corticosterone exposure results in albuminuria, sex-specific hypotension, and altered heart rate responses to restraint stress in aged adult mice. *Am J Physiol Renal Physiol* **308**, F1065-F1073.
- O'Sullivan L, Cuffe JS, Paravicini TM, Campbell S, Dickinson H, Singh RR, Gezmish O, Black MJ & Moritz KM. (2013). Prenatal exposure to dexamethasone in the mouse alters cardiac growth patterns and increases pulse pressure in aged male offspring. *PLoS One* **8**, e69149.
- Ojeda NB, Grigore D, Robertson EB & Alexander BT. (2007a). Estrogen protects against increased blood pressure in postpubertal female growth restricted offspring. *Hypertension* **50**, 679-685.
- Ojeda NB, Grigore D, Yanes LL, Iliescu R, Robertson EB, Zhang H & Alexander BT. (2007b). Testosterone contributes to marked elevations in mean arterial pressure in adult male intrauterine growth restricted offspring. *Am J Physiol Regul Integr Comp Physiol* **292**, R758-R763.
- Ojeda NB, Johnson WR, Dwyer TM & Alexander BT. (2007c). Early renal denervation prevents development of hypertension in growth-restricted offspring. *Clin Exp Pharmacol Physiol* **34**, 1212-1216.
- Ojo AO, Hanson JA, Wolfe RA, Leichtman AB, Agodoa LY & Port FK. (2000). Long-term survival in renal transplant recipients with graft function. *Kidney Int* **57**, 307-313.

- Ong KK, Ahmed ML, Emmett PM, Preece MA & Dunger DB. (2000). Association between postnatal catch-up growth and obesity in childhood: prospective cohort study. *BMJ* **320**, 967-971.
- Ortiz LA, Quan A, Zarzar F, Weinberg A & Baum M. (2003). Prenatal dexamethasone programs hypertension and renal injury in the rat. *Hypertension* **41**, 328-334.
- Otsuka F, Kramer MC, Woudstra P, Yahagi K, Ladich E, Finn AV, de Winter RJ, Kolodgie FD, Wight TN & Davis HR. (2015). Natural progression of atherosclerosis from pathologic intimal thickening to late fibroatheroma in human coronary arteries: a pathology study. *Atherosclerosis* **241**, 772-782.
- Painter RC, de Rooij SR, Bossuyt PM, Phillips DI, Osmond C, Barker DJ, Bleker OP & Roseboom TJ. (2006). Blood pressure response to psychological stressors in adults after prenatal exposure to the Dutch famine. *J Hypertens* **24**, 1771-1778.
- Palmer SK, Moore LG, Young DA, Cregger B, Berman JC & Zamudio S. (1999). Altered blood pressure course during normal pregnancy and increased preeclampsia at high altitude (3100 meters) in Colorado. *Am J Obstet Gynecol* **180**, 1161-1168.
- Park JS, Valerius MT & McMahon AP. (2007). Wnt/beta-catenin signaling regulates nephron induction during mouse kidney development. *Development* **134**, 2533-2539.
- Parraguez VH, Atlagich M, Araneda O, García C, Muñoz A, De los Reyes M & Urquieta B. (2011). Effects of antioxidant vitamins on newborn and placental traits in gestations at high altitude: comparative study in high and low altitude native sheep. *Reprod Fertil Dev* **23**, 285-296.
- Peyronnet J, Dalmaz Y, Ehrstrom M, Mamet J, Roux JC, Pequignot JM, Thoren HP & Lagercrantz H. (2002). Long-lasting adverse effects of prenatal hypoxia on developing autonomic nervous system and cardiovascular parameters in rats. *Pflugers Arch* **443**, 858-865.
- Phipps K, Barker DJP, Hales CN, Fall CHD, Osmond C & Clark PMS. (1993). Fetal growth and impaired glucose tolerance in men and women. *Diabetologia* **36**, 225-228.

- Pollock CA, Bostrom TE, Dyne M, Györy AZ & Field MJ. (1992). Tubular sodium handling and tubuloglomerular feedback in compensatory renal hypertrophy. *Pflügers Archiv* **420**, 159-166.
- Prior LJ, Davern PJ, Burke SL, Lim K, Armitage JA & Head GA. (2014). Exposure to a high-fat diet during development alters leptin and ghrelin sensitivity and elevates renal sympathetic nerve activity and arterial pressure in rabbits. *Hypertension* **63**, 338-345.
- Radhakrishnan J, Remuzzi G, Saran R, Williams DE, Rios-Burrows N, Powe N, Bruck K, Wanner C, Stel VS, Venuthurupalli SK, Hoy WE, Healy HG, Salisbury A, Fassett RG, O'Donoghue D, Roderick P, Matsuo S, Hishida A, Imai E & Iimuro S. (2014). Taming the chronic kidney disease epidemic: a global view of surveillance efforts. *Kidney Int* **86**, 246-250.
- Ramadoss J, Tress U, Chen WJ & Cudd TA. (2008). Maternal adrenocorticotropin, cortisol, and thyroid hormone responses to all three-trimester equivalent repeated binge alcohol exposure: ovine model. *Alcohol* **42**, 199-205.
- Ravelli AC, van der Meulen JH, Michels R, Osmond C, Barker DJ, Hales C & Bleker OP. (1998). Glucose tolerance in adults after prenatal exposure to famine. *Lancet* **351**, 173-177.
- Ream M, Ray AM, Chandra R & Chikaraishi DM. (2008). Early fetal hypoxia leads to growth restriction and myocardial thinning. *Am J Physiol Regul Integr Comp Physiol* **295**, R583-R595.
- Rettig R, Folberth C, Stauss H, Kopf D, Waldherr R & Unger T. (1990). Role of the kidney in primary hypertension - a renal transplantation study in rats. *Am J Physiol* **258**, F606-F611.
- Robillard JE, Weitzman RE, Burmeister L & Smith FG. (1981). Developmental aspects of the renal response to hypoxemia in the lamb fetus. *Circ Res* **48**, 128-138.
- Rodgers A & Neal B. (1999). Less salt does not necessarily mean less taste. *Lancet* **353**, 1332.
- Rouwet EV, Tintu AN, Schellings MWM, van Bilsen M, Lutgens E, Hofstra L, Slaaf DW, Ramsay G & le Noble FAC. (2002). Hypoxia induces aortic hypertrophic growth, left ventricular

dysfunction, and sympathetic hyperinnervation of peripheral arteries in the chick embryo. *Circulation* **105**, 2791-2796.

Rudolph AM & Heymann MA. (1968). The fetal circulation. *Ann Rev Med* **19**, 195-206

Rueda-Clausen CF, Morton JS & Davidge ST. (2008). Effects of hypoxia-induced intrauterine growth restriction on cardiopulmonary structure and function during adulthood. *Cardiovasc Res* **81**, 713-722.

Rueda-Clausen CF, Morton JS, Dolinsky VW, Dyck JRB & Davidge ST. (2012a). Synergistic effects of prenatal hypoxia and postnatal high-fat diet in the development of cardiovascular pathology in young rats. *Am J Physiol Regul Integr Comp Physiol* **303**, R418-R426.

Rueda-Clausen CF, Morton JS, Lopaschuk GD & Davidge ST. (2010). Long-term effects of intrauterine growth restriction on cardiac metabolism and susceptibility to ischaemia/reperfusion. *Cardiovasc Res*, cvq363.

Rueda-Clausen CF, Morton JS, Oudit GY, Kassiri Z, Jiang Y & Davidge ST. (2012b). Effects of hypoxia-induced intrauterine growth restriction on cardiac siderosis and oxidative stress. *J Dev Orig Health Dis* **3**, 350-357.

Rumballe BA, Georgas KM, Combes AN, Ju AL, Gilbert T & Little MH. (2011). Nephron formation adopts a novel spatial topology at cessation of nephrogenesis. *Dev Biol* **360**, 110-122.

Rurak D. (1978). Plasma vasopressin levels during hypoxaemia and the cardiovascular effects of exogenous vasopressin in foetal and adult sheep. *J Physiol* **277**, 341-357.

Ruta L-AM, Dickinson H, Thomas MC, Denton KM, Anderson WP & Kett MM. (2010). High-salt diet reveals the hypertensive and renal effects of reduced nephron endowment. *Am J Physiol Renal Physiol* **298**, F1384-F1392.

Graber SE & Krantz SB. (1978). Erythropoietin and the Control of Red Cell Production. *Annu Rev Med* **29**, 51-66.

- Sacks FM, Svetkey LP, Vollmer WM, Appel LJ, Bray GA, Harsha D, Obarzanek E, Conlin PR, Miller ER, 3rd, Simons-Morton DG, Karanja N & Lin PH. (2001). Effects on blood pressure of reduced dietary sodium and the Dietary Approaches to Stop Hypertension (DASH) diet. DASH-Sodium Collaborative Research Group. *N Engl J Med* **344**, 3-10.
- Saez F, Castells MT, Zuasti A, Salazar F, Reverte V, Loria A & Salazar FJ. (2007). Sex differences in the renal changes elicited by angiotensin II blockade during the nephrogenic period. *Hypertension* **49**, 1429-1435.
- Sahin FK, Koken G, Cosar E, Saylan F, Fidan F, Yilmazer M & Unlu M. (2008). Obstructive sleep apnea in pregnancy and fetal outcome. *Int J Gynaecol Obstet* **100**, 141-146.
- Salinas C, Blanco C, Villena M, Camm E, Tuckett J, Weerakkody R, Kane A, Shelley A, Wooding F & Quy M. (2010). Developmental origin of cardiac and vascular disease in chick embryos incubated at high altitude. *J Dev Orig Health Dis* **1**, 60-66.
- Samuelsson AM, Morris A, Igosheva N, Kirk SL, Pombo JM, Coen CW, Poston L & Taylor PD. (2010). Evidence for sympathetic origins of hypertension in juvenile offspring of obese rats. *Hypertension* **55**, 76-82.
- Sarnak MJ, Levey AS, Schoolwerth AC, Coresh J, Culeton B, Hamm LL, McCullough PA, Kasiske BL, Kelepouris E, Klag MJ, Parfrey P, Pfeffer M, Raij L, Spinosa DJ & Wilson PW. (2003). Kidney disease as a risk Factor for development of cardiovascular disease. A Statement From the American Heart Association Councils on Kidney in Cardiovascular Disease, High Blood Pressure Research, Clinical Cardiology, and Epidemiology and Prevention **108**, 2154-2169.
- Santos RA. (2014). Angiotensin-(1-7). *Hypertension* **63**, 1138-1147.
- Savolainen SM, Foley JF & Elmore SA. (2009). Histology atlas of the developing mouse heart with emphasis on E11.5 to E18.5. *Toxicol Pathol* **37**, 395-414.
- Schedl A. (2007). Renal abnormalities and their developmental origin. *Nat Rev Genet* **8**, 791-802.

- Schlegel RN, Moritz KM & Paravinici TM. (2016). Maternal hypomagnesemia alters renal function but does not program changes in the cardiovascular physiology of adult offspring. *J Dev Orig Health Dis*, 1-8.
- Schmidt K, Pesce C, Liu Q, Nelson RG, Bennett PH, Karnitschnig H, Striker LJ & Striker GE. (1992). Large glomerular size in Pima Indians: lack of change with diabetic nephropathy. *J Am Soc Nephrol* **3**, 229-235.
- Schock-Kusch D, Geraci S, Ermeling E, Shulhevich Y, Sticht C, Hesser J, Stsepankou D, Neudecker S, Pill J, Schmitt R & Melk A. (2013). Reliability of transcutaneous measurement of renal function in various strains of conscious mice. *PLoS ONE* **8**, e71519.
- Schreiber A, Shulhevich Y, Geraci S, Hesser J, Stsepankou D, Neudecker S, Koenig S, Heinrich R, Hoecklin F, Pill J, Friedemann J, Schweda F, Gretz N & Schock-Kusch D. (2012). Transcutaneous measurement of renal function in conscious mice. *Am J Physiol Renal Physiol* **303**, F783-F788.
- Schultheis PJ, Clarke LL, Meneton P, Miller ML, Soleimani M, Gawenis LR, Riddle TM, Duffy JJ, Doetschman T & Wang T. (1998). Renal and intestinal absorptive defects in mice lacking the NHE3 Na⁺/H⁺ exchanger. *Nat Genet* **19**, 282-285.
- Shah A, Reyes LM, Morton JS, Fung D, Schneider J & Davidge ST. (2016). Effect of resveratrol on metabolic and cardiovascular function in male and female adult offspring exposed to prenatal hypoxia and a high-fat diet. *J Physiol* **594**, 1465-1482.
- Sibley CP, Coan PM, Ferguson-Smith AC, Dean W, Hughes J, Smith P, Reik W, Burton GJ, Fowden AL & Constancia M. (2004). Placental-specific insulin-like growth factor 2 (Igf2) regulates the diffusional exchange characteristics of the mouse placenta. *Proc Natl Acad Sci U S A* **101**, 8204-8208.
- Simon DB, Karet FE, Hamdan JM, Di Pietro A, Sanjad SA & Lifton RP. (1996). Bartter's syndrome, hypokalaemic alkalosis with hypercalciuria, is caused by mutations in the Na-K-2Cl cotransporter NKCC2. *Nat Genet* **13**, 183-188.

- Singh RR, Cullen-McEwen LA, Kett MM, Boon WM, Dowling J, Bertram JF & Moritz KM. (2007). Prenatal corticosterone exposure results in altered AT1/AT2, nephron deficit and hypertension in the rat offspring. *J Physiol* **579**, 503-513.
- Singh RR, Denton KM, Bertram JF, Jefferies AJ & Moritz KM. (2010). Reduced nephron endowment due to fetal uninephrectomy impairs renal sodium handling in male sheep. *Clin Sci (Lond)* **118**, 669-680.
- Skarsgard P, Van Breemen C & Laher I. (1997). Estrogen regulates myogenic tone in pressurized cerebral arteries by enhanced basal release of nitric oxide. *Am J Physiol Heart Circ Physiol* **273**, H2248-H2256.
- Song R & Yosypiv IV. (2012). Development of the kidney medulla. *Organogenesis* **8**, 10-17.
- Song S, Meyer M, Türk TR, Wilde B, Feldkamp T, Assert R, Wu K, Kribben A & Witzke O. (2009). Serum cystatin C in mouse models: a reliable and precise marker for renal function and superior to serum creatinine. *Nephrol Dial Transplant* **24**, 1157-1161.
- St Clair D, Xu M, Wang P, Yu Y, Fang Y, Zhang F, Zheng X, Gu N, Feng G & Sham P. (2005). Rates of adult schizophrenia following prenatal exposure to the Chinese famine of 1959-1961. *JAMA* **294**, 557-562.
- Stangenberg S, Nguyen LT, Chen H, Al-Odat I, Killingsworth MC, Gosnell ME, Anwer AG, Goldys EM, Pollock CA & Saad S. (2015). Oxidative stress, mitochondrial perturbations and fetal programming of renal disease induced by maternal smoking. *Int J Biochem Cell Biol* **64**, 81-90.
- Stein AD, Zybert PA, Van der Pal-de Bruin K & Lumey L. (2006). Exposure to famine during gestation, size at birth, and blood pressure at age 59 y: evidence from the Dutch Famine. *Eur J Epidemiol* **21**, 759-765.
- Stephenson JL. (1987). Models of the urinary concentrating mechanism. *Kidney Int* **31**, 648-661.
- Stevens LA, Fares G, Fleming J, Martin D, Murthy K, Qiu J, Stark PC, Uhlig K, Van Lente F & Levey AS. (2005). Low rates of testing and diagnostic codes usage in a commercial clinical

laboratory: evidence for lack of physician awareness of chronic kidney disease. *J Am Soc Nephrol* **16**, 2439-2448.

Sulyok E, Varga F, Györy E, Jobst K & Csaba IF. (1979). Postnatal development of renal sodium handling in premature infants. *J Pediatr* **95**, 787-792.

Susser ES & Lin SP. (1992). Schizophrenia after prenatal exposure to the Dutch Hunger Winter of 1944-1945. *Arch Gen Psychiatry* **49**, 983-988.

Tapanainen PJ, Bang P, Wilson K, Unterman TG, Vreman HJ & Rosenfeld RG. (1994). Maternal hypoxia as a model for intrauterine growth retardation: effects on insulin-like growth factors and their binding proteins. *Pediatr Res* **36**, 152-158.

Tazuke SI, Mazure NM, Sugawara J, Carland G, Faessen GH, Suen L-F, Irwin JC, Powell DR, Giaccia AJ & Giudice LC. (1998). Hypoxia stimulates insulin-like growth factor binding protein 1 (IGFBP-1) gene expression in HepG2 cells: A possible model for IGFBP-1 expression in fetal hypoxia. *P Natl Acad Sci USA* **95**, 10188-10193.

te Velde SJ, Ferreira I, Twisk JW, Stehouwer CD, van Mechelen W & Kemper HC. (2004). Birthweight and arterial stiffness and blood pressure in adulthood—Results from the Amsterdam Growth and Health Longitudinal Study. *Int J Epidemiol* **33**, 154-161.

Thomas MC, Burns WC & Cooper ME. (2005). Tubular changes in early diabetic nephropathy. *Adv Chronic Kidney Dis* **12**, 177-186.

Thomas R, Kanso A & Sedor JR. (2008). Chronic kidney disease and its complications. *J Prim Care* **35**, 329-vii.

Tintu A, Rouwet E, Verlohren S, Brinkmann J, Ahmad S, Crispi F, van Bilsen M, Carmeliet P, Staff AC & Tjwa M. (2009). Hypoxia induces dilated cardiomyopathy in the chick embryo: mechanism, intervention, and long-term consequences. *PLoS ONE* **4**, e5155.

Tintu AN, Noble FA & Rouwet EV. (2007). Hypoxia disturbs fetal hemodynamics and growth. *Endothelium* **14**, 353-360.

- Titze J. (2015). A different view on sodium balance. *Curr Opin Nephrol Hypertens* **24**, 14-20.
- Tomat AL, Inserra F, Veiras L, Vallone MC, Balaszczuk AM, Costa MA & Arranz C. (2008). Moderate zinc restriction during fetal and postnatal growth of rats: effects on adult arterial blood pressure and kidney. *Am J Physiol Regul Integr Comp Physiol* **295**, R543-549.
- Tschöp M, Strasburger CJ, Hartmann G, Biollaz J & Bärtsch P. (1999). Raised leptin concentrations at high altitude associated with loss of appetite. *Lancet* **352**, 1119-1120.
- Tsuchida S, Matsusaka T, Chen X, Okubo S, Niimura F, Nishimura H, Fogo A, Utsunomiya H, Inagami T & Ichikawa I. (1998). Murine double nullizygotes of the angiotensin type 1A and 1B receptor genes duplicate severe abnormal phenotypes of angiotensinogen nullizygotes. *J Clin Invest* **101**, 755-760.
- Vehaskari VM, Stewart T, Lafont D, Soye C, Seth D & Manning J. (2004). Kidney angiotensin and angiotensin receptor expression in prenatally programmed hypertension. *Am J Physiol Renal Physiol* **287**, F262-267.
- Vilar J, Gilbert T, Moreau E & Merlet-Bénichou C. (1996). Metanephros organogenesis is highly stimulated by vitamin A derivatives in organ culture. *Kidney Int* **49**, 1478-1487.
- Villamor E, Kessels CGA, Ruijtenbeek K, van Suylen RJ, Belik J, De Mey JGR & Blanco CE. (2004). Chronic in ovo hypoxia decreases pulmonary arterial contractile reactivity and induces biventricular cardiac enlargement in the chicken embryo. *Am J Physiol Regul Integr Comp Physiol* **287**, R642-R651.
- Vio F, Salazar G & Infante C. (1991). Smoking during pregnancy and lactation and its effects on breast-milk volume. *Am J Clin Nutr* **54**, 1011-1016.
- Vries WB, Bal MP, Homoet-van der Kraak P, Kamphuis PJGH, Leij FR, Baan J, Steendijk P, Weger RA, Bel F & Oosterhout MFM. (2006). Suppression of physiological cardiomyocyte proliferation in the rat pup after neonatal glucocorticosteroid treatment. *Basic Res Cardiol* **101**, 36-42.

- Walker KA, Cai X, Caruana G, Thomas MC, Bertram JF & Kett MM. (2012). High nephron endowment protects against salt-induced hypertension. *Am J Physiol Renal Physiol* **303**, F253-F258.
- Wallimann T, Wyss M, Brdiczka D, Nicolay K & Eppenberger HM. (1992). Intracellular compartmentation, structure and function of creatine kinase isoenzymes in tissues with high and fluctuating energy demands: the 'phosphocreatine circuit' for cellular energy homeostasis. *Biochem J* **281** (Pt 1), 21-40.
- Walton SL, Singh RR, Tan T, Paravicini TM & Moritz KM. (2016). Late gestational hypoxia and a postnatal high salt diet programs endothelial dysfunction and arterial stiffness in adult mouse offspring. *J Physiol* **594**, 1451-1463.
- Wang JC & Bennett M. (2012). Aging and atherosclerosis mechanisms, functional consequences, and potential therapeutics for cellular senescence. *Circ Res* **111**, 245-259.
- Wang Q, Hummler E, Maillard M, Nussberger J, Rossier BC, Brunner HR & Burnier M. (2001). Compensatory up-regulation of angiotensin II subtype 1 receptors in alpha ENaC knockout heterozygous mice. *Kidney Int* **59**, 2216-2221.
- Warner Matthew J & Ozanne Susan E. (2010). Mechanisms involved in the developmental programming of adulthood disease. *Biochem J* **427**, 333-347.
- Weber KT. (1989). Cardiac interstitium in health and disease: the fibrillar collagen network. *J Am Coll Cardiol* **13**, 1637-1652.
- Weinberger MH & Fineberg NS. (1991). Sodium and volume sensitivity of blood pressure. Age and pressure change over time. *Hypertension* **18**, 67-71.
- Weismann DN & Robillard JE. (1988). Renal hemodynamic responses to hypoxemia during development: relationships to circulating vasoactive substances. *Pediatr Res* **23**, 155-162.
- Welham SJ, Wade A & Woolf AS. (2002). Protein restriction in pregnancy is associated with increased apoptosis of mesenchymal cells at the start of rat metanephrogenesis. *Kidney Int* **61**, 1231-1242.

- Wen CP, Cheng TYD, Tsai MK, Chang YC, Chan HT, Tsai SP, Chiang PH, Hsu CC, Sung PK, Hsu YH & Wen SF. (2008). All-cause mortality attributable to chronic kidney disease: a prospective cohort study based on 462 293 adults in Taiwan. *Lancet* **371**, 2173-2182.
- Werns SW, Walton JA, Hsia HH, Nabel EG, Sanz ML & Pitt B. (1989). Evidence of endothelial dysfunction in angiographically normal coronary arteries of patients with coronary artery disease. *Circulation* **79**, 287-291.
- Westerterp-Plantenga MS. (1999). Effects of extreme environments on food intake in human subjects. *Proc Nutr Soc* **58**, 791-798.
- Westerterp-Plantenga MS, Westerterp KR, Rubbens M, Verwegen CRT, Richelet J-P & Gardette B. (1999). Appetite at “high altitude” [Operation Everest III (Comex-'97)]: a simulated ascent of Mount Everest. *J Appl Physiol* **87**, 391-399.
- Wickman C & Kramer H. (2013). Obesity and kidney disease: potential mechanisms. *Semin Nephrol* **33**, 14-22.
- Wiig H, Schröder A, Neuhofer W, Jantsch J, Kopp C, Karlsen TV, Boschmann M, Goss J, Bry M, Rakova N, Dahlmann A, Brenner S, Tenstad O, Nurmi H, Mervaala E, Wagner H, Beck F-X, Müller DN, Kerjaschki D, Luft FC, Harrison DG, Alitalo K & Titze J. (2013). Immune cells control skin lymphatic electrolyte homeostasis and blood pressure. *J Clin Invest* **123**, 2803-2815.
- Wilkinson L, Kurniawan ND, Phua YL, Nguyen MJ, Li J, Galloway GJ, Hashitani H, Lang RJ & Little MH. (2012). Association between congenital defects in papillary outgrowth and functional obstruction in *Crim1* mutant mice. *J Pathol* **227**, 499-510.
- Wilkinson LJ, Neal CS, Singh RR, Sparrow DB, Kurniawan ND, Ju A, Grieve SM, Dunwoodie SL, Moritz KM & Little MH. (2015). Renal developmental defects resulting from in utero hypoxia are associated with suppression of ureteric β -catenin signaling. *Kidney Int* **87**, 975-983.

- Williams P, McMahon A & Boustead R. (2003). A case study of sodium reduction in breakfast cereals and the impact of the Pick the Tick food information program in Australia. *Health Prom Int* **18**, 51-56.
- Williams SJ, Campbell ME, McMillen IC & Davidge ST. (2005a). Differential effects of maternal hypoxia or nutrient restriction on carotid and femoral vascular function in neonatal rats. *Am J Physiol Regul Integr Comp Physiol* **288**, R360-367.
- Williams SJ, Hemmings DG, Mitchell JM, McMillen IC & Davidge ST. (2005b). Effects of maternal hypoxia or nutrient restriction during pregnancy on endothelial function in adult male rat offspring. *J Physiol* **565**, 125-135.
- Wilson DH, Adams RJ, Tucker G, Appleton S, Taylor AW & Ruffin RE. (2006). Trends in asthma prevalence and population changes in South Australia, 1990-2003. *Med J Aust* **184**, 226.
- Wilson MJ, Lopez M, Vargas M, Julian C, Tellez W, Rodriguez A, Bigham A, Armaza JF, Niermeyer S, Shriver M, Vargas E & Moore LG. (2007). Greater uterine artery blood flow during pregnancy in multigenerational (Andean) than shorter-term (European) high-altitude residents. *Am J Physiol Regul Integr Comp Physiol* **293**, R1313-1324.
- Wintour EM, Moritz K, Butkus A, Baird R, Albiston A & Tennis N. (1999). Ontogeny and regulation of the AT1 and AT2 receptors in the ovine fetal adrenal gland. *Mol Cell Endocrinol* **157**, 161-170.
- Wintour EM, Moritz KM, Johnson K, Ricardo S, Samuel CS & Dodic M. (2003). Reduced nephron number in adult sheep, hypertensive as a result of prenatal glucocorticoid treatment. *J Physiol* **549**, 929-935.
- Wlodek ME, Mibus A, Tan A, Siebel AL, Owens JA & Moritz KM. (2007). Normal lactational environment restores nephron endowment and prevents hypertension after placental restriction in the rat. *J Am Soc Nephrol* **18**, 1688-1696.
- Wlodek ME, Westcott K, Siebel AL, Owens JA & Moritz KM. (2008). Growth restriction before or after birth reduces nephron number and increases blood pressure in male rats. *Kidney Int* **74**, 187-195.

- Wlodek ME, Westcott KT, O'Dowd R, Serruto A, Wassef L, Moritz KM & Moseley JM. (2005). Uteroplacental restriction in the rat impairs fetal growth in association with alterations in placental growth factors including PTHrP. *Am J Physiol Regul Integr Comp Physiol* **288**, R1620-1627.
- Woods LL, Ingelfinger JR, Nyengaard JR & Rasch R. (2001). Maternal protein restriction suppresses the newborn renin-angiotensin system and programs adult hypertension in rats. *Pediatr Res* **49**, 460-467.
- Woods LL, Ingelfinger JR & Rasch R. (2005). Modest maternal protein restriction fails to program adult hypertension in female rats. *Am J Physiol Regul Integr Comp Physiol* **289**, R1131-1136.
- Woods LL, Weeks DA & Rasch R. (2004). Programming of adult blood pressure by maternal protein restriction: Role of nephrogenesis. *Kidney Int* **65**, 1339-1348.
- World Health Organisation. (2001). Iron Deficiency Anaemia. Geneva.
- World Health Organisation. (2009). WHO Fact Sheet: Cardiovascular Diseases (CVDs). Geneva.
- World Health Organisation. (2012). Obesity and Overweight: Fact Sheet. Geneva.
- World Health Organisation. (2015). Global Status Report on Noncommunicable Diseases 2014. Geneva.
- Wreford NG. (1995). Theory and practice of stereological techniques applied to the estimation of cell number and nuclear volume in the testis. *Microsc Res Tech* **32**, 423-436.
- Xia S, Lv J, Gao Q, Li L, Chen N, Wei X, Xiao J, Chen J, Tao J, Sun M, Mao C, Zhang L & Xu Z. (2015). Prenatal exposure to hypoxia induced Beclin 1 signaling-mediated renal autophagy and altered renal development in rat fetuses. *Reprod Sci* **22**, 156-164.

- Xu Y, Williams SJ, O'Brien D & Davidge ST. (2006). Hypoxia or nutrient restriction during pregnancy in rats leads to progressive cardiac remodeling and impairs postischemic recovery in adult male offspring. *FASEB J* **20**, 1251-1253.
- Xue Q & Zhang L. (2009). Prenatal hypoxia causes a sex-dependent increase in heart susceptibility to ischemia and reperfusion injury in adult male offspring: role of protein kinase C ϵ . *J Pharmacol Exp Ther* **330**, 624-632.
- Yamagata K, Takahashi H, Tomida C, Yamagata Y & Koyama A. (2002). Prognosis of asymptomatic hematuria and/or proteinuria in men. *Nephron* **91**, 34-42.
- Yu HCM, Burrell LM, Black MJ, Wu LL, Dilley RJ, Cooper ME & Johnston CI. (1998). Salt induces myocardial and renal fibrosis in normotensive and hypertensive rats. *Circulation* **98**, 2621-2628.
- Yu J, Carroll TJ, Rajagopal J, Kobayashi A, Ren Q & McMahon AP. (2009). A Wnt7b-dependent pathway regulates the orientation of epithelial cell division and establishes the cortico-medullary axis of the mammalian kidney. *Development* **136**, 161-171.
- Yuan BX & Leenen FH. (1991). Dietary sodium intake and left ventricular hypertrophy in normotensive rats. *Am J Physiol* **261**, H1397-1401.
- Yusuf S, Wood D, Ralston J & Reddy KS. (2015). The World Heart Federation's vision for worldwide cardiovascular disease prevention. *The Lancet* **386**, 399-402.
- Zambrano E, Martínez-Samayoá PM, Bautista CJ, Deás M, Guillén L, Rodríguez-González GL, Guzmán C, Larrea F & Nathanielsz PW. (2005). Sex differences in transgenerational alterations of growth and metabolism in progeny (F2) of female offspring (F1) of rats fed a low protein diet during pregnancy and lactation. *J Physiol* **566**, 225-236.
- Zamudio S, Baumann MU & Illsley NP. (2006). Effects of chronic hypoxia in vivo on the expression of human placental glucose transporters. *Placenta* **27**, 49-55.
- Zamudio S, Droma T, Norkyel KY, Acharya G, Zamudio JA, Niermeyer SN & Moore LG. (1993). Protection from intrauterine growth retardation in Tibetans at high altitude. *Am J Phys Anthropol* **91**, 215-224.

- Zamudio S, Kovalenko O, Vanderlelie J, Illsley NP, Heller D, Belliappa S & Perkins AV. (2007). Chronic hypoxia in vivo reduces placental oxidative stress. *Placenta* **28**, 846-853.
- Zamudio S, Palmer SK, Dahms TE, Berman JC, Young DA & Moore LG. (1995a). Alterations in uteroplacental blood flow precede hypertension in preeclampsia at high altitude. *J Appl Physiol* **79**, 15-22.
- Zamudio S, Palmer SK, Droma T, Stamm E, Coffin C & Moore LG. (1995b). Effect of altitude on uterine artery blood flow during normal pregnancy. *J Appl Physiol* **79**, 7-14.
- Zhang J, Massmann GA, Rose JC & Figueroa JP. (2010). Differential effects of clinical doses of antenatal betamethasone on nephron endowment and glomerular filtration rate in adult sheep. *Reprod Sci* **17**, 186-195.
- Zhou L & Liu Y. (2016). Wnt/ β -catenin signaling and renin–angiotensin system in chronic kidney disease. *Curr Opin Nephrol Hypertens* **25**, 100-106.
- Zohdi V, Moritz KM, Bubb KJ, Cock ML, Wreford N, Harding R & Black MJ. (2007). Nephrogenesis and the renal renin-angiotensin system in fetal sheep: effects of intrauterine growth restriction during late gestation. *Am J Physiol Regul Integr Comp Physiol* **293**, R1267-1273.